



SPATIAL MODELLING, ANALYSIS AND PREDICTION OF HENDRA DISEASE
OUTBREAKS IN SOUTH EAST QUEENSLAND, AUSTRALIA

A Thesis Submitted by

Jahnavi Burnham, MSc GIS

For the award of

Doctor of Philosophy

2017

Abstract

Hendra Virus (HeV) is an emerging zoonotic disease that was first identified in 1994 and has only been found in Australia. It can be transmitted to other horses, humans and dogs with a high fatality rate of >79 per cent in horses and 57 per cent in humans giving it both veterinary and public health significance. Fruit bats (*Pteropus* spp.) commonly known as flying-foxes have been identified as the natural host of the virus. From 1994 to 2015 inclusive, there have been more than 70 sporadic confirmed cases of HeV infection in horses. All cases have occurred in Queensland and in north-east New South Wales. The research on the HeV has almost begun immediately after the first outbreak. Government organisations as well as scientists and academicians from a broad range of disciplines, including the animal health, environmental and social sciences, are working together to develop a 'One Health' approach that will help minimise the impact of HeV. This research uses a GIS-based spatial approach to research and determine the potential factors that can explain the dispersal of HeV outbreaks in the south east Queensland, Australia. The aim of this research is to identify the equine population 'at risk' and thus identifying the human population 'at risk' in the study area.

A preliminary spatial analysis examined the relationship between the Hendra disease outbreaks and the roosting sites of flying foxes in the study area. There are four main roosting site categories which are permanent (continuous or seasonal use), temporary (occupied or unoccupied), abandoned and destroyed. This analysis showed a strong relationship between the outbreak events and the existence of temporary and seasonal flying fox roosting sites within a 10 kms range. But very few disease outbreak incidents have a permanent roosting site in their range. This provided a strong case for further study into the seasonal behaviour of flying foxes, particularly in breeding season. This analysis revealed that variables such as species and their foraging range, breeding time, equine data, and environment aspects such as types of vegetation and seasonal changes could provide suitable factors for the determination of potential factors that can explain the dispersal of HeV outbreaks in the study area.

Based on the preliminary results, a further analysis was done on the roosting sites by considering factors such as the species of flying foxes, foraging range and pregnancy period. Global Moran's I method (inverse distance conceptualisation) was used to identify the presence of significant spatial clustering of the three flying fox species at various foraging ranges (10, 20, 30, 40 and 50 kms) in the study area. Global Moran's I revealed significant clustering of *P. alecto* and *P. scapulatus* species. The analysis of *P. alecto* species showed significant clustering at all foraging range intervals with high occurrence at 50 kms, which is their maximum foraging range. The results of *P. scapulatus* species showed maximum significant clustering occurring at 10 kms range. Kernel density estimation (KDE technique) analysis helped in establishing a strong relationship between *P. alecto* and *P. scapulatus* species density and the outbreak events in the study area and revealed the density hotspots of these species. Buffer analysis established an initial relationship between *P. alecto* and *P. poliocephalus* species birth periods and the outbreak incidents.

The ordinary least squares (OLS) regression analysis was carried out using the 'incident rate' as a dependent variable and black flying foxes, grey-headed flying foxes and pregnancy period as independent variables. This model has a statistically significant heteroscedasticity ($p < 0.05$) which suggests the use of Robust P to determine the coefficient significance for consideration. Goodness-of-fit measure indicated a model performance of 0.7. Ordinary least squares (OLS) regression identified *P. poliocephalus* species as statistically significant at a global context across the study area. The variance inflation factor (VIF) values indicated no redundancy among the variables. Moran's I test (Index = -0.02, $P = 0.8$) indicated no significant clustering among the residuals. An exploratory method approach was exercised to calibrate the model for local regression (GWR), which used the most significant exploratory variables that could explain the trends of dispersion of HeV in the study area. Geographically weighted regression (GWR) analysis performed to study the local spatial variations of the explanatory variables in the study area identified *P. alecto* and *P. poliocephalus* species as having a significant positive relationship in most of the regions. 'Pregnancy/Birth period' variable exhibited a significant negative relationship to the HeV incidents in the study area. The goodness-of-fit measure indicated an improvement from 0.7 (global model) to 0.8. Moran's I test (Index = -0.02, $P = 0.9$) indicated no significant clustering among the

residuals. The spatial variability of the local parameter estimates of each variable in the GWR model has been tested and a significant spatial variability was present in the variables.

An in-depth analysis was carried out to determine the correlation between food source vegetation and the flying foxes roosting sites in the study area. Using spatial analyst tools, the major vegetation subgroups (MVS) present within 20 kms range of *P. alecto* and *P. poliocephalus* roosting sites were identified. The identification of abundance of food sources for individual species within their minimum foraging range indicated a strong correlation between their site locations and the vegetation subgroups present. A 10 kms range vegetation study on the incident locations identified the presence of 'food sources' of both species. The clustering of the food resource vegetation present near the incidence was studied using Getis-Ord General G Statistic method, which indicated statistically high clustering with 99% confidence level at 3 kms distance threshold. A 10 kms range vegetation study on the equine properties in the study area identified the food source vegetation of both significant species. The clustering of the food source vegetation present near the equine properties was studied using high/low clustering/Getis-Ord General G Statistic method, which indicated statistically significant high clustering at 3, 5 and 10 kms distance thresholds. The vegetation analysis revealed a strong correlation between the roosting sites, food source vegetation and the equine properties.

Based on the above analysis, three prediction models were produced to identify the equine population 'at risk' in the study area. These models were based on the presence of the significant species identified in the GWR model and the clustering of their food source vegetation in statistically significant high clusters within 20 kms from the equine properties. Flowering season of the food source vegetation was considered as an additional risk factor. These models have successfully identified the equine population 'at risk'. The risk percentage of a probable outbreak event varies for each equine property depending on their exact location and their contributing factors. The prediction model(s) is an effective tool to identify the potential population (both equine and human) 'at risk', which can assist with Health Service Planning, policy implications, decision making and ongoing disease surveillance. This research successfully established the correlation between the HeV outbreak

events, flying fox species and their roosting sites, food source vegetation and seasons spatially. The factors influencing the dispersal of HeV outbreak events in the study area were understood. This study reveals the capability of GIS-based surveillance system to issue early warnings and precautionary measures to the identified population 'at risk'. This research also makes evidence based practice of disease mitigation, planning and prevention and control strategies for HeV achievable.

Certification of Thesis

This thesis is entirely the work of *Jahnavi Burnham* except where otherwise acknowledged. The work is original and has not previously been submitted for any other award, except where acknowledged.

Student and supervisors signatures of endorsement are held at USQ.

Dr Albert Kon-Fook Chong

Principal Supervisor

Dr Xiaoye Liu

Associate Supervisor

Dedication

To my loving family

Acknowledgements

I would like to thank Dr. Albert Chong, my principal supervisor, for his encouragement and ongoing assistance throughout the research journey. I am very grateful to my associate supervisor, Dr. Xiaoye Liu, for her support and suggestions on the research. I am very grateful for my supervisory team who have provided me excellent guidance to work enthusiastically and develop critical thinking abilities. I am extremely thankful to them for their invaluable suggestions and constant encouragement. Special thanks to Dr. Antony Moore from University of Otago, New Zealand for providing a great feedback on the research and providing invaluable guidance.

I would like to thank my colleagues and friends in the university, work place and my personal life for their sincere and ongoing support. I would like to give special thanks to Ms. Paulina Lee for her selfless feedback and suggestions on my research and reports. I would like to give my supreme thanks to my beloved husband, my children and my family members for their years of lasting support, encouragement and love.

I gratefully acknowledge the funding received towards my PhD from the Commonwealth of Australia through Research Training Scheme (RTS). I acknowledge the Queensland Centre for Emerging Infectious Diseases, Biosecurity Queensland - Department of Agriculture, Fisheries and Forestry for their data support in the research. I would like to thank Mr. Craig Smith, senior scientist from Biosecurity Queensland for his help in processing the data sharing agreement with the department. I am grateful to the Department of Environment and Heritage Protection, Queensland for their data contribution in this research. Finally, there are many people I would like to thank who made this thesis possible. I could not name each person who encouraged, assisted and supported me in this research and personal life. I would like to express my gratitude to them. This research would not have been achievable without them.

Associated Publications

Journals

Burnham, J and Chong, AK (2016) 'Factors Explaining the Dispersal of HeV Disease in South-East Queensland', *Geocarto International*, pp 1-16. DOI: 10.1080/10106049.2016.1161080

Burnham, J, Chong, AK, Liu, X and Moore, A (2015) 'Preliminary spatial analysis of Hendra disease outbreaks in South East Queensland', *The Globe*, Vol 76, pp 39-45.

Refereed Conference Proceedings

Burnham, J, Chong, AK, Liu, X and Moore, A (2014) 'Preliminary spatial analysis of Hendra disease outbreaks in South East Queensland', in the proceedings of The seventh National Cartographic Conference GeoCart'2014, 42nd ANZMapS Conference and the 3rd ICA Symposium on Cartography for Australasia and Oceania, The University of Auckland.

Burnham, J and Chong, AK (2016) 'An Investigation of the Food Sources and Roosting Sites as Potential Factors of HeV Dispersion in South East Queensland, Australia', International conference on GIS and Geomatics Engineering 2016 (ICGGE'16), (In progress to be published in the 'International Journal of Applied Engineering Research (IJAER)' SCOPUS ISSN no 0973-4562).

Burnham, J and Chong, AK (2016) 'Examining the Spatial Relationship between Equine Population and Food Source Vegetation of Flying-foxes in South East Queensland, Australia', in the proceedings of The 8th National Cartographic Conference, GeoCart'2016, and the 4th ICA Regional Symposium on Cartography for Australasia and Oceania.

Other Publications during the Candidature

Burnham, J (2014) 'Crime analysis mapping in the UK: a GIS analysis of burglaries in Leicestershire', in the proceedings of The seventh National Cartographic Conference GeoCart'2014, 42nd ANZMapS Conference and the 3rd ICA Symposium on Cartography for Australasia and Oceania, The University of Auckland.

Table of Contents

Abstract	II
Acknowledgements	VIII
Associated Publications	IX
List of Abbreviations	XIII
List of Tables	XIV
List of Figures	XVI

Chapter 1 – Introduction

1.1 Overview	1
1.2 Problem Statement and Research Gap	4
1.3 Research Aim and Questions	5
1.4 Research Objectives	6
1.5 Scope of the Research	7
1.6 Significance of the Research	8
1.7 Limitations of the Research	9
1.8 Thesis Organization	9

Chapter 2 – Literature Review

2.1 HeV	11
2.1.1 Introduction	11
2.1.2 Overview	11
2.1.3 HeV Biology, Distribution, Transmission and Other Influential Factors	14
2.1.4 HeV Research	21
2.1.5 Summary	26
2.2 Flying Foxes	27
2.2.1 Introduction	27
2.2.2 Overview	27
2.2.3 Flying Fox Ecology, Foraging Distances, Food Resources & Behaviours	29

2.2.4 Flying Foxes Research and Virus Prevalence	38
2.2.5 Summary	43
2.3 Spatial Epidemiology	43
2.3.1 Introduction	43
2.3.2 Overview	44
2.3.3 Disease Mapping	48
2.3.4 Spatial Analysis	51
2.3.5 Exploratory Data Analysis and Visualization	54
2.3.6 Spatial Autocorrelation	61
2.3.7 Spatial Data Modelling	65
2.3.8 Regression Analysis	66
2.3.9 Geographical Information Systems (GIS) in Epidemiology	71
2.3.10 Summary	76

Chapter 3 – Methodology

3.1 Introduction	78
3.2 Study Area	78
3.3 Data Collection, Processing and Integration	81
3.3.1 Data Collection	81
3.3.2 Data Processing and Integration	84
3.4 Flying Fox Roosting Site Visits	92
3.5 Spatial Analyses Methods	103
3.5.1 Buffer Analysis	103
3.5.2 Spatial Analyst Tools	106
3.5.3 Spatial Autocorrelation	108
3.5.4 Kernel Density	111
3.5.5 High/low clustering	113
3.6 Regression Analysis	116
3.6.1 Ordinary Least Squares (OLS) Regression	119
3.6.2 Geographically Weighted Regression (GWR)	121
3.6.3 Model Calibration for Regression Analysis	124
3.7 Methodology Flowchart	127
3.8 Summary	128

Chapter 4 – Analysis and Results

4.1 Introduction	129
4.2 Preliminary Spatial Analysis of HeV Outbreaks and the Roosting Sites (Hypothesis 1)	129
4.3 Factors Explaining the Dispersal of the HeV Disease (Hypothesis 2)	134
4.3.1 Measuring Spatial Autocorrelation (Global Moran’s I) of the Flying Fox Species	134
4.3.2 Examining and Establishing the Primary Relationship(s) between the Individual species Distribution, Incidents and Birth Period(s)	136
4.3.3 Regression Modelling	144
4.3.4 Ordinary Least Squares (OLS) Analysis	148
4.3.5 Geographically Weighted Regression (GWR) Analysis	152
4.4 Food Source Vegetation Analysis (Hypothesis 3)	158
4.4.1 An Investigation of the Food Sources and Roosting Sites as Potential Factors of HeV Dispersion	158
4.4.2 Examining the Spatial Relationship between the Equine Population and Food Source Vegetation of the Flying Foxes	179
4.5 Models to Identify Population ‘at risk’ (Hypothesis 4)	183
4.5.1 Model 1	183
4.5.2 Model 2	186
4.5.3 Model 3	189
4.6 Flowchart of the Results	191
4.7 Summary	192
Chapter 5 – Discussion	196
Chapter 6 – Conclusion	205
References	208

Appendices

Appendix-1 Data and Statistics	233
Appendix-2 Regression Model Calibration Results	254
Appendix-3 Spatial Autocorrelation and Regression Analysis	263
Appendix-4 Food Source Vegetation Analysis	276
Appendix-5 Abstracts of the Associated Publications	294

List of Abbreviations

AAHL	Australian Animal Health Laboratory
AAW	Australian Animal Welfare
AICc	Akaike Information Criterion
AURIN	Australia's urban intelligence network
AVA	Australian Veterinary Association
CDC	Centers for Disease Control and Prevention
CDNA	Communicable Diseases Network Australia
CFSPH	Center for Food Security and Public Health
CSF	Cerebrospinal Fluid
CSIRO Organization	Commonwealth Scientific and Industrial Research Organization
CSR	Complete Spatial Randomness
CV	Cross Validation
DAF	Department of Agriculture and Fisheries
DEPI	Department of Environment and Primary Industries
DILGP	Department of Infrastructure, Local Government and Planning
DoE	Department of Environment
DPI	Department of Primary Industries
EDA	Exploratory Data Analysis
EHP	Department of Environment and Heritage Protection
EPBC	Environmental Protection and Biodiversity Conservation Act
ESDA	Exploratory Spatial Data Analysis
ESRI	Environmental Systems Research Institute
GDA	Geocentric Datum of Australia
GIS	Geographical Information System
GWR	Geographically Weighted Regression
HeV	HeV
IUCN	International Union for Conservation of Nature
KDE	Kernel Density Estimation
MAUP	Modifiable Areal Unit Problem
MVG	Major Vegetation Groups
MVS	Major Vegetation Sub-groups
NERP	National Environment Research Programme
NFFMP	National Flying Fox Monitoring Programme
NPDO	National Pest and Disease Outbreaks
NSW	New South Wales
OLS	Ordinary Least-Squares Regression
QLD	Queensland
SEQ	South East Queensland
VIC	Victoria
VIF	Variance Inflation Factor
WHO	World Health Organization

List of Tables

Table 3.1: Summary of the major data sets obtained	82
Table 3.2: HeV outbreak incidents considered in the study	83
Table 3.3: Flying fox roosting sites status description	86
Table 3.4: The syntax of the buffer analysis in ArcGIS	104
Table 3.5: Summary of the tools in the Extraction Toolset – Spatial Analyst	107
Table 3.6: Syntax of the Spatial Autocorrelation tool in ArcGIS	109
Table 3.7: Syntax of the Kernel Density tool in ArcGIS	112
Table 3.8: Syntax of the High/low Clustering tool in ArcGIS	114
Table 3.9: The Difference in the interpretation of High/Low Clustering and Spatial Autocorrelation tools	115
Table 3.10: Summary of the issues in the modelling of Regression Analyses	117
Table 3.11 Summary of the syntax of the OLS regression technique	120
Table 3.12: Summary of the syntax of the GWR regression technique	122
Table 3.13 Model calibrated using the GWR technique	126
Table 4.1: The Percentage of flying fox roosting sites in each category	130
Table 4.2: The results of the Spatial Autocorrelation of the Flying Fox species at various foraging ranges	135
Table 4.3: Moran’s I results of the significant models	148
Table 4.4: Summary of OLS results	149
Table 4.5: Summary of GWR regression model results	153
Table 4.6: Major vegetation groups on the black flying fox roosting sites in the study area	159
Table 4.7: Major vegetation groups on the black Flying fox roosting sites	161
Table 4.8: List of black flying fox food source vegetation and its count	164
Table 4.9: Summary of the cluster analysis results of black flying foxes food source vegetation	165
Table 4.10: List of major vegetation groups on the grey-headed flying fox roosting sites in the study area	167
Table 4.11: List of major vegetation subgroups on the grey-headed flying fox roosting sites in the study area	168

Table 4.12: List of grey-headed flying fox food source vegetation and its count in the study area	171
Table 4.13: Summary of the cluster analysis results of grey-headed flying foxes food source vegetation	172
Table 4.14: List of major vegetation groups on the HeV outbreak sites in the study area	174
Table 4.15: List of major vegetation subgroups on the HeV outbreak sites in the study area	174
Table 4.16: List of flying fox food source vegetation and its count near the outbreak events in the study area	177
Table 4.17: Summary of the cluster analysis results of food source vegetation near the outbreak events	178
Table 4.18: List of flying fox food source vegetation and its count near the outbreak events in the study area	181
Table 4.17: Summary of the cluster analysis results of food source vegetation near the equine properties	183
Table 4.18: Cluster analysis results of black flying foxes food source vegetation near the equine population ‘at risk’	185
Table 4.19: Cluster analysis results of grey-headed flying Foxes food source vegetation near the equine population ‘at risk’	188
Table A1.1: List of HeV incidents	233
Table A1.2: List of permanent continuous use roosting sites in the study area	235
Table A1.3: List of permanent seasonal use roosting sites in the study area	236
Table A1.4: List of temporary occupied roosting sites in the study area	238
Table A1.5: List of temporary unoccupied roosting sites in the study area	240
Table A1.6: List of abandoned roosting sites in the study area	242
Table A1.7: List of destroyed roosting sites in the study area	243
Table A1.8: List of MVG in the study area	246
Table A1.9: List of MVS in the study area	247
Table A1.10: Statistics calculated in the study of HeV Outbreaks	248
Table A3.1: Significantly positive estimates of black flying foxes	269
Table A3.2: Significantly positive estimates of grey-headed flying foxes	271
Table A3.3: Significantly negative estimates of grey-headed flying foxes	273
Table A3.4: Significantly negative estimates of pregnancy/birth period	274

List of Figures

Figure 2.1: HeV outbreak events as of July, 2013	13
Figure 2.2: Electron micrograph of HeV	15
Figure 2.3: Henipavirus outbreaks and Pteropus distribution map	16
Figure 2.4: Temporal pattern of the HeV outbreaks	20
Figure 2.5: Types of flying foxes that occur in Australia	28
Figure 2.6: Flying fox species distribution map of Australia	29
Figure 2.7: Original map of Cholera cases by John Snow	49
Figure 2.8: Kernel estimation of a point pattern	56
Figure 2.9: Estimation of A K function	58
Figure 3.1: Map of Queensland with an inset map showing SEQ region	79
Figure 3.2: Map of the study area and the local councils in the region	81
Figure 3.3: GIS database creation workflow	83
Figure 3.4: HeV outbreak events in the study area	85
Figure 3.5: Flying fox roosting sites by species in the study area	87
Figure 3.6: Flying fox roosting site statuses in the study area	87
Figure 3.7: Registered equine properties in the study area	88
Figure 3.8: Registered equine properties sample	89
Figure 3.9: MVG and MVS in the study area	90
Figure 3.10: Flying fox colony location - site 1	93
Figure 3.11: Loders Creek flying fox colony statistics	94
Figure 3.12: Flying foxes in Loders Creek	95
Figure 3.13: Loders Creek flying fox colony view	95
Figure 3.14: A closer view of the flying foxes in the Loders Creek colony	96
Figure 3.15: Cascades Gardens flying fox colony statistics	98
Figure 3.16: A view of flying foxes in the Cascades Gardens colony	99
Figure 3.17: Flying foxes spotted in dense vegetation at Cascades Gardens	100
Figure 3.18: Vegetation at the Cascades Gardens flying fox colony	101
Figure 3.19: Water catchment near the Cascades Gardens colony	102
Figure 3.20: Native Fruits at the Cascades Gardens colony	102
Figure 3.21: Flow chart of the methodology	127
Figure 4.1: A 20 kms radius buffer of the outbreak incidents	131

Figure 4.2: A 10 kms buffer of the incidents with respect to the temporary and permanent seasonal roosting sites	132
Figure 4.3: A 10 kms buffer of the incidents with respect to the permanent continuous roosting sites	133
Figure 4.4(a): KDE analysis of black flying foxes in the study area	137
Figure 4.4(b): KDE analysis of grey-headed flying foxes in the study area	138
Figure 4.4(c): KDE analysis of little red flying foxes in the study area	139
Figure 4.5: A 20 Kms range study of the incidents	141
Figure 4.6 (a): Birth period study of the black flying foxes	142
Figure 4.6 (b): Birth period study of the grey-headed flying foxes	143
Figure 4.6 (c): Birth period study of the little red flying foxes	144
Figure 4.7: Scatter plot matrix of the model variables	145
Figure 4.8: Graph of the AIC values of all models in Regression Modelling	146
Figure 4.9: Spatial variability test for significant model 1 using GWR4.0	147
Figure 4.10: Spatial variability test for significant model 2 using GWR4.0	147
Figure 4.11: Spatial variability test for significant model 2 using GWR4.0	147
Figure 4.12: OLS regression residuals map	150
Figure 4.13: OLS regression diagnostics	151
Figure 4.14: The graph of the OLS regression residuals	151
Figure 4.15: GWR model residuals map	153
Figure 4.16 (a): Local estimates of the back flying foxes in the study area	154
Figure 4.16 (b): Local estimates of the grey-headed flying foxes	155
Figure 4.16 (c): Local estimates of the pregnancy period variable	156
Figure 4.17: Local R-Squared values of the GWR model across the study area	157
Figure 4.18: Black flying fox roosting sites in the study area	159
Figure 4.19: Major vegetation subgroups within 20 kilometers range of the black flying fox roosting sites	162
Figure 4.20: Identification of food resources within 20 kms range of the black flying fox roosting sites	163
Figure 4.21: Grey-headed flying fox roosting sites in the study area	166
Figure 4.22: Major vegetation subgroups within 20 kms range of the grey-headed flying fox roosting sites	169
Figure 4.23: Identification of food resources within 20 kms range of the grey-headed flying fox roosting sites	170

Figure 4.24: HeV outbreak events with MVS in the study area	173
Figure 4.25: Major vegetation subgroups within 10 kms range of the HeV outbreak sites	175
Figure 4.26: Identification of flying fox food resources within 10 kms range of the HeV outbreak sites	176
Figure 4.27: Major vegetation subgroups within 10 kilometers range of the equine properties	180
Figure 4.28: Identification of flying fox food resources within 10 kms range of the equine properties	181
Figure 4.29: Equine population ‘at risk’ in the study area based on model 1	184
Figure 4.30: Equine population ‘at risk’ based on model 2	187
Figure 4.31: Equine population ‘at risk’ in the study area based on model 3	190
Figure 4.32: Summary of the results	191
Figure A1.1: Full legend of MVG	244
Figure A1.2: Full legend of MVS	245
Figure A2.1: GWR result of the significant model 1 using ArcGIS	254
Figure A2.2: GWR result of the significant model 1 using GWR4.0	255
Figure A2.3: Spatial Autocorrelation test of significant model 1 residuals	256
Figure A2.4: GWR result of the significant model 2 using ArcGIS	257
Figure A2.5: GWR result of the significant model 2 using GWR4.0	258
Figure A2.6: Spatial Autocorrelation test of significant model 2 residuals	259
Figure A2.7: GWR result of the final model using ArcGIS	260
Figure A2.8: GWR result of the final model using GWR4.0	261
Figure A2.9: Spatial Autocorrelation test of the final model residuals	262
Figure A3.1: Spatial Autocorrelation report of the black flying foxes at their minimum foraging range	263
Figure A3.2: Spatial Autocorrelation report of the grey-headed flying foxes at their minimum foraging range	264
Figure A3.3: Spatial Autocorrelation report of the little red flying foxes at their minimum foraging range	265
Figure A3.4: Summary of the OLS results	266
Figure A3.5: The variable distributions and relationships of the OLS model	266
Figure A3.6: The histogram of the OLS model’s standard residuals	267
Figure A3.7: Spatial Autocorrelation report of the OLS standard residuals	268

Figure A4.1: Legend of the MVS identified within 20 kms range of the black flying fox roosting sites in the study area	276
Figure A4.2 (a): High/Low Clustering report of the food source vegetation of black flying foxes at 3 kms	277
Figure A4.2 (b): High/Low Clustering report of the food source vegetation of black flying foxes at 5 kms	277
Figure A4.2 (c): High/Low Clustering report of the food source vegetation of black flying foxes at 10 kms	278
Figure A4.3: Legend of the MVS identified within 20 kms range of the grey-headed flying fox roosting sites in the study area	279
Figure A4.4 (a): High/Low Clustering report of the food source vegetation of grey-headed flying foxes at 3 kms	280
Figure A4.4 (b): High/Low Clustering report of the food source vegetation of grey-headed flying foxes at 5 kms	280
Figure A4.4 (c): High/Low Clustering report of the food source vegetation of grey-headed flying foxes at 10 kms	281
Figure A4.5: Legend of the MVS identified within 10 kms range of the HeV incidents in the study area	282
Figure A4.6 (a): High/Low Clustering report of the flying foxes food source vegetation within 10 kms incident range at 3 kms	283
Figure A4.6 (b): High/Low Clustering report of the flying foxes food source vegetation within 10 kms incident range at 4 kms	283
Figure A4.6 (c): High/Low Clustering report of the flying foxes food source vegetation within 10 kms incident range at 5 kms	284
Figure A4.6 (d): High/Low Clustering report of the flying foxes food source vegetation within 10 kms incident range at 10 kms	284
Figure A4.7: Legend of the MVS identified within 10 kms range of the registered equine properties in the study area	285
Figure A4.8 (a): High/Low Clustering report of the flying foxes food source vegetation within 10 kilometers range of equine properties at 3 kms	286
Figure A4.8 (b): High/Low Clustering report of the flying foxes food source vegetation within 10 kms range of equine properties at 5 kms	286
Figure A4.8 (c): High/Low Clustering report of the flying foxes food source vegetation within 10 kms range of equine properties at 10 kms	287

Figure A4.9 (a): High/Low Clustering report of the black flying foxes food source vegetation near the equine Properties ‘at risk’ at 3 kms	288
Figure A4.9 (b): High/Low Clustering report of the black flying foxes food source vegetation near the equine properties ‘at risk’ at 5 kms	288
Figure A4.9 (c): High/Low Clustering report of the black flying foxes food source Vegetation near the equine properties ‘at risk’ at 10 kms	289
Figure A4.9 (d): High/Low Clustering report of the black flying foxes food source Vegetation near the equine properties ‘at risk’ at 15 kms	289
Figure A4.9 (e): High/Low Clustering report of the black flying foxes food source Vegetation near the equine properties ‘at risk’ at 20 kms	290
Figure A4.10 (a): High/Low Clustering report of the grey-headed flying foxes food source vegetation near the equine properties ‘at risk’ at 3 kms	291
Figure A4.10 (b): High/Low Clustering report of the grey-headed flying foxes food source vegetation near the equine properties ‘at risk’ at 5 kms	291
Figure A4.10 (c): High/Low Clustering report of the grey-headed flying foxes food source vegetation near the equine properties ‘at risk’ at 10 kms	292
Figure A4.10 (d): High/Low Clustering report of the grey-headed flying foxes food source vegetation near the equine properties ‘at risk’ at 15 kms	292
Figure A4.10 (e): High/Low Clustering report of the grey-headed flying foxes food source vegetation near the equine properties ‘at risk’ at 20 kms	293

1. Chapter One – Introduction

1.1 Overview

Spatial epidemiology involves the description and analysis of geographically indexed health data with respect to demographic, environmental, behavioural, socio-economic, genetic, and infectious risk factors (Elliot et al 2004). It is a part of geographic analyses dating back to the 1800s when maps of disease rates in different countries began to emerge to characterize the spread and possible causes of outbreaks of infectious diseases such as yellow fever and cholera (Walter 2000). In recent decades, it grew in complexity, sophistication, and utility. The practice of ecologic studies is extended by spatial epidemiology that use explanations of the distribution of diseases in different places to better understand the ecology of disease (Doll 1980, Keys 1980). Haining (2003) described spatial epidemiology as the analysis of spatial and a space-time distribution of disease data which enables the identification of populations with high relative risks for particular diseases and may help to isolate the possible casual factors for subsequent analysis by individual study level designs.

Epidemiology can be defined as a scientific study of a disease, which includes analysing the occurrence and distribution of the disease and its associated factors (Medical Dictionary). The ability of GIS to integrate and manipulate complex data has emerged it as a powerful tool in epidemiological studies. The traditional epidemiological studies such as cohort or case control studies enable us to identify excess disease rates or trends and perform further analysis for hypothesis testing (Seng et al 2005). Use of GIS technology in spatial epidemiological and public health studies gained momentum after researchers started using it for more than visual representations i.e. maps. GIS in spatial epidemiology has been tremendous in understanding diseases in a different dimension. With the assistance of this powerful tool, the disease clusters could be identified and other influencing factors such as environmental, socio-economic and climatic could be linked to diseases. While

geographical visualization serves the need to reveal the spatial patterns, the statistical awareness in GIS determines the significance of these patterns.

HeV (HeV) is a rare zoonotic disease and was first reported in a suburb of Hendra, Brisbane, Australia in the year 1994. This outbreak of the disease resulted in the death of 13 horses and the trainer. Fruit bats commonly known as flying foxes (*Pteropus spp.*) were consequently identified as the natural reservoirs of HeV (Halpin et al 2000). The virus was initially named as *Equine Morbillivirus*, after further genetic analysis, it was placed in a new genus within the family of *Paramyxiviridae*, which was found more appropriate; and hence renamed as 'HeV' where the first outbreak occurred (CSIRO 2011, Field et al 2007). In the year 2011, Australia witnessed an unprecedented spike in the number of HeV cases in horses in both Queensland and New South Wales (Hume et al. 2012). The cases included 18 outbreaks and 24 cases in horses reported; and also with a dog tested positive for the first time (DAFF 2014). As of December 2012, there were 80 confirmed outbreak events including equine and human cases (Smith et al 2014). Between 1994 and July 2013 there have been 48 clusters of the disease in Australia which have resulted in four human deaths. The confirmed human cases stand at seven giving it a very high Case Fatality Rate (CFR) of 57 per cent. It has also caused the deaths of 90 horses. Since 2011 two dogs have become infected; and both were subsequently euthanized.

HeV outbreaks have only occurred in Australia so far, where the virus is endemic in flying foxes. Flying foxes are found throughout tropical and sub-tropical Asia and Australia and on islands of the Indian and western Pacific Oceans (DEPI VIC 2015). Seropositive flying foxes have been found from Darwin in North Central Australia to Melbourne in South Eastern Australia. Equine cases been reported from Eastern Australia, in the States of Queensland and New South Wales. Antibodies detected in flying foxes in Papua New Guinea might be caused by HeV or a related virus. Currently there is no evidence that HeV exists in other areas. However, henipaviruses or antibodies to these viruses have been detected in bats on several continents. Most of these viruses are poorly characterized (CFSPH 2015).

In horses, HeV is transmitted mainly by ingesting food or water contaminated with infected flying fox body fluids and excretions. The virus is then being passed onto humans who come into contact with infected horse's nasal discharge, blood, saliva or urine (AAW 2012). The studies show strong evidences that the disease is not bat-to-human transmissible and horses act as medium for disease transmission to humans. Horses to other species and bats to other species transmissions are however possible (Australian Biosecurity 2009). The mode of transmission and incubation period of HeV was documented by Communicable Diseases Network Australia (CDNA). The typical incubation period in horses appears to be 5-16 days. The prevalence of the HeV appears to be uncertain in flying fox populations but the reason behind this is not known.

Clinical signs of the humans presented with the infection include self-limiting influenza-like illness (two cases), influenza-like illness complicated by severe pneumonic illness contributing to death (one case), aseptic meningitis with apparent recovery, then death from encephalitis 13months later (one case), acute influenza-like illness followed by encephalitis and seroconversion, followed by recovery (one case) and death (two cases). In horses, the virus clearly targets the endothelial cells of blood vessels, with clinical signs dependent on the sequence in which organs are affected. Typical clinical signs include body temperature, increased heart rate, respiratory or neurological signs or a mix, frothy nasal mucus, sweating, balance difficulties and rapid deterioration (CDNA 2011 and BetterHealth Victoria 2014).

The powerful analytical modelling and mapping capabilities of GIS may serve as a good decision-support and decision-making tool for disease investigations, monitoring, modelling, predictions, preventions and resource allocations (Davenhall 2002). The availability of the data and the functionality of GIS will be a great advantage for this research, which concentrates on studying the HeV outbreaks from a spatial epidemiological prospective.

1.2 Problem Statement and Research Gap

Some of the transmissible diseases such as HeV are challenging to monitor through normal surveillance programs, as these diseases are affected by various external factors and the impact of these factors on them are likely to be very high. The biological and ecological researches for analysing these kinds of rare diseases might not be sufficient for disease surveillance and risk predictions in certain circumstances. Identification of a spill-over of any zoonotic virus involves one of the human, livestock or wildlife deaths with a certain degree of medical, emotional and economic misery. A research survey study conducted on the studies on HeV in the south western United States revealed that exploring the virus spreads in an epidemiological aspect with targeted study helped the public health officials in reducing the risk of infections by forecasting the locations and their future outbreak occurrence levels. These researches are categorised as cost-effective and long run theories (Calisher et al 2006).

Differences in modelling approaches, disease transmission intensity and data dimensions space-time would influence the analysis and could be a reason for a less accurate model for the disease surveillance (Seng et al 2005 and Cressie 2000). Using a precise set of spatial analysis and modelling techniques can make the predictions more reliable. An accurate modelling technique demands detailed understanding of the HeV such as its eco-biological factors, transmission and environmental factors that may affect the disease distribution. Studying the various factors and their relationship with the HeV outbreak events could assist in the understanding the disease dynamics. This would provide necessary information in developing a model that can explain the HeV dispersal in the study area.

In the case of rare disease outbreaks like HeV, GIS will be suitable as a tool to identify the main factors (geographical, environmental and other factors) of disease transmission, to use it as disease monitoring, to identify population at risk, prediction models and generate warning systems according to spatial distributions. GIS in public health research starts from epidemiologists using the traditional maps to observe the relationships between location, environment and diseases outbreaks. GIS

is well adopted by these types of researches varying from vector-borne diseases to lead hazards in the public health field for its analysis and display capabilities (Clarke et al 1996).

Many of the epidemiological and public health projects are GIS-based. GIS, especially in the last decade emerged as an innovative, important and even essential tool for some researches. As GIS involves a lot of interdisciplinary work, the appropriate methods remain as the important part of the research. Statistical work and models are crucial in a successful research involving GIS (Waller 1996). There is always a major gap in the current GIS-based researches, when it comes to model development and statistical analysis, which is yet to be, filled (Miranda et al 2013). The capability and reliability of GIS in spatial data handling, manipulation and analysis, and the accuracy and improvements in regression techniques makes GIS an appropriate technology to employ for HeV research. This study will concentrate on investigating, analysing, and visualizing HeV outbreaks in the study area using appropriate GIS techniques.

This research provides a framework to fill the existing need for HeV research and monitoring announced by the Queensland Government (Edmonston et al 2011). This research studies the correlation between the HeV outbreaks and the factors such as the flying fox species, roosting sites and their status, foraging range, pregnancy/birth period, seasonal changes, and the food source vegetation of the flying fox species. By considering the climatic, environmental, behavioural and other influential factors of the hosts, this research may explain the dispersal of the HeV outbreak events in the study area.

1.3 Research Aim and Questions

The overall aim of this research is to analyse the spatial patterns of the HeV cases, study the factors that may explain the HeV dispersal in the study area and identify the population ‘at risk’ using a prediction model by incorporating GIS techniques. Using the spatial analytical tools in GIS, this research will establish a relationship between the outbreak events and their influential factors such as species, foraging

range, pregnancy period, birth and lactation period, seasons and food source vegetation. A spatial epidemiological study of the HeV outbreaks will help answer the following set of questions:

- i) How the outbreak events are spatially distributed in the study area?
- ii) What is the correlation between the roosting sites and the outbreak events?
- iii) What are the factors that are influencing the disease transmission?
- iv) How can these factors explain the dispersal of the outbreak events in the study area?
- v) What is the correlation between the food source vegetation of flying foxes and the outbreak events?
- vi) How to identify population ‘at risk’?

This work attempts to fill in the requirement of a good GIS-based research to study the HeV outbreaks in the study area spatially and temporally. This research can provide the epidemiologist with an effective tool to identify the potential population (both equine and human) ‘at risk’ and thus helps in the formation of evidence-based disease mitigation strategies.

1.4 Research Objectives

In order to achieve the research aim, a list of objectives is stated below:

- i) Detailed study on the HeV Outbreak events and the reservoir hosts.
- ii) Research the relevant spatial analyses, modelling and mapping techniques that are best suited for spatial epidemiological study of the HeV outbreak events and the influential factors.
- iii) Develop a technique to integrate all the relevant data from various sources and format according to the requirements of the GIS software.
- iv) Calibrate a prediction model that could identify population ‘at risk’ in the study area.

The hypotheses to be addressed and tested in this research are as follows:

- i) **Hypothesis 1** - the HeV Outbreak events in the study area are correlated to the flying fox roosting sites.
- ii) **Hypothesis 2** – the crucial factors that could explain the HeV dispersal in the study area can be identified using an appropriate spatial modelling technique.
- iii) **Hypothesis 3** – the food source vegetation play an important role in the outbreak events.
- iv) **Hypothesis 4** – Based on the influential factors, it is possible to identify the population ‘at risk’ by formulating a prediction model.

1.5 Scope of the Research

This research concentrates on the spatial analyses, modelling and mapping of the HeV outbreak events in south east Queensland, Australia. The selection of the study area is dependent of the data resource available for the detailed research of the outbreak events. South East Queensland (SEQ) was classified as an interim Australian bioregion, which consists of 11 cities and regional councils (Queensland Government 2009). The Toowoomba city from the Toowoomba Regional Council, which is located in the SEQ, was excluded from the study due the data availability (Refer *Section 3.2*). HeV incident data was provided by the Queensland Department of Agriculture, Fisheries and Forestry (DAFF) under a data sharing agreement. For this study, a total of 11 equine related incidents that occurred from 1994 to 2011 in the study area were examined. The incident data is disclosed by its location (longitude and latitude coordinates) and date of occurrence.

The flying foxes spatial data set used in the study area is obtained from the Department of Environment and Heritage Protection, Queensland (EHP). The collection of the data is continuous and is updated every three months by EHP. The data contained abundance of spatial information such as the roosting site locations, total flying fox population at each site, type of occupancy and individual species population at each site. The data reveal the presence of three types of species - *P. alecto*, *P. poliocephalus* and *P. scapulatus* in the study region.

The Queensland vegetation data containing the major vegetation groups (MVG) and major vegetation subgroups (MVS) for the study were obtained from the Department of the Environment and Energy, Australia database. The datasets are National Vegetation Information System (NVIS) version 4.2. The major software's used this research are ESRI ArcGIS versions 10.2 and 10.5 and Geographically Weighted Regression version 4.0 (GWR4).

1.6 Significance of the Research

This study attempts to study the HeV outbreaks events from spatial epidemiological prospective. By studying the outbreak events spatially, this research can be a great support for evidence-based health service planning, policy implications, decision making and ongoing disease surveillance. GIS in epidemiology enables the researchers to isolate the high disease prevalence areas, identify the population at-risk, resource and budget allocations In the case of rare disease outbreaks like HeV, GIS is a perfect as a tool to identify the main causes (geographical, environmental and other factors) of outbreaks for disease monitoring. This study can help in developing prediction models and generating warning systems in the study area and furthermore, provide a good base for future research.

Some of the key points that indicate the significance of this research:

- i) Identifies any underlying spatial patterns of the outbreak events.
- ii) Reveal the correlation(s) between HeV outbreak events and its influential factors.
- iii) Helps in understanding the HeV dispersal in the study area.
- iv) Creates a model to identify population (both equine and human) 'at risk'.
- v) Generate early warnings with precautionary measures to the identified population 'at risk'.
- vi) Provides epidemiologists with an effective evidence-based planning system.
- vii) Assists in developing disease mitigation strategies.

HeV research was considered challenging and complicated and much remains to be learnt (Australian Biosecurity 2009). There was a need for further research to understand the spatial and temporal patterns of the virus for effective surveillance and management of the disease. The Queensland government announced a pressing need for current research on the spatial and temporal occurrences of the virus outbreaks and further study into ecological and environmental factors as causes of the disease (DAF 2015). This research used GIS as a crucial tool to determine the main factors (geographical, environmental and other factors) of HeV disease transmission.

1.7 Limitations of the Research

The main caveat of this study was the geographical location selected due to the availability of resources. The findings might vary when the dynamics of the HeV disease and the medium host were to be studied at a larger scale. The findings of this research were highly dependent of the data as the study was based on empirical data-driven analysis and hence limited by data accuracy. The flying fox species data was recorded manually, which might have some degree of error. One of the important factors of this research was; it was a spatial GIS-based approach to understand the HeV disease outbreak events, its transmission and the factors influencing the disease dispersal in the study area. This study was built on the research that have been published so far on the HeV, its biology, transmission and their reservoir host – flying foxes.

1.8 Thesis Organization

This thesis contains six chapters mainly addressing various spatial analyses, mapping and modelling techniques employed to study the HeV outbreak events spatially and temporally. These chapters are classified as follows:

- i) Chapter One is an introduction to the study.
- ii) Chapters Two consists of reviews of the published literature related to the research.

- iii) Chapters Three discusses the research methodology.
- iv) Chapter Four provides the analysis and results.
- v) Chapter Five and Six present discussion, conclusions and recommendations.

A brief structure of what each chapter contains is given below:

Chapter One gives an overview of the research topic. The problem statement, research aim, objectives, scope, significance and limitations of the research are summarised in this chapter. A number of key points that represent the significance of this study are listed in this chapter.

Chapter Two reviews the literature published in regards to the HeV biology, distribution, transmission and other influential factors. The flying fox ecology, foraging distances, food resources and behaviours were reviewed in this chapter. Spatial epidemiology, spatial analysis, disease mapping and GIS in epidemiology were also reviewed in this chapter.

Chapter Three presents the methodology of this research. The background of the study area, data collection, data integration and pre-processing and site visits are detailed in this chapter. The calibration of regression model for the study is discussed in this chapter. This chapter presents the modelling, mapping and analyses techniques employed for this research.

Chapter Four presents the analysis and results achieved from various spatial analyses and modelling techniques. The results are visualized using various maps where applicable in this chapter. The prediction model(s) are discussed in this chapter.

Chapter Five documents a detailed discussion of the results, summaries the main findings of the thesis, discusses the limitations of the research and suggests recommendations for future work.

Chapter Six concludes the thesis.

2. Chapter Two – Literature Review

2.1 HeV

2.1.1 Introduction

The section 2.1 in chapter 2 provides an outline of the HeV history and the academic research on its occurrence in Australia. An overview is provided in section 2.1.2 and section 2.1.3 provides a review of various aspects of HeV such as its biology, distribution, transmission, impact and influential factors of the virus to better understand the infection risk and disease dynamics. Section 2.1.4 covers the academic research on the HeV so far and a summary is provided in section 2.1.5.

2.1.2 Overview

HeV is an emerging zoonotic disease that was first identified in 1994 and has only been found in Australia. It can be transmitted to other horses, humans and dogs with a high fatality rate of >79 per cent in horses and 57 per cent in humans giving it both veterinary and public health significance. Fruit bats (*Pteropus* species), also known as flying foxes, are the only known natural reservoir (CDNA 2010). Human infections have occurred as a result of direct exposure to body substances from infected or dead horses. To date there has been no known transfer of HeV from person to person or from flying foxes to other animals apart from horses (AVA 2016). From 1994 to 2015 inclusive, there have been more than 70 sporadic confirmed cases of HeV infection in horses. All cases have occurred in Queensland and in north-east New South Wales (NPDO 2016).

An outbreak of acute respiratory disease occurred in a stable in September 1994 in the Brisbane suburb of Hendra, Queensland, Australia. Twenty one horses were infected with 14 fatalities (Hess et al 2011). The disease also spread to two people and one of them, a well-known racehorse trainer Mr Vic Rail, died following a severe influenza-like illness. The novel symptoms and rapid spread of the disease and its appearance in both horses and man brought together teams of scientists and veterinarians at the Commonwealth Scientific and Industrial Research Organisation's

(CSIRO) Australian Animal Health Laboratory (AAHL) and the Queensland Department of Primary Industry. All known exotic infectious diseases, such as African horse sickness, were excluded by tests at AAHL and within a month a new virus was isolated and diagnostic procedures to identify it were established (CSIRO 2016).

A novel equine virus belonging to the family *Paramyxoviridae* was isolated (Hess et al 2011). The virus was initially called *equine morbillivirus*, but later renamed “*HeV*” after the suburb where the outbreak occurred. Since the first outbreak there have been 12 clusters of HeV infection recorded in horses with seven people infected four of whom have died. A subsequent lethal outbreak at Mackay, Queensland in October 1995 claimed the life of a farmer. It was revealed that 13 months before his terminal illness (and a month after the first outbreak at Hendra) the farmer had assisted at the necropsy of two horses that had died on his property. Analysis of tissue samples from the horses retrospectively confirmed that they had been infected with HeV. This determined that the virus was able to cause both respiratory and encephalitic disease. A similar pattern of transmission from horse to man was responsible for the deaths of two Queensland veterinarians, in 2008 and 2009 (CSIRO 2016).

The occurrence of outbreaks at Hendra and Mackay occurred within a month of each other and it was concluded that the source of the virus (the so-called reservoir host) would either be capable of migrating the 600 miles between the two sites or be present at both sites. A search for the animal reservoir host for this newly described disease revealed that all four species of flying fox found in Australia could harbour the virus without ill effect. HeV itself was isolated from two species of flying foxes in the year 2000. Using experimentally infected flying foxes confirmed the absence of any clinical symptoms following infection with doses of virus that would be lethal for horses. Indeed some flying foxes shrugged off the infection without generating any detectable antibody. This is consistent with flying foxes being the natural host or reservoir of HeV (CSIRO 2016).

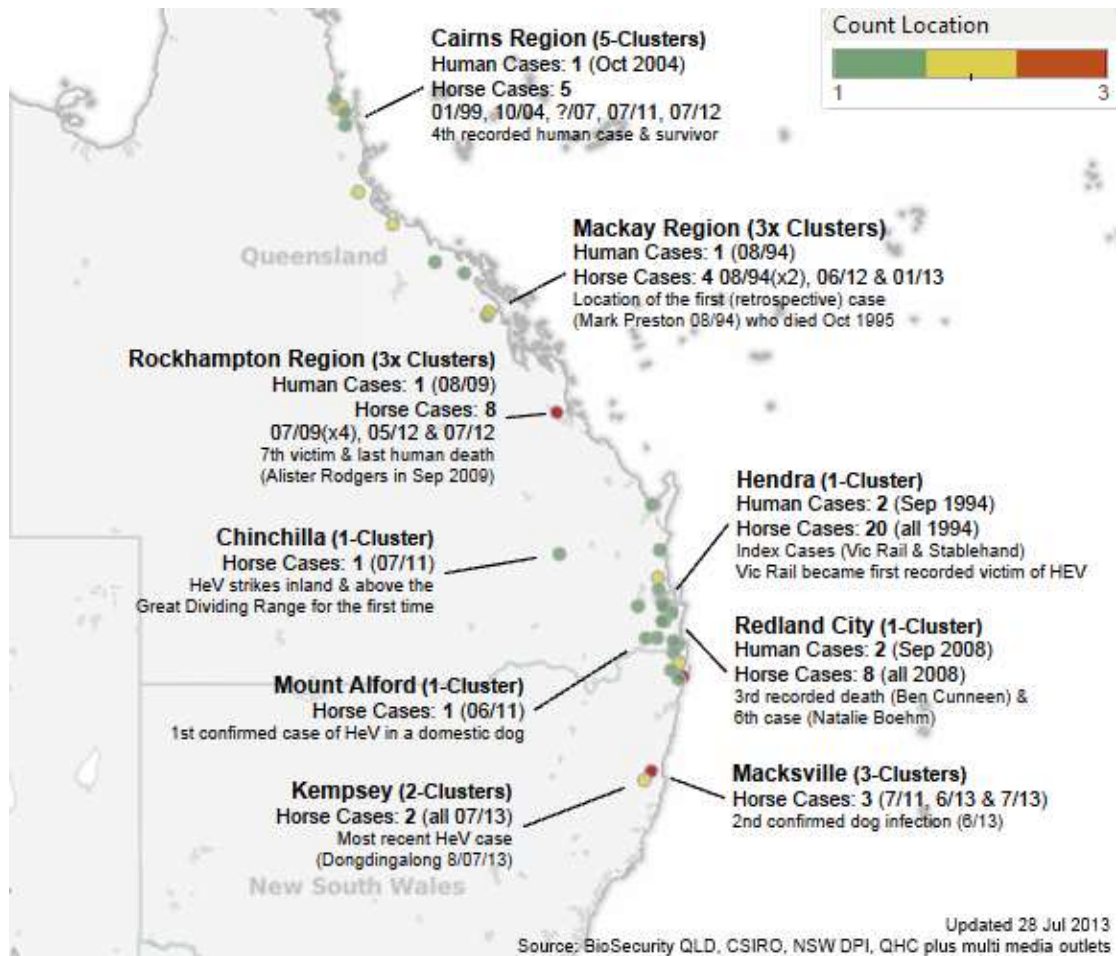


Figure 2.1: HeV outbreak events as of July, 2013 (Source: Random Analytics 2013).

Since 1994 to July 2013 there have been 48 clusters of the disease in Australia which have resulted in four human deaths. The confirmed human cases stand at seven giving it a very high Case Fatality Rate of 57 per cent. It has also caused the deaths of 90-horses. Since 2011 two dogs have become infected; and both were subsequently euthanized. Figure 2.1 shows the HeV outbreak events as of July, 2013. In 2011, the outbreaks spiked to record levels with 18 recorded clusters with deaths of 23 horses in a calendar year (eight in NSW and 10 in Queensland) and also the first euthanasia of an infected dog, which sparked a great deal of concern across the horse industry, as well as veterinary and public health sectors and with the public at large (AAW 2012, Random Analytics 2013, Thompson 2016 and CSIRO 2016).

2.1.3 HeV Biology, Distribution, Transmission and Other Influential Factors

2.1.3.1 Biology

HeV is a member of the family *Paramyxoviridae* and one of two virus species in the genus *Henipavirus* (the other being *Nipah virus*). HeV was first isolated in 1994 from specimens obtained during an outbreak of respiratory and neurologic disease in horses and humans in Hendra, a suburb of Brisbane, Australia. The tests that are used to diagnose HeV and Nipah virus include detection of antibody by ELISA (IgG and IgM), real time polymerase chain reaction (RT-PCR), and virus isolation attempts. In most countries, handling HeV needs to be done in high containment laboratories. Laboratory diagnosis of a patient with a clinical history of HeV or NV can be made during the acute and convalescent phase of the disease by using a combination of tests including detection of antibody in the serum or the cerebrospinal fluid (CSF), viral RNA detection (RT-PCR) in the serum, CSF, or throat swabs, and virus isolation from the CSF or throat swabs (CDC 2014).

Both viruses are predominant in overlapping populations from India to Australia. The emergence of HeV virus in Australia has raised a number of questions relating to their natural history (Field et al 2001). AAHL characterised the virus using a number of laboratory procedures and visualised the virus in affected horse and human tissues by electron microscope which confirmed that the virus was the causative agent of the outbreak.

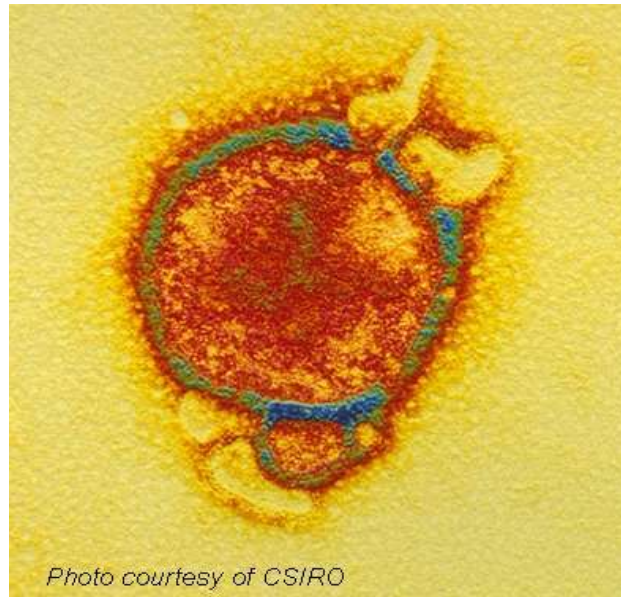


Figure 2.2: Electron micrograph of HeV (Source: CSIRO 2016).

Figure 2.2 shows us the typical HeV Cell in a slide of a cross section of a blood vessel taken from the lung of an infected horse. The multinucleated (giant) cells are situated on the lining of the blood vessel. These giant cells are caused by the action of the fusion protein of HeV. In the bottom panel a fluorescent stain has been used on the slide to highlight the virus, in yellow/green (CSIRO 2016).

The virus infects wide range of cells but primarily the endothelial cells, which form the thin, inside layer of blood vessels. Rapid molecular tests were developed to detect the virus with genome sequencing data. The available laboratories and epidemiological data were reviewed to obtain information of the animal(s) which may harbour the virus in nature. Flying foxes were targeted for further investigation as they fulfilled the criteria as a possible viral reservoir host. Flying foxes were present in the outbreak regions and they have the capability to move between the outbreaks locations. The hosts could have possibly had indirect contact with the horses during the outbreaks. In 1996, sampling of sick/injured flying foxes in temporary captivity showed that several species of Australian flying foxes had antibodies to HeV. All mainland *pteropoid* species – the black, grey headed, little red and spectacled flying foxes have antibodies to HeV. The flying foxes which were infected experimentally develop a *viraemia* – the virus that enters into blood stream. Flying foxes excreted the virus in their urine, faeces and saliva for about a week.

However, the flying foxes did not indicate any signs of illness like horses (Australian Biosecurity 2009).

2.1.3.2 Distribution

HeV infections have been seen only in Australia, where the virus is endemic in flying foxes. Seropositive flying foxes have been found from Darwin in north central Australia to Melbourne in south eastern Australia (CFSPH 2015). The HeV incidents have been reported from Cairns in northern Queensland down to Kempsey on the New South Wales Mid North Coast. East of the Great Dividing Range holds majority of the cases with one outbreak recorded west of the range in chinchilla, Queensland in 2011 (DPI NSW 2016). Figure 2.3 shows the overall distribution of the Henipavirus and Pteropus including HeV distribution in Australia, which is within the Pteropus home range.

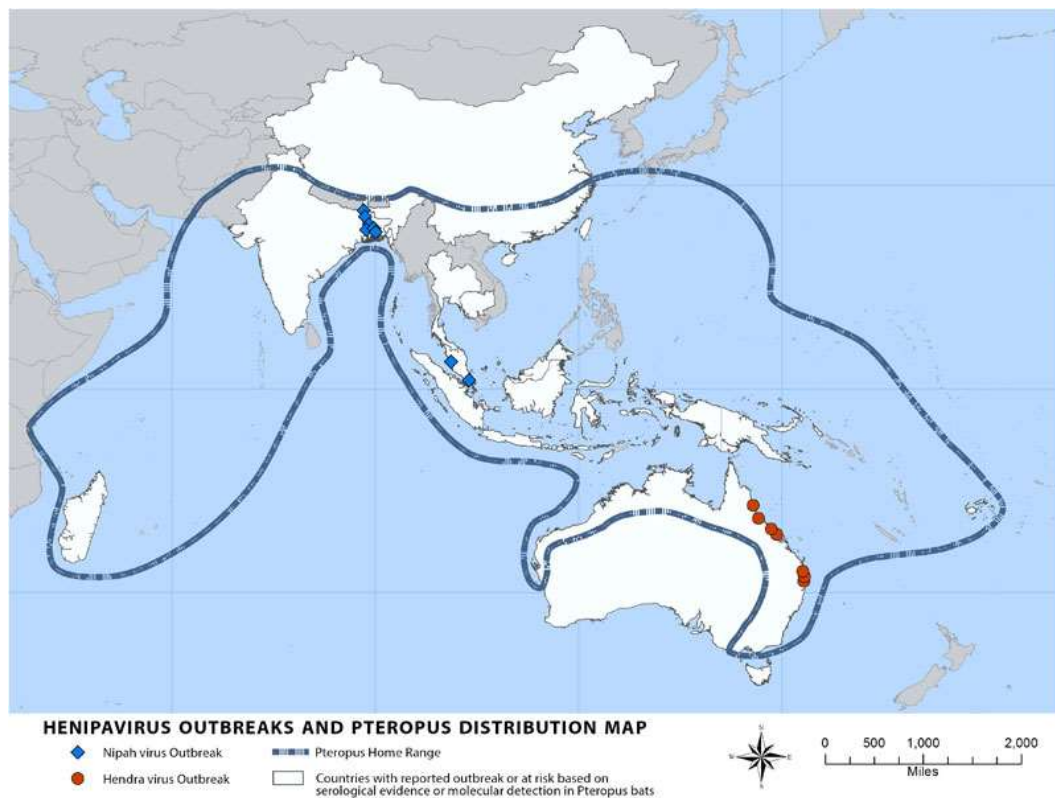


Figure 2.3: Henipavirus outbreaks and Pteropus distribution map (Source: CDC 2014).

2.1.3.3 Transmission

HeV is transmitted mainly by ingesting food or water contaminated with infected flying fox body fluids and excretions in horses. The virus can then be passed onto humans who come into close contact with infected horse's nasal discharge, blood, saliva or urine (AAW 2012). The studies show strong evidences that the disease is not bat-to-human transmissible and horses act as medium for disease transmission to humans. Horses to other species and bats to other species transmissions are however possible (Australian Biosecurity 2009).

The mode of transmission and incubation period of HeV is documented as below by Communicable Diseases Network Australia (CDNA 2010):

Mode of transmission

Bat-to-horse

The Spill-over from flying foxes to horses is rare (32 documented events from 1994 to October 2011, 9 in NSW and 23 in Queensland); possibly occurring through contamination of horse feed by infectious fluids from bats such as bat urine/reproductive products.

Horse-to-person

Seven human cases have been documented as of September 2011 and all of them had a high level of exposure to respiratory secretions and/or other body fluids of horses subsequently diagnosed with HeV infection. With the evidence available, it is highly likely that the mode of transmission is via substantial direct exposure of mucous membranes to respiratory secretions or blood from an infected horse. Indirect exposure to respiratory secretions or blood, and direct or indirect exposure to other body fluids, may also contribute to overall transmission risk. Airborne exposure is not supported by the current evidence as a significant mode of transmission.

Horse-to-horse

Transmission between horses is possible and has been more efficient in stabled situations, with spread between multiple horses occurring in all stabled situations to date – Hendra (1994), Redlands (2008) and Cawarral (2009), all in Queensland.

Bat-to-person

Current evidence does not suggest that this occurs. A study of 128 bat carers who have daily contact with bats and/or a history of bat bites, found no individuals with antibodies to HeV.

Person-to-person

Current evidence does not suggest that this occurs. A Serological testing in 169 health care worker contacts and four household contacts of the first three human cases found no individuals with antibodies to HeV. However it is suggested to avoid close contact with respiratory secretions and other body fluids of symptomatic human cases.

Person-to-horse

Current evidence does not suggest that this occurs. However it is desirable for suspected human cases to avoid close contact with horses until the diagnosis has been clarified.

Experimental

Other species like mice, rats, rabbits, chickens and dogs did not develop the disease having immunisation to the virus. Unlike the above, cats and guinea pigs were highly vulnerable but no cases have emerged so far. The cats that are experimentally infected with HeV resembled the lethal respiratory disease in humans and horses. This raised the possibility of cats transmitting the virus to horses but there has been no evidence in reality. The attempts to recreate transmission in cats-to-cats, cats-to-horses, horses-to-horses, horses-to-cats and bats-to-bats have been largely unsuccessful (Field et al 2001).

Other

A dog developed antibodies to HeV on a property with three infected horses in July 2011. There is no evidence that bat-to-dog or dog-to-person or dog-to-horse transmission occurs.

Incubation period which is defined as the time from exposure to the appearance of the first clinical signs of infection (Australian Biosecurity 2009) is as follows:

Humans

The incubation period in humans is between 5 and 21 days, however the evidence is limited.

Horses

The typical incubation period in horses appears to be 5-16 days.

Queensland department of health has stated that the people infected by HeV (both deceased and infected) have become unwell with influenza-like symptoms and encephalitis – an inflammation of the brain. The diagnosis can be made by blood and urine tests. In some cases, testing of nasal swabs, tissues samples and cerebrospinal fluid (CSF) is required. The infectious period - time during which an infected person can infect others in humans should be considered until their recovery. There is no specific treatment for HeV infection yet. Treatment is mainly supportive to help relieve symptoms and to reduce complications from the illness. It is suggested that people who are suspected to have the virus or have been in close contact with horses that might have the infection should be reviewed by an infectious diseases specialist, and may require hospital admission.

2.1.3.4 Other Influential Factors

The prevalence of the HeV appears to be uncertain in flying fox populations but the reason behind this is not known. Pregnancies, birthing period and/or lactation were associated with HeV infection in some studies, but not others. The influence of the above factors remains uncertain. The nutritional stress could also be influencing the infection fluctuations, while the environmental conditions such as temperature might influence the virus survival and transmission to horses. HeV infections in equine

population appear to be seasonal. Equine cases have mostly occurred in cooler months from May to October in subtropical areas, with a peak in July. In the northern tropics, the cases have been seen year around. The absence of any seropositive horses in two surveys, which tested approximately 4000 horses, suggested that infections were rare in horses. The infections appeared more regularly between 2006 and 2009, with two incidents reported each year, and unexpectedly high numbers of cases were reported in 2011 (18 incidents with 23 cases) and 2012-2013 (12 incidents between January 2012 and July 2013). The reason for the recent increase in cases seems to be unclear, although increased testing and recognition might play some role (CFSPH 2015). Figure 2.4 demonstrates the graph where the virus infections were higher during cooler months.

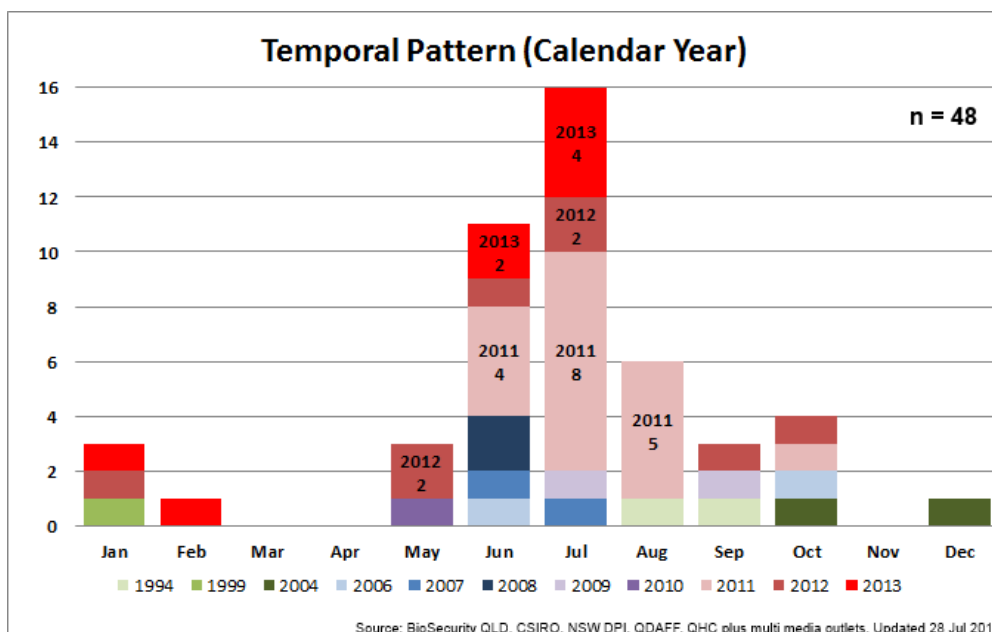


Figure 2.4: Temporal pattern of the HeV outbreaks (Source: Random Analytics 2013).

DPI NSW (2012) and QLD Horse Council (2012) made some recommendations for the horse owners to exercise some precautions in areas with flying foxes to help minimise the risk of their horses being infected. The recommendations are as follows:

- i) Do not place feed and water under trees.

- ii) Cover feed and water containers with a shelter so they cannot be contaminated from above.
- iii) Do not leave food lying about that could attract flying foxes, such as apples, carrots, or molasses.
- iv) Inspect paddocks regularly and identify trees that are flowering or fruiting,
- v) Remove horses from paddocks where fruiting or flowering trees have temporarily attracted flying foxes.
- vi) If the horse(s) cannot be removed from the paddock, erect temporary or permanent fencing to keep horses from grazing under trees.
- vii) If these measures are not practical, consider stabling horses, or removing them from the paddock before dusk and overnight, when flying foxes are most active.
- viii) Clean up any fruit debris under the trees before horses are returned to the paddock.

Apart from the above recommendations, the horse owners can watch for some signs that the flying foxes are feeding/visiting, which include tooth marks on fruit on or under the tree, large compressed pieces of fruit skin and flesh on the ground under the tree (spats), broken twigs or shoots, debris under the tree including: leaves, broken branches and partly eaten fruit or flowers and fruit distributed up to 100 metres from the tree. There are also specific trees that are safer and can help reduce the risk of infection - casuarinas (she oaks), conifer or cypress, brachychitons e.g. flame trees, bottle trees and kurrajongs, bamboo, bougainvilleas, jacarandas, olives, fiddlewoods, tipuanas, and other deciduous or evergreen trees that don't flower or produce soft fruits (NSW DPI 2012, QLD Horse Council 2012).

QLD Horse Council (2010) suggested a safe property design to minimise the risk of the HeV infection and to address other biosecurity issues. It recommends that the property should have a quarantine/isolation/sick bay area where one can isolate the new horse/horses that come on to your property. This reduces the risk of them introducing a disease or parasite. The council recommends isolation for about 3 weeks. This area can be a simple paddock with double fencing set a little away from the rest of the horse areas, to a separate stable block.

2.1.4 HeV Research

HeV has sparked a great deal of concern by being one of the rarest diseases with high fatality rate for both equine and human population. This prompted the establishment of the National HeV Research Program, to fund research leading to strategies to minimise the impact of the virus. The Australian, Queensland and New South Wales governments announced funding of \$12 million in July 2011 to accelerate research on HeV following the unprecedented number of outbreak incidents in Queensland and New South Wales. The funds were allocated through a \$9 million National HeV Research Program consisting of commissioned projects and an open funding program with an allocation of \$3 million by the National Health and Medical Research Council (DAF 2015). There were a total of 20 projects under the National HeV Research Program out of which eight were managed by the Rural Industries Research and Development, eight were managed by the NHMRC, and the remaining four were by the Queensland and the New South Wales State Governments (Thompson 2016).

The research highlights of the recent compendium of findings from the National HeV Research Program (2016) are:

- i) For the first time scientists have identified biomarkers that could indicate periods of increased HeV risk, by analysing the urinary metabolic profiles for flying foxes when they experience conditions, yet to be identified, that cause an increase in the replication of HeV.
- ii) A project revealed that the length of time the virus survived did not influence the pattern of ‘spillover’ events from flying foxes to horses, but rather that

transmission of HeV was likely to involve relatively direct contact of horses with flying fox excreta shortly after excretion.

- iii) Research into the possibility that HeV could persist in animals that had clinically recovered from the disease, posing a risk of re-infection or later transmission to other humans and animals, ruled out the likelihood of recurrence.
- iv) A series of projects examined the way in which HeV and its family group of henipaviruses replicate and interact with hosts; information with important ramifications for finding antidotes to other global viruses such as Nipah and the distantly related Ebola virus. One therapy was found to reduce HeV by up to 98 per cent and may prove its potential in future studies.
- v) There is the potential for transmission of HeV to people from acutely infected dogs.
- vi) The wide-ranging social, regulatory and policy impacts of HeV were revealed in a longitudinal cohort study of 1149 horse owners. The study used surveys and interviews to assess how horse owners perceived the risk of HeV, their uptake of risk mitigation practices such as the vaccine and their engagement with government and industry stakeholders such as veterinarians.

A study by Edson et al (2015) revealed that the flying fox urine is the most important route of HeV excretion in naturally infected flying-foxes and it should be considered a priority sample from a diagnostic or surveillance screening perspective. A total of 2840 individual flying foxes were captured and sampled across 10 roost sites over the 28-month period for this study. HeV is less likely to be detected in blood and faeces, and minimally in saliva and nasal discharge. Spleen and kidney were the tissues most likely to yield virus. Numerous diverse and previously unknown paramyxoviruses were detected, but no new henipaviruses (Field et al 2016). Research findings by Field et al (2016) indicated that HeV could be maintained in isolated flying fox populations via periodic recurrence of dormant infection, as well as by the immigration of infected individuals. The survival of the virus in the environment varied with latitude and season, and the effect of ambient temperature on survival could explain both the winter cluster of equine cases and sporadic cases at other times of year.

A serial cross-sectional serological study over a 25-month period with 521 individual samples, investigated the pattern of infection in the population of flying-foxes. The results of this study have shown that age, pregnancy and lactation plays as significant risk factors. The pregnant animals have highest antibody titres. Females are significantly higher than males in this. HeV infection in a population of *Pteropus conspicillatus* is likely to be endemic rather than episodic, as previously proposed for HeV in flying foxes. The evidence for seasonal viral activity suggested that the immunity to the virus may wax and wane on a seasonal basis. The study advised that life cycle of the reservoir species has to be considered when modelling a risk management strategy of the disease (Breed et al 2011).

Another study by Field et al (2015) on the Spatiotemporal aspects of HeV Infection in flying foxes in Eastern Australia has provided an advanced understanding of the virus infection dynamics in flying foxes and thereby, understanding of the fundamental drivers for virus spillover to horses, and indirectly humans. Largely, the findings show how the virus excretion by flying foxes in eastern Australia varies over space and time. They showed a non-linear relationship between mean HeV excretion prevalence and latitude, with excretion prevalence highest in southern QLD and northern NSW. They demonstrated a consistent, strong winter peaking of excretion in southern QLD and central and northern NSW. The findings were consistent with the observed spatiotemporal pattern of infection in horses, and demonstrate that HeV infection prevalence in flying foxes is a fundamental determinant of infection in horses

According to Plowright et al (2014), the emergence of bat viruses in recipient hosts requires at least five hierarchical enabling conditions. The probability of occurrence of each is conditional on the occurrence of the preceding condition; removal of any condition should prevent spillover. The study found no evidence that the prevalence of HeV in bat populations was associated with population density, and therefore that decreases in host density would reduce virus prevalence. It was mentioned that differentiating causal from correlational factors is a major challenge as the enabling conditions for spillover have many conditions that occur simultaneously and have common environmental drivers. For example, winter in subtropical Australia is the peak of resource scarcity for both bats and horses. Flying foxes are likely to migrate

to human-dominated landscapes in search of food, increasing their co-occurrence with horses, their vulnerability to nutritional stress and possibly excretion of HeV. Cooler temperatures may maximize virus survival, increasing the cumulative dose available to horses. Low productivity of pastures leads to horse consumption of contaminated fruit or grass, as well as poor horse condition and higher susceptibility.

A study estimated HeV survival with a Weibull distribution and calculated parameters from data generated in laboratory experiments. The virus survival rates are based on air temperatures 24 hours after excretion ranged from 2 to 10 % in summer, where as it was 12 to 33 % in winter. Based on the analyses, the study concluded that the most likely pathways of transmission did not require long periods of virus survival and were likely to involve relatively direct contact with flying fox excreta shortly after excretion (Martin et al 2015). Simulation modelling by Scanlan et al (2015) showed that the virus survival varied with location and with season, that factors such as the timing of virus excretion during the night and microclimate account for less variation in virus survival than does temperature variation between years. The model showed that the effect of ambient temperature on the virus survival in the environment reflects both the annual clustering of HeV cases in the Australian winter as well as occasional sporadic cases at other times of year. This study supports previous study by Field et al (2011) to understand the HeV infection dynamic in flying foxes and stated the need for further work to elaborate other contributing causal components.

A study to model the risk prediction for HeV transmission from flying foxes to horses (Skerratt et al 2016) concluded that the timing and geographical distribution of HeV spillover events cannot be explained by virus survival in the environment, as they occurred when the suitability of temperatures for survival was intermediate to very low. The study believes that the winter-dominant seasonal pattern of HeV transmission to horses in southern Queensland and northern New South Wales is likely driven by an additional seasonal factor apart from virus survival.

CSIRO announced the development of a prototype vaccine for horses in May 2011. After thorough testing, Equivac® HeV was launched in November 2012 by CSIRO and its associated partners. By March 2013 it was confirmed that horses were

immune to a lethal exposure of the HeV six months post vaccination by CSIRO scientists. The Equivac® HeV is a world-first commercial vaccine for a Bio-Safety Level-4 disease agent. This vaccine enables commercial and private equine activities to continue with minimal negative impact by increasing personal safety for horse owners, vets and others regularly interacting with horses. The Australian Veterinary Association now recommends that all horses in Australia are vaccinated against the HeV (CSIRO 2016). Immunising the horses is being viewed as a single approach to protect equine, human and environmental health (Middleton et al 2014).

2.1.5 Summary

HeV is a rare zoonotic disease that spills from flying foxes to horses and was first identified and described in 1994 following the outbreak of a new disease fatally affecting horses and humans in south east Queensland. The virus was initially called *equine morbillivirus*, but later renamed “*HeV*” after the suburb where the outbreak occurred. There are strong evidences supporting the bat to-horse to-human transmission of virus but there are no evidences supporting the bat-to-human, human-to- human or human-to-horse transmissions (CDNA 2010). In the year 2011, Australia witnessed an unprecedented spike in the number of HeV cases in horses in both Queensland and New South Wales. There were 80 confirmed outbreak events in Australia as of December, 2012 (Smith et al 2014).

The research on the HeV has almost begun immediately after the first outbreak. Government organisations as well as scientists and academicians from a broad range of disciplines, including the animal health, environmental and social sciences, are working together to develop a 'One Health' approach that will help minimise the impact of HeV. Currently, a vaccine is available for horses which have been introduced after thorough testing. ‘Equivac®’ – the HeV vaccine was launched in November 2012 by CSIRO and its associated partners. Apart from the vaccine, the DPI NSW (2012) and QLD Horse Council (2012) made some recommendations for the horse owners to exercise some precautions in areas with flying foxes to help minimise the risk of their horses being infected and thus reducing the risk of being infected themselves. QLD Horse Council (2010) also suggested a safe property

design to minimise the risk of the HeV infection and to address other biosecurity issues.

2.2 Flying Foxes

2.2.1 Introduction

The section 2.2 in chapter 2 provides a review of flying foxes in Australia particularly in South East Queensland. An overview is provided in section 2.2.2 and section 2.2.3 provides a detailed study of flying foxes - their roosting sites, diet, vegetation, foraging distances and behaviour. Section 2.2.4 covers the academic research of flying foxes in regards to the HeV and a summary is provided in section 2.2.5.

2.2.2 Overview

Species belonging to the *Pteropus* genus are part of the order Chiroptera (meaning ‘handwing’), generally known as bats. They were previously considered members of the Megachiroptera sub-order, a classification still popular in literature. *Pteropus* species are also known as flying foxes or fruit bats. This group comprises the largest bats in the world with some species weighing over 1000 grams and having a wingspan of 1.7 metres. They are generally characterised by large, well-developed eyes, simple external ears and an inability to use true echolocation, relying rather on their eyesight and strong sense of smell to find food. Bats are often considered carriers of many infectious diseases, and Australian flying foxes are associated with Lyssa, Hendra, Nipah and Menangle viruses (Australian Museum 2013).

The *Pteropid bats* commonly known as flying foxes were found to be the natural reservoirs for HeV. The emergence of HeV in Australia has raised a number of questions relating to their natural history (Halpin et al 2000, Field et al 2001). There are five Australian *Pteropus* species of which four are found on the mainland in primarily coastal regions, and one is found on Christmas Island. According to the International Union for Conservation of Nature, the current conservation status for most of these species is stable (Australian Museum 2013). All the four species of

Pteropus flying foxes are found in Queensland. The species are commonly known as black (*Pteropus alecto*), grey-headed (*Pteropus poliocephalus*), little red (*Pteropus scapulatus*) and spectacled (*Pteropus conspicillatus*) flying foxes. Flying foxes are nomadic animals and their movement patterns and local distribution are determined by variations in climate and the flowering and fruiting patterns of their preferred food plants (DEPI VIC 2011). They have an important ecological role because of their feeding behaviour which helps pollinate and disperse the seeds of native trees. They spread the pollen of valuable plants as they feed and thus playing an important role in our environment. Some plants even rely on flying foxes to pollinate their species (Wildlife QLD 2016). Figure 2.5 shows the four species of flying foxes that occur in Australia.



Figure 2.5: Types of flying foxes that occur in Australia (Source: BatReach 2016).

HeV outbreaks are only seen in Australia so far, where the virus is endemic in flying foxes. Flying foxes are found throughout tropical and sub-tropical Asia and Australia and on islands of the Indian and western Pacific Oceans (DEPI VIC 2011). Seropositive flying foxes have been found from Darwin in north central Australia to Melbourne in south eastern Australia. Equine cases been reported from eastern Australia, in the states of Queensland and New South Wales. Antibodies detected in flying foxes in Papua New Guinea might be caused by HeV or a related virus. Currently there is no evidence that HeV exists in other areas. However, henipaviruses or antibodies to these viruses have been detected in bats on several continents. Most of these viruses are poorly characterized (CFSPH 2015). Figure 2.6

shows the distribution of all four species of flying foxes in Australia and the approximate extent of the “HeV Belt”.

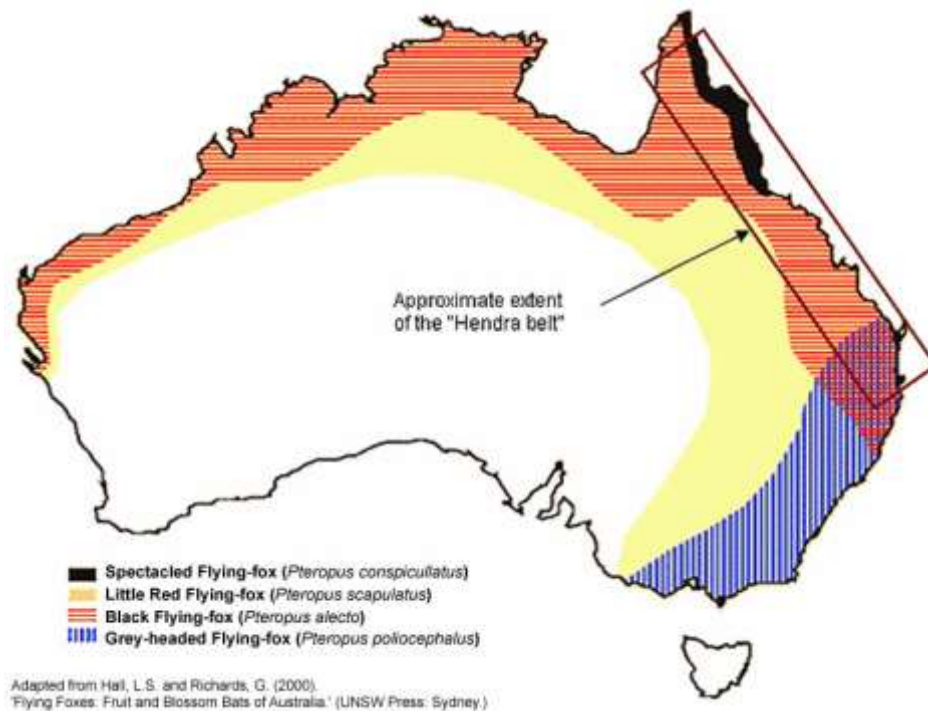


Figure 2.6: Flying fox species distribution map of Australia (Source: Agriculture Victoria 2016).

2.2.3 Flying Fox Ecology, Foraging Distances, Food Resources and Behaviours

2.2.3.1 Black Flying Fox (BFF)

The black flying fox was first described by Temminck in 1837 from a specimen from Menado, Indonesia. In 1867, Peters described a black flying fox from Rockhampton. The south-eastern limit of black flying-foxes has been moving southwards for at least 60 years. In 1930, the southern limit was Rockhampton and in 1960 it was the Tweed River, northern NSW. By 2002 they could be found further south than Port Macquarie. The black flying fox is the largest of the four mainland species in terms of body size in Australia (Wildlife QLD 2016).

Description

The Black flying fox is covered in short black fur but can sometimes also have a reddish-brown or yellow-brown colour. Its belly fur can have a frosted appearance if the fur is flecked with grey tips. The lower legs of this bat are unfurred and faint red-brown eye rings may be present. It is quite a large flying fox with weights ranging from 500 – 1000 g and forearm lengths ranging from 153 – 191 mm in adults (Australian Museum 2013). The wingspan of the black flying fox is about 1m (Wildlife QLD 2016).

Habitat

The black flying foxes are commonly found in tropical and subtropical forests, and in woodlands. They form camps in mangrove islands in river estuaries, paperbark forests, eucalypt forests and rainforests, and are mainly found along coastal and near coastal northern Australia from Shark Bay in Western Australia to central New South Wales (Wildlife QLD 2016, Australian Museum 2013).

Roosting sites

Large groups of black flying foxes can reach hundreds of thousands of individuals and form permanent camps for daytime roosting. It is a high roosting species and seeks fairly dense leaf cover (Australian Museum 2013).

Life History

The Black flying fox has a long life-span and can live for over 20 years in captivity and can live closer to 15 years in the wild. Like all *Pteropus* species, this bat has a slow lifecycle and low fecundity (ability of the female to produce numerous young) (Wildlife QLD 2016, Australian Museum 2013).

Breeding

Mating occurs in March to April when large males establish a territory on a branch. Females become pregnant before the bats disperse into generally smaller camps for the winter, and re-congregate into large camps during spring and summer, when birthing occurs. Females give birth to one offspring annually around late September – December. The young are completely dependent up to 4 weeks, at which point they will be left at the camp nightly while the mother forages. During this 4-week period,

the young cannot fly and must grip its mother's fur and nipple. At 2-3 months, the young can fly and they will start to leave the camp nightly to feed. They are weaned at about 5 months, and become sexually mature at about 2 years old, but most females will not reproduce before 3 (Australian Museum 2013, Red List 2008).

Food Resources/Vegetation

Black flying foxes fly out at dusk to feed on blossoms and fruits. They prefer blossom of eucalypts, paperbarks and turpentine's, as well as a variety of other native and introduced blossom and fruits. They have been seen to eat the leaves of trees by chewing the leaves into a bolus, swallowing the liquid and then spitting out the fibre. The Black flying fox uses its clawed thumbs to hold and manipulate food (Wildlife QLD 2016, Australian Museum 2013).

Foraging Distance

The foraging range of black flying foxes is approximately 15 – 50 km and will travel this distance from their camps at night. Like other flying foxes, these are a migratory species, and individuals move large distances in search for food. In favourable conditions, they can return to same camp locations over the years (Wildlife QLD 2016, Australian Museum 2013 and Red List 2008).

Distribution

Black flying foxes are found around the northern coast of Australia and inland wherever permanent water is found in rivers (Wildlife QLD 2016).

Conservation Status

They are currently listed as Lower Risk Least Concern according to the IUCN Red List of Threatened Species (Wildlife QLD 2016, Red List 2008).

2.2.3.2 Grey-Headed Flying Fox (GHFF)

The grey-headed flying fox was the first Australian flying fox species discovered by Europeans. The first grey-headed flying fox specimen was reported as collected in New Holland and described by Temminck in 1825. Their numbers have declined

drastically since European colonisation from many millions to a few hundred thousand. The known range for grey-headed flying foxes has contracted southwards by about 750 km and their southern limit during winter has expanded into Victoria. They are the largest Australian fruit bat and are endemic to Australia. Grey-headed flying foxes have sophisticated vocal communication, making more than 30 specific calls (Wildlife QLD 2016).

Description

The grey-headed flying fox is the only one to have a distinctly broad and complete collar of brownish-orange fur. It is also the only flying-fox to have thick leg fur which extends all the way to the ankles. Its body fur is long and dark brown to grey while its head fur is somewhat paler. It can sometimes be mistaken for the Black flying fox as they are quite similar in size. The average weights vary from 600 – 1000 g and the forearm lengths vary from 152 – 177 mm. The wingspan is about 1m (Wildlife QLD 2016, Australian Museum 2013 and Churchill 2008).

Habitat

The grey-headed flying foxes live in camps that can contain multiple *Pteropus* species. In general, they maintain traditional camps and visit these with varying frequencies in response to patchy food availability. They live in a large variety of habitats including rainforests, mangroves, paperbark swamps, wet and dry sclerophyll forests and cultivated areas. These bats commonly form their camps in gullies that are not far from water and usually in dense canopy vegetation (Wildlife QLD 2016, Australian Museum 2013).

Roosting Sites

The social organisation of grey-headed flying foxes revolves around traditional camps. These roost sites are extremely important as they are the locations for mating, birth and rearing of young, as well as refuges from predators. These camps can contain up to several hundred thousand individuals during summer and migrations to form smaller camps occur during winter. Changing camp sites usually depends on food availability and the sizes of different camps vary (Wildlife QLD 2016, Australian Museum 2013 and Churchill 2008).

Life History

Grey-headed flying-foxes are capable of living over 20 years in captivity; however they rarely live past 6 years in the wild. The majority of females reach sexual maturity at 3 years of age and if conditions are favourable, they will continue reproducing every year (Australian Museum 2013, DeHaven 2005).

Breeding

The mating of grey-headed flying foxes occurs throughout the year but most conceptions happen in March or April. A single young is born after 6 months and is carried by its mother for 4 to 5 weeks. At 5 weeks, it is left at the camp while the mother forages and is dependent on the mother for 4 to 5 months. Mothers are able to identify their young through unique calls and their sense of smell when returning from foraging (Wildlife QLD 2016, Australian Museum 2013).

Food Resources/Vegetation

These flying foxes forage on fruits and blossoms of more than 80 species of plants and mostly refer eucalypt blossom with native figs being the most popular fruit. They chew leaves and appear to eat the salt glands from mangroves. They also forage in gardens, parks and orchards and may fly many kms from roost site to feed. Some round trips are about 30 km (Wildlife QLD 2016).

Foraging Distance

The nightly feeding range of grey-headed flying foxes is 20-50km from camp and in winter, adults can migrate up to 750km from their summer camps (Wildlife QLD 2016).

Distribution

The grey-headed flying foxes occur along the east coast of Australia from Rockhampton to western Victoria and inland to the western slopes (Wildlife QLD 2016).

Conservation Status

The Grey-headed Flying-fox is listed as a 'vulnerable' species by the IUCN due to continuing declines in population of about 30% over the last 20 years. These bat numbers are predicted to continue declining through threats such as habitat

destruction, direct killing as a pest species of orchards and competition for resources with black flying foxes. They are federally listed as ‘vulnerable’ under the ‘Environment Protection and Biodiversity Conservation Act 1999’ and also the ‘NSW Threatened Species Conservation Act 1995, schedule 2’. In Victoria they are listed as ‘threatened’ under the ‘Flora and Fauna Guarantee Act 1988’. They are ranked as a critical priority under the Department of Environment and Heritage Protection ‘Back on Track species prioritisation framework’ and a Recovery Plan for this species exists (Australian Museum 2013, EHP QLD 2013, Red List 2008 and DeHaven 2005).

2.2.3.3 Little Red Flying Fox (LRFF)

Little red flying foxes are the most widespread species of mega bats in Australia and the only species of Australian flying fox that regularly roosts in clusters as up to 30 have been seen hanging together in a tight bunch. The weight of their clusters can cause severe damage to their roost trees. They are nomadic and their movements depend on food resources. Peters first described the little red flying fox in 1862, from a specimen collected on Cape York (Wildlife QLD 2016).

Description

The little red flying foxes vary in colour from reddish brown to light brown, and there are patches of light, creamy, brown fur where the wing membrane and shoulder meet. Their head is covered with greyish fur and, in some forms found in northern Queensland, grey fur continues down the back. The wings are brown and semi-transparent when seen flying during the day, which helps identify the species. The average weight 300–600g and the head-body length is 125–200mm (Wildlife QLD 2016).

Habitat

Little red flying foxes is a highly nomadic species and is tolerant of a number of different environments, enduring different temperature and humidity ranges and having the largest distribution of the Pteropus genus in Australia. As a result, this species extends further inland than any other species of flying foxes (Wildlife QLD 2016, Australian Museum 2013 and Red List 2008).

Roosting Sites

The roosting sites of little red flying foxes are usually fairly congested and can become extremely noisy during the active periods, mainly early morning and late afternoon. They are largely nomadic due to the unpredictability of food supplies (Australian Museum 2013).

Life History

The little red flying foxes can have an average lifespan of over 15 years in captivity; however there is currently no information on their lifespan in the wild (Australian Museum 2013).

Breeding

Unlike other species, the little red flying foxes have a breeding cycle that begins in November – January when mating occurs. Birthing occurs from March – May in camps. Once the young are born, they suckle for one month and are then left at the roost and suckle periodically until they are able to fly, which is around 2 months of age. For several months thereafter, they are semi-independent until they can perform necessary adult behaviours (Wildlife QLD 2016, Australian Museum 2013).

Food Resources/Vegetation

The little red flying foxes feed mostly on eucalypt or melaleuca nectar, as well as native and cultivated fruits, leaves, growing shoots, bark, sap and insects. When food is scarce, these bats will raid orchards and damage these crops. While they usually feed at dusk and night, they have been known to feed during overcast days. The groups congregate during the day at roosting sites that are near water (Wildlife QLD 2016, Australian Museum 2013).

Foraging Distance

The little red flying foxes only travel up to 20–30km from camp to feed (Wildlife QLD 2016).

Distribution

They are distributed in coastal and subcoastal regions from Shark Bay in Western Australia through to northern Victoria and, in certain circumstances, South Australia.

As nomads they range a long distance inland, depending on the availability of flowering trees (Wildlife QLD 2016).

Conservation Status

This species is listed as a species of ‘least concern’ by the IUCN and is listed as ‘Least Concern’ under the ‘Nature Conservation Act 1992’ in Queensland and is ranked as a low priority under the Department of Environment and Heritage Protection ‘Back on Track species prioritisation framework’. It is, however, locally threatened by clearing in parts of its range (EHP QLD 2016, Australian Museum 2013).

2.2.3.4 Spectacled Flying Fox (SFF)

Spectacled flying foxes were first described in 1850 by Gould. They are important seed dispersers and pollinators of rainforest flora. These flying foxes have the smallest known distribution and smallest population of the four Australian mainland *Pteropus* flying foxes (Wildlife QLD 2016).

Description

The spectacled flying foxes are very similar in appearance to black flying foxes as they are almost completely black. However, it is distinguishable by a patch of straw-coloured fur on their collar and prominent straw-coloured to dirty brown fur surrounding both eyes. This fur can sometimes extend towards the nose. In some cases, the body fur is tipped with grey, giving it a grizzled appearance. The size of adults can vary from 500 – 1000 g in weight and 150 – 183 mm in forearm length (Wildlife QLD 2016, Australian Museum 2013).

Habitat

The spectacled flying fox is distinguished from other Australian flying foxes by being the only rainforest specialist. They are integral to the rainforest regeneration through seed dispersal and pollination (Australian Museum 2013).

Roosting Sites

The spectacled flying foxes usually roost in camps that only include their own species. They are frugivorous, meaning that fruit makes up a large portion of their diet. The camps of spectacled flying foxes have well-defined territories of feeding trees and they can become quite aggressive and territorial after dusk when feeding occurs (Wildlife QLD 2016, Australian Museum 2013).

Life History

The life-span of spectacled flying foxes is at least 17 years in captivity, however little is known about their lifespan in the wild. Like all *Pteropus* species, they have a slow life cycle and low fecundity (Wildlife QLD 2016, Australian Museum 2013).

Breeding

Mating of the spectacled flying foxes occurs in March to May but sexual activity occurs for the entire first half of the year. The females give birth to one offspring annually around late September – December. The young are nursed for over 5 months and, once they are weaned, will continue living in the camp in ‘nursery trees’ (Australian Museum 2013).

Food Resources/Vegetation

The spectacled flying foxes are specialist fruit eaters that feed mostly on rainforest fruits, some eucalyptus nectar and pollen. They disperse seeds of at least 26 species of rainforest canopy trees (Wildlife QLD 2016).

Foraging Distance

The foraging range of spectacled flying foxes is 20–30 km and it is dictated by food availability (Wildlife QLD 2016, Australian Museum 2013).

Distribution

Of all the mainland Australian *Pteropus* species, the spectacled flying fox has the smallest distribution and population size. Their distribution is limited to within rainforests or areas closer than 6 km to rainforest. As a result of this, they are restricted to the coastal region of north-eastern Queensland and have a patchy range

extending from Cape York to coastal central Queensland (Australian Museum 2013, Red List 2008).

Conservation Status

The spectacled flying fox is listed as a species of 'least concern' by the IUCN. However, it is considered vulnerable largely due to habitat destruction such as large-scale clearing of coastal and upland habitats and persecution by fruit-growers (electrocution and shooting). They have been federally listed as 'Vulnerable' under the 'Environment Protection and Biodiversity Conservation Act 1999' (Australian Museum 2013, Red List 2008).

2.2.4 Flying Foxes Research and Virus Prevalence

On 31st May 2012, there were six new research projects totalling just over \$2 million announced, including \$794,717 to CSIRO Ecosystem Sciences (Dr David Westcott) for the project 'Implementing a National Flying Fox Monitoring programme' (NFFMP). The Minister approved an additional \$700,000 towards the NFFMP under the 'Emerging Priorities' of the National Environment Research Programme (NERP). Monitoring is described as the process of collecting data on the abundance of a species and its distribution. It is a critical activity in biodiversity conservation because it provides insight into the status of a species and over time provides an indication into population trends and other ecological factors. This information is necessary to assess the kind of management required and to measure the effectiveness of management. Monitoring of flying foxes is considered even more important because two species, the grey-headed flying fox and the spectacled flying fox, which are listed as threatened under the Commonwealth *Environmental Protection and Biodiversity Conservation Act 1999* (EPBC Act) and relevant state legislation. The results of the program will help inform responses to public concerns about the impact of flying foxes on industry, agriculture and public health, including any potential Hendra outbreaks (DoE 2013).

The recent findings of NFFMP revealed that the distribution of flying foxes is highly variable, with the animals moving in and out of camps seasonally, apparently in response to varying food resources. The grey headed and spectacled flying foxes -

whose entire distributions were covered by the monitoring, have shown a dramatic change in their distribution over the last decades with a shift to smaller camps located in urban and peri urban areas. This is a similar distribution to that of horses. The data showed a severe decline in the abundance of the spectacled flying fox, sufficient to warrant a change in its status to endangered, while the number of grey headed flying foxes was found to be stable to declining. HeV in horses mostly correlated with incursions of the spectacled flying fox and black flying fox (Westcott 2016)

A study to investigate the HeV dynamics in flying foxes to determine the prevalence of viral co-infections during the spillover events found that peak periods of HeV spillover from flying foxes are associated with a peak in other viral infections. It was revealed by the scientists that the flying fox colonies with a high HeV prevalence contain a correspondingly high prevalence of other viruses, including paramyxoviruses from the general *Henipavirus* and *Rubulavirus*. An analysis of urine collected from flying foxes during the 2011 HeV spillover events has resulted in the isolation of more than 40 viruses, including a large number of new viruses which are yet to be classified. Seasonal trend in the presence of viruses was identified, indicating that environmental triggers may be associated with spillover events. A secondary objective of this study was to examine urinary metabolic profiles for flying foxes when they experience conditions that increase the replication of HeV, such as nutritional stress, movement stress, pregnancy, birth or lactation. This is believed to be the first metabolomics analysis performed on flying fox samples, with the aim of identifying biomarkers that could indicate periods of increased HeV risk (Baker 2016, Barr et al 2015).

Field et al (2016) investigated the flying fox dispersal and HeV risk. The study analysed whether the disturbance of flying fox roosts leads to an increase in stress levels and HeV infection and excretion in dispersing animals, which might potentially increase the risk of spillover of the virus to horses. The study found no association between disturbance of the roosts and HeV excretion, indicating that roost dispersal does not cause increased HeV infection and excretion in dispersing flying foxes. No association was found between roost disturbance and concentration of the stress hormone cortisol, but found an underlying association between cortisol

concentration, season and region, suggesting that other factors, possibly biological or environmental play a role in determining levels of cortisol in flying foxes. A need for a 'best practice' approach was mentioned to study the dispersal of flying fox roosts, as the nature or timing of the activity had a clear impact on the level of behavioural distress exhibited by the animals. While flying foxes have some capacity to escape roost disturbance, their increasing urban presence may make them the target of ongoing harassment, with unknown consequences.

A cross-disciplinary study by McFarlane et al (2011) demonstrated a significant occurrence of Hendra spillover events 1994–2010 within the dry season. In this study, the climatic and vegetation primary productivity variables are compared for the dispersed and heterogenic 1994–2010 outbreak sites. The significant occurrence of spillover events within the dry season ($p=0.013$, 95% CI (0.57–0.98)) suggests seasonal forcing of transmission across species, or seasonal forcing of virus excretion by the reservoir host. The preliminary investigations of the spatial determinants of Hendra disease locations are also presented in this study. The postal areas in the Australian state of Queensland in which flying fox roosts occur are approximately forty times more likely (OR=40.5, (95% CI (5.16, 317.52)) to be the location of Hendra spillover events. The study found that the result appears to be independent of density of horses at these locations. The limitations of the study include scale of host resource use, land use change and limitations of existing data that challenge. This study serves as a good base for further investigations of a broad range of potential climatic and environmental influences on the spillover events.

A three year longitudinal study to detect virus in the urine of free-living flying foxes (a putative route of excretion) to investigate HeV infection dynamics indicated that the virus excretion occurs periodically rather than continuously, and in geographically disparate flying fox populations in the state of Queensland. A total of 1672 pooled urine samples from 67 sampling events was collected and tested between 1 July 2008 and 30 June 2011, with 25% of sampling events and 2.5% of urine samples yielding detections. The proportion of positive samples was statistically associated with year and location. The lack of any detection in the Northern Territory suggests prevalence may vary across the range of flying foxes in Australia. The findings suggested that the flying foxes can excrete virus at any time

of year, and that the apparent seasonal clustering of HeV incidents in horses and associated humans with 70% occurring between June to October. This reflects factors other than the presence of virus and identification of these factors will strengthen risk minimization strategies for horses and ultimately humans (Field et al 2011).

The study conducted by Field et al (2015) to identify key spatial and temporal factors associated with excretion in flying-foxes over a 2300 km latitudinal gradient from northern QLD to southern NSW aimed to strengthen the knowledge of HeV ecology in flying foxes to improve spillover risk prediction. A generalised linear model was employed in this study, to investigate the spatiotemporal associations with HeV detection in 13,968 samples from 27 roosts. A non-linear relationship between mean HeV excretion prevalence and five latitudinal regions was identified, with excretion moderate in northern and central QLD, highest in southern QLD/northern NSW, moderate in central NSW, and negligible in southern NSW. Highest HeV positivity occurred where black or spectacled flying foxes were present; nil or very low positivity rates occurred in exclusive grey-headed flying fox roosts. The little red flying foxes are evidently not a significant source of virus, as their periodic extreme increase in numbers at some roosts was not associated with any concurrent increase in HeV detection. The study identified consistent, strong winter seasonality to excretion in the southern QLD/northern NSW and central NSW regions.

Plowright et al (2008) initiated a longitudinal field study of HeV in little red flying foxes and examined individual and population risk factors for infection in order to determine probable modes of intraspecific transmission. The study investigated whether seasonal changes in host behaviour, physiology and demography affect host-pathogen dynamics. The results showed that pregnant and lactating females had significantly higher risk of infection. This may explain previously observed temporal associations between HeV outbreaks and flying fox birthing periods. The field data implied that the HeV is transmitted horizontally via faeces, urine or saliva. The highest seroprevalence was observed when animals showed evidence of nutritional stress, suggesting that environmental processes that alter flying fox food sources, such as habitat loss and climate change, may increase HeV infection and

transmission. These results of HeV in flying fox populations suggest possible causal links between environmental change and HeV emergence.

The latitudinal range shifts study of Australian flying foxes revealed that both black and grey-headed flying foxes range is not shifting in a manner driven by climate change as supposed to. The study obtained historical locality records from a wide range of sources (including banding and museum records, government wildlife databases and unpublished records), and filtered them for reliability and spatial accuracy. The latitudinal distribution of each species was compared between eight time-periods: 1843–1920, 1921–1950, five 10-year intervals between 1950 and 2000, and 2001–2007. The findings suggest that neither the northern or southern range limits of grey-headed flying foxes (Mackay, Queensland and Melbourne, Victoria respectively) changed over time. Black flying foxes range limit extended southward by 1168 km during the twentieth century (from approximately Rockhampton, Queensland to Sydney, New South Wales). The percentage of total records that were black flying foxes increased from 8% prior to 1950 to 49% in the early 2000s, and local count data showed that its abundance increased from several hundred to more than 10,000 individuals at specific roost sites, as range expansion progressed. The study concluded that neither climate change nor habitat change could provide simple explanations to explain black flying foxes observed rapid range shift (Roberts et al 2011).

A study on the urban habituation, ecological connectivity and epidemic dampening of the flying foxes suggested that multiple factors in the changing landscape of Australia and the demography of flying foxes contribute to HeV dynamics in bats and spill-over hosts. The models in the study predicted urban habituation of flying foxes increases the epidemiological linkage between flying foxes and horses, providing plausible scenarios for the recent apparent increased frequency of HeV outbreaks in Australia. The study described a counterintuitive ‘epidemic dampening’ effect, where decreasing reservoir host population connectivity can favour a sporadic, high force of infection that may facilitate pathogen emergence into an aberrant host. The results suggested that the anthropogenic driven changes to flying fox ecology may result in more intense, sporadic, lethal outbreaks of HeV in livestock and people (Plowright et al 2011).

2.2.5 Summary

The *Pteropid* bats commonly known as flying foxes were found to be the natural reservoirs for HeV. The emergence of HeV in Australia has raised a number of questions relating to their natural history (Halpin et al 2000, Field et al 2001). There are five Australian *Pteropus* species of which four are found on the mainland in primarily coastal regions, and one is found on Christmas Island. Flying foxes are nomadic animals and their movement patterns and local distribution are determined by variations in climate and the flowering and fruiting patterns of their preferred food plants. They have an important ecological role because of their feeding behaviour which helps pollinate and disperse the seeds of native trees (DEPI VIC 2011). Computer modelling of flying foxes revealed that the virus does not persist as a constant endemic infection in discrete populations of bats but persists throughout the range of flying foxes in a pulsing pattern (Australian Biosecurity 2009).

HeV research is considered challenging and complicated and much remains to be learnt (Australian Biosecurity 2009). There is a need for further research to understand the spatial and temporal patterns of the virus for effective surveillance and management of the disease. The Queensland government announced a pressing need for current research on the spatial and temporal occurrences of the virus outbreaks and further study into ecological and environmental factors as causes of the disease (DAF 2015). In the case of rare outbreaks like the HeV, GIS is a vital tool to identify the main factors (geographical, environmental and other factors) of disease transmission, for disease monitoring, identifying at-risk populations, producing prediction models and generating warning systems according to spatial distributions (See Section 2.3.9).

2.3 Spatial Epidemiology

2.3.1 Introduction

The section 2.3 in chapter 2 discusses spatial epidemiology, including spatial data exploration, visualization, spatial autocorrelation, spatial clustering, data modelling as well as disease mapping and GIS applications in epidemiology which are closely related to disease monitoring and surveillance. Section 2.2.2 provides an overview of

spatial epidemiology, and geographical representation and mapping of diseases is covered in section 2.2.3. Spatial data exploration and visualization is discussed in Section 2.2.4. The topics spatial autocorrelation, spatial clustering and spatial data modelling are covered in sections 2.3.5, 2.3.6 and 2.3.7 respectively. Section 2.3.8 details regression model frameworks, and the literature referred to GIS applications in epidemiology, specifically in HeV studies is covered in 2.3.9. Finally, a summary of the section is provided in 2.3.10.

2.3.2 Overview

Spatial epidemiology provides researchers with a map-based description and analysis of infectious and non-infectious diseases. This approach utilises epidemiological data and other health-related data including but not limited to demographic data, genetic and molecular data, environmental data and behavioural data. In modern research, it has emerged as an innovative way in studying the spread and possible causes of infectious disease outbreaks such as cholera, malaria, dengue and yellow fever. This new field of study emerged in early 1800s (Walter 2000) and it has since advanced in sophistication and complexity. The spatial approach in the epidemiological/health studies can play a crucial part in measuring the variability in the risk factors concerning the health status of the communities, environmental hazards and socio-economic profiles. GIS plays a pivot role in the analysis of spatial distribution of disease data across space and time, which is increasingly recognized in the spatial epidemiological research.

A review of spatial methods in epidemiology from 2000 – 2010 to understand the impact of place on health as a key element of epidemiologic investigation revealed that the space and place have been key dimensions of epidemiology and public health for decades, yet advanced spatial methods have been relatively slow to trickle into epidemiology. The study notes that, there are many rich tools to employ in this day for a more sophisticated treatment of space and to understand better the interacting contributions to health of individual characteristics and spatially varying place-based factors. The most common spatial methods were found to be distance calculations, spatial aggregation, clustering, spatial smoothing and interpolation, and spatial regression. It concluded that the increased use of spatial methods is likely to

continue, in tandem with interest in the relationship between place and health, as spatial software tools become more accessible and geographically referenced data become more available (Auchincloss et al 2012). A study by Nuckols et al (2004) discussed the three major scientific disciplines, namely geospatial science, environmental science and epidemiology, in which GIS was used in exposure assessment for epidemiology studies. The study emphasised how an epidemiological study must be able to estimate the exposure and critical time windows with respect to the disease latency period.

‘Disease ecology is inherently integrative and spatial, and GIS provides the environment in which the biophysical, social, behavioural, and cultural worlds can be combined for a systemic understanding of health and disease’ – (Queensland Health 2005). Kulldroff (1999) and Elliot et al (2000) stated that applications of GIS in epidemiological studies date from late 19th century. The studies attempted to observe the spatio-temporal patterns of various communicable and non-communicable diseases in different parts of the world. Most of the studies revealed significant information about the diseases and that helped in further investigations. Exploratory methods in GIS are valuable in searching for regions of high disease prevalence. This helps to investigate and improve the understanding the disease distribution from a spatio-temporal perspective (Nuckols et al 2004, Seng et al 2005). Gatrell et al (1997) discussed three types of GIS methods in public and environmental health application. They are visualization, exploratory and modelling. He mentioned that exploratory and visualization is closely related and is often recognised as ‘exploratory visualization’. Visualization involves displaying the locations and influential variables on maps and showing variations in space and time whereas exploratory analysis enables the analyst to explore and investigate the spatial data trend which helps in identifying the disease pattern and generate hypothesis. Cluster identification is one of the important exploratory methods in epidemiology.

In epidemiology there have been considerable advances in the development of methods for the detection of clustering and clusters of health events, together with productive links between statisticians, epidemiologists, and geographers in demonstrating the usefulness of GIS-based approaches. Langford et al (1996) stated

that multilevel or hierarchical methods were being promoted actively in health research, and given an explicitly spatial dimension; links are needed between these tools and GIS environments. Significance should be given to the importance of building closer research links between those using GIS for epidemiology and those using it in health care planning. GIS should be used in the needs assessment process, such 'needs' being represented, in part at least, by the areas of high mortality and morbidity i.e. the 'clusters' to which the attention has been given – identified by other GIS-based analyses. GIS, in the reshaped form of a spatial decision support system, can play a valuable role in bringing the two health research backgrounds together (Gatrell et al 2005).

The occurrence of disease is the primary interest of an epidemiologist in as categorized by time, person and place where as spatial epidemiology emphasizes the latter. Describing and understanding variations in disease from a distinctly analytical spatial perspective and as an area of medical research it is one of growing importance. In general, health, population and exposure data are available in either point (exact location) or count data (aggregated level). Point data is considered more accurate due to its geographical representation but it is rarely available in some cases. Therefore, it is recommended only if there is sufficient evidence to warrant the use of such data. On the other hand, using aggregated data for exploratory analysis is easier than case control or cohort studies; however, they are prone to biases and misclassifications (Elliot et al 2000).

Data of epidemiological or public health interest often occur as spatial information during each of several time periods. Most of the analytical techniques require the pooling of information in administrative areas with well-defined geographic boundaries (e.g., counties, municipalities, and health districts), and the presentation of the spatial process with maps constrained to them. Nobre et al (1995) has introduced two temporal analytical techniques in their work – time series analysis and temporal cluster analysis. The time series analysis has is quite useful in different contexts for monitoring tasks. The implementation of this technique into an integrated system for use in public health will lead to a better assessment of its impact and utility (Nobre et al 1995). Spatio-temporal analytical technique was also reviewed by Nobre et al (1995) in their work, which emphasizes on space-time

interaction among health events, or health events and environmental variables which are important in epidemiological studies and disease surveillance.

The ability of GIS to integrate and manipulate complex data has emerged it as a powerful tool in epidemiological studies. The traditional epidemiological studies such as cohort or case control studies enable us to identify excess disease rates or trends and perform further analysis for hypothesis testing (Seng et al 2005). Use of GIS technology in epidemiological and public health studies gained momentum after researchers started using it for more than visual representations i.e. maps. GIS in epidemiology has been tremendous in understanding the disease in a different dimension. With the assistance of this powerful tool, the disease clusters could be identified and other influencing factors such as environmental, socio economic and climatic could be linked to the diseases. While geographical visualization serves the need to reveal the spatial patterns, the statistical awareness in GIS determines the significance of these patterns.

The introduction and implementation of GIS technology in public health and epidemiology benefits in analysing the prevalence and geographic distribution of a disease outbreak in a space-time sense (Lawson et al 2001). GIS technology is being widely used for disease monitoring, research hypotheses generation and identifying populations at risk for its high capability in data interpretation, manipulation and modelling (Seng et al 2005, Gupta et al 2003). GIS serves as an effective tool for spatial analysis, modelling and visualisation of epidemiological and environmental data; and recent studies have shown significant and increasing use of GIS applications in public health and epidemiology (Shittu et al 2010, Busgeeth et al 2004 and Gupta et al 2003). The powerful analytical modelling and mapping capabilities of GIS can serve as a good decision-support and decision-making tool for disease investigations, monitoring, simulation, predictions, preventions and resource allocations (Davenhall 2002).

2.3.3 Disease Mapping

Mapping is a visual representation of geographical distribution, and disease mapping refers to the representation of disease or outbreak location, summary measures or statistics for a specific group of individuals in their geographical association (Lawson et al 2001). The mapping of disease incidence and prevalence has long been a part of public health, epidemiology, and the study of disease in human populations (Koch 2005). The advantage of disease mapping is that they might any significant spatial patterns that may not be recognized in tabular representation of the data (Elliot et al 2004). Disease mapping identifies possible disease clusters, to define and monitor epidemics, to provide baseline data on health patterns, and to show changes in disease patterns over time. It may also be useful for initial exploration of relationships between exposure and disease, particularly; acute health effects. It may at times involve small area maps of disease which are much more difficult to produce and interpret in a meaningful way. Caution needs to be exercised in their interpretation due to the factors of latency period and migration (Jarup 2004), variable representation and spatial resolution (Elliot et al 2004).

In general, the disease distribution may occur within specific population groups with a spatial distribution and may vary in various aspects. It is extremely important to be aware of the spatial patterns of the underlying causes/factors to be able to detect the true disease pattern (Seng et al 2005). The interpretation of the map should be dependent on the type of the disease i.e. infectious or non-infectious as a map that demonstrates the distribution of an infectious disease could be invaluable in identifying the cause of the outbreak, mainly if it is represented as points. The mapping of non-infectious diseases is useful in hypothesis generation (Lawson et al 2001).

Koch (2004) studied a series of maps of the 1854 cholera outbreak in Soho, London - historical and contemporary which serve as an example of the manner and degree to which a map-maker's intent defines the context that determines the content of the resulting map. These maps include John Snow's original maps; E.W. Gilbert's 1958 version of Snow's map; Andrew D. Cliff and Peter Haggett's 1988 maps; Edward Tufte's 1983 revision of Gilbert's 1958 map; Monmonier's 1990s revision of the

Gilbert-Tufte map; and the US Centers for Disease Control's (CDC) 2001 map based on Snow, Gilbert, and Tufte. The study concluded that the maps reflect specific phenomena of interest to map-makers, who choose from the available data to fashion idiosyncratic interpretations of those phenomena.

The cholera outbreak map by John Snow, a physician in London is still the best acknowledged example of disease mapping. It demonstrated the correlation between the cholera cases and the water supply contamination in the year 1854. The infected well was identified from the concentration of cases around the Broad Street water pump by incidence mapping (Snow et al 1994). Figure 2.7 shows the original map by John Snow showing the clusters of cholera cases in the London epidemic of 1854.

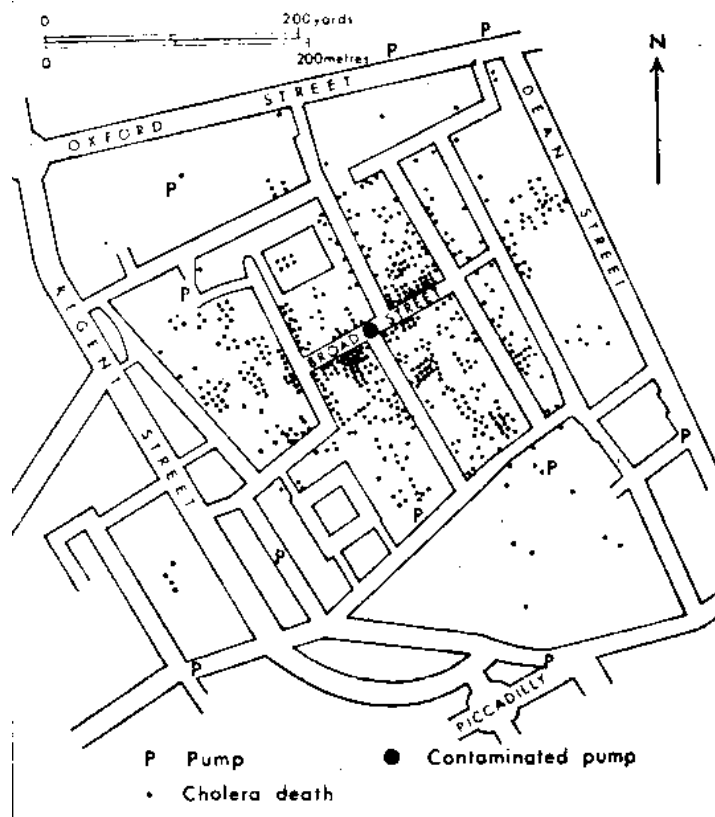


Figure 2.7: Original map of Cholera cases by John Snow (Source: Epidemiology Inside 2016).

Walter (1993) discussed the theories of graphical perception which suggested that the interpretation of maps is complex relative to other types of graphical material. In his study, it was found that the maps with various types of spatial pattern were visually

distinguishable; comparisons between variants of the same map, however, using different shading and plotting symbols indicated that the method of data representation also had a strong effect on visual perception. The study showed enough evidence for a learning effect in complex maps. The study concluded that the relationship between the visual assessments and a statistical measure of spatial autocorrelation was significant but imperfect. In their review of cognitive aspects of designing statistical maps, Sirken et al (1993) have concluded that map reading actually is best viewed as consisting of a series of reading stages which include Map Orientation, Legend Comprehension, Map/legend Integration and Discerning and Spatial Patterns and Relationships. They suggest that the sensory processes are important in map orientation and the legend comprehension stages whereas the integration of the map with the legend depends more on perception, and the discernment of patterns makes use of comprehension, memory, and reasoning.

In the introductory guide to disease mapping, Lawson et al (2001) has discussed the visual perception and construction of a disease map as below:

Construction of the Map

Construction of the map should consider the aspects such as the data, the area and the choice of scale. The area should be chosen with great care and sometimes this may be predefined. As study of the incidence or disease prevalence must have boundaries such as town, city or a country. Maps are usually characterised by the scale chosen to represent the geographical distribution of the disease of interest (Lawson et al 2001).

Map Transformation

The next step is chose the form of the symbolic representation. This is a well-known practice. The map is usually constructed from the standard spatial coordinate systems such as longitude-latitude, east-north etc. and in these cases there is no further need to consider any changes. In some rare cases, there might be a need to consider other representation systems, usually when mapping very large scale distributions (e.g. Worldwide) (Lawson et al 2001).

Symbolic Representation

Symbolization is considered as an important characteristic of cartography. Misinterpretation of maps usually arises from inappropriate symbolization, which affects the accuracy of the results and conclusions drawn from the map. The most commonly used symbols in disease mapping are points, lines, colour and shading symbols. Point symbols represent case events in disease mapping and the choice of type and size should correspond with the underlying population. The size of the point symbol is suggested to be inversely proportional to the population density at the specific location (Bailey et al 1995, Seng et al 2005). Lawson et al (2001) emphasized on using the appropriate symbols and monochrome colour schemes for disease mapping, which was found to be most effective.

Processing of Data and Data Aggregation

This stage involves further processing that typically occurs when the information from the spatial structure or its associated attributes is unavailable under the current representation system. Data interpolation/smoothing and transformation are the two steps that need to be considered to fulfil the requirement. Sometimes, specific algorithms may be required to determine the best values from interpolation to use at the locations other than the observed data (Lawson et al 2001). Data aggregation is also an important aspect that needs to be taken into consideration in mapping and misinterpretation might occur when areas are mapped according to the aggregated data leading to the loss of data variation (Seng et al 2005).

Interpretation of Maps

Disease maps are derived from statistical data and it is recommended to include some form of accompanying table of the data used in the map. If not possible, a secondary map showing the variability or the reliability of the data estimates such as relative risks can be displayed on the map. A full overview of recommendations for disease mapping is available in a WHO workshop report (Lawson et al 2001).

2.3.4 Spatial Analysis

Spatial data analysis is considered as a branch of data analysis where the geographical referencing of objects contains important information. In data

collection, specifically in some areas of experimental science, the indexes that distinguish different cases can be exchanged without any loss of information. The information relevant to understanding the variation in the data is available within the observations and indexing does not have any relevant information. But, in the case of spatial data, the indexing may contain crucial information. The collection of techniques and models that explicitly use the spatial referencing of each data case is defined as spatial analysis. In spatial analysis, it is required to make assumptions on the data describing spatial relationships or interactions between cases. The results of spatial analysis highly depend on the re-arrangements of spatial distributions of values and reconfiguration of the spatial structure (Goodchild et al 2004, Haining 1994).

Goodchild et al (2004) refers spatial data matrix as the point of contact for spatial analysis and GIS. The spatial data matrix consists of rows and columns where rows refer to cases and columns refer to the attributes measured at each of the cases, and the last columns provide the spatial referencing. At the simplest level, there might be two last columns containing a pair of coordinates: latitude and longitude, or x and y in some projected coordinate system. GIS permits a vast array of operations based on this approach to representation. There are many published methods of spatial analysis that are available in the form of standard products of commercial GIS vendors. A variety of GIS products and extensions are also available as open software or freeware, through academic and other organizations and communities (Ungerer et al 2002).

Bailey et al (1995) categorized the spatial data analysis into three main divisions - visualizing the data, exploratory data analysis and methods for development of statistical models. Pfeiffer (1996) mentioned that during most analyses, a combination of techniques will be used with the data first being displayed visually, followed by exploration of possible patterns and possibly modelling. Point patterns, spatially continuous and area data are the methods used in spatial data analysis. The spatial perspective in the spatial data analysis allows easy access to information on the relative locations of objects and events, and also proximity (Goodchild et al 1992).

Goodchild et al (2005) has mentioned that the below conditions that are mostly likely the reason for someone to choose GIS-based spatial analysis rather than the statistical spatial analysis, although the list is certainly not complete and the items are not intended to be mutually exclusive.

- i) The data are geographically referenced;
- ii) Geographical references are essential to the analysis;
- iii) The data include a range of vector data types (support for vector analysis among non GIS packages appears to be much less common than support for raster analysis);
- iv) Topology – representation of the connections between objects – is important to the analysis;
- v) The curvature of the Earth’s surface is important to the analysis, requiring support for projections and for methods of spatial analysis on curved surfaces;
- vi) The volume of data is large, since alternatives like spreadsheets tend to work only for small datasets;
- vii) Data must be integrated from a variety of sources, requiring extensive support for reformatting, resampling, and other forms of format change;
- viii) Geographical objects under analysis have large numbers of attributes, requiring support from integrated database management systems, since many alternatives lack such integration;
- ix) The background of the investigator is in geography, or a discipline with strong interest in geographical data;
- x) The project involves several disciplines, and must therefore transcend the software traditions and preferences of each;
- xi) Visual display is important, and when the results must be presented to varied audiences;
- xii) The results of the analysis are likely to be used as input by other projects, or when the data are being extensively shared.

There are some issues that affect the interpretation and results of the spatial analysis such as selection bias, confounding factors, gross error, modifiable areal unit problem (MAUP) and edge effects. Bias and confounding factors are closely related

and remain as a major problem in data analysis. Bias happens when the variables are deviated from 'true' values and confounder factor refers to the secondary variables which are associated with the outcome (Elliot et al 2000). Understanding of the underlying demography, topography and disease epidemiology is essential in parameter selections and thus a likelihood of producing more reliable results. Gross error can be detected by identifying the extreme data values from the overall distribution. It is considered important as it tends to affect the mean or standard deviation especially in a small sample.

MAUP effects are divided into two major components – scale effects and zone effects. Scale effects refers to the variation in numerical results that may be obtained at different levels of spatial aggregation of data whereas zoning effects are the variation in numerical results arising from the spatial portioning by a fixed level of aggregation. Various specialized methods have been developed to address these problems such as spatial interaction models, statistical reporting units, monte-carlo simulation, simulated annealing and genetic algorithms (Seng et al 2005). Edge effects play an important role in spatial statistical applications and mainly result in spatial censoring (Lawson et al 2001). Lawson et al (2001) introduced several methods for resolving edge effects including utilizing weight relating to the external boundary proximity, guard area and simulating missing data. Rogerson (2001) suggested using buffer zones to include the important features that affect analysis according to the area of interest. Rogerson (2001) recognized the shape and size of the study areas as one of the boundary problems, which can affect measurement and interpretation.

2.3.5 Exploratory Data Analysis and Visualization

Good (1983) described exploratory data analysis (EDA) as a collection of techniques to summarize data properties, identify data trends, detect data errors and unusual features. Hypothesis generation, and may also be used to study the model results and identify influential data effects. Exploratory spatial data analysis (ESDA) is described as a set of techniques to explore spatial data, which involves summarizing spatial data properties, detecting spatial patterns, hypothesis generations and

identifying unusual trends on the map (Seng et al 2005). Exploratory data analysis is aimed at developing hypotheses and makes extensive use of graphical views of the data such as maps, histograms, graphs or scatter plots. It makes certain assumptions about the data and must be robust to extreme data values (Pfeiffer 1996). ESDA techniques are visually and numerically resistant, comprising of EDA techniques and additional methods to analyse spatial relationships (Haining 1998).

Hypothesis testing is considered important in numerical ESDA as the clustering and event concentrations would be studied to identify the significance from a statistical aspect. This serves as an exploratory tool with a null model being proposed and the test statistics are constructed to assist in decision making to either accept or reject the null hypothesis (Haining 1998). The advances in GIS have made it easier to conduct the spatial pattern analysis. Bailey et al (1995) has divided the spatial point patterns tools into four methods – *Kernel estimation, K-function, Nearest Neighbour Distance and Quadrat Methods*. The following sub-sections (2.3.5.1 and 2.3.5.2) discuss the Kernel Estimation and the K function as they are most commonly used in studying spatial clustering (Bailey et al 1995, Gatrell et al 1996).

2.3.5.1 Kernel Estimation

Kernel estimation is an exploratory tool for examining the first-order properties such as global or larger scale trend of point processes (Gatrell et al 1996). It is employed to obtain a smooth estimation of univariate or multivariate probability density from a sample of observation. This method lacks the predictive ability.

If s represents a vector location anywhere in the region, R then the intensity $\lambda(s)$, is an estimate of the intensity of the point pattern at s (Equation 2.1).

$$\hat{\lambda}_{\tau}(s) = \sum_{i=1}^n \frac{1}{\tau^2} k\left(\frac{s - s_i}{\tau}\right)$$

Equation 2.1

$k()$ represents the kernel weighting function which is expressed in standardized form i.e. centred at the origin and having a total volume of 1 under the curve. It is then

centred on s and 'stretched' according to the parameter $\tau > 0$, which is referred to as the bandwidth. The value of τ provides the required degree of smoothing in the estimate. Graphically, it can visualize a three-dimensional function that 'visits' each point s on the fine grid (Figure 2.8). The distances to each observed event, s_i that lies within the region of influence are measured and contribute to the intensity estimate at s according to how close they are to s . A suitable contouring algorithm or some form of raster display may then be used to represent the resulting intensity estimates as a continuous surface showing the R intensity variations (Gatrell et al 1996).

Choosing appropriate bandwidth is considered important as the kernel estimate $\lambda\tau(s)$ is intended to be sensitive to the choice of bandwidth, τ . As this increase, there is more smoothing of the spatial variation in intensity which can result in a flat appearance and neglected local features and when it is reduced, it can yield a 'spiky' estimate. However, it is possible to use a local bandwidth adjustment technique known as adaptive kernel estimation to improve the kernel estimation (Gatrell et al 1996). The kernel estimation closer to the boundary of R may be subjected to the edge effect due to the possibility of neighbours outside the boundary. Constructing a guard area inside the perimeter of R is recommended to address this issue. The points inside the guard area will not be computed but are allowed to contribute the estimation. According to Gatrell et al (1996), kernel estimation is able to produce valuable results in estimating the relative intensity of different types of events.

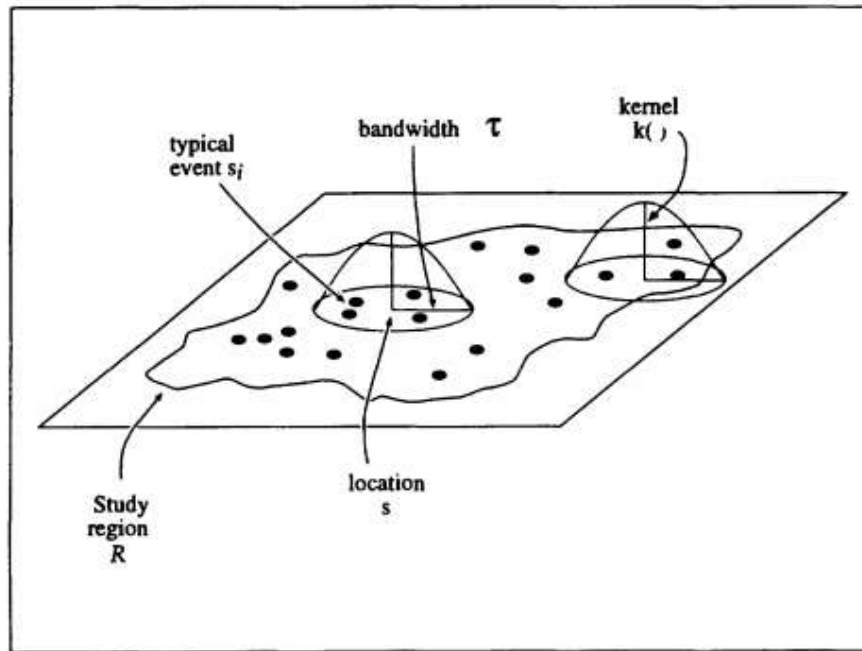


Figure 2.8: Kernel estimation of a point pattern (Source: Gatrell et al 1996).

2.3.5.2 The K function

K function is a very useful technique to estimate the second-order properties i.e. local or small scale effects of the process that gave rise to the data. It describes the spatial dependencies over a wide range of scales. The assumption of stationary when examining the spatial dependencies over a very small scale in region, R is highlighted by Bailey et al (1995). When a point process is stationary and isotropic, there is a close mathematical relationship between the second-order intensity and an alternative characterization of second-order properties known as the K function (Ripley 1981, Gatrell et al 1996).

Equation 2.2 defines the K function, where $E(\cdot)$ denotes expectation, $\#$ means ‘the number of’ and λ is the intensity (or mean number of events per unit area).

$$\lambda K(d) = E(\#(\text{events} \leq \text{distance } d \text{ of an arbitrary event}))$$

Equation 2.2

An estimation of the K function is given by equation 2.3, where R is the area of region and $I_d(d_{ij})$ is an indicator function that has value of 1 when d_{ij} is less than d (Boots et al 1988). When the edge effect is considered, ω_{ij} is included as the conditional probability that an event is observed in R with distance d_{ij} from i_{th} event. Therefore, the final estimation of $K(d)$ is equation 2.4, which is obtained by replacing the unknown density λ with an estimate n/R , where n is the observed number of events.

$$\hat{K}(d) = \frac{1}{\lambda^2 R} \sum_{i \neq j} \sum I_d(d_{ij})$$

Equation 2.3

$$\hat{K}(d) = \frac{R}{n^2} \sum_{i \neq j} \sum \frac{I_d(d_{ij})}{w_{ij}}$$

Equation 2.4

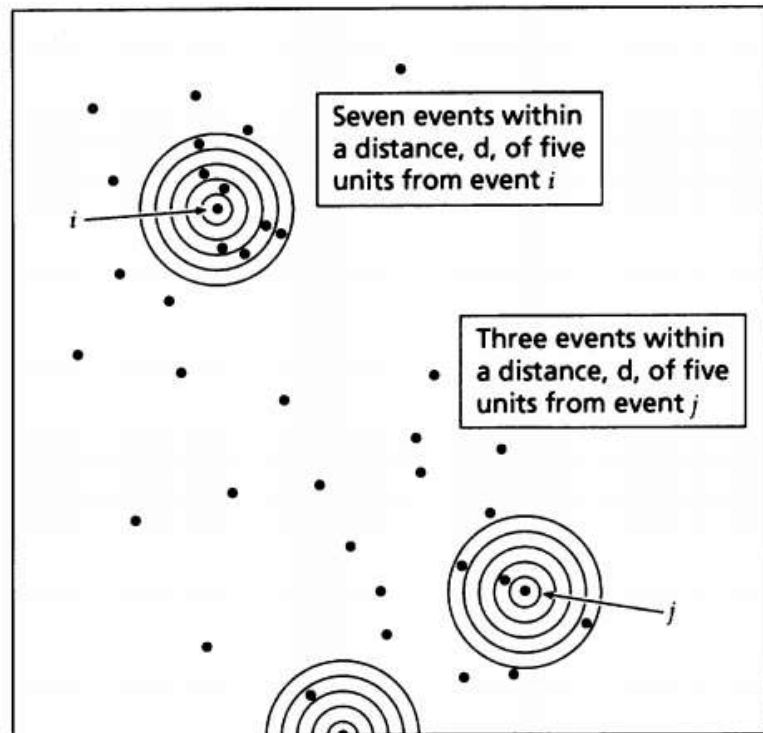


Figure 2.9: Estimation of A K function (Source: Gatrell et al 1996).

Figure 2.9 refers to the visualization of the K function estimate without the edge effect. An event is 'visited' and around this event is a set of concentric circles at a fine spacing is constructed. The cumulative number of events within each of these distance 'bands' is counted. Every other event is assumed to be similarly 'visited' and the cumulative number of events within distance bands up to a radius d around all events becomes the estimate of $K(d)$ when scaled by R/n^2 (Gatrell et al 1996).

2.3.5.3 Visualization as a Method of Exploring Spatial Data

The term visualization in the cartographic literature can be traced back at least four decades (Philbrick 1953, MacEachren et al 1997) and it has an important role in exploratory data analysis, which enables the data being analysed to be seen (Bailey et al 1995). The graphical display of data and other statistics and summary information are considered as the basic tools for seeking spatial trends, hypothesis generation and for evaluation of data into the proposed models. Visualizing the spatial data refers to the mapping in a spatial data analysis context (Bailey et al 1995, Seng et al 2005). MacEachren et al (1990) developed a simple cognitive model to identify key parts of the user display interaction that occurs during exploratory map-based visual analysis. They emphasized on developing cartographic tools that prompt pattern identification and on the potential for visualization errors – the errors that are similar in nature to the Type I and Type II errors associated with traditional statistically-based hypothesis testing.

Visualization of data can be described as maintaining the data points with some smoothing effect to detect the complex spatial patterns (Haining 1998). The comprehensive tools serves as the data analyses supporting tools rather than just producing graphics as the final report (Wise et al 1998). The data visualization approaches has been classified into two areas – rendering and manipulation by Buja et al (1996). Rendering is defined as the process of building the graphic plot which involves the determination of type of information to display and the output plot type. Manipulation involves the operation of individual plots and organization of multiple plots to explore the data. Identification of data set properties (finding gestalt), posing queries and making comparisons are the tasks in data exploration in visualization (Buja et al 1999).

Exploratory analysis of spatial data can be significantly enabled when visualization in geographic space is dynamically linked to presentation of data in attribute space (Andrienko et al 2001). Usage of the brushing technique for linking maps and statistical graphics by simultaneous highlighting of corresponding objects was suggested by Monmonier (1989). Most often linking between maps and dot plots or scatter plots is considered (Buja et al 1986; Dykes 1997). Simultaneous representation of more than two variables can be done using parallel coordinate plots. This kind of graphic is very useful for visual data exploration and data mining (Andrienko et al 2001).

Andrienko et al (2001) introduced a painting-based data visualisation method, which is applicable to several (more than two) comparable attributes called dominant attribute mapping method. This method consists of ascribing an object to a class according to the value of the dominant attribute. The attribute with the largest value is considered dominant and the other approaches involve prior normalisation of attribute values. This method is intended to support the following exploratory activities:

- i) Overall view on spatial co-distribution of attribute values;
- ii) Finding spatial clusters of objects similar to each other in terms of the considered attributes;
- iii) Detecting objects with anomalies or disproportion among the values of the attributes.

In a nutshell, 'visualization' is a comprehensive term that refers to an array of methods that are used to provide insight into data through visual representations and includes the areas of geographic, information, and scientific visualization, which refer to the visual representation and exploration of geographic data, of nonnumeric datasets, and of large, multivariate datasets that use high-end computing, respectively (Knigge et al 2006). Knigge et al (2006) suggests that the data exploration, exploratory spatial data analysis (ESDA), and visualization using GIS and other visualization software, can be employed to facilitate an 'iterative process' in the analysis of data whereby researchers can recursively explore data in order to identify

themes and processes, raise new questions, and begin to build theories. Grounded visualization is suggested by the authors (Knigge et al 2006), which is a set of analyses that could be broadly used in various disciplines. The method is sensitive to scale issues (from local to global and back again) and can integrate mobility. It greatly depends on qualitative and quantitative measures of context (historical and geographical).

Pang (2001) discussed visualizing uncertainty in geo-spatial data in which the author mentioned that there is more than one way to classify how uncertainty can be visualized. First one is by how uncertainty itself is represented; another is by how uncertainty is encoded into visualization. In the second one, there are two general ways of combining uncertainty to a visualization which is either by mapping uncertainty information as an additional piece of data or creating new visualization primitives and abstractions that incorporate uncertainty information. MacEachren (1992) has addressed the difference between data quality and uncertainty. It is suggested that mapping in pairs (side-by-side with a map of uncertainty), sequential presentation in which a user might be warned about uncertainty with an initial map which is followed by a map of the data and bivariate maps in which both the data of interest and the uncertainty estimate are incorporated in the same map are the best practices. Bordoloi et al (2004) presented an interactive visualization technique for spatial probability density function data and implemented a hierarchical clustering and visualization scheme for spatial pdf data in their study which allows for a multiple level of detail exploration of dataset.

2.3.6 Spatial Autocorrelation

“Everything is related to everything else, but near things are related than distant things” –’s First Law of Geography (Tobler 1970). Tobler’s First Law is often considered as the core of spatial autocorrelation statistics, which are quantitative techniques for analysing correlations relative to distance (Rogerson 2001). The concept of spatial autocorrelation may be viewed as a special case of correlation but has a meaning of its own. The correlation statistics were designed to show relationships between or among variables, spatial autocorrelation shows the correlation within variables across georeferenced space. The statistics were initially

designed to identify a theoretical condition in which no spatial autocorrelation is present. (Getis 2008). Hubert et al (1981) defined spatial autocorrelation as - “Given a set S containing n geographical units, spatial autocorrelation refers to the relationship between some variable observed in each of the n localities and a measure of geographical proximity defined for all $n(n - 1)$ pairs chosen from n .” Spatial autocorrelation is often used to measure the spatial dependency and spatial association.

Goodchild (1986) defines spatial autocorrelation as one of the relatively small set of techniques that deals simultaneously with both locational and attributes information. Spatial interaction modelling and location-allocation belong to the same set. A set of spatial features may or may not be similar in attributes, and their proximity will determine how similar they are in spatial location. Spatial autocorrelation often compares the two sets of similarities. Positive similarity occurs when the similar values (either high or low) are located in close proximity to each other whereas negative similarity (or dissimilarity) occurs when features which are close together in space tend to be more dissimilar in attributes than features which are further apart. Zero similarity occurs when the attributes are independent of location. The degree of spatial autocorrelation of a pattern is dependent on the scale. Goodchild (1986) notes the practical importance of spatial autocorrelation is that it provides a type of information about a spatially distributed phenomenon which is not available in any other form of statistical analysis. This information is important for appropriate interpretation of the data.

Fotheringham et al (2002) says that the spatial autocorrelation is measured by several statistics with slightly different formulations; however, they are all incorporated within geographical weighing, which indeed represents the localised versions of general statistics. Global statistics attempt to characterize the stable pattern of spatial dependence for the entire dataset (Unwin 1996) and local statistics are referred to as spatial disaggregation's of global statistics (Fotheringham et al 2002). A global model is calibrated using the data which is equally weighted and assumed to be constant over space (stationary), where the local variations in relations are unobserved. Moran's I is the most widely used global statistic to study the spatial dependency of the data (Moran 1950, Getis et al 1992). The local statistics recognize

the association between a single point and its neighbours within a specified distance and are able to identify a localized pattern where no global pattern has been detected using an autocorrelation statistic (Getis et al 1996). Fotheringham et al (2002) suggests that the local models capture the *non-stationary* process (which varies across space) and spatial dependence.

2.3.6.1 Moran's I

Moran's *I* coefficient is a very well know global statistic which is used to measure the degree of similarity between each areal unit and its contagious neighbours of autocorrelation. For a spatial proximity matrix *W*, spatial correlation in attribute *y_i*, the Moran's *I* is summarised in equation 2.5.

$$I = \frac{n}{S_0} \frac{\sum_{i=1}^n \sum_{j=1}^n w_{i,j} z_i z_j}{\sum_{i=1}^n z_i^2}$$

Equation 2.5

Where,

Z_i is the deviation of an attribute for feature 'i'

W_{ij} is the spatial weight between the features 'i' and 'j'

n is equal to the total of features

S₀ is the aggregate of all the spatial weights

'Moran's *I*' calculates the mean and deviation of any observation from the mean and follows the comparison of the value at any location with the value at other locations. The *W_{ij}* is a contiguity matrix, where if the zone *i* and *j* are adjacent, it will receive a weight of 1 and vice versa. The weighted Moran's *I* is similar to the correlation coefficient, which varies between -1.0 to +1.0 and the result is the sum of the cross-product values at different locations. The higher *I* value indicates more spatial autocorrelation compared to the lower *I* value. The negative value closer to 0 describes the lack of spatial dependencies. The *I* value above the theoretical mean depicts a positive autocorrelation and value below the theoretical mean depicts a

negative autocorrelation. This method does not pinpoint the local effects and the results are highly dependent on the spatial unit (Getis et al 1996, Levine 2002).

2.3.6.2 Getis-Ord Local G

The G_i statistic is known to be useful for identifying “hot and/or cold spots” and to check for heterogeneity in the dataset. G_i statistics are the ratio of the sum of values in neighbouring locations, defined by a given distance, to the sum over all observations (Getis et al 1992). The $G_i(d)$ is defined by Getis et al (1992) as in the equation 2.6.

$$G_i(d) = \frac{\sum_j w_{ij}(d)x_j}{\sum_j x_j}, j \text{ not equal to } i$$

Equation 2.6

Where $\{\omega_{ij}(d)\}$ is a symmetric one/zero spatial weight matrix with ones for all links defined as being within distance d of a given i ; all other links are zero including the link of point i to itself. A slightly different form of G_i was suggested by Ord et al (1995), $G_i(d)$ originally proposed for elements of a symmetric binary weights matrix, was extended to variables that do not have a natural origin and to non-binary standardised weight matrices (AURIN 2016). The statistic for each region i is defined as equation 2.7.

$$G_i(d) = \frac{\sum_j w_{ij}(d)x_j - W_i \bar{x}(i)}{s(i) \{[(n-1)S_{1i}^*] - W_i^{*2}/(n-1)\}^{1/2}}, j \neq i$$

Equation 2.7

Where ω_{ij} is the spatial weight matrix element, X_j is the variable and d is the distance threshold from i . Similarly, if ω_{ij} is included and not equal to 0, the standardized G_i statistic is given in equation 2.8.

$$G_i(d) = \frac{\sum_j w_{ij}(d)x_j - W_i \bar{x}}{s \{[(nS_{1i}^*) - W_i^{*2}]/(n-1)\}^{1/2}}, \text{ all } j$$

Equation 2.8

The Getis-Ord G_i is a statistic for local spatial association and their individual components are not related to the global statistic of spatial association (G). The results firstly produce the G_i ; for each area i as a standardised z-value. Getis et al (1992) argued that inference, as with global measures are based on calculating a standardised value and comparing this against a null which is assumed to follow a normal distribution. However a normally distributed null may not be an appropriate assumption, as Local G_i are not independent of each other by design (Ord et al, 1995) (AURIN 2016).

2.3.7 Spatial Data Modelling

Spatial data modelling in epidemiology involves GIS integration with standard statistical and epidemiological methods. GIS has the increased spatial statistical capabilities to accommodate the epidemiological data, perform spatial statistical analysis, display results – mapping and modelling the patterns that occur over time and space. These capabilities enable researchers, scientists and academicians to evaluate the statistical analysis and prediction models. Rogerson (2001) defined a model as a tool to simplify the relationship between variables for further study. By studying a model, critical information could be derived to either support or reject the null hypothesis.

Spatial modelling is undergoing its own shifts of emphasis and bringing with it new challenges for spatial data analysis as to how to assess correspondence between model output and real data. Goodchild et al (2004) says that the spatial data analysis have been developed for, and implemented in, many different contexts. Haining (1987) used unilateral spatial auto regressions to estimate population and income multipliers for towns organized in a central place system. Anselin (1988), treating the field as a branch of econometrics (spatial econometrics), developed a statistical modelling strategy, with software to implement the methodology that follows the strategy used in certain forms of time-series econometric modelling. There are numerous examples of the use of spatial regression modelling in a wide variety of fields (Goodchild et al 2004).

Haining (1998) mentioned that the variation between observed quantities at different locations must be taken into consideration in statistical models for spatial data

through the mean or the correlation structure. Fitting a statistical model to data enables the potential to further research the parameters. The modelling process starts with determining a model consisting of signal and noise and probability distribution. A likelihood function should be employed in the analysis and the joint probability of data is assumed to have fixed unknown values. In general terms, data modelling can be distinguished into two areas – descriptive and explanatory. Descriptive modelling describes the spatial pattern and explanatory modelling is a mathematical expression involving the predictions. The data in the descriptive modelling involves only one variable with the locations and is described by a simple functional representation of variation (it could be as few parameters as possible). Explanatory data modelling consists of many variables and deals with the variation of covariance and predictors (Haining 1998). Multi-agent modelling is another system-wide level which allows the individuals to migrate around the space responding to global and local conditions in different segments of the space (Goodchild et al 2004).

The aim of the descriptive modelling is to summarize the spatial variation of response variable without the existence of covariance in the model. The models for continuous valued variables include trend surface and covariance and semi-variogram modelling. Auto-logistics, auto-binomial and auto-poisson models are used to model discrete value area data. Explanatory models describe the interaction between dependent and independent variables. Some descriptive models can be extended to exploratory models by including the predictor variables or covariates. In the modelling, spatial data incorporates the spatial dependence between the data which improves the power of the model. Initially, an exploratory analysis is conducted with the aim of identifying the structure of dependence in the data. There are two basic types of exploratory modelling, which is spatial regression that allows the incorporation of the spatial effect and those of Global form and those of Local form (Lopes et al 2007, Fotheringham et al 2000).

2.3.8 Regression Analysis

Regression analysis is a statistical tool to investigate the relationships between variables. The investigator seeks to ascertain the causal effect of one variable upon another. The data is assembled to study the underlying variables of interest and

employs regression to estimate the quantitative effect of the causal variables upon the variable that they influence. It assesses the “statistical significance” of the estimated relationships i.e. the degree of confidence that the true relationship is close to the estimated relationship (Skyes 1992).

A simple linear regression examines the linear relationship between two continuous variables - one response (y) and one predictor (x). A linear regression line is denoted in equation 2.9 of the form, where X is the explanatory variable and Y is the dependent variable.

$$Y = a + bX$$

Equation 2.9

The slope of the line is b, and a is the intercept (the value of y when x = 0). When the two variables are related, it is possible to predict a response value from a predictor value with better than chance accuracy. Regression provides the line that "best" fits the data. This line can then be used to either examine how the response variable changes as the predictor variable changes or predict the value of a response variable (y) for any predictor variable (x). The multiple linear regression examines the linear relationships between one continuous response and two or more predictors (Minitab 2016). The multiple linear regression model is given in the equation 2.10 where \hat{Y}_t denotes the “dependent” variable and X_1, \dots, X_k denote the “independent” variables, with the value of variable X_k in period t (or in row t of the data set) denoted by X_{kt} . The error in the model is assumed to be independent without the spatially correlated measurement error. Other unobserved predictors are also considered to be spatially uncorrelated.

$$Y_t = b_0 + b_1 X_{1t} + \dots + b_k X_{kt}$$

Equation 2.10

The following assumptions must hold when building a linear regression model (Christensen 1997).

- i) The dependent variable must be continuous. Linear regression is not the correct method to predict a categorical variable.
- ii) The data modelling meets the "iid" criterion. That means the error terms are independent from one another and identically distributed.
- iii) The error term is normally distributed with a mean of zero.

2.3.8.1 Ordinary Least Square (OLS) Regression

OLS is well known among all the regression techniques and it is a global regression technique. This technique is often mentioned as a straight forward method and is the proper starting point for all the spatial regression analyses. A global model of the variables that are needed to be predicted will be provided and this creates a single equation to represent this process. This is a method to estimate the parameters and is based on set of assumptions (Bailey et al 1995). The mathematical equation of an OLS regression model for multiple explanatory variables is given in equation 2.11.

$$Y = \alpha + \beta_1 X_1 + \beta_2 X_2 + \beta_3 X_3$$

Equation 2.11

The OLS regression model can be extended to include multiple explanatory variables by simply adding additional variables to the equation. The form of this model is the same as with a single response variable (Y), but in the above equation 2.11, Y is predicted by multiple explanatory variables (X1 to X3) and for n variables it is X1 to Xn (Hutcheson 2011).

The following assumptions should be met for most precise OLS regression (Minitab 2016):

- i) The regression model is linear in the coefficients. Least squares can model curvature by transforming the variables (instead of the coefficients). You must specify the correct functional form in order to model any curvature.
- ii) Residuals have a mean of zero. Inclusion of a constant in the model will force the mean to equal zero.

- iii) All predictors are uncorrelated with the residuals.
- iv) Residuals are not correlated with each other (serial correlation), have a constant variance and are normally distributed.
- v) No predictor variable is perfectly correlated ($r=1$) with a different predictor variable. It is best to avoid imperfectly high correlations (multicollinearity) as well.

The common approaches in making sure the above assumptions are met includes examining residual plots, using lack of fit tests, and viewing the correlation between predictors using the Variance Inflation Factor (VIF).

The simplicity of the model makes it appropriate as a starting method; however there are certain limitations for this model. OLS results are only accurate if the data and the regression model satisfies all the assumptions inherently required by this method. This method cannot be efficient when variables have same values. The results of an OLS regression depend on the spatial autocorrelation and statistically significant spatial autocorrelation of regression residuals almost always indicates one or more key explanatory variables are missing from the model. The main limitation of the OLS analysis is that the results cannot be mapped. When misspecification is the result of trying to model non-stationary variables using a global model (OLS is a global model), then Geographically Weighted Regression may be used to improve predictions and to better understand the non-stationarity (regional variation) inherent in the explanatory variables (ESRI 2013).

2.3.8.2 Geographically Weighted Regression (GWR)

For any spatial analysis, knowledge regarding the extent of spatial association in the data is very important (Getis et al 1996). There are tools being used such as Moran's I and Geary's C to determine the spatial association of the variables, however it is necessary to acquire a technique to measure the spatial dependency of local statistic. Correlation and regression techniques are often used in investigating the relationships between the events and their influencing factors (Haining 1998, Seng 2005). GWR measures the spatial dependency i.e. non-stationary in a dataset and summarises relationship between the explanatory variables by local regression

parameters (Fotheringham et al 2002). It is a multivariate approach to analysing spatial data (Fotheringham et al 2002, Brunson et al 1996).

Mathematical and Statistical Algorithm

GWR technique is easily understood because of its traditional regression based framework and it is an extension of global multiple regression - OLS. GWR analysis is always an improvement (Malczewski 2004) over the global regression analysis (OLS). The mathematical equation for this regression model is given in equation 2.12.

$$y_i = a_0(u_i, v_i) + \sum_k a_k(u_i, v_i)x_{ik} + \sum_i$$

Equation 2.12

Where (u_i, v_i) represents the co-ordinates of the i -th point in space and $a_k(u_i, v_i)$ is a realisation of the continuous function $a_k(u, v)$ at the point i (Fotheringham et al 1997, Charlton et al 2006). The global model is considered as a special case of GWR model, where the parameter surface is assumed to be constant over space. In GWR model calibration, observed data near to point i have more influence than the data located farther from i , in the estimation of the $a_k(u_i, v_i)$'s. The weighted least squares provide basics for understanding of GWR operation. Algebraically, the GWR estimator is given in equation 2.13.

$$a(u_i, v_i) = (X^t W(u_i, v_i) X)^{-1} X^t W(u_i, v_i) y$$

Equation 2.13

Where $W(u_i, v_i)$ is an n by n matrix for which the off-diagonal elements are zero and the diagonal elements denote the geographically weighting if the observed data of i (Charlton et al 2009). $X^t W(u_i, v_i) y$ is the geographically weighted variance-covariance matrix and y is the vector of the values of the dependent variable. The statistical interference of GWR model helps us to determine whether an observed pattern is due to random variation or a true spatial trend in the local model.

GWR technique is able to assess error residuals by comparing the measured and predicted values. Residuals for location without the measured data and the associated confidence information are provided through the goodness of fit statistics (R-Squared value). In global regression models, such as OLS, results are unreliable when two or more variables exhibit multicollinearity. GWR builds a local regression equation for each feature in the dataset. If the values in the model for a particular explanatory variable cluster spatially there will be problems with local multicollinearity. If categories cluster spatially, there is strong risk of encountering local multicollinearity issues and results in the presence of local multicollinearity are unstable. A regression model is considered misspecified if it has a missing a key explanatory variable and it is recommended to identify this variable (using OLS). A model is misspecified if there is statistically significant spatial autocorrelation among the regression residuals and/or unexpected spatial variation among the coefficients of one or more explanatory variables (ESRI 2016).

Testing and Visualization

The results of GWR can be evaluated by monte-carlo simulation test. The tests will determine the significance level of the GWR model. Visual Representation of geographical distribution is referred as mapping and disease mapping is the representation of disease locations and summary/statistics for a specific group of individuals in their geographical distribution (Lawson et al 2001) and they may reveal important patterns (Elliott et al 2004). The possibility of visual representation of the results is an added advantage for GWR technique.

2.3.9 Geographical Information Systems (GIS) in Epidemiology

Use of GIS technology in epidemiological and public health studies gained momentum after researchers started using it for more than visual representations i.e. maps. Apart from the statistical analysis, epidemiologists have traditionally used maps to analyse the relationship between location, environment and disease. GIS, especially in the last decade emerged as an innovative, important and even essential tool in epidemiology due to its capabilities in studying the above mentioned relationships as well as spatial analysis and visualization capabilities. As GIS

involves a lot of interdisciplinary work, the appropriate methods remain as the important part of the research. There are a number of famous researches that contributed in finding out the key issues in the cases of deadly diseases such as cholera, malaria, rabies, dengue fever and other infectious and non-infectious outbreaks around the world.

GIS applications in spatial epidemiology and disease surveillance range from, but not limited to monitoring vector-borne diseases, chronic disease (Beck et al 1994, Muttitanon et al 2002, Ali et al 2003, Seng et al 2005, CDC GIS 2012), identification of high risk locations and populations (Bithell 2000, Baum et al 2010), addressing community health problems such as cancers incidence (McCall et al 2003) and studying healthcare services accessibilities and planning (Luo et al 2003). A research survey conducted on the studies of HeVes in the south-western United States revealed that exploring the virus spreads in an epidemiological aspect with targeted study helped the public health officials in reducing the risk of infections by forecasting the locations and their future outbreak occurrence levels. These researches are categorised as cost effective long run theories (Calisher et al 2006). Public health studies, disease mapping and monitoring programs started to employ GIS technology to observe the spatio-temporal patterns and make policy implications (Perry 1994, Han et al 2003, Wiafe et al 2007).

A research on malaria in Kenya led to an outcome that suggested that the climate affects the transmission of the disease. This research incorporated climate-based statistical model and provided a basis for an estimate of the annual morbidity and mortality burden in children (Snow et al 1998). This was a great outcome for a rational disease control. Another study used GIS to map three different diseases – HIV, tuberculosis and malaria in Africa. The study observed the general trends of the diseases and their impact on the public health services in Africa. The study was carried out as part of health planning and management strategy and they employed exploratory data analysis for their study (Tanser et al 2002).

GIS is used as a management and policy implication tool to make decisions on the allocation of the resources, prioritization of control areas, planning and management of field operations for African animal *trypanosomosis* in sub-saharan Africa. Various

aspects such as abundance, distribution and mapping were studied using GIS. The research was conducted on local and national level to make sure the policies are technically feasible (Hendrickx 2001). A Bayesian geo-statistical model has been developed to predict the intensity of the infection with *Schistosoma Mansoni* in East Africa, a parasite disease. To study the morbidity, the study combined the data of school children and environmental data for the identification of risk factors. It explained the geographical heterogeneity in infection intensity and developed a predictive map (Clements et al 2006). Various studies were conducted on the neglected tropical diseases such as *Chagas* in South America, human African *trypanosomiasis*, *leishmaniasis*, *lymphatic filariasis*, *onchocerciasis*, *schistosomiasis*, *soil-transmitted helminthiasis* and *trachoma* by Brooker et al (2007). The main aim of their research was to study different parasite species in varying transmission settings for an improved understanding of spatial risk factors, behavioural, demographic and epidemiological risk factors. This research was planned to serve as a guide for regional and national level integrated disease control. Authors stated that the geo-spatial techniques needs attention to make them go hand-in-hand with public health studies (Brooker et al 2007).

Descriptive epidemiological analysis study using GIS of the cholera outbreaks in Abeokuta, Nigeria by Shittu et al (2010) revealed that the municipal water consumption was found to be associated with illness. The epidemiological surveillance data showed a total of one hundred and fifteen cases and 11 deaths with case fatality rate of 9.6%. The age group of 15 years and above accounted for 68.3% of the cases and 90.9% of the deaths. The post epidemic environmental investigation showed progressive contamination along distribution points. The study states that cholera is still a major cause of morbidity and mortality among youth and ageing population in Nigeria.

Eisen et al (2010) discussed the advances in mapping and GIS technologies and their progress in the fields of spatial and space-time modelling in preventing and controlling emerging vector-borne diseases. The benefits of spatial and space-time risk modelling mentioned in the study includes identification of risk patterns for exposure to vectors and vector-borne pathogens, and an improved understanding of how socioeconomic and environmental factors affect the vectors and influence

transmission of their associated pathogens. The study has found that the GIS-based spatial and space-time risk modelling have proven effective tools to develop risk surfaces (maps) to inform policy makers, control programs, and the public. The study emphasized on the moving of GIS technology and modelling approaches from the research arena into operational vector and disease control programs.

A case study by Lessler et al (2016) revealed that the global clustering statistics are an important tool for spatial analytics that can be used to better understand the transmission of an infectious disease. The τ -statistic presents one approach for measuring the global clustering and has an easy interpretation. It overcomes challenges encountered when analysing infectious disease data. The authors stated that the τ -statistic provides a valuable tool to capture spatial dependence in epidemiological terms but it should be used alongside existing measures of spatial dependence, in particular as it provides a qualitatively different tool to other approaches. Grabowski et al (2014) analysed the dynamics of HIV transmission in Uganda using spatial clustering statistics technique. The results suggested that the frequent HIV introductions into communities play a critical role in ongoing HIV incidence and showed limited spatial clustering of HIV cases outside of households, multiple circulating HIV viruses within communities, and a significant proportion of incidence resulting from extra-community partnerships.

Field et al (2015) studied the spatio-temporal aspects of HeV infection in eastern Australia. The study aimed to identify the key spatial and temporal factors associated with excretion in flying foxes over a 2300 km gradient from northern QLD to southern NSW which encompassed all known equine case locations to improve spillover risk prediction and exposure risk mitigation strategies, and thus better protect horses and humans. This study employed a generalised linear model to investigate spatiotemporal associations with HeV detection in 13,968 samples from 27 roosts. A non-linear relationship was identified between the mean HeV excretion prevalence and five latitudinal regions. The study successfully identified the highest HeV positivity in the areas with black or spectacled flying foxes and nil to very low positivity rates occurred in exclusive grey-headed flying fox roosts. Little red flying foxes were significantly not related to the source of virus. The study also identified a

consistent and strong relationship between winter seasonality and the virus excretion in southern QLD, northern NSW and central NSW regions.

Smith et al (2014) investigated the flying fox species density as a possible spatial risk factor for HeV infection in horses in eastern Australia. The study aimed to inform the risk mitigation by identifying spatial and environmental risk factors for equine infection using multiple analytical approaches to investigate the relationship between plausible variables and reported HeV infection in horses. The study employed techniques such as spatial autocorrelation, Getis-Ord G_i^* and geographically weighted regression. The study showed black and spectacled flying foxes are strongly positively correlated to equine case locations, suggesting these species are more likely a source of infection of HeV for horses. The horse density, climate and vegetation variables were not found significant risk factors in the study. However, the authors advised that their GWR model suggests additional unidentified risk factors exist at the property level.

McCallum's (2016) research concentrated on developing models that will enable prediction of flying fox colony dynamics, patterns of high prevalence and intensity of HeV infection in such colonies, and the subsequent risk of transmission of HeV to horses. A spatial model of flying fox colony dynamics was developed and it detected the evidence that 'pulses' of HeV activity in south east QLD are associated with colony size, which in turn can be predicted using remotely sensed satellite data. The research suggests that the models will be based on data analysis of flying fox colony sizes through time and also with the information on dynamics of prevalence of infection at a colony level.

A research on emerging infectious diseases is conducted to understand their effect on socio-economic, environmental and ecological factors of 315 diseases emerged during 1940 and 2004 found that there are significant correlations with the above factors and based on those, it is estimated that the hotspot regions could be identified. The research concluded with a message that global resources to counter disease emergence are poorly allocated (Jones et al 2007). Another case study on the infectious diseases across New Brunswick, Canada and Maine, USA, showed the effectiveness of surveillance system and cross-border visualization, analysis and

sharing of the disease information through interactive maps via distributed network. This project developed service oriented architecture for online disease mapping that is interoperable. The output of this research is a strong message that the development of standard health services and spatial data infrastructure can enhance the efficiency of the health surveillance (Gao et al 2008). A case study on forecasting disease for increased preparedness talked about the modelling of the diseases based on the statistical relationships established between past case numbers and environmental predictors (Myers et al 2000). It mentioned that a wide possible range of environmental and other factors should be considered as there are high chances that these relationships would persist into the future. These models can be extremely powerful and the reason why diseases like cancer adopted statistical route.

The large volume of literature relating to the use of GIS for medical geography purposes includes but not limited to Albert et al (2000), Cromley et al (2002), Bazemore et al (2003), Jerrett et al (2003), Kaushal et al (2003), and Busgeeth et al (2004). The last aforementioned studied the epidemiological issues in conjunction with GIS. Although there are several GIS applications for epidemiological applications (Colak 2005, Ulugtekin et al 2007), there is always a need for proper model which can investigate the significant factors of the disease. Disease mapping, location analysis, spatial statistics and modelling are very well supported by GIS, but there is pressing need to develop an analysis tool that can appropriately conducts fore-epidemiological research and analysis (Ogbonna 2012).

2.3.10 Summary

The ability of GIS to integrate and manipulate complex data has emerged it as a powerful tool in epidemiological studies. Use of GIS technology in epidemiological and public health studies gained momentum after researchers started using it for more than visual representations i.e. maps. GIS in epidemiology has been tremendous in understanding the disease in a different dimension. With the assistance of this powerful tool, the disease clusters could be identified and other influencing factors such as environmental, socio economic and climatic could be linked to the diseases. While geographical visualization serves the need to reveal the spatial patterns, the statistical awareness in GIS determines the significance of these

patterns. GIS technology is being widely used for disease monitoring, research hypotheses generation and identifying populations at risk for its high capability in data interpretation, manipulation and modelling (Seng et al 2005, Gupta et al 2003). It serves as an effective tool for spatial analysis, modelling and visualisation of epidemiological and environmental data; and recent studies have shown significant and increasing use of GIS applications in public health and epidemiology (Shittu et al 2010, Busgeeth et al 2004 and Gupta et al 2003). The powerful analytical modelling and mapping capabilities of GIS can serve as a good decision-support and decision-making tool for disease investigations, monitoring, simulation, predictions, preventions and resource allocations (Davenhall 2002).

In summary, spatial and ecological data together with epidemiological data can enable a new potential to analyse the variables which play an important role in disease transmission and discovering underlying spatial patterns. This is essential for health service planning, policy implications, decision making and ongoing disease surveillance. GIS in epidemiology enables the researchers to isolate the high disease prevalence areas, identify the population at-risk, resource and budget allocations. In the case of rare disease outbreaks like HeV, GIS would be perfect as a tool to identify the main causes (geographical, environmental and other factors) of outbreaks for disease monitoring. This would help in developing prediction models and generating warning systems in the study area. The next chapter discusses the epidemiology data and study area for the research of HeV outbreaks investigation in Australia. A detailed methodology from data preparation, integration and management to spatial analysis, modelling, mapping and predictions is covered in chapter three.

3. Chapter Three – Methodology

3.1 Introduction

This chapter details the study area chosen and the data collected to study the HeV outbreak events. Data plays a major role in any information systems related research. This section provides all the necessary information in regards to the data collected from various resources, how it was manipulated and managed to achieve the results. The spatial analyses, modelling and visualization techniques employed in this study are discussed in detail in this chapter. The methodology used to accomplish the research aim, questions and objectives described in chapter 1 are discussed in the following sections. In general, this chapter covers the spatial techniques and regression analysis of HeV outbreaks and its influential factors in the study area.

3.2 Study Area

The study area for this research is limited to south east Queensland (SEQ), Australia. The area is chosen based on the data resources available and the time frame for a detailed study on the HeV outbreaks and its influential factors. SEQ is a geographical, political and administrative region of the Queensland State, Australia (Department of Environment and Energy 2013). The population of SEQ is estimated at 3.4 million, which is majority of the Queensland state's population (Queensland Treasury 2011). SEQ extends 240 kms from Noosa in the north to the Gold Coast, New South Wales border in the south, and 140 kms west to Toowoomba. The area covers up to 22,420 sq. kms and consists of 11 local government areas. Figure 3.1 shows the Queensland Map with an inset map showing the SEQ region.

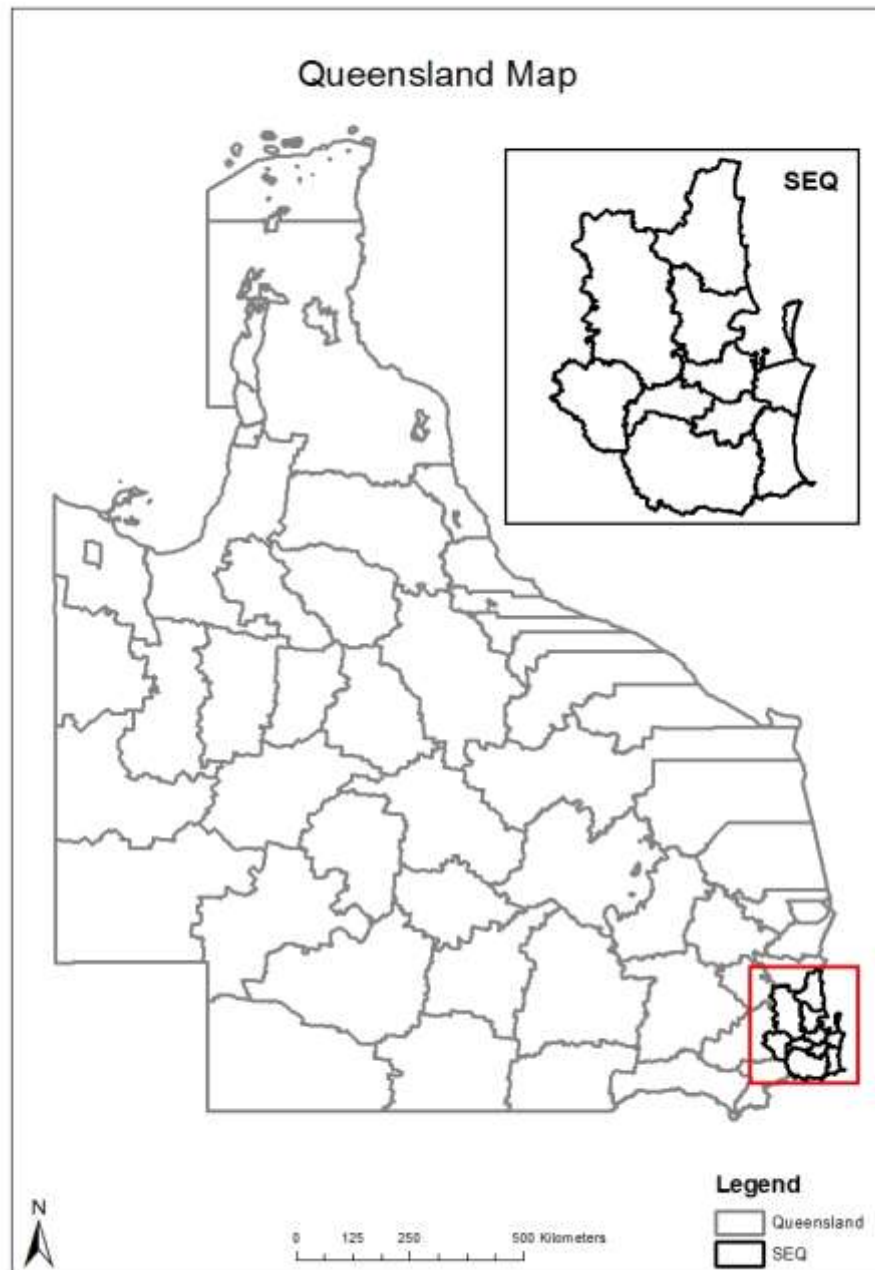


Figure 3.1: Map of Queensland with an inset map showing SEQ region.

SEQ is considered as the economic, social and cultural hub of Queensland, which has been a subject to sustained high levels of growth since the early 2000s (Department of Infrastructure, Local Government and Planning (DILGP) 2017).

According to the DILGP (2017), the South East Queensland Regional Plan includes the local government areas of:

- i) Brisbane City Council
- ii) City of Gold Coast Council
- iii) Ipswich City Council
- iv) Lockyer Valley Regional Council
- v) Logan City Council
- vi) Moreton Bay Regional Council
- vii) Noosa Shire Council
- viii) Redland City Council
- ix) Scenic Rim Council
- x) Somerset Regional Council
- xi) Sunshine Coast Council
- xii) Toowoomba Regional Council (Part of)

The major cities in SEQ region include Brisbane, Gold Coast and Sunshine Coast. The Toowoomba city is included in both SEQ region and within Western Downs region due to its importance in both regions as a gateway city providing access to the west of the state. The Toowoomba city was excluded from the study due to the availability of limited data. Some government entities (State Library of Queensland, Queensland Water Information etc.) does not include Toowoomba city as part of SEQ region in their data sets regardless of its inclusion in the regional plan (2009), which made it challenging to obtain the relevant data with Toowoomba city included for the study. Figure 3.2 shows the map of the study area and the local councils in the region.

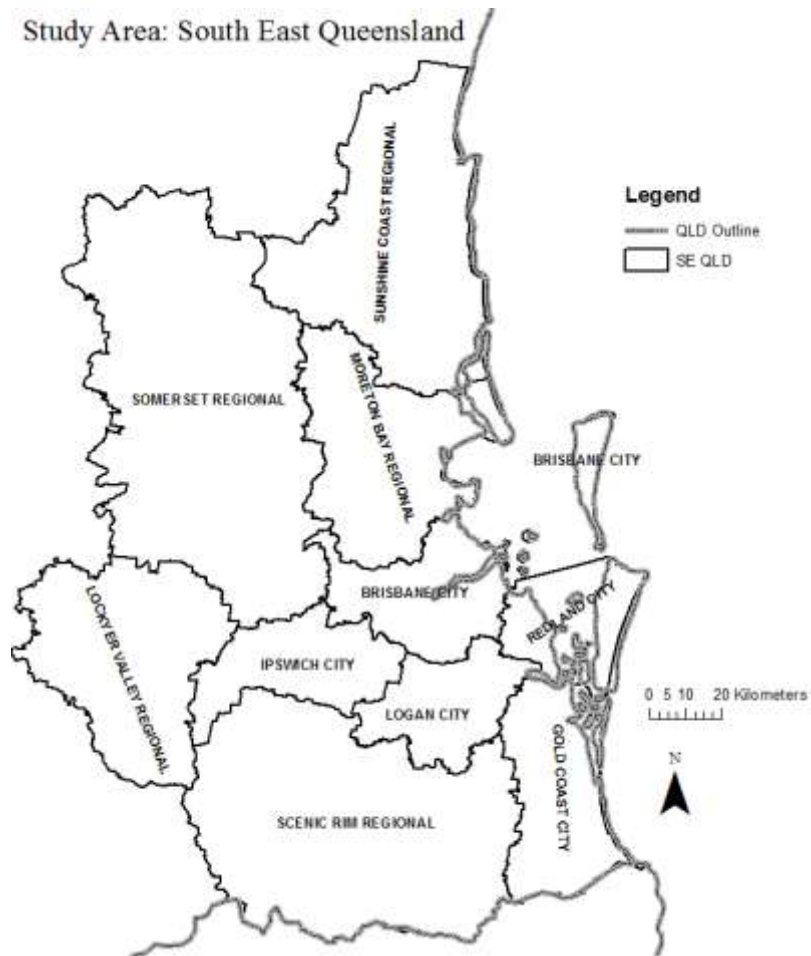


Figure 3.2: Map of the study area and the local councils in the region.

3.3 Data Collection, Processing and Integration

3.3.1 Data Collection

The data required for this research was collected from various sources. Once the data was collected, it was manipulated and integrated into the GIS system. Spatial data usually consists of administrative boundaries, point/vector data (longitude and latitudes), remote sensing imagery (raster data) and topographic maps. This research used a combination of both vector and raster datasets. The data without any spatial reference to it is known as aspatial data. Table 3.1 summarizes the major data sets used in this research.

Table 3.1: Summary of the major data sets obtained.

Data	Format	Source	Year Obtained
HeV Outbreak Incidents	Excel	Queensland Centre for Emerging Infectious Diseases	2014 – Data Sharing Agreement
Registered Equine Properties	Excel	Queensland Centre for Emerging Infectious Diseases (DAFF)	2014 – Data Sharing Agreement
Flying Foxes Data	Excel	Department of Environment and Heritage Protection, Queensland	2014 – Data Sharing Agreement
Queensland Administrative Boundary	Shapefile (Vector)	Queensland Government Data	2014
Queensland Local Government Areas	Shapefile (Vector)	Queensland Government Data	2014
Major Vegetation Groups	Raster (Scale: 1:250k)	Department of the Environment and Energy	2015
Major Vegetation Subgroups	Raster (Scale: 1:250k)	Department of the Environment and Energy	2015

The vegetation data obtained consists of the raster data for the whole of Australia. The major vegetation groups (MVG) and major vegetation subgroups (MVS) data for the SEQ has been extracted from the above datasets. Department of Environment and Energy states that the information is based on the data in the National Vegetation Information System, other mapped vegetation information, expert advice and key references in regards the dataset’s accuracy. The grid size was calculated by default in ArcGIS ‘Spatial Analyst’ during the analysis based on the original resolution. ESRI highly recommends the usage of the in-built grid size calculator formula for the third-party datasets. Apart from the major data sets defined above, the other data (aspatial) such as foraging range, pregnancy/birth periods and other relevant information has been obtained from Wildlife Queensland (2016) and has been appropriately cited where relevant. Figure 3.3 shows the flowchart of the GIS database creation for the research.

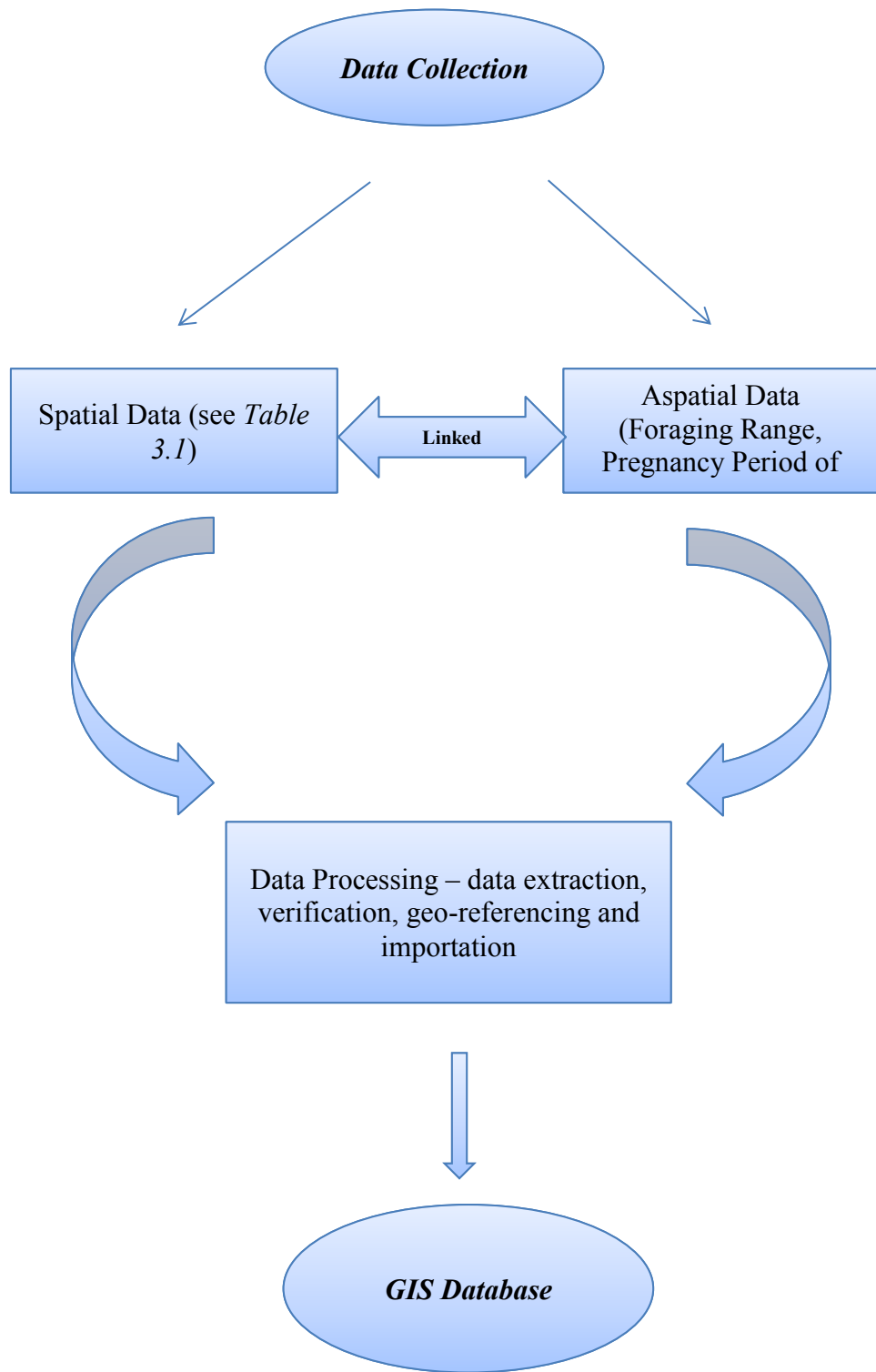


Figure 3.3: GIS database creation workflow.

3.3.2 Data Processing and Integration

This section details the data processing and integration steps undertaken for the study. The HeV incident data, flying fox data and equine data used in this are explained.

HeV Incidents Data

In total, 11 outbreak incidents occurred between the years 2006-2011 were considered in this study. An additional 3 outbreak events that occurred in the year 2012 were included in the vegetation analysis. Table 3.2 shows the outbreak incidents studied. The incident that occurred in the year 1994 in the suburb of Brisbane was not included in the study considering the relevance of the current flying fox data to it.

Figure 3.4 shows the HeV outbreak events in the study area considered for the research. For a full list of outbreak events provided by Queensland Centre for Emerging Infectious Diseases, see *Appendix 1*.

Table 3.2: HeV outbreak incidents considered in the study.

Year of Occurrence	Month of Occurrence	Place of Occurrence
2006	June	Peachester
2008	June	Redland Bay
2010	May	Tewantin
2011	June	Logan Reserve
2011	June	park Ridge
2011	June	Boonah-Mt. Alford
2011	June	Beaudesert-Biddaddaba
2011	July	Beaudesert-Kerry
2011	July	Boondall
2011	August	Gold Coast-Hinterland
2011	October	Beachmere

HeV Outbreak Events

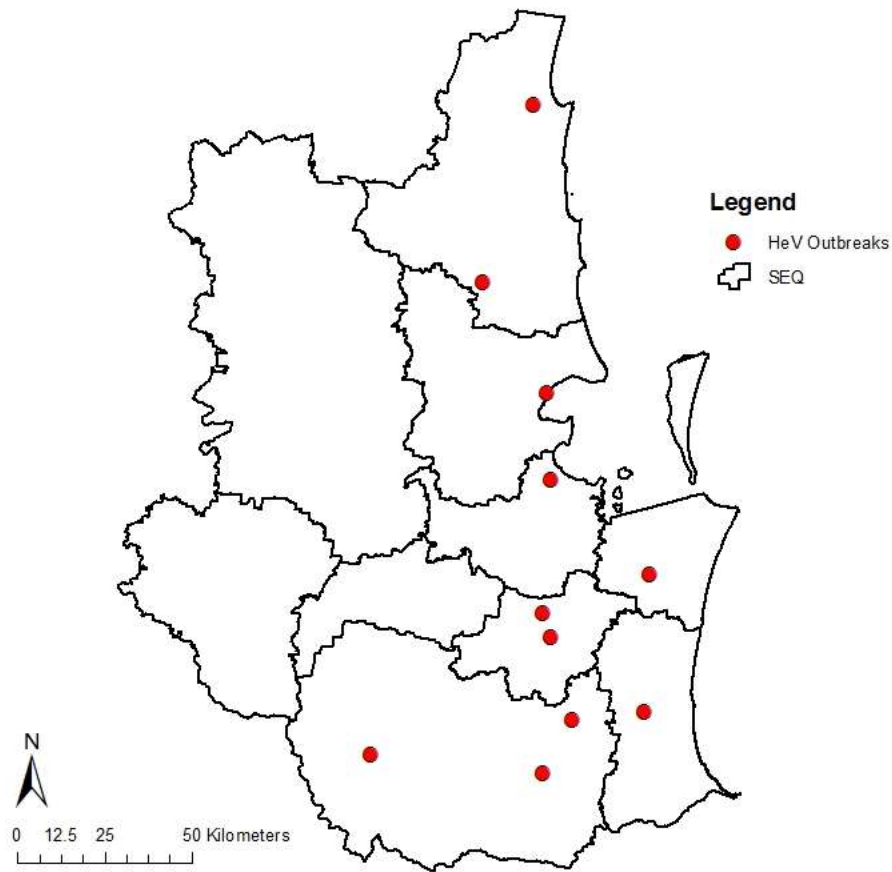


Figure 3.4: HeV outbreak events in the study area.

Flying Fox Data

The flying fox data contained detailed information about the size of each camp, species information and the type of the roosting site. There are approximately, 5,200 roosting sites in Queensland. The flying fox camps were categorized into six types - permanent continuous use, permanent seasonal use, temporary occupied, temporary unoccupied, abandoned and destroyed. Abandoned and destroyed roosting sites were excluded from the study with most of sites having no flying fox population. Based on our three-year observation, local foxes remain in the same camp site all year round.

Nevertheless, the data was carefully selected and edited for the analysis making sure there is a presence of all three species in each site in significant numbers and reflecting the occupancy at the time of the incidents.

Table 3.3 gives a detailed description of the above categories of the flying fox roosting site status.

Table 3.3: Flying Fox roosting sites status description (Source: EHP 2014).

Camp type	Status	Description
Permanent	continuous use	90% of all records include the presence of flying foxes Roost has been known for 2 years or more
	Seasonal	80% of all records include the presence of flying foxes Roost has been known for 2 years or more
Temporary	Occupied	Roost doesn't satisfy permanent classification. Most recent record includes the presence of flying foxes
	Unoccupied	Roost doesn't meet permanent/abandoned/destroyed category. Most recent record has absence of flying foxes
Abandoned	-	Roost on database but no record of use in the last 5 years
Destroyed	-	This would be manually entered based on the vegetation being destroyed either legally or illegally

Figure 3.5 shows the flying fox roosting sites in the study area. Figure 3.6 shows the statuses of the flying fox roosting sites present in the study area. For detailed information on the flying fox roosting sites see *Appendix 1*.

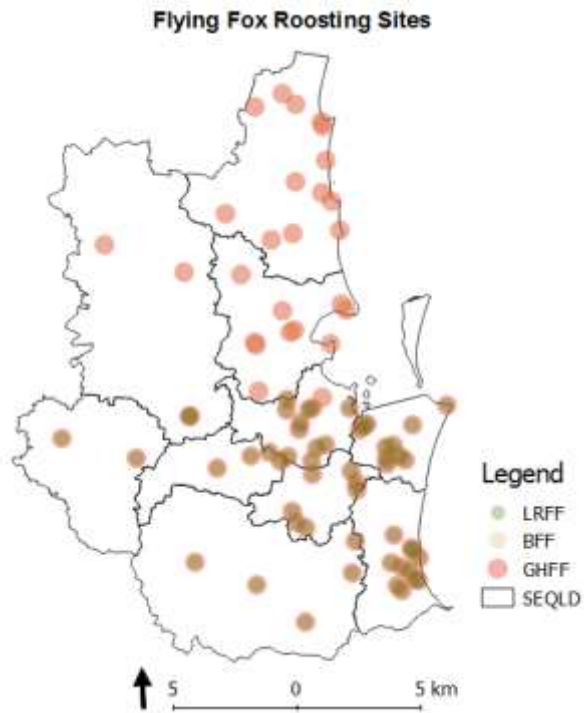


Figure 3.5: Flying fox roosting sites by species in the study area.

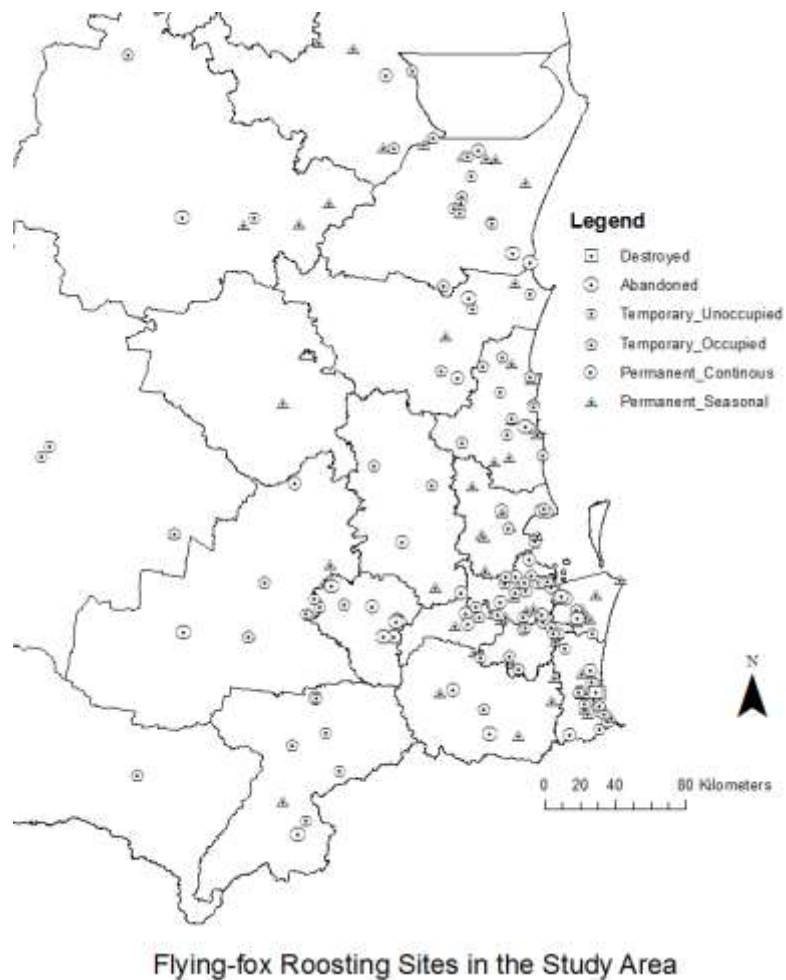


Figure 3.6: Flying fox roosting site statuses in the study area.

Equine Data

There are 16,986 registered equine properties in the study area. Figure 3.7 shows the registered equine properties in the study area.

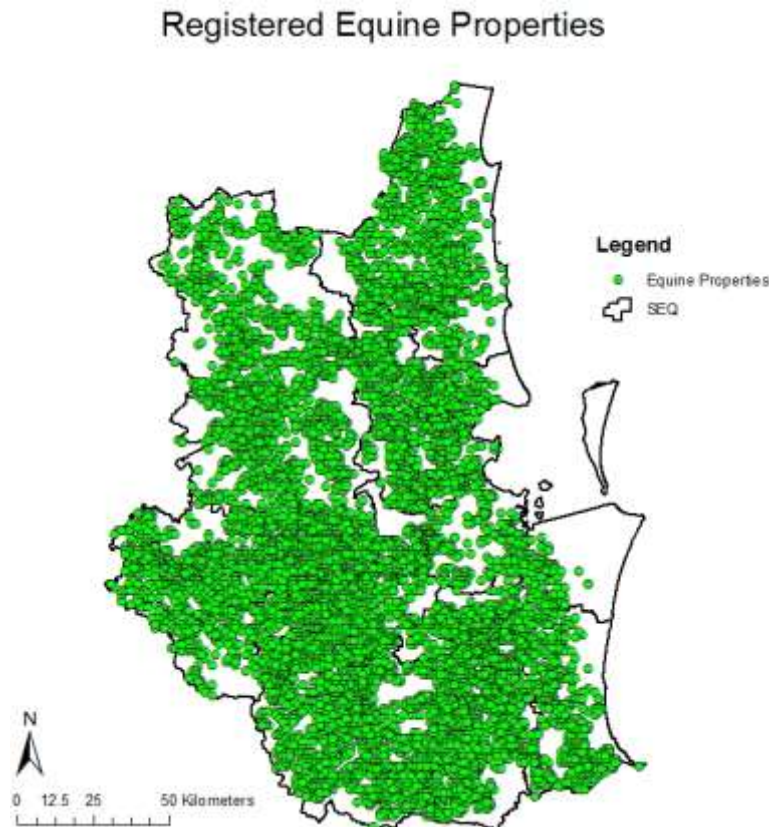


Figure 3.7: Registered equine properties in the study area.

As there were a total of 16,986 registered equine properties in the study area, a sample was chosen for the study. Using the geoprocessing tools in ArcGIS - buffer and clip, the data of the properties within 10 Km range from the outbreak events in the study area was extracted. There were 4,082 registered properties in this range. A further sample of 200 random properties (5% approximately; 1:13 outbreak event and equine property ratio) were selected across the study area for a detailed study. Figure 3.8 shows the registered equine properties sample chosen for a detailed study.

Registered Equine Properties Sample

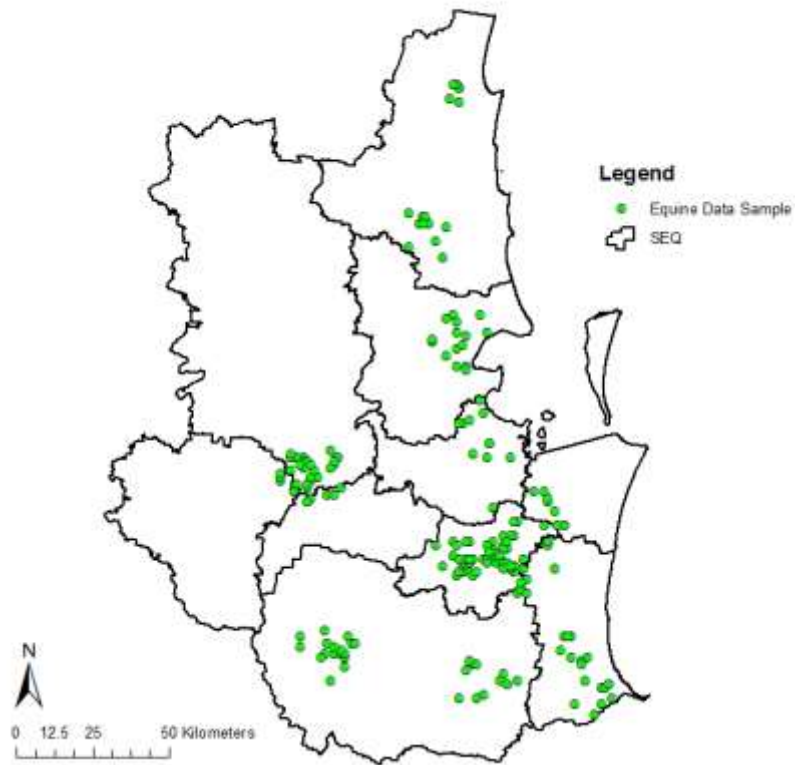


Figure 3.8: Registered equine properties sample.

Vegetation Data

The raster data sets of major vegetation groups and major vegetation subgroups were obtained for Australia. Using geoprocessing tool – extract by mask, the raster data sets for SEQ were cropped according to the study area boundary. MVG data set has been used for referencing purposes whereas MVS data set has been used for a detailed vegetation study. Figure 3.9 (a) and (b) shows the major vegetation groups and major vegetation subgroups in the study area. For full legend of both MVG and MVS of the data sets, see *Appendix 1*. There are 20 major vegetation groups and 28 major vegetation subgroups in the study area. The full list of these groups and subgroups is included in *Appendix 1*.

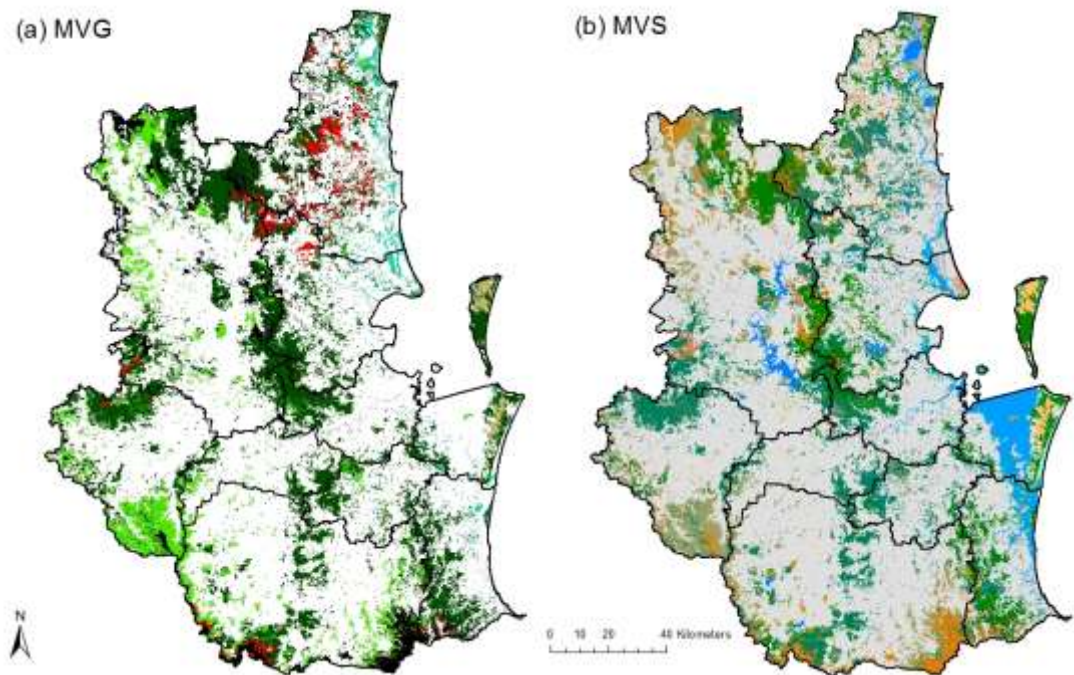


Figure 3.9: MVG and MVS in the study area.

Data Processing of Aspatial Data

Each flying fox roosting site (spatial data) in the study area was assigned with individual species density, average foraging range of the camp, approximate pregnancy/birth period of the camp and an incident rate (aspatial data). In this way, the aspatial data was linked to the spatial data for analysis. The flying fox species density, average foraging range and the pregnancy/birth period statistics (average pregnancy plus lactation period at individual roost) were calculated manually for each roosting site using the flying-fox population and species attribute data. The information used to calculate the average foraging range and pregnancy period for the analysis are based on the flying-foxes fact sheet from wildlife preservation society of Queensland (Wildlife Queensland 2016, see section 2.2.3). Each flying fox roosting site in the study was assigned an ‘incident rate’ for the regression analysis. This was calculated using the number of incidents present within the 20 kms range of each site. To view the calculated data see *Appendix 1*.

Flying foxes species density was calculated using the equation 3.1.

$$\text{Species Density} = \left(\frac{\text{Individual species population at each roost}}{\text{Total number of flying foxes in the study area}} \right) * 100$$

Equation 3.1

The average foraging distance (in kms) of each site was calculated by equation 3.2.

$$\begin{aligned} \text{Avg. Foraging Range} \\ &= ((\text{Species 1 density} * \text{their avg. foraging range}) \\ &+ (\text{Species 2 density} * \text{their avg. foraging range}) \\ &+ (\text{Species 3 density} * \text{their avg. foraging range}))/3 \end{aligned}$$

Equation 3.2

The average pregnancy period (in days) of each site was calculated using equation 3.3.

$$\begin{aligned} \text{Avg. Pregnancy Period} \\ &= ((\text{Species} - 1 \text{ density} \\ &* \text{their pregnancy and lactation period}) + (\text{Species} \\ &- 2 \text{ density} * \text{their pregnancy and lactation period}) \\ &+ (\text{Species} - 3 \text{ density} \\ &* \text{their pregnancy and lactation period}))/3 \end{aligned}$$

Equation 3.3

The incident rate for each roosting site was calculated using equation 3.4.

Incident Rate

$$= \left(\frac{(\text{no. of incidents in the 20 kms range}) * (\text{flying fox population density})}{11} \right) * 100$$

Equation 3.4

Data Verification

The quality of the data was validated through filtering the null values, duplicates and any repeats. For spatial data, ArcGIS was used to verify the above and for aspatial data, Microsoft Excel was used. Data aggregation was performed at various levels depending on the application in the study. The spatial data was appropriately projected using ArcGIS. The maps were projected using ‘The Geocentric Datum of Australia (GDA)’. The raster data sets of the imagery were geo-referenced according to the ground control points.

3.4 Flying Fox Roosting Site Visits

It is important to have knowledge on the flying foxes, their roosting sites and their preferred living conditions to carry an in-depth analysis. To gain some additional knowledge and do some fact checking, two roosting sites in the study area were visited. The names of the sites are Loders Creek and Cascade Gardens. They are located on the Gold Coast, Queensland. Site 1 – Loders Creek is a natural bat colony and Site 2 – Cascades Gardens colony is a part of flying fox revegetation project.

Site 1 – Loders Creek

Loders Creek is a suburban area of Southport. The flying fox colony at the Loders Creek consists of all three species that occurs in the study area. Figure 3.10 shows a view of the site 1 location and figure 3.11 shows the statistics of the Loders Creek flying fox colony obtained from the Department of the Environment’s National Flying Fox Monitoring Viewer (2017).



Figure 3.10: Flying fox colony location - site 1.

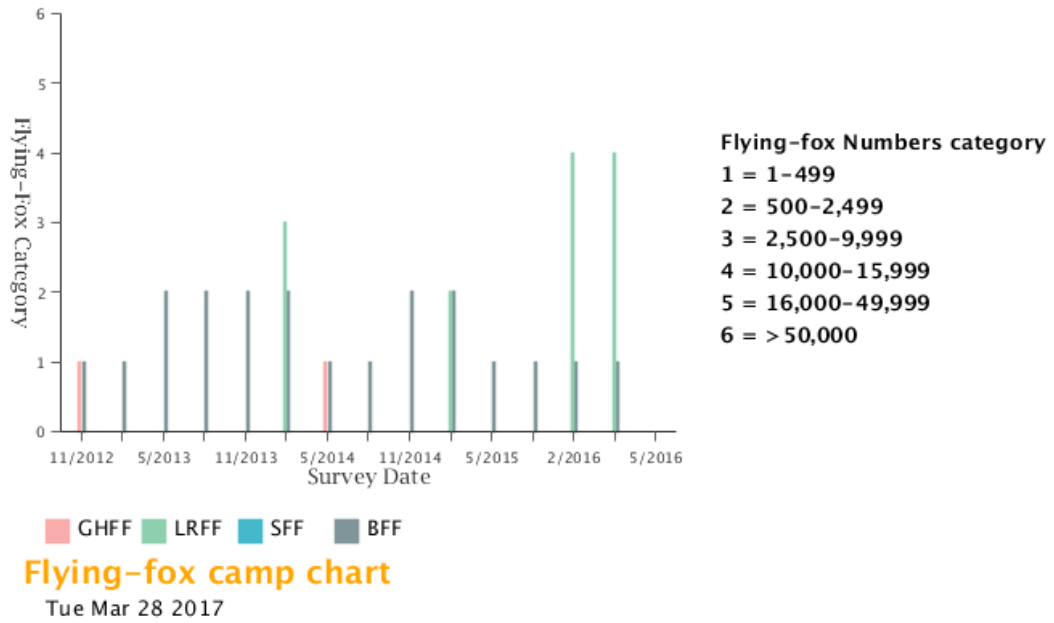


Figure 3.11: Loders Creek flying fox colony statistics (Source: Department of the Environment 2017).

Loders Creek flying fox colony is considered large with an estimated 30,000 flying fox population. Recently, the residents of the Southport has complained to the Gold Coast City Council as the colony being a nuisance to the area with constant noise and bat dropping in the yards and driveways. However, the colony is yet to be relocated due to its size (Gold Coast Bulletin 2016). Figure 3.12 shows the flying foxes in the Loders Creek.



Figure 3.12: Flying foxes in Loders Creek (Source: Gold Coast Bulletin 2016).



Figure 3.13: Loders Creek flying fox colony view.

Figure 3.13 shows a distant view of the flying fox colony at Loders Creek. The flying foxes in this colony are spread over a wide area on both tall and short vegetation. The vegetation appeared to be rainforest type with a great access to water (alongside the creek).



Figure 3.14: A closer view of the flying foxes in the Loders Creek colony.

Figure 3.14 shows a closer view of the flying foxes in the Loders Creek colony which was backed on to a residential property. There were a lot of droppings of these flying foxes in the backyard of the property. There was an abundance of food sources available in the vegetation, mainly the native fruiting trees. A sample count of these

trees in an area of 200 square metres has revealed a total of 31 native fruiting trees in this colony location.

Site 2 – Cascades Gardens

Cascades Gardens flying fox colony is part of the award-winning Cascades Gardens Flying Fox Revegetation Project 2004-2006. It is located on the southern end of the Surfers Paradise in a popular park. The colony consists of two species that occurs in the study area. In recent years the roosting site had deteriorated to such a degree that many individuals were starting to relocate to the public recreation areas of the park. This project was created and administered by the Bat Rescue team (Bat Rescue Inc. 2017).

A grant of \$16,000 was obtained through Threatened Species Network for on ground works. Additional support was received from Jupiters Ltd, Wildlife Preservation Society QLD, Queensland Parks and Wildlife Service (Southern Region), Gold Coast City Council and DDW Fauna. The total value of the project, including the additional support was approximately \$100,000 (Bat Rescue Inc. 2017).

A GOLD GECKO AWARD was received by Bat Rescue Gold Coast Branch for this project from the Gold Coast and Hinterland Environment Council in December 2006.

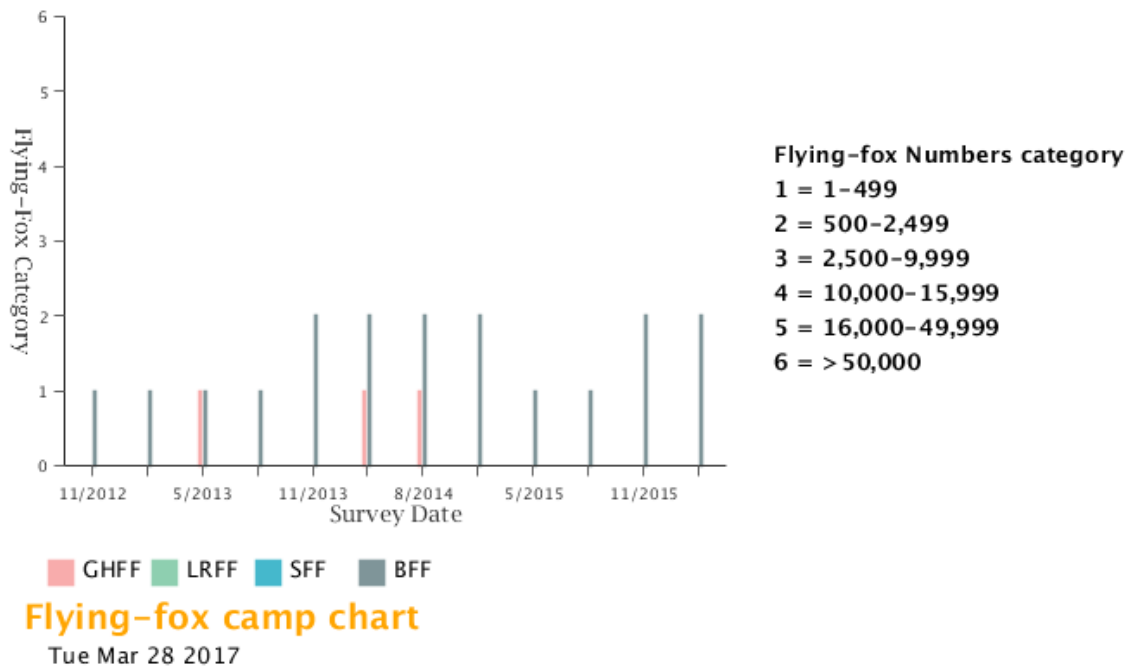


Figure 3.15: Cascades Gardens flying fox colony statistics (Source: Department of the Environment 2017).

Figure 3.15 shows the Cascades Gardens flying fox colony statistics provided by the Department of the Environment’s National Flying Fox Monitoring Viewer. The colony had a resident population of approximately 5,000 flying foxes including Black and Grey-headed flying fox species. But, in the recent years the roosting site had deteriorated to such a degree that many of these individuals were starting to relocate to the public recreation areas of the park (Bat Rescue Inc. 2017).



Figure 3.16: A view of flying foxes in the Cascades Gardens colony.

Figure 3.16 shows a view of the flying foxes in the Cascades Gardens colony. The flying foxes were widely spread in several areas of the park as mentioned by the Bat Rescue Inc. (2017). Some flying foxes preferred tall vegetation and some were spotted in the dense vegetation. A few flying foxes in this colony were also spotted on very low/shorter type of vegetation. Figure 3.17 shows the flying foxes in dense vegetation at the Cascades Gardens.



Figure 3.17: Flying foxes spotted in the dense vegetation at the Cascades Gardens.



Figure 3.18: Vegetation at the Cascades Gardens flying fox colony.

Figure 3.18 shows the vegetation that is present at the Cascades Gardens flying fox colony. It is mainly the rainforest vegetation; however there was some cleared vegetation at other parts of the park.



Figure 3.19: Water catchment near the Cascades Gardens colony.



Figure 3.20: Native Fruits at the Cascades Gardens colony.

Figure 3.19 shows the water catchment adjacent with the Cascades Gardens colony. Figure 3.20 shows the native fruits at the colony. There was an abundance of food sources available for the flying foxes in this colony. A sample count of the native fruiting trees in an area of 200 square metres has revealed a total of 44 trees in this colony location.

3.5 Spatial Analyses Methods

This section discusses the spatial analyses methods used to test the hypothesis mentioned in *section 1.4*.

3.5.1 Buffer Analysis

Buffer analysis is a simple yet important spatial technique used to determine the area or features covered within a specified location of a geographic feature. It is available in the 'Analysis Toolbox' under the 'Proximity Tools' in ArcGIS. It creates buffer polygons around input features to a specified distance. The output buffer features are created from the buffer offsets created by the buffer routine traverses of each input feature's vertices (ESRI 2016).

ESRI (2017) mentioned that the important feature of the buffer tool is the Method parameter which determines how the buffers are constructed. Euclidean and geodesic are the two basic methods available for constructing buffers. The Euclidean buffers measure distance in a two-dimensional Cartesian plane. It calculates the Euclidean distance between two points on a flat surface. This method is the most commonly used and works well for analysing distances around features in a projected coordinated system concentrated in a relatively small area. In a projected coordinate system with areas where distances and the shape of features are distorted, the features are more accurate near the origin of the projection (the centre of the state/zone). For a dataset with both low and high distortion areas, the Euclidean buffers will be more accurate in the low distortion areas and less accurate in the high distortion areas.

Geodesic buffers refer to the actual shape of the earth i.e. an ellipsoid or a geoid. In this method, the distances are calculated between two points on a curved surface as opposed to the Euclidean buffers. These are suitable when the region is fairly large/even such as the ‘whole globe’ as the features will be more dispersed. It is also more suitable method if the spatial reference of the input features distorts distances. The geodesic buffers are best visualized when viewed on a three-dimensional globe. The ‘method’ parameter determines the type of buffers created. Planar is the default option in ArcGIS, which determines the method to use based on the coordinate system of the input features. A gridded coordinate system creates Euclidean buffers and a geographical coordinate system creates geodesic buffers if the linear units (metres, feet etc.) are specified (ESRI 2017). The Syntax of the buffer analysis is described in the Table 3.4.

Table 3.4: The syntax of the buffer analysis in ArcGIS (Source: ESRI 2017).

Parameter	Explanation	Datatype
Input Features (Required)	The feature layer or feature class to be buffered.	Feature Layer
Output Feature Class (Required)	The feature class that will be created and to which the resulting features will be written.	Feature Class
Distance [value or field] (Required)	The distance used to create buffer zones around Input Features. Either a value or a numeric field can be used to provide buffer distances. If a negative buffer distance is specified, the buffer offsets will be generated inside, instead of outside, of the input features. This is only valid for polygon feature classes. If the distance units are not specified, or entered as 'Unknown', the units of the Input Features are used (or if the Output Coordinate System environment has been set, its units will be used).	Linear unit Field
Side Type (Optional)	Options to buffer to one side of a line or outside polygons <ul style="list-style-type: none"> FULL - A buffer will be generated on both sides of the line. If the input is a polygon the result will include the area inside the 	String

	<p>polygon. This is the default.</p> <ul style="list-style-type: none"> • LEFT - the buffer will be generated on the LEFT side of the line. • RIGHT - the buffer will be generated on the RIGHT side of the line. • OUTSIDE_ONLY - the area inside of the input polygon features will be excluded from the resulting buffer. 	
End Type (Optional)	<p>For lines, the shape of the buffer at the line end points.</p> <ul style="list-style-type: none"> • ROUND—End will be in the shape of a half circle. This is the default. • FLAT—Creates rectangular line endings with the middle of the short side of the rectangle coincident with the end point of the line. 	String
Dissolve Type (Optional)	<p>Specifies whether a dissolve will be performed to remove buffer feature overlap.</p> <ul style="list-style-type: none"> • NONE—Individual buffer for each feature is maintained, regardless of overlap. This is the default. • ALL—Dissolves all the buffers together into a single feature and removes any overlap. • LIST—Dissolves by a given list of fields. 	String
Dissolve Field(s) (Optional)	<p>List of field(s) for the dissolve. Buffer polygons that share the same set of values in their Dissolve Field(s) will be dissolved together.</p>	Field

Buffer analysis was primarily employed in this study for testing **Hypothesis 1** (see *Section 1.4*), which is to understand the correlation between the roosting sites and the HeV outbreak events in the study area (Burnham et al 2015). It was utilised to examine and visualise the relationship between individual flying fox species pregnancy/birth periods and the incidents. It was also employed secondarily in the vegetation study to highlight the 10 and 20 kms area from the flying fox roosting sites, equine properties and outbreak events for an in-depth analysis. The Euclidean

buffer was used as the method parameter in this study. The data used has a gridded coordinate system (GDA) and the size of the study area is relatively small, which are both suitable for Euclidean buffer method.

3.5.2 Spatial Analyst Tools

The spatial Analyst extension in ArcGIS version 10.3 provides a set of spatial analysis and modelling tools for raster (cell-based) and vector (feature) data. ESRI (2016) has broken down the capabilities of Spatial Analyst into categories of related functionality. Identifying the category based on the need will help in employing the particular tool to use. There are a few ways to access the Spatial Analyst functionality in ArcGIS. It can be accessed using the tool dialog box, Python or a Model (ESRI 2016).

The list of categories available in ‘Spatial Analyst’ is:

- i) Conditional
- ii) Density
- iii) Distance
- iv) Extraction
- v) Generalization
- vi) Groundwater
- vii) Hydrology
- viii) Interpolation
- ix) Local
- x) Map Algebra
- xi) Math (general)
- xii) Math Bitwise
- xiii) Math Logical
- xiv) Math Trigonometric
- xv) Multivariate
- xvi) Neighbourhood
- xvii) Overlay

- xviii) Raster Creation
- xix) Reclass
- xx) Solar Radiation
- xxi) Segmentation and Classification
- xxii) Surface
- xxiii) Zonal

‘Extraction’ category was utilised in this study for the food source vegetation analysis of the flying foxes to test **Hypothesis 3** (see *Section 1.4*). This toolset allows extracting a subset of cells from a raster by either the cells’ attributes or their spatial location. The cell values for specific locations can also be obtained as an attribute in a point feature class or as a table. Table 3.5 provides summary of the tools available in the ‘Extraction’ category of the Spatial Analyst Tools.

Table 3.5: Summary of the tools in the Extraction Toolset – Spatial Analyst (Source: ESRI 2016).

Tool	Description
Extract by Attributes	Extracts the cells of a raster based on a logical query.
Extract by Circle	Extracts the cells of a raster based on a circle.
Extract by Mask	Extracts the cells of a raster that correspond to the areas defined by a mask.
Extract by Points	Extracts the cells of a raster based on a set of coordinate points.
Extract by Polygon	Extracts the cells of a raster based on a polygon.
Extract by Rectangle	Extracts the cells of a raster based on a rectangle.
Extract Multi Values to Points	Extracts cell values at locations specified in a point feature class from one or more rasters and records the values to the attribute table of the point feature class.
Extract Values to Points	Extracts the cell values of a raster based on a set of point features and records the values in the attribute table of an output feature class.

Sample	<p>Creates a table that shows the values of cells from a raster, or set of rasters, for defined locations. The locations are defined by raster cells or by a set of points.</p> <p>The input rasters can be two-dimensional or multidimensional. The structure of the output table changes when the input rasters are multi-dimensional.</p>
---------------	--

‘Extract by Attributes’ and ‘Extract by Mask’ tools from the above toolset were used in this study for the vegetation analysis as they are very useful in extracting information from raster data sets. ‘Extract by Mask’ operation was employed to extract the major vegetation groups and subgroups information for the study area from the original dataset. ‘Extract by Attributes’ tool was used to identify the food sources from the vegetation subgroups data of the flying fox species from the dataset extracted earlier. Using the query builder, the food sources were isolated using their ‘ID’ and ‘IN’ clause was used for extracting multiple attributes at once.

3.5.3 Spatial Autocorrelation

Global Moran’s I for spatial autocorrelation tool in ArcGIS was used to measure the spatial autocorrelation in this study. It is available in the ‘Analysing Patterns Toolset’ in ArcGIS. Spatial clustering serves as a reflection of risk condition of a disease, however, it may be affected by common unobserved factors/variables (Lawson et al 2001) and is best for the initial analysis to detect and analyse the clusters (Wakefield et al 2001) at the global level across the study area. The autocorrelation is measured by the spatial autocorrelation tool based on both feature locations and feature values simultaneously. For a given set of features and an associated attribute, the tool evaluates whether the pattern is clustered, dispersed or random. The tool gives the Moran’s I Index value and a z-score and p-value to evaluate the significance of the Index (ESRI 2017).

The syntax of the spatial autocorrelation tool in ArcGIS is described in table 3.6.

Table 3.6: Syntax of the Spatial Autocorrelation tool in ArcGIS (Source: ESRI 2017).

Parameter	Explanation
Input Feature Class	The feature class for which spatial autocorrelation will be calculated.
Input Field	The numeric field used in assessing spatial autocorrelation.
Conceptualization of Spatial Relationships	<p>Specifies how spatial relationships among features are defined.</p> <ul style="list-style-type: none"> • INVERSE DISTANCE - Nearby neighbouring features have a larger influence on the computations for a target feature than features that are far away. • INVERSE DISTANCE SQUARED - Same as INVERSE DISTANCE except that the slope is sharper, so influence drops off more quickly, and only a target feature's closest neighbours will exert substantial influence on computations for that feature. • FIXED DISTANCE BAND - Each feature is analysed within the context of neighbouring features. • ZONE OF INDIFFERENCE - Features within the specified critical distance (Distance Band or Threshold) of a target feature receives a weight of one and influence computations for that feature. • CONTIGUITY EDGES ONLY - Only neighbouring polygon features that share a boundary or overlap will influence computations for the target polygon feature. • CONTIGUITY EDGES CORNERS - Polygon features that share a boundary, share a node, or overlap will influence computations for the target polygon feature. <p>GET SPATIAL WEIGHTS FROM FILE - Spatial relationships are defined by a specified spatial weights file. The path to the spatial weights file is specified by the Weights Matrix File parameter.</p>

Distance Method	<p>Specifies how distances are calculated from each feature to neighbouring features.</p> <ul style="list-style-type: none"> • EUCLIDEAN DISTANCE - The straight-line distance between two points (as the crow flies) • MANHATTAN DISTANCE - The distance between two points measured along axes at right angles; calculated by summing the (absolute) difference between the x- and y-coordinates
Standardization	<p>Row standardization is recommended whenever the distribution of your features is potentially biased due to sampling design or an imposed aggregation scheme.</p> <ul style="list-style-type: none"> • NONE - No standardization of spatial weights is applied. • ROW - Spatial weights are standardized; each weight is divided by its row sum (the sum of the weights of all neighbouring features).

The spatial autocorrelation tool was primarily used in testing the **Hypothesis 2** (see *Section 1.4*). Inverse distance conceptualization of spatial relationships was employed to study the clustering of the flying fox species in the study area. It was secondarily employed to test the autocorrelation among the Ordinary Least Squares (OLS) and Geographically Weighted Regression (GWR) analysis residuals.

The results of the spatial autocorrelation tool are interpreted within the context of null hypothesis. The null hypothesis states that the attribute being analysed is randomly distributed among the features in the study area. When the p-value of the analysis is statistically significant, the null hypothesis can be rejected.

The interpretations of the spatial autocorrelation results are:

- **The p-value is not statistically significant** – The null hypothesis may be accepted and the spatial distribution of feature values is a result of random spatial processes.
- **The p-value is statistically significant and the z-score is positive** – the null hypothesis may be rejected and the spatial distribution of high/low values in

the data set is more spatially clustered than expected if underlying spatial processes were random.

- **The p-value is statistically significant and the z-score is negative** – the null hypothesis may be rejected and the spatial distribution of high/low values in the data set are more spatially dispersed than expected if underlying spatial processes were random.

3.5.4 Kernel Density

The kernel density tool is available in the density tools category in the Spatial Analyst Toolbox ArcGIS (see *Section 3.5.2*). It is referred as kernel density estimation (KDE) technique. The KDE technique is well-suited for analysing data visually (Chainey 2010) and serves as a good spatial technique to examine the relationships. It calculates magnitude-per-unit area from point or polyline features using a kernel function to fit a smoothly tapered surface to each point or polyline. The default search radius or bandwidth is calculated based on the spatial configuration and the number of input points.

The algorithm used by ArcGIS 10.2.1 or above versions to calculate the default search radius or bandwidth for the analysis is as follows (ESRI 2017):

- Calculation of the mean centre of the input points.
- Calculation of the distance from the (weighted) mean centre for all points.
- Calculation of the (weighted) median of these distances, D_m .
- Calculate the (weighted) Standard Distance, SD .
- Application of the equation 3.5 to calculate the bandwidth.

$$SearchRadius = 0.9 * \min \left(SD, \sqrt{\frac{1}{\ln(2)} * D_m} \right) * n^{-0.2}$$

Equation 3.5

Where:

- SD is the standard distance
- D_m is the median distance
- n is the number of points if no population field is used, or if a population field is supplied, n is the sum of the population field values

The KDE technique was employed in this study to establish the primary relation between the flying fox species density and the incidents as part of testing the **Hypothesis 2** (see *Section 1.4*) of the study. Using this technique, density hot spot maps were created for each species in the study area. The bandwidth for the KDE analysis for each species was set at 0.4598 degrees, which was calculated by the default search radius (bandwidth) algorithm of ArcGIS. Different bandwidth radii were tested (0.22 and 0.68 degrees) in generating the density hot spots but the default density calculated by ArcGIS yielded the best output with no errors such as missing neighbours (ESRI 2017).

The syntax for the KDE technique in ArcGIS is described in table 3.7.

Table 3.7: Syntax of the Kernel Density tool in ArcGIS (Source: ESRI 2017).

Parameter	Explanation	Data Type
In features	The input features (point or line) for which to calculate the density.	Feature Layer
Population field	Field denoting population values for each feature. The population field is the count or quantity to be spread across the landscape to create a continuous surface. Values in the population field may be integer or floating point.	Field
Cell size (Optional)	The cell size for the output raster dataset. This is the value in the environment if specifically set. If the environment is not set, then cell size is the shorter of the width or height of the output extent in the output spatial reference, divided by 250.	Analysis Cell Size

Search radius (Optional)	<p>The search radius within which to calculate density. Units are based on the linear unit of the projection of the output spatial reference.</p> <p>The default search radius (bandwidth) is computed specifically to the input dataset using a spatial variant of Silverman's Rule of Thumb that is robust to spatial outliers (that is, points that are far away from the rest of the points).</p>	Double
---------------------------------	---	--------

3.5.5 High/low clustering

The high/low clustering tool measures the degree of clustering of either high or low using the Getis-Ord General G statistic. It is available in the ‘Analysing Patterns Toolset’. This tool returns four values: Observed General G, Expected General G, z-score, and p-value. Global statistic such as Getis-Ord General G assesses the overall pattern and trend of the data. It is an appropriate method if the values are fairly evenly distributed across the study area. As an inferential statistic tool, the results produced are interpreted within the context of null hypothesis, which states that there is no spatial clustering of feature values. When p value is statistically significant, the null hypothesis can be rejected. In case of null hypothesis rejection, the sign of the Z score becomes important. If the result is a positive Z score, it indicates that the high values are clustered together. If the result is a negative Z score, it indicates that the low values are clustered together.

This tool was employed for testing **Hypothesis 3** (see Section 1.4), which studied the food source vegetation of the flying foxes. It was used to study the clustering of the food source vegetation in the study area. Inverse distance conceptualization of spatial relationships was used in this analysis. Table 3.8 shows the syntax of the high/low clustering tool in ArcGIS.

Table 3.8: Syntax of the High/low Clustering tool in ArcGIS (Source: ESRI 2016).

Parameter	Explanation	Data Type
Input Feature Class	The feature class for which the General G statistic will be calculated.	Feature Layer
Input Field	The numeric field to be evaluated.	Field
Generate Report (Optional)	NO REPORT - No graphical summary will be created. This is the default. GENERATE REPORT - A graphical summary will be created as an HTML file.	Boolean
Conceptualization of Spatial Relationships	Specifies how spatial relationships among features are defined. <ul style="list-style-type: none"> • INVERSE DISTANCE • INVERSE DISTANCE SQUARED • FIXED DISTANCE BAND • ZONE OF INDIFFERENCE • CONTIGUITY EDGES ONLY • CONTIGUITY EDGES CORNERS • GET SPATIAL WEIGHTS FROM FILE 	String
Distance Method	Specifies how distances are calculated from each feature to neighbouring features. <ul style="list-style-type: none"> • EUCLIDEAN DISTANCE • MANHATTAN DISTANCE 	String
Standardization	Row standardization is recommended whenever the distribution of your features is potentially biased due to sampling design or an imposed aggregation scheme. <ul style="list-style-type: none"> • NONE • ROW 	String
Distance Band or Threshold Distance (Optional)	Specifies a cut-off distance for the inverse distance and fixed distance options. Features outside the specified cut-off for a target feature are ignored in analyses for that feature.	Double

The null hypothesis for both the High/Low Clustering (Getis-Ord General G) and the Spatial Autocorrelation (Global Moran's I) tool is complete spatial randomness (CSR). The values are randomly distributed among the features in the dataset, reflecting random spatial processes at work. However, the interpretation of z-scores for the High/Low Clustering tool is very different from the interpretation of z-scores for the Spatial Autocorrelation (Global Moran's I) tool (ESRI 2017). Table 3.9 shows the difference in the interpretation of these results.

Table 3.9: The Difference in the interpretation of High/Low Clustering and Spatial Autocorrelation tools (Source: ESRI 2017).

Result	High/Low Clustering	Spatial Autocorrelation
The p-value is not statistically significant.	The null hypothesis cannot be rejected. It is quite possible that the spatial distribution of feature attribute values is the result of random spatial processes.	
The p-value is statistically significant, and the z-score is positive.	The null hypothesis may be rejected.	The null hypothesis may be rejected. The spatial distribution of high values and/or low values in the dataset is more spatially clustered than would be expected if underlying spatial processes were truly random.
The p-value is statistically significant, and the z-score is negative.	The null hypothesis may be rejected.	The null hypothesis may be rejected. The spatial distribution of high values and low values in the dataset is more spatially dispersed than would be expected if underlying spatial processes were truly random.

3.6 Regression Analysis

The Spatial Statistics Toolbox in ArcGIS provides an effective set of tools for quantifying spatial patterns such as hotspot analysis and regression analysis. Regression analysis tools allow to model, examine, explore spatial relationships, explain the factors behind observed spatial patterns in the study area and even predict the future events. This study has utilised OLS and GWR regression techniques in testing **Hypothesis 2** (see *Section 1.4*). Linear relationships between two variables can be either positive or negative but with regression analyses makes an attempt to demonstrate the degree to which one or more variables (independent variables) potentially promote positive or negative change in other variable (dependent variable). The main terms in the regression analyses are described by ESRI (2016) as below:

Dependent variable - this variable represents the process of the subject that is being predicted or understood.

Independent/Explanatory variables - these are the variables used to model or to predict the dependent variable values.

Regression coefficients – the Regression Coefficients are computed by the regression tool. They are values, one for each explanatory variable, that represent the strength and the type of relationship the explanatory variable has to the dependent variable

P-values - most regression methods perform a statistical test to compute a probability, called a p-value, for the coefficients associated with each independent variable. The null hypothesis for this statistical test states that a coefficient is not significantly different from zero. Small p-values reflect small probabilities and suggest that the coefficient is, indeed, important to your model with a value that is significantly different from zero.

R2/R-squared - Multiple R-squared and adjusted R-squared are both statistics derived from the regression equation to quantify model performance. The value of R-squared ranges from 0 to 100 percent. The adjusted R-squared value is always lower than the multiple R-squared values as it reflects model complexity (the number of variables). Consequently, the adjusted R-squared value is a more accurate measure of model performance.

Residuals - These are the unexplained portion of the dependent variable, represented in the regression equation as the random error term ϵ . The difference between the observed y-values and the predicted y-values are called the residuals. The magnitude of the residuals from a regression equation is one measure of model fit. Large residuals indicate poor model fit.

The common issues that may arise during regression analyses and modelling and how they may affect the analysis are described in table 3.10.

Table 3.10: Summary of the issues in the modelling of Regression Analyses (Source: ESRI 2016).

Issues	Reason	Solution
Omitted explanatory variables (misspecification)	When key explanatory variables are missing from a regression model, coefficients and their associated p-values cannot be trusted.	Map and examine OLS residuals and GWR coefficients.
Non-linear relationships	OLS and GWR are both linear methods. If the relationship between any of the explanatory variables and the dependent variable is nonlinear, the resultant model will perform poorly.	Create a scatter plot matrix graph to elucidate the relationships among all variables in the model. Alternatively, use a nonlinear regression method.
Data outliers	Influential outliers can pull modelled regression relationships away from their true best fit, biasing	Create a scatter plot matrix and other graphs (histograms) to examine extreme data values. Correct or remove outliers

	regression coefficients.	if they represent errors.
Nonstationarity	If relationships between the dependent and explanatory variables are inconsistent across the study area, computed standard errors will be artificially inflated.	The OLS tool in ArcGIS automatically tests for problems associated with Nonstationarity (regional variation) and computes robust standard error values. When the probability associated with the Koenker test is small (< 0.05 , for example), the statistically significant regional variation is present and the robust probabilities should be used to determine if an explanatory variable is statistically significant or not.
Multicollinearity	Multicollinearity leads to an over counting type of bias and an unstable/unreliable model.	The OLS tool in ArcGIS automatically checks for redundancy. Each explanatory variable is given a computed VIF value. When this value is large (> 7.5), redundancy is a problem and the offending variables should be removed from the model or modified by creating an interaction variable or increasing the sample size.
Inconsistent variance in residuals	When the model predicts poorly for some range of values, results will be biased.	The OLS tool in ArcGIS automatically tests for inconsistent residual variance (called heteroscedasticity) and computes standard errors that are robust to this problem. When the probability associated with the Koenker test is small (< 0.05 , for example), the robust probabilities must be used to determine if an explanatory variable is statistically significant or not.
Spatially correlated residuals	auto- When there is spatial clustering of the under-/over predictions coming out of the model, it introduces an over counting type of bias and renders the model unreliable.	Run the Spatial Autocorrelation tool on the residuals to ensure they do not exhibit statistically significant spatial clustering. Statistically significant spatial autocorrelation is almost always a symptom of misspecification (a key variable is missing from the model).
Normal distribution bias	When the regression model residuals are not normally distributed with	The OLS tool in ArcGIS automatically tests whether the residuals are normally distributed.

<p>a mean of zero, the p-values associated with the coefficients are unreliable.</p>	<p>When the Jarque-Bera statistic is significant (< 0.05, for example), the model is likely misspecified (a key variable is missing from the model) or some of the relationships you are modelling are nonlinear.</p>
--	---

The steps followed in this study in the modelling of regression analyses to understand the dispersal of the HeV outbreak events in the study area are:

- i) Model calibration using GWR (see *Section 3.6.3*).
- ii) Using OLS method to select the significant independent variables.
- iii) Spatial autocorrelation (Moran’s I) test on the residuals to ensure that there are no significant variables missing that could possibly better explain the dispersal of HeV outbreak events.
- iv) GWR analysis on the independent variables from the OLS model.
- v) Spatial autocorrelation (Moran’s I) test on the residuals of GWR.

3.6.1 Ordinary Least Squares (OLS) Regression

The OLS technique is a well-known regression technique and was employed in this study to understand the HeV outbreak patterns globally across the study area. It is also considered as a proper starting point for all spatial regression analyses (ArcGIS 2016). The OLS tool produces an output feature class and optional tables with coefficient information and diagnostics. The results from OLS regression technique can only be trusted if the data and the regression model satisfy all the assumptions inherently required by this method (see *Table 3.10*). The output diagnostics of OLS include corrected Akaike Information Criterion (AICc), Coefficient of Determination, Joint F statistic, Wald statistic, Koenker's Breusch-Pagan statistic, Jarque-Bera statistic, uncorrected AIC and Sigma-squared values (ESRI 2017).

Table 3.11 shows the syntax of the OLS technique in ArcGIS.

Table 3.11 Summary of the syntax of the OLS regression technique (Source: ESRI 2017).

Parameter	Explanation	Data Type
Input Feature Class	The feature class containing the dependent and independent variables for analysis.	Feature Layer
Unique ID Field	An integer field containing a different value for every feature in the Input Feature Class.	Field
Output Feature Class	The output feature class to receive dependent variable estimates and residuals.	Feature Class
Dependent Variable	The numeric field containing values for what you are trying to model.	Field
Explanatory Variables	A list of fields representing explanatory variables in your regression model.	Field
Coefficient Output Table (Optional)	The full path to an optional table that will receive model coefficients, standardized coefficients, standard errors, and probabilities for each explanatory variable.	Table
Diagnostic Output Table (Optional)	The full path to an optional table that will receive model summary diagnostics.	Table
Output Report File (Optional)	The path to the optional PDF file if chosen. This report file includes model diagnostics, graphs, and notes to help you interpret the OLS results.	File

To assess the model performance of OLS technique both Multiple R-Squared and Adjusted R-Squared values should be interpreted whose values range from 0.0 to 1.0. The Coefficient, Probability or Robust Probability, and Variance Inflation Factor (VIF) should be considered to assess each explanatory variable in the model. The coefficient for each explanatory variable reflects both the strength and type of relationship the explanatory variable has to the dependent variable. When the sign associated with the coefficient is negative, the relationship is negative. The statistically significant probabilities have an asterisk (*) next to them. These variables that are significant are important to the regression model if theory/common sense supports a valid relationship with the dependent variable. The

VIF measures redundancy among the explanatory variables. The VIF values larger than about 7.5 should be removed (one by one) from the regression model.

The Joint F-Statistic and Joint Wald Statistic are measures of overall model statistical significance of the OLS technique. The Joint F-Statistic is trustworthy only when the Koenker (BP) statistic is not statistically significant and if the Koenker (BP) statistic is significant, the Joint Wald Statistic should be used to determine overall model significance. The Koenker (BP) Statistic assesses model stationarity. It is a test to determine whether the explanatory variables in the model have a consistent relationship to the dependent variable both in geographic space and in data space. The Jarque-Bera statistic measures the model bias by indicating whether or not the residuals are normally distributed (ESRI 2016).

3.6.2 Geographically Weighted Regression (GWR)

The GWR technique is a local model of the variable or process for understanding the spatial patterns by fitting a regression equation to every feature in the data set. It constructs the equations by incorporating the dependent and independent/exploratory variables of features falling within the bandwidth of each target feature. The shape and size of the bandwidth is dependent on user input for the Kernel type, Bandwidth method, Distance, and Number of neighbour's parameters. Model design errors often indicate a problem with global or local multicollinearity and using OLS technique can determine the problem of multicollinearity. Problems with local multicollinearity may prevent the AIC and CV Bandwidth method from resolving an optimal distance/number of neighbours (ESRI 2016).

Usage of gridded data is always recommended as it is important whenever distance is a component of the analysis, as it is for GWR to select Fixed for Kernel type. For linear regression analysis similar to GWR, it is important for dependent and explanatory variables to have numeric fields containing a variety of values and is not appropriate for predicting binary outcomes. Nominal or categorical data in a GWR model should be used with caution as the categories cluster spatially; there is strong risk of encountering local multicollinearity issues. "Dummy" explanatory variables

cannot be used to represent different spatial regimes in a GWR model (ESRI 2016). GWR is a linear model subject to the same requirements as OLS and the severe model errors are same for both (see Table 3.10).

Table 3.12 summarises the syntax of the GWR technique in ArcGIS.

Table 3.12: Summary of the syntax of the GWR regression technique (Source: ESRI 2016).

Parameter	Explanation	Data Type
In features	The feature class containing the dependent and independent variables.	Feature Layer
Dependent field	The numeric field containing values for what you are trying to model.	Field
Explanatory field	A list of fields representing independent explanatory variables in your regression model.	Field
Out feature class	The output feature class to receive dependent variable estimates and residuals.	Feature Class
Kernel type	Specifies if the kernel is constructed as a fixed distance, or if it is allowed to vary in extent as a function of feature density. FIXED - The spatial context (the Gaussian kernel) used to solve each local regression analysis is a fixed distance. ADAPTIVE - The spatial context (the Gaussian kernel) is a function of a specified number of neighbours. Where feature distribution is dense, the spatial context is smaller; where feature distribution is sparse, the spatial context is larger.	String
Bandwidth method	Specifies how the extent of the kernel should be determined. When AICc or CV is selected, the tool will find the optimal distance or number of neighbours for you. AICc - The extent of the kernel is determined using the Akaike Information Criterion (AICc).	String

CV - The extent of the kernel is determined using Cross Validation.

BANDWIDTH PARAMETER - The extent of the kernel is determined by a fixed distance or a fixed number of neighbours.

distance (Optional)	The distance whenever the kernel type is FIXED and bandwidth method is BANDWIDTH PARAMETER.	Double
Number of neighbours (Optional)	The exact number of neighbours to include in the local bandwidth of the Gaussian kernel when kernel type is ADAPTIVE and the bandwidth method is BANDWIDTH PARAMETER.	Long
Weight field (Optional)	The numeric field containing a spatial weighting for individual features.	Field
Coefficient raster workspace (Optional)	A full pathname to the workspace where all of the coefficient rasters will be created.	Folder
Cell size (Optional)	The cell size (a number) or reference to the cell size (a pathname to a raster dataset) to use when creating the coefficient rasters. The default cell size is the shortest of the width or height of the extent specified in the geoprocessing environment output coordinate system, divided by 250.	Analysis Cell Size
Prediction explanatory field (Optional)	A list of fields representing explanatory variables in the Prediction locations feature class. These field names should be provided in the same order (a one-to-one correspondence) as those listed for the input feature class Explanatory variables parameter. If no prediction explanatory variables are given, the output prediction feature class will only contain computed coefficient values for each prediction location.	Field
Out prediction feature class (Optional)	The output feature class to receive dependent variable estimates for each feature in the Prediction locations feature class.	Feature Class

Fixed kernel type and AICc bandwidth method were used in this study. The bandwidth method is the most important parameter for GWR technique. It controls the degree of smoothing in the model. The program chooses a bandwidth or neighbour value by selecting the corrected Akaike Information Criterion (AICc) or Cross Validation (CV) for the Bandwidth method parameter. They both identify an optimal fixed distance or optimal adaptive number of neighbours. The Residual Squares is the sum of the squared residuals in the model. The smaller the measure, the closer the fit of the GWR model to the observed data. This value is used in a number of other diagnostic measures. R-Squared is a measure of goodness of fit. Its value varies from 0.0 to 1.0, with higher values being preferable. The adjusted R-squared value normalizes the numerator and denominator by their degrees of freedom. This has the effect of compensating for the number of variables in a model, and consequently, the Adjusted R2 value is almost always smaller than the R2 value (ESRI 2016). The spatial variability of the local parameter estimates of each variable has been tested using GWR4 software. The results achieved using the GWR technique was used test the **Hypothesis 4** in generating model(s) to identify population ‘at risk’.

3.6.3 Model Calibration for Regression Analysis

The model for the regression analyses was calibrated using the GWR technique in an exploratory method (Fotheringham et al 2012). Based on the literature review, 4 potential explanatory factors were chosen that could potentially explain the HeV outbreak events dispersal in the study area. This model calibration technique by Fotheringham et al (2012) uses a statistical model-building procedure in order to establish if any further reduction in the set were possible. By doing this, a reduced set of highly significant explanatory variables of HeV outbreak events were achieved.

The following steps are followed to achieve the most significant model for the analyses:

- i) **Iteration 1** – the 4 explanatory variables were individually included in a simple model with incident rate as the dependent variable by GWR. Using the Akaike Information Criterion (AIC) and R-Squared value (as R-Squared

value improves, the AICc value decreases), a goodness-of-fit statistic was computed. The best model using the goodness-of-fit measure was retained.

ii) Iteration 2 – using the model established in iteration 1, each of the remaining 3 variables not selected for the model was entered into the model in turn, so that 3 new models, each containing two independent variables, were obtained. These models were then calibrated by GWR. The best model based on the goodness-of-fit was retained.

iii) Iteration 3 - using the model established in iteration 2, each of the remaining 2 variables not selected for the model was entered into the model in turn, so that 2 new models, each containing three independent variables, were obtained. These models were then calibrated by GWR. The best model based on the goodness-of-fit was retained.

iv) Iteration 4 – using the model in iteration 3, a final model adding the remaining 1 variable was calibrated using GWR. The goodness-of-fit of this model is less than the model retained in the iteration 3.

The final model is selected from the iteration 3, which produced the best goodness-of-fit measure out of all. This model was used for the regression analyses. Table 3.13 shows the model calibrated using the GWR technique for the study. Further details of the model calibration were documented in *Section 4.3.3*. The additional documentation of the significant model(s) calibrated in the four iterations was documented in *Appendix 2*.

Table 3.13 Model calibrated using the GWR technique.

	Model variables	AIC	R-Squared	Significance
Iteration 1	Black flying foxes (Bff)	1239	0.68	
	Grey headed flying foxes (Ghff)	1189	0.82*	Significant model 1
	Foraging Range (FR)	1442	0.36	
	Pregnancy Period (PP)	1439	0.56	
Iteration 2	Ghff, Bff	1165	0.86**	Significant model 2
	Ghff, FR	1178	0.82	
	Ghff, PP	1182	0.85	
Iteration 3	Ghff, Bff, FR	1195	0.80	
	Ghff, Bff, PP	1143	0.88***	Final model
Iteration 4	Ghff, Bff, FR, PP	1222	0.76	

Notes:

* Indicates significant model 1 obtained from iteration 1

** Indicates significant model 2 obtained from iteration 2

*** Indicates significant model 3, which is the final model obtained from iteration 3

3.7 Methodology Flowchart

A summary of the methodology used in this study is detailed in flowchart presented in the figure 3.21.

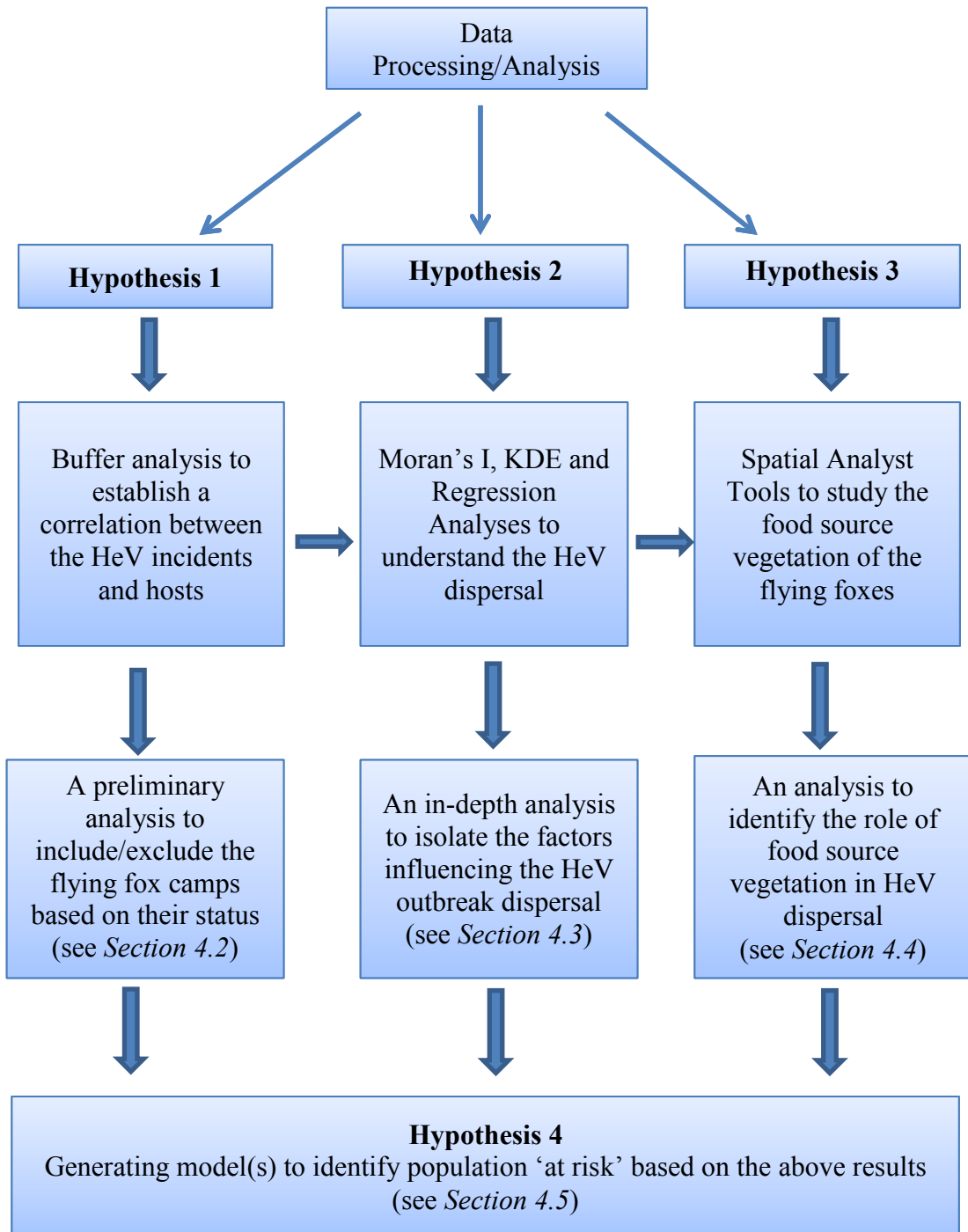


Figure 3.21: Flow chart of the methodology.

Fig 3.21 visualises the hypotheses tested in this study and their relationship to one another. Hypothesis 4 is to generate final model(s) based on the results from previous hypotheses. The flowchart can be described as process/methods used in the research.

3.8 Summary

In general, section 3.2 declared the study area considered for the research. The data collection, processing and integration steps involved in this were documented in section 3.3. Section 3.4 detailed the flying fox roosting site visits in the study area. The site visits provided an insight into the roosting site vegetation and in general their preference of a location.

Hypothesis 1

Buffer analysis was employed primarily to understand the correlation between the HeV outbreak events and flying fox roosting sites. Section 3.5 documented the spatial analyses methods in ArcGIS that were used to test Hypothesis 1.

Hypothesis 2

The Spatial Autocorrelation technique was used to study the autocorrelation among the variables and KDE were used to establish a primary relationship between the HeV outbreaks and the density of the flying foxes. The regression analyses and the model building using GWR technique were detailed in Section 3.6. The regression analyses were used in the study to test Hypothesis 2. It was employed to understand the factors influencing the virus dispersal in the study area.

Hypothesis 3

The spatial analyst toolset was used to examine the correlation between the food source vegetation, flying fox species and the HeV incidents. Section 3.5 outlined the detailed information in regards to the spatial analyst toolset that was used in testing Hypothesis 3.

Hypothesis 4

The results from Hypothesis 1, 2 and 3 were used in producing the model(s) to identify the population 'at risk' (Hypothesis 4). The models were documented in Chapter 4, *section 4.5*.

4. Chapter Four – Analysis and Results

4.1 Introduction

This chapter documents the analyses and results of the HeV outbreak incidents study. The analyses carried out to test the hypotheses mentioned in *Section 1.4* is detailed here and the results were presented. This section outlines the methodologies discussed in chapter 3. Section 4.2 details the preliminary spatial analyses of the HeV outbreaks. Section 4.3 provides the analyses and results of the factors explaining the dispersal of the HeV disease in the study area. Section 4.4 discusses the food source vegetation analysis of the flying foxes. Identification of population ‘at risk’ has been detailed in section 4.5. The results were visualized throughout the chapter where appropriate. Section 4.6 shows the flowchart of the summary of the results.

4.2 Preliminary Spatial Analysis of HeV Outbreaks and the Roosting Sites (Hypothesis 1)

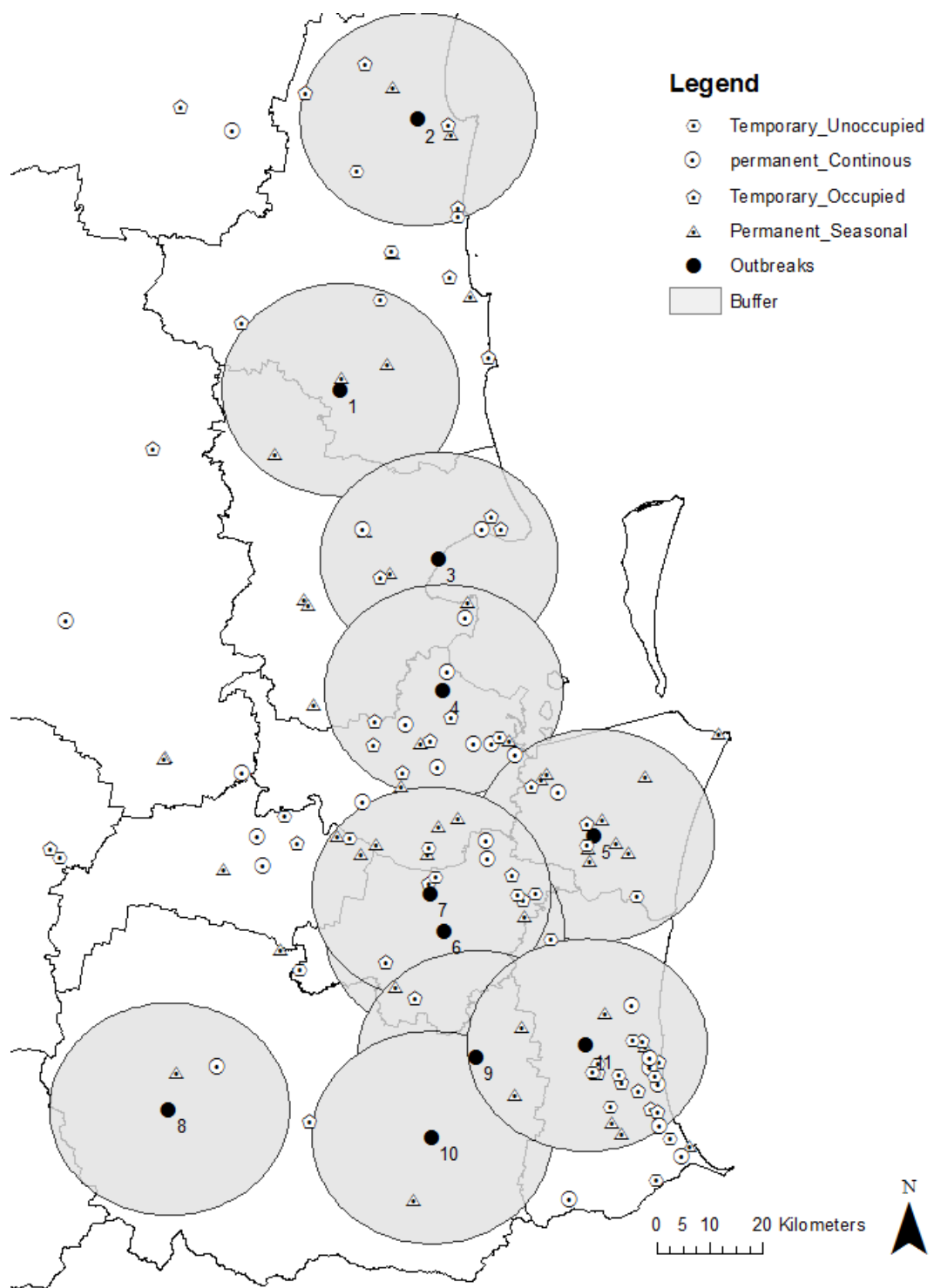
A buffer analysis was carried out on the HeV outbreak locations with a 20 kms range to determine the presence of the roosting sites within the outbreak region. This analysis examines the status of the flying fox roosting sites that were spatially correlated with the outbreak events in the study area. This establishes the preliminary correlation between the outbreak events and the flying fox roosting sites.

The specific 20 kms range has been used based on the study of the flying fox characteristics (Wildlife QLD 2016, see *Section 2.2*) and their travel distances - ‘foraging range’. The forage range for the four types of flying-foxes – black, grey-headed, little red and spectacled flying foxes vary. Black flying fox groups travel up to 50 kms from their camps to foraging areas and use the same camp for many years, whereas little red flying foxes and spectacled flying foxes only travel 20 – 30 kms from camp to feed. Grey-headed flying foxes nightly feeding range is 20 - 50 kms from their camps. The minimum home range distance is used for initial buffer analysis i.e. 20 kms.

The flying fox roosting sites were divided into six categories by Department of Environment and Heritage Protection (EHP), Queensland (see *Section 3.3*). Table 4.1 shows the percentage of flying fox roosting sites in each category.

Table 4.1: The Percentage of Flying Fox roosting sites in each category.

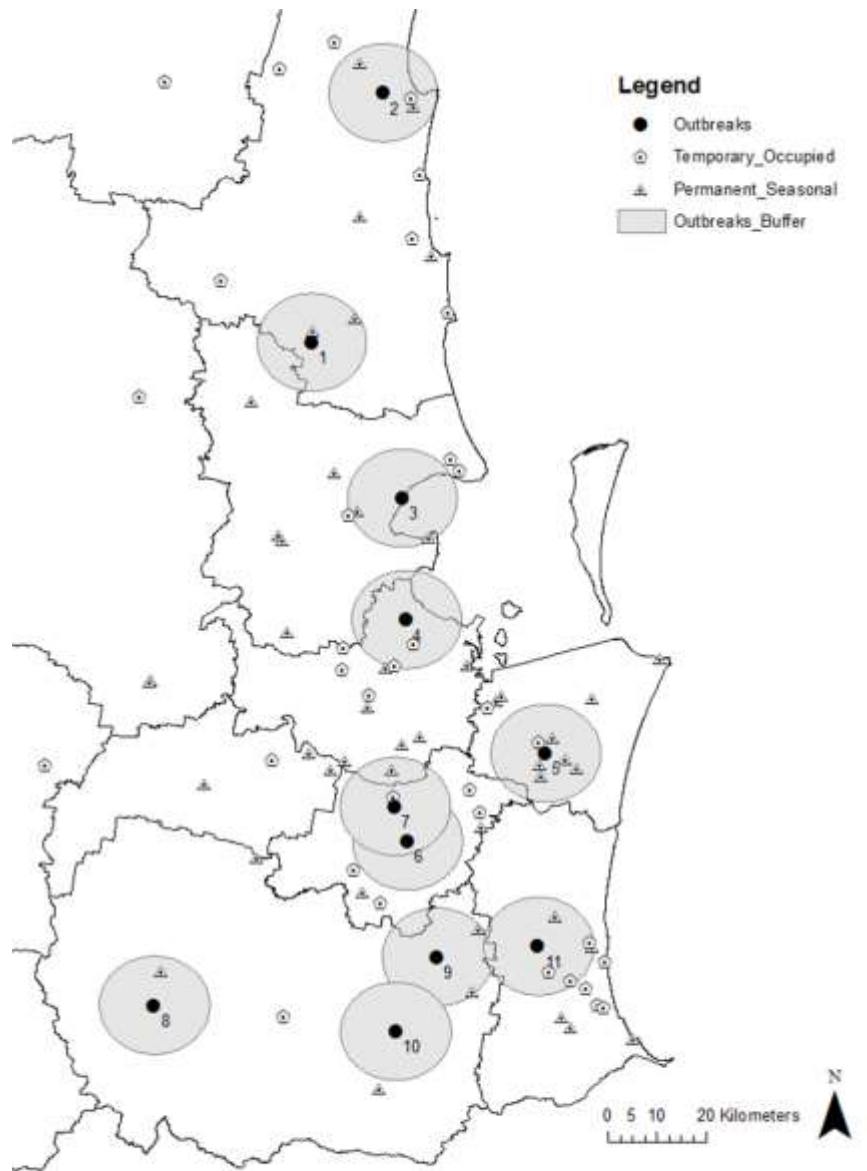
Status	Percentage of roosting sites
Permanent Seasonal Use	30.98%
Temporary Unoccupied	23%
Temporary Occupied	22.53%
Permanent Continuous Use	15.95%
Abandoned	7.04%
Destroyed	0.5%



20 kilometres Radius Buffer of the Outbreak Incidents

Figure 4.1: A 20 kms radius buffer of the outbreak incidents.

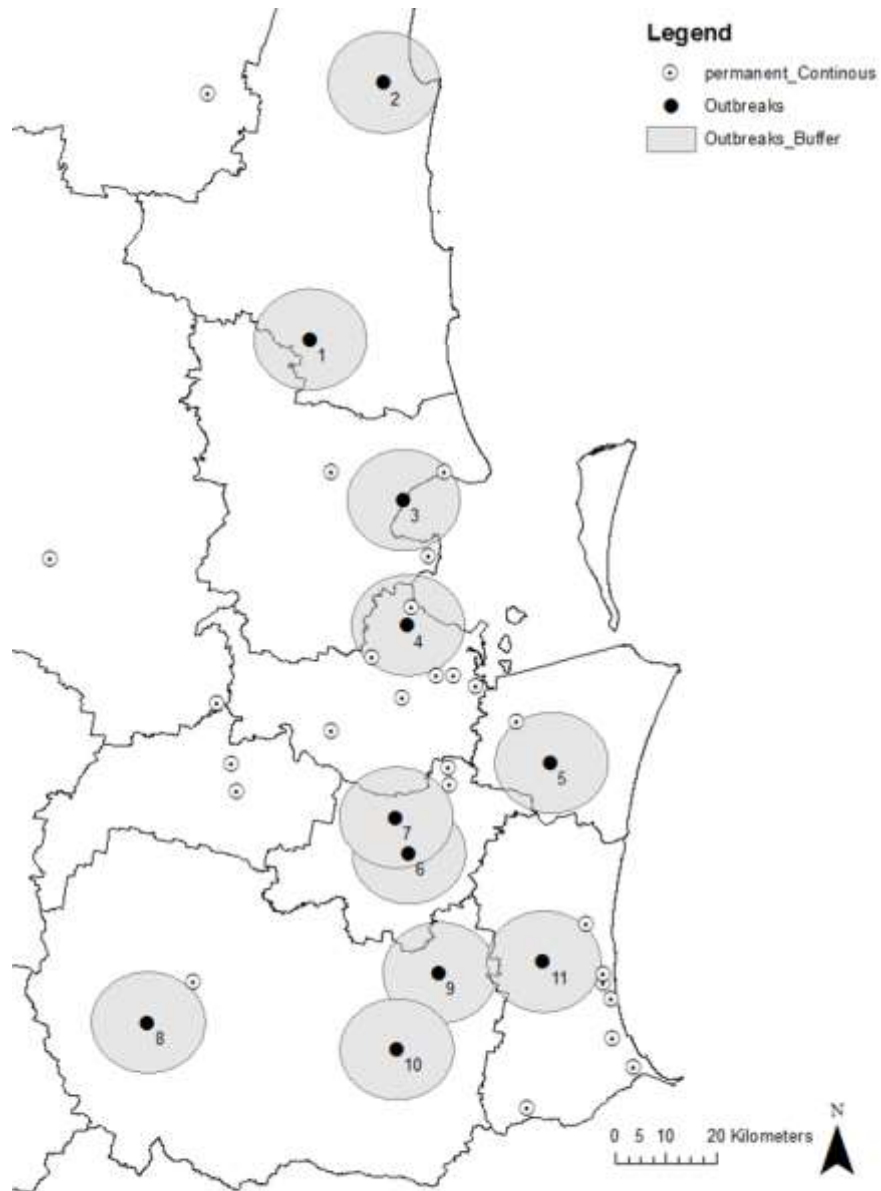
Figure 4.1 shows a 20 kms buffer of the outbreak incidents in the study area. There is a significance presence of the roosting sites in this buffer range and the presence of permanent seasonal sites in almost every incident's buffer range can be seen in the map. A further 10 kms radius buffer analysis is conducted on the temporary and permanent seasonal sites. Figure 4.2 shows a 10 kms buffer with respect to the temporary and seasonal roosting sites.



10 kms Buffer to Observe the Presence of Temporary and Seasonal Roosting Sites

Figure 4.2: A 10 kms buffer of the incidents with respect to the temporary and permanent seasonal roosting sites.

From figure 4.2, it is evident that permanent seasonal and temporary occupied roosting sites displays stronger spatial relationship to outbreak incidents as approximately 91% (10 out of 11 incidents) of the incidents have either one or both of these sites in the outbreak incidents buffer range. It is also evident that the permanent seasonal roosting sites displays stronger relationship than the temporary occupied sites with the presence of multiple roosting sites at each incident range.



10 kms Buffer to Observe the Presence of Permanent Roosting Sites

Figure 4.3: A 10 kms buffer of the incidents with respect to the permanent continuous roosting sites.

Figure 4.3 shows a 10 kms buffer of the outbreak incidents with respect to the permanent continuous roosting sites in the study area. The analysis shows a lower probability for a significant spatial relationship with permanent continuous roosting sites in the study area. Only 19% (2 out of 11 incidents) of the incidents have the permanent roosting site in their range and another couple of incidents have the permanent roosting on the border of the range.

The preliminary analysis of the HeV outbreak incidents and the roosting sites has identified a strong spatial relationship between the outbreak events and the permanent seasonal and temporary occupied roosting sites in the study area.

4.3 Factors Explaining the Dispersal of the HeV Disease (Hypothesis 2)

4.3.1 Measuring Spatial Autocorrelation (Global Moran's I) of the Flying Fox Species

Spatial clustering is best for the initial analysis to detect and analyse the clusters (Wakefield et al 2000) at the global level across the study area. Global Moran's I method (inverse distance conceptualisation) was used to identify the presence of significant spatial clustering of the three flying foxes species at various foraging ranges (10, 20, 30, 40 and 50 kms) in the study area, namely: black flying foxes, grey-headed flying foxes and little red flying foxes. The flying fox species data by EHP (2014) was used to measure the spatial autocorrelation. The autocorrelation of each species has been studied from 10 kms to 50 kms, which is the maximum foraging range (Wildlife QLD 2016, see *Section 2.2*). The 10 km range was selected for an in depth study of the flying fox clustering. The purpose of performing this analysis is to examine at what foraging range each species maintains high correlation (or no correlation). The results of this analysis would be significant in further study of the overall trend of the incidents with respect to the distribution of the flying fox species across the study area.

Table 4.2 shows the summary of the results of the spatial autocorrelation reports of the three flying fox species in the study area at various foraging ranges. For detailed reports of the autocorrelation at their minimum foraging range, see *Appendix 3*. The minimum foraging range was taken into consideration for most of the study.

Table 4.2: The results of the Spatial Autocorrelation of the Flying Fox species at various foraging ranges.

Species	10 kms	20 kms	30 kms	40 kms	50 kms
Black					
Index	0.064	0.035	0.04	0.05	0.065
Z-score	1.73	2.03	3.37	5.14	7.81
P value	<i>0.083</i>	<i>0.041</i>	<i>0.0007</i>	<i>0.0000</i>	<i>0.0000</i>
Confidence Level	90%	95%	99%	99%	99%
Inference	Clustered	Clustered	Clustered	Clustered	Clustered
Grey-Headed					
Index	0.025	0.009	0.004	0.002	0.023
Z-score	0.94	0.96	0.97	3.38	3.63
P value	<i>0.3472</i>	<i>0.3314</i>	<i>0.3308</i>	<i>0.0007</i>	<i>0.0002</i>
Confidence Level	-	-	-	99%	99%
Inference	Random	Random	Random	Clustered	Clustered
Little Red					
Index	0.154	0.15	0.12	N/A	N/A
Z-score	3.88	7.45	9.03		
P value	<i>0.0001</i>	<i>0.0000</i>	<i>0.0000</i>		
Confidence Level	99%	99%	99%		
Inference	Clustered	Clustered	Clustered		

The analysis of the black flying foxes showed significant clustering at all the foraging range intervals with high occurrence at 50 kms at a confidence level of 99%, which is their maximum foraging range. Grey-headed flying foxes showed random clustering at 10, 20 and 30 kms range. The maximum clustering for grey headed flying foxes occurred at 40 kms foraging range at a confidence level of 99%. The results of the little red flying foxes showed maximum significant clustering occurring at 10 kms range at a confidence level of 99%.

4.3.2 Examining and Establishing the Primary Relationship(s) between the Individual species Distribution, Incidents and Birth Period(s)

4.3.2.1 Kernel Density Analysis

Kernel density estimation technique was employed for observing the spread of the individual flying fox species population density across the study area and to generate hotspot maps for each species. Using the flying-fox species density data, the maps were created to visualise the species density hot spots. This method was used to establish the primary relation between the flying-fox species density and the incidents. The bandwidth for the KDE analysis for each species was set at 0.4598 degrees, which was calculated by the default search radius (bandwidth) algorithm of ArcGIS. Different bandwidth radii were tested (0.22 and 0.68 degrees) in generating the density hot spots but the default density calculated by ArcGIS yielded the best output with no errors such as missing neighbours. A density hot spot map was created for each species and the incidents were overlaid on the map to visualise the relationship between the two variables in the study area.

Figure 4.4 – a, b and c shows the KDE analysis of the black, grey-headed and little red flying foxes in the study area.

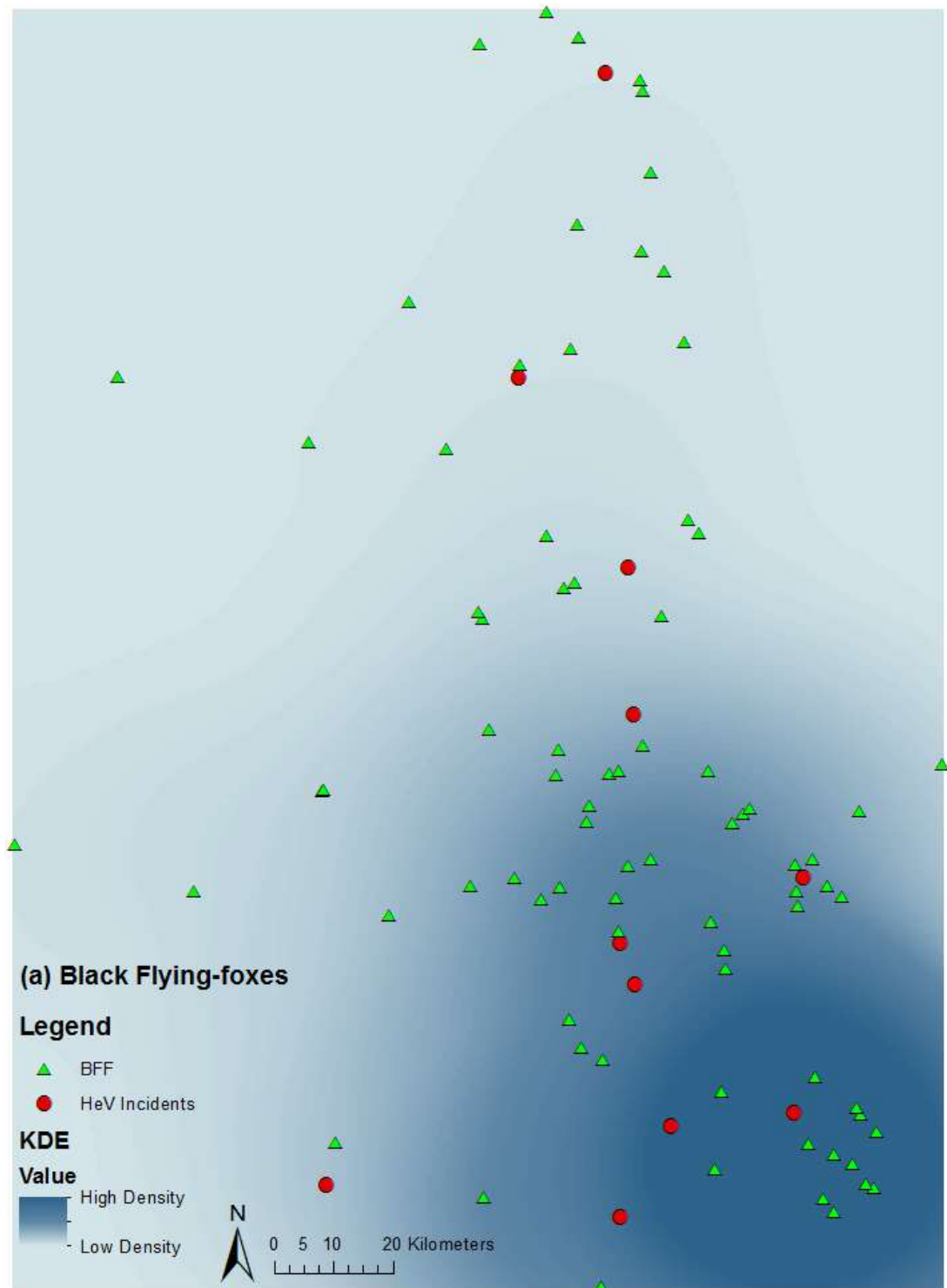


Figure 4.4(a): KDE analysis of black flying foxes in the study area.

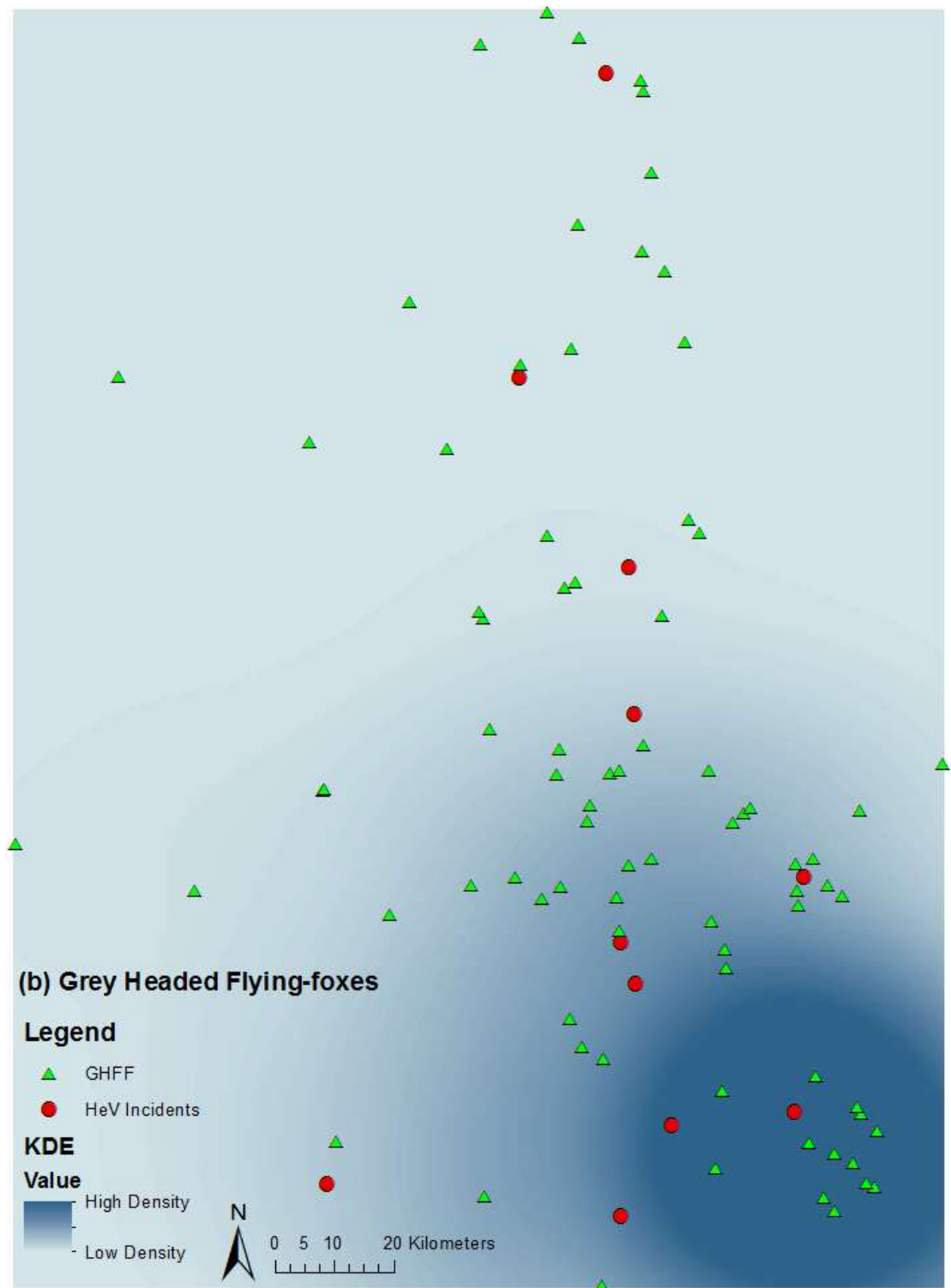


Figure 4.4(b): KDE analysis of grey-headed flying foxes in the study area.

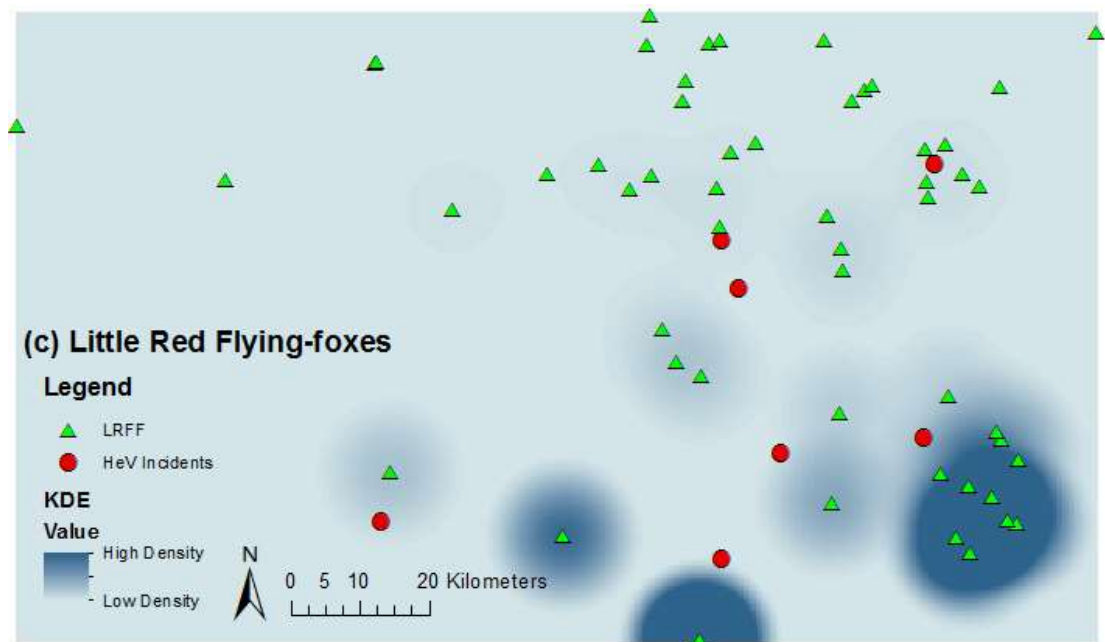


Figure 4.4(c): KDE analysis of little red flying foxes in the study area.

Through the KDE technique, it is evident that the black and grey-headed flying foxes are highly correlated to the HeV outbreak incidents in the study area. The little red flying foxes show little to no correlation to the outbreak incidents in the study area.

4.3.2.2 Birth Period Study of the Flying Foxes

Buffer analysis was employed to examine and visualise the relationship between individual flying fox species birth periods and the incidents in the study area. Each species of flying foxes have different breeding and birthing seasons (Wildlife QLD 2016, see *Section 2.2*), which usually last for 3 - 4 months. Incident data from DAFF and birth period data collected from Wildlife Queensland (2016) has been used in this method. The roosting data was edited to best reflect the status of the roosting sites at the time of the incident. Vegetation analysis (see *Section 4.4*) identified an abundance of food resources near these camp sites in the study area and hence it was assumed that the flying foxes in these camps do not migrate or at least to an extent that a roosting site is empty.

A 10 kms buffer was created for each incident and they were labelled using the month of the incident occurrence. The roosting sites of individual species were then projected on the buffer map to examine if the incident occurrence month falls within the birth periods of each species roosting site in the buffer range. Buffer analysis was useful in visualising the data and in studying the presence of number of individual species roosting sites that matched the month of occurrence of the disease within the buffer range to establish a base for further detailed study. Spatial clustering of the three species at 10 - 50 kms (See Table 4.2) indicated significant clustering of black and little red flying foxes at 10 and 20 kms range.

A radius of 10 and 20 kms were initially chosen to study the relationship between individual species birth periods and the month of occurrence of Hendra disease. As the 20 km range has overlapping incidents, the 10 km buffer was used for the better understanding of correlation. Figure 4.5 shows the 20 km range study of the incidents with majorly overlapping incident ranges.

Black Flying-foxes - 20 Kilomtres Buffer

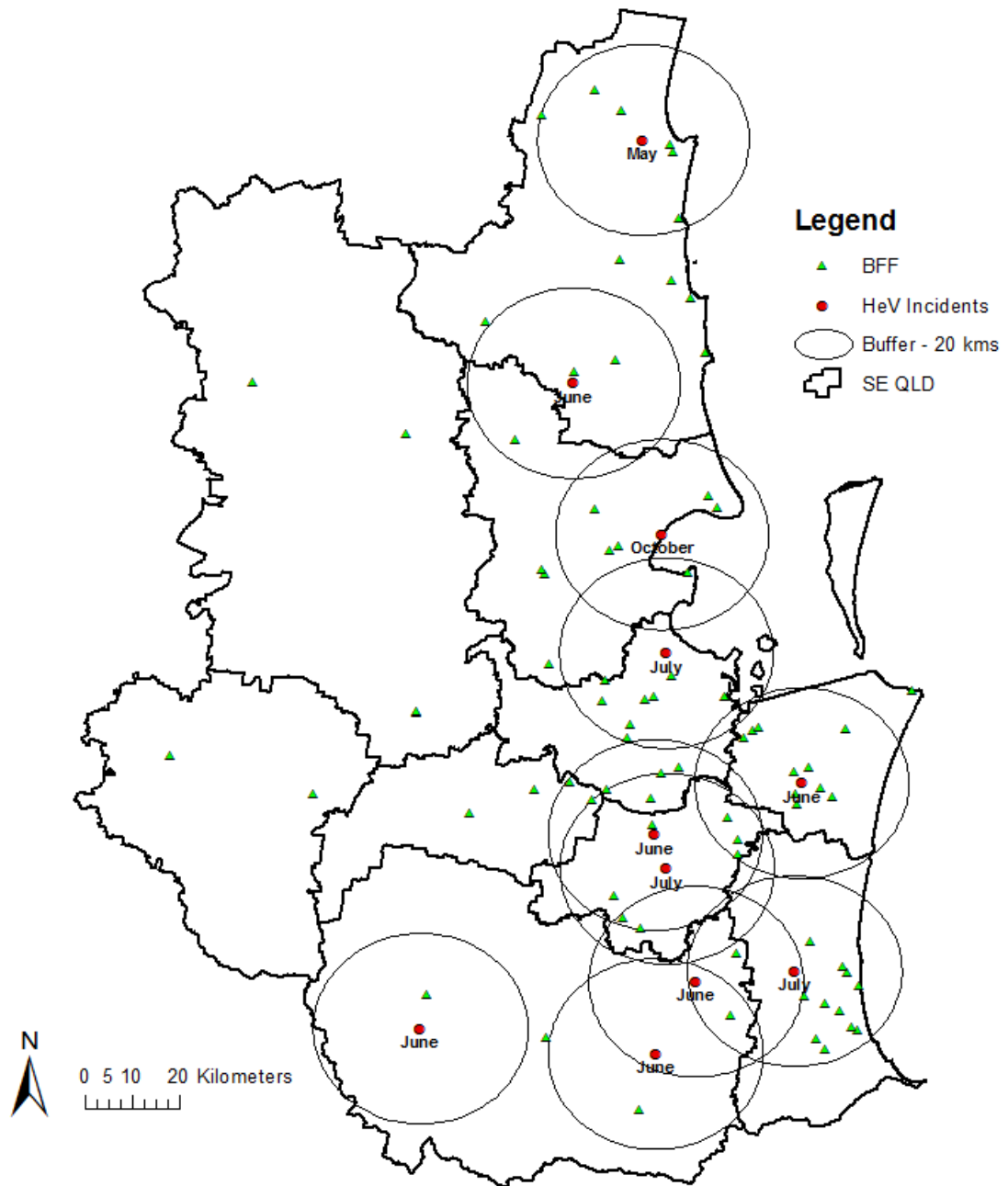


Figure 4.5: A 20 Kms range study of the incidents.

The birth/pregnancy period of black flying foxes lasts from June to February and the birth/pregnancy period of grey-headed flying foxes lasts from April to October (Wildlife QLD 2016). Figure 4.6 (a) shows the birth period study of the black flying foxes.

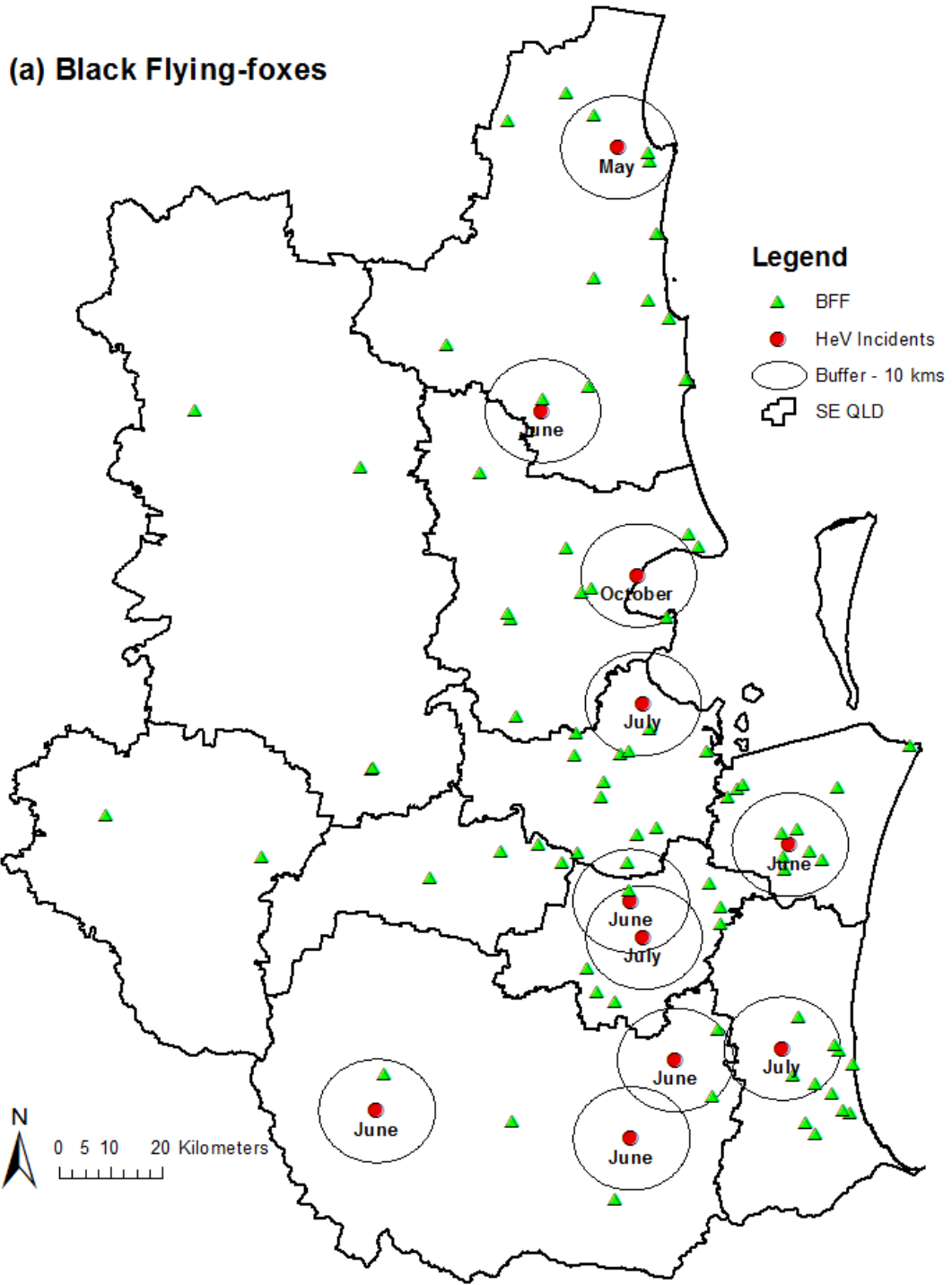


Figure 4.6 (a): Birth period study of the black flying foxes.

(b) Grey Headed Flying-foxes

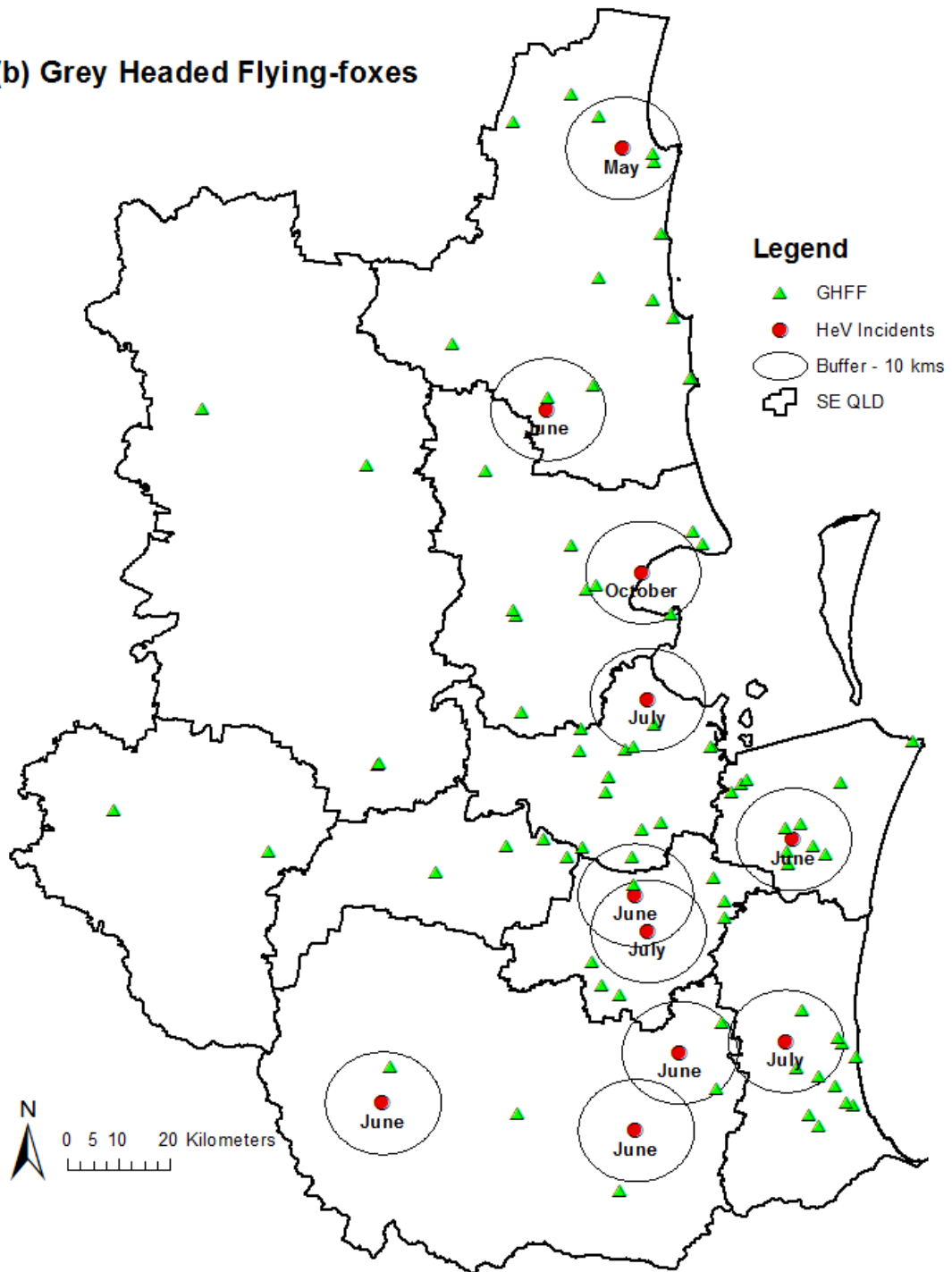


Figure 4.6 (b): Birth period study of the grey-headed flying foxes.

Figure 4.6 (b) shows the birth period study of the grey-headed flying foxes. Ten incidents have fallen within the birth/pregnancy period of the black flying foxes and grey-headed flying foxes with more than one roosting site in the buffer range.

The birth period of little red flying foxes lasts from January to May (Wildlife QLD 2016). Figure 4.6 (c) shows that none of the incidents have fallen within the birth/pregnancy period of the little red flying foxes. The buffer analysis established a primary relationship between the HeV outbreak incidents and the birth/pregnancy periods of black and grey-headed flying foxes in the study area.

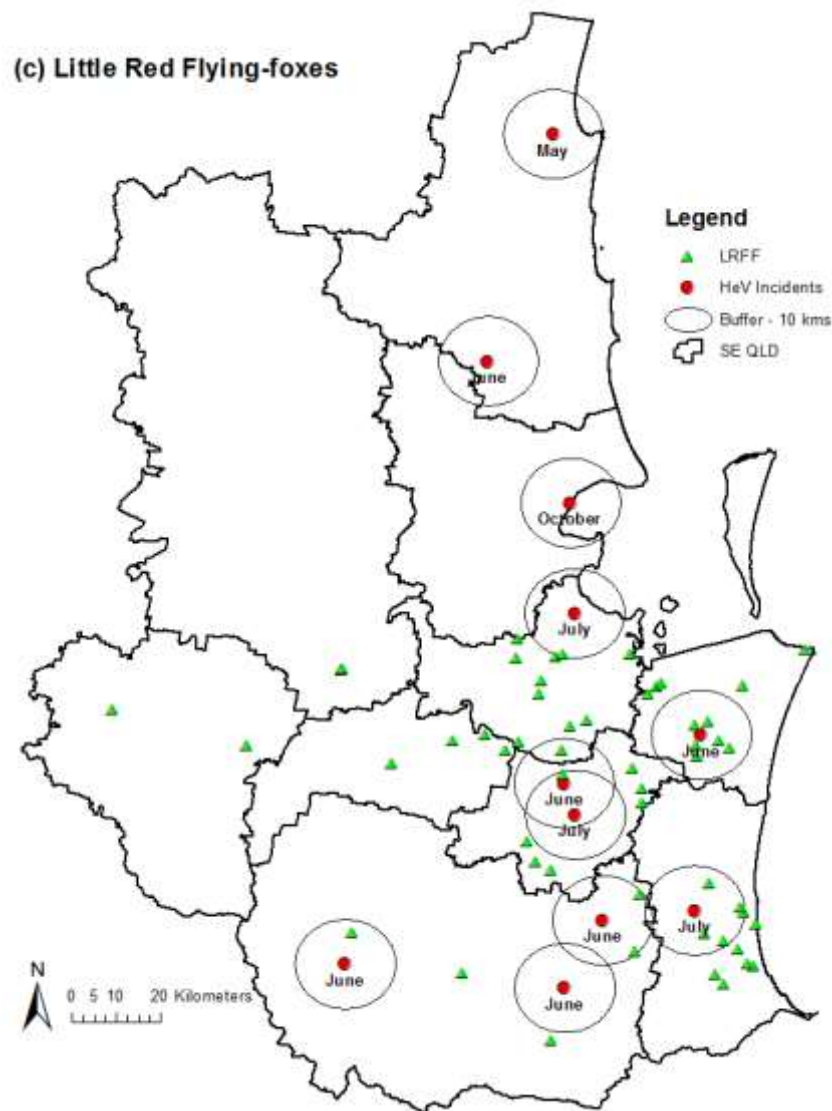


Figure 4.6 (c): Birth period study of the little red flying foxes.

4.3.3 Regression Modelling

By creating a scatterplot matrix for the model variables, it is possible to address the model bias issues. A nonlinear relationship between the dependent variable and one

of the explanatory variables is a common cause of model bias. If the dependent variable exhibits a nonlinear relationship with the explanatory variables, it may not be included in the model. OLS and GWR are linear regression models that assume the relationships between the models are linear. When the relationships are not linear, transforming the variables (log and exponential) can create relationships that are more linear (ESRI 2016). Based on the analysis in *section 4.3.2*, the independent variables chosen for the regression analysis are black flying fox species, grey-headed flying fox species, average foraging range and average pregnancy/birth period.

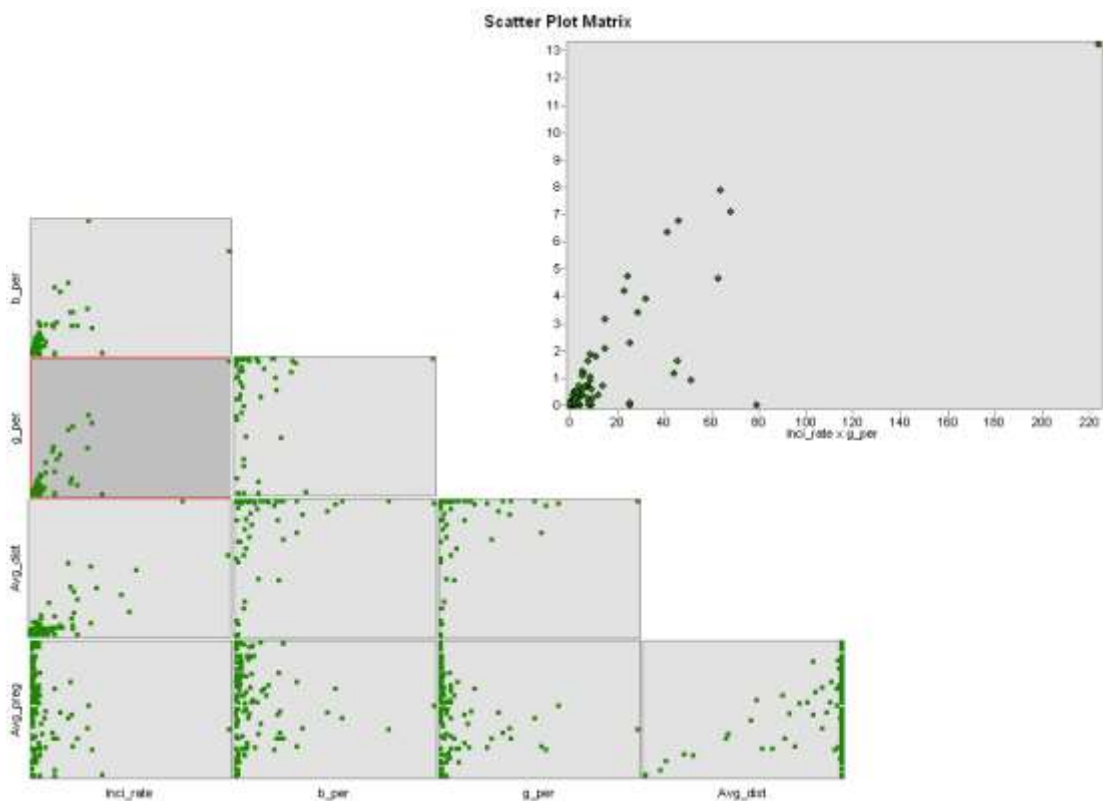


Figure 4.7: Scatter plot matrix of the model variables.

Figure 4.7 shows the scatter plot matrix of the regression model variables in the study. The independent variables black flying foxes, grey-headed flying foxes, average foraging range and average pregnancy/birth period exhibited a fairly linear relationship to the dependent variable – incident rate.

The method used in the modelling of the regression model is documented in *section 3.6.3*. Figure 4.8 shows the graph of the AIC values of all models used in the

regression modelling. The model with low AIC value and high R-squared value was selected as the significant model in all iterations (represented in colour 'Red').

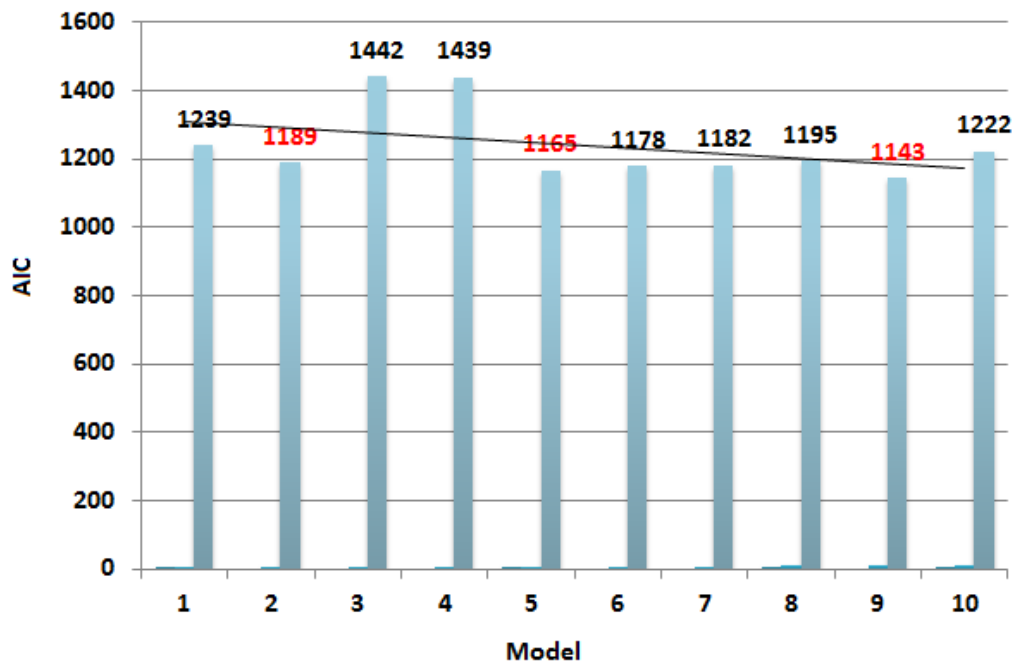


Figure 4.8: Graph of the AIC values of all models in the Regression Modelling.

Iteration 1 (significant model 1): Iteration 1 includes models 1, 2, 3 and 4. Independent variable – Grey-headed flying foxes (AIC – 1189, R-Squared – 0.82).

Iteration 2 (significant model 2): Iteration 2 includes models 5, 6 and 7. Independent variables – Grey-headed flying foxes and Black flying foxes (AIC – 1165, R-Squared – 0.82).

Iteration 3 (significant model 3): Iteration 3 includes models 8 and 9. Independent variables – Grey-headed flying foxes, Black flying foxes and average pregnancy period (AIC – 1143, R-Squared – 0.88). This is the final regression model used in the study to understand the HeV dispersal in the study area.

Iteration 4 (no significant model): Iteration 4 includes model 10 and it returned no significant model(s).

The spatial variability of the local parameter estimates of each variable has been tested using GWR4 software for each significant model from iteration 1, 2 and 3 and significant spatial variability was present in the variables of the final model. Figures 4.9 and 4.10 shows the results of the spatial variability test using GWR4.0 software.

```

*****
Geographical variability tests of local coefficients
*****
Variable      F          DOF for F test  DIFF of Criterion
-----
Intercept     0.257684    0.753 158.247    1.366108
Note: positive value of diff-Criterion (AICC, AIC, BIC/MDL or CV) suggests no spatial variability in terms of model selection criteria.
F test: in case of no spatial variability, the F statistics follows the F distribution of DOF for F test.
*****

```

Figure 4.9: Spatial variability test for significant model 1 using GWR4.0.

```

*****
Geographical variability tests of local coefficients
*****
Variable      F          DOF for F test  DIFF of Criterion
-----
Intercept     0.257684    0.753 158.247    1.366108
Note: positive value of diff-Criterion (AICC, AIC, BIC/MDL or CV) suggests no spatial variability in terms of model selection criteria.
F test: in case of no spatial variability, the F statistics follows the F distribution of DOF for F test.
*****

```

Figure 4.10: Spatial variability test for significant model 2 using GWR4.0.

Spatial variability was not present among the variables in significant model 1 and 2. A Positive “DIFF of Criterion” value that is greater than or equal to two suggests that the local term is better to be assumed as global. Significant model 1 and 2 has a positive value which is lesser than 1. Figure 4.11 shows the spatial variability test results of the final regression model. There was significant spatial variability present among the variables in the final model, which means these variables are better suited for a local model compared to a global model. For full test results of the three significant models in all iterations, see *Appendix 2*.

```

*****
Geographical variability tests of local coefficients
*****
variable      F          DOF for F test  DIFF of criterion
-----
Intercept     4.583933    6.893 134.769    -14.788531
perB          18.343303    3.689 134.769    -54.737133
perG          35.094427    3.065 134.769    -85.240322
perR          7.145171     5.597 134.769    -26.075265
Note: positive value of diff-Criterion (AICC, AIC, BIC/MDL or CV) suggests no spatial variability in terms of model selection criteria.
F test: in case of no spatial variability, the F statistics follows the F distribution of DOF for F test.
*****

```

Figure 4.11: Spatial variability test for significant model 2 using GWR4.0.

Moran's I test was performed on the residuals of the three significant models to check whether there is a key variable missing from each model. Table 4.3 shows the Moran's I test results of the three significant models.

Table 4.3: Moran's I results of the significant models.

	Moran's I	Z-score	P-value	Clustering
Significant Model 1	-0.12	-0.87	0.3	Random
Significant Model 2	-0.13	-1.04	0.2	Random
Final Model	-0.02	-0.12	0.9	Random

Final model indicated no significant clustering among the residuals. This indicates that the model is not misspecified. The test reports of the Moran's I was included in *Appendix*

4.3.4 Ordinary Least Squares (OLS) Analysis

OLS regression technique was employed to study the spatial trends of the HeV dispersion globally across the study area. The data sets used to perform this analysis were the same ones used for model calibration, which includes the incident data (DAFF 2014), flying fox species density data (EHP 2014), and the average foraging range and pregnancy/birth period of each camp. The model calibrated using the statistical model building procedure by Fotheringham, Kelly and Charlton (2012) (see section 3.6.3); with black flying fox density, grey-headed flying fox density and pregnancy period as explanatory variables. The OLS method calculated the probability and robust probability for each explanatory variable which may be required in cases of nonstationary relationships (nonstationary is determined using Koenker p-value in OLS output summary). The globally significant explanatory variable was identified using the OLS analysis. Koenker (BP) statistic measures the

relationship between the predicted values and changes in magnitudes (heteroscedasticity).

Table 4.4: Summary of OLS results.

Global Regression Model: Results					
Variable	t- statistic	Probability	Robust probability	VIF	Significance
<i>Black flying foxes</i>	1.26	0.2	0.53	3.58	
<i>Grey-headed flying foxes</i>	8.9	0.00*	0.00*	3.8	Significant
<i>Pregnancy Period</i>	-0.86	0.39	0.56	1.14	

Table 4.4 indicates that the independent variable ‘grey headed flying-foxes’ was globally significant at 99% confidence level across the study area. The variance inflation factor (VIF) values indicated no redundancy among the variables. Figure 4.12 shows the OLS regression residuals map.

OLS Regression Residuals Map

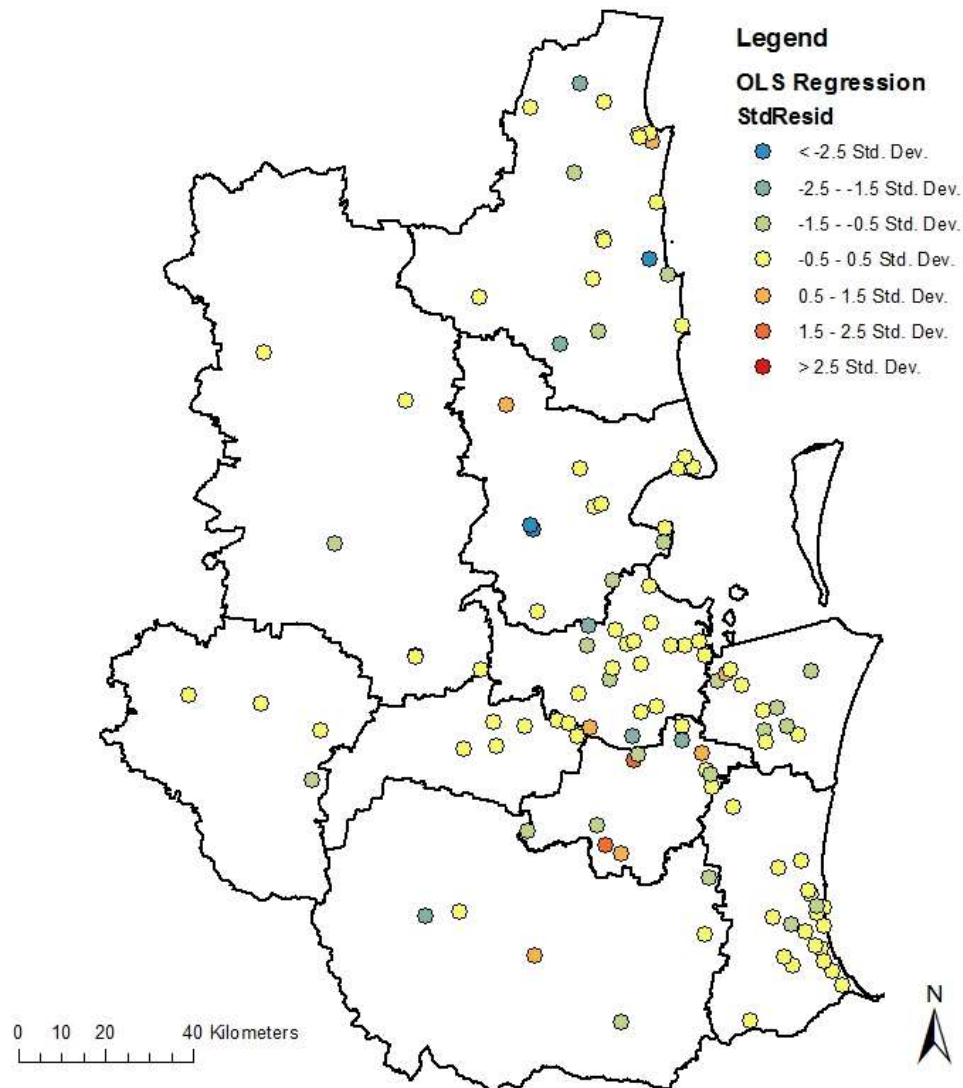


Figure 4.12: OLS regression residuals map.

This model has a statistically significant heteroscedasticity ($p < 0.05$) which suggests the use of Robust P to determine the coefficient significance for consideration. Goodness-of-fit measure indicated a model performance of 0.7. Moran's I test ($Index = -0.02, P = 0.8$) indicated no significant clustering among the residuals (see *Appendix 3*). Figure 4.13 shows the diagnostics of the OLS regression model. Figure 4.14 shows the graph of the OLS regression residuals. Full report of the OLS regression analysis is documented in *Appendix 3*.

OLS Diagnostics

Input Features:	Regression	Dependent Variable:	INCI_RATE
Number of Observations:	160	Akaike's Information Criterion (AICc) [d]:	1253.074281
Multiple R-Squared [d]:	0.712587	Adjusted R-Squared [d]:	0.707059
Joint F-Statistic [e]:	128.924029	Prob(>F), (3,156) degrees of freedom:	0.000000*
Joint Wald Statistic [e]:	37.607245	Prob(>chi-squared), (3) degrees of freedom:	0.000000*
Koenker (BP) Statistic [f]:	48.716507	Prob(>chi-squared), (3) degrees of freedom:	0.000000*
Jarque-Bera Statistic [g]:	4117.110363	Prob(>chi-squared), (2) degrees of freedom:	0.000000*

Figure 4.13: OLS regression diagnostics.

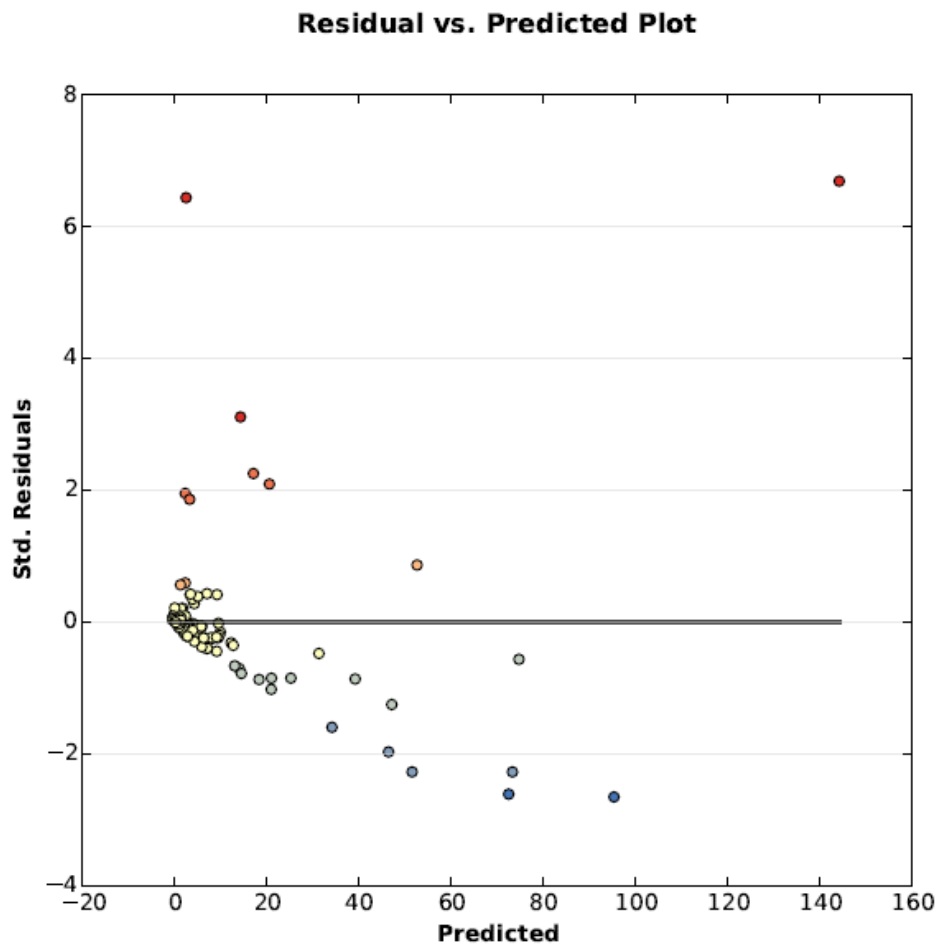


Figure 4.14: The graph of the OLS regression residuals.

The graph of the OLS residuals (model over and under predictions) in relation to the predicted dependent variable values should have little structure and look random.

This is an indicator for a properly specified model. For a misspecified model, the graph provides clues for better understanding of the dependent variable.

4.3.5 Geographically Weighted Regression (GWR) Analysis

The model building was carried out utilizing methods recommended in Fotheringham, Kelly and Charlton (2012) who built a set of most significant explanatory variables (see *Section 3.6.3*) among all the variables considered – species density, average foraging range and pregnancy/birth period; that could possibly explain the HeV dispersion in the study area. GWR technique assists in understanding and exploring of the spatial relationships at local level across the study area by fitting a regression equation to individual feature in the dataset. The shape and size of the bandwidth is dependent on user input for the kernel type, bandwidth method, distance, and number of neighbours' parameters (Fotheringham et al 2002). The model produced (explanatory variables - black flying fox density, grey-headed flying fox density and pregnancy period) using the data mentioned above in the model building procedure was used to study the locally varying spatial trends of the HeV incidents across the study area. The spatial variability among the local parameter estimates produced by GWR analysis of each variable has been tested using GWR4 software (see *Section 4.3.3*). The t values of each parameter estimate of each independent variable were mapped for a detailed study of the local relationships. The local R-squared values of the GWR regression model were mapped to visualise the overall performance of the model in the study area.

Table 4.5 shows the results of the GWR regression model. The goodness-of-fit measure indicated an improvement from 0.7 (global model, see table 3) to 0.88. Moran's I test ($Index = -0.02, P = 0.9$) indicated no significant clustering among the residuals (see *Appendix 2*).

Table 4.5: Summary of GWR regression model results.

VARNAME	Variable	Definition
Bandwidth	0.322621	
ResidualSquares	8523.058328	
EffectiveNumber	28.821755	
Sigma	8.06059	
AICc	1143.849672	
R2	0.889239	
R2Adjusted	0.865747	
Dependent Variable	0	Incident Rate
Explanatory Variable	1	Black Flying Foxes Density
Explanatory Variable	2	Grey-headed Flying Foxes Density
Explanatory Variable	3	Pregnancy Period

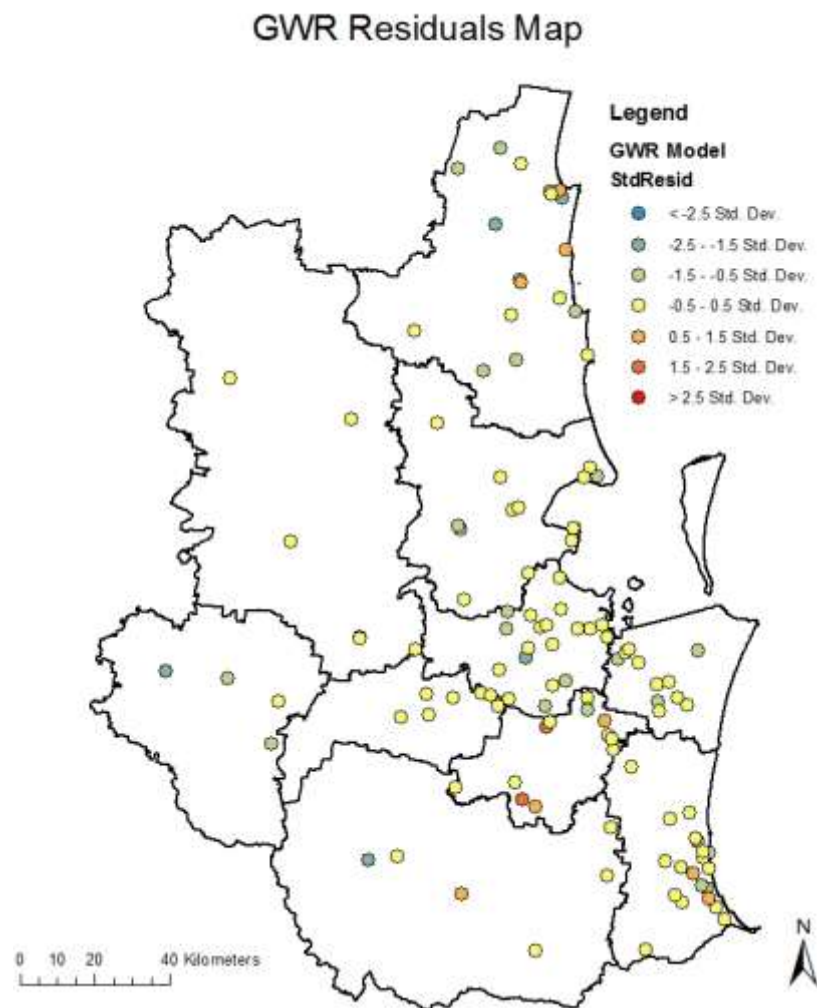


Figure 4.15: GWR model residuals map.

Figure 4.15 shows the regression residuals map of the GWR model in the study area. The t values of each parameter estimate of the independent variables were mapped for a detailed study of the local relationships. Figure 4.16 (a), (b) and (c) shows the significant local estimates of the GWR model variables – black flying foxes, grey-headed flying foxes and pregnancy period respectively.

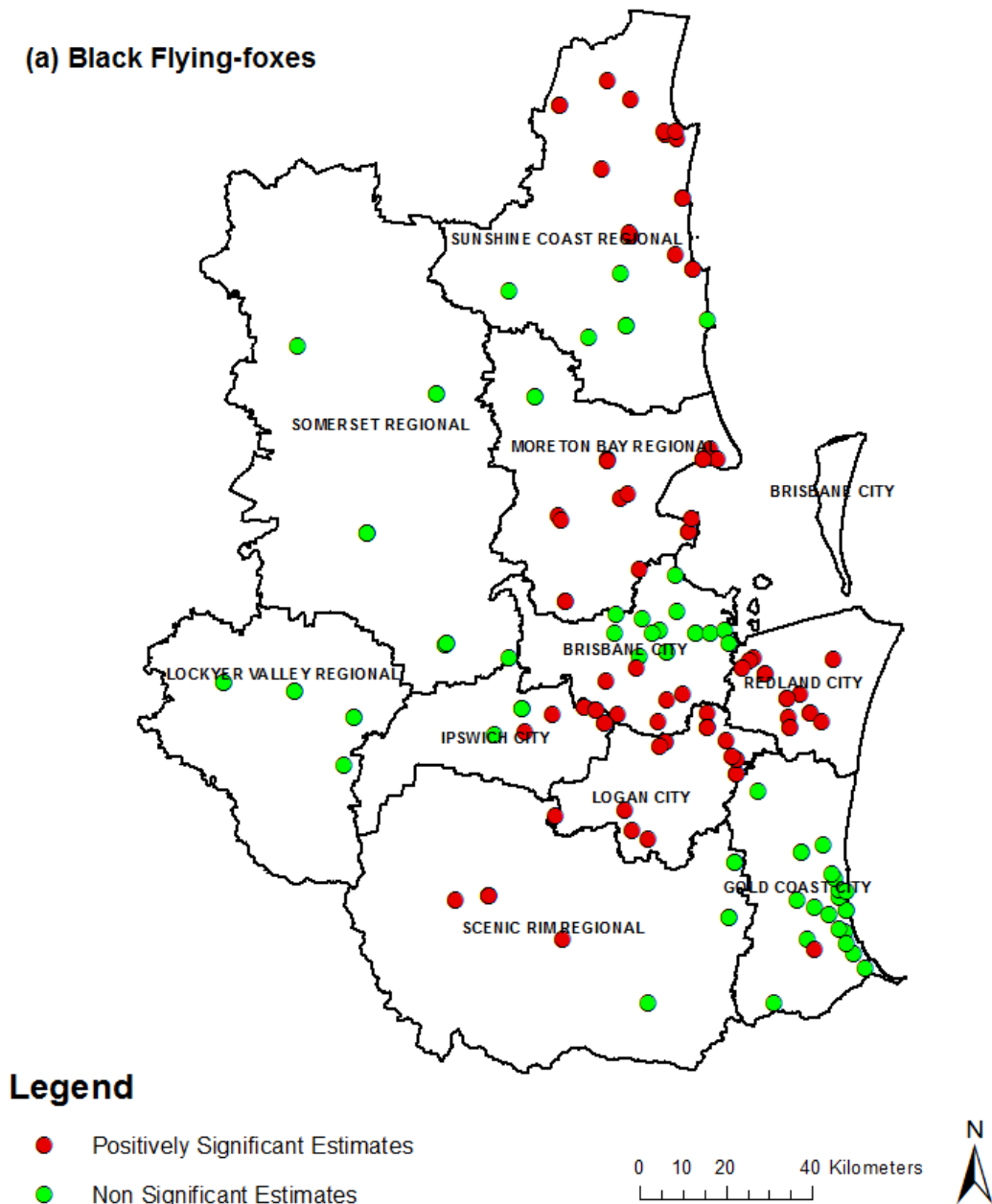


Figure 4.16 (a): Local estimates of the back flying foxes in the study area.

The black flying foxes showed positive significance in the regions of Logan, Redland, Scenic Rim and parts of Brisbane, Moreton Bay, and Sunshine Coast Regions. The grey headed flying-foxes showed positive significance in the regions of Brisbane, Ipswich, Gold Coast, Scenic Rim, Logan and Redland regions in the study area.

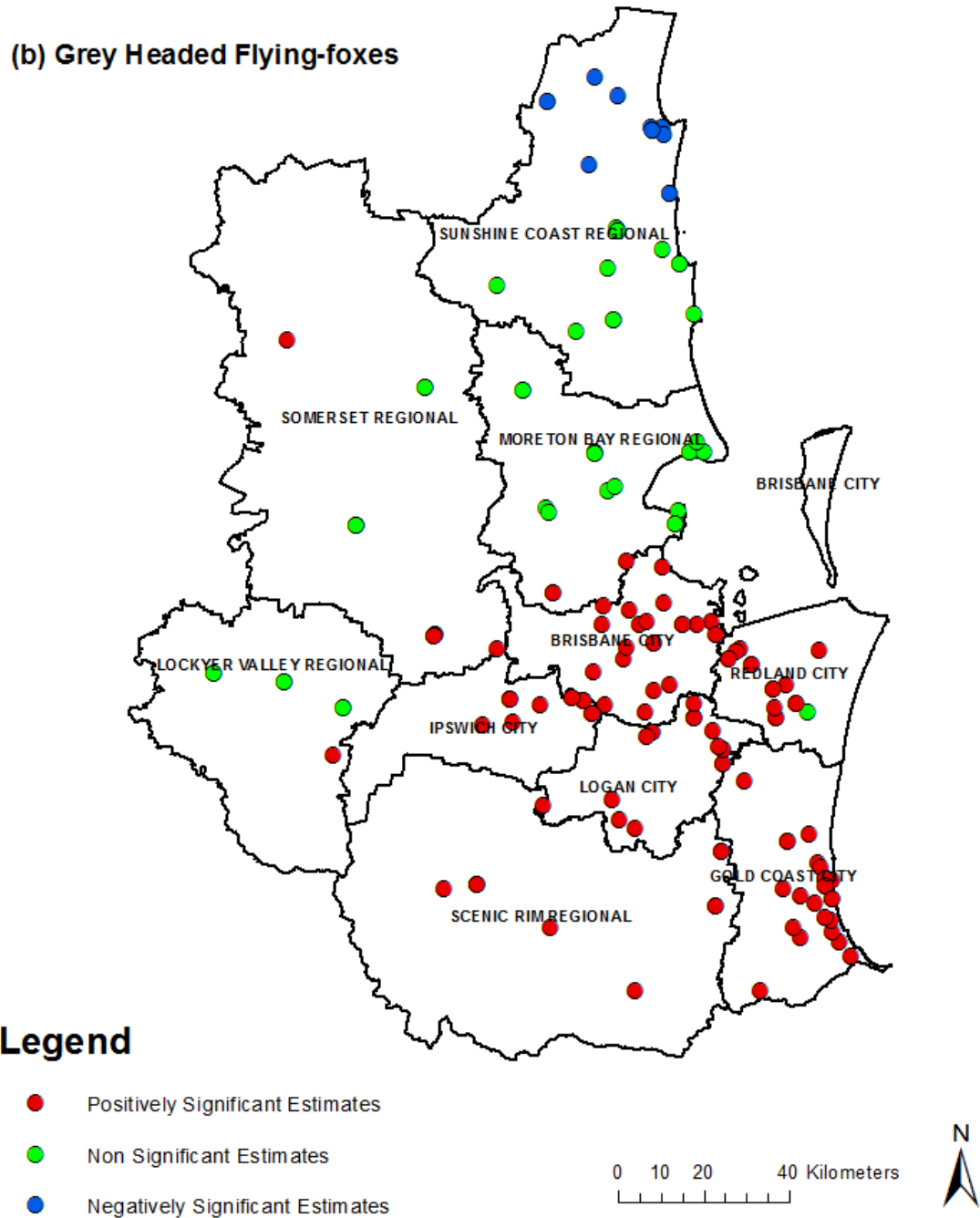


Figure 4.16 (b): Local estimates of the grey-headed flying foxes in the study area.

The black flying foxes showed a positive correlation where the grey-headed flying foxes displayed a negative correlation in the region of Sunshine Coast. The grey-headed flying foxes showed no significance in the region of Moreton Bay where black flying foxes showed a strong positive correlation in the study area.

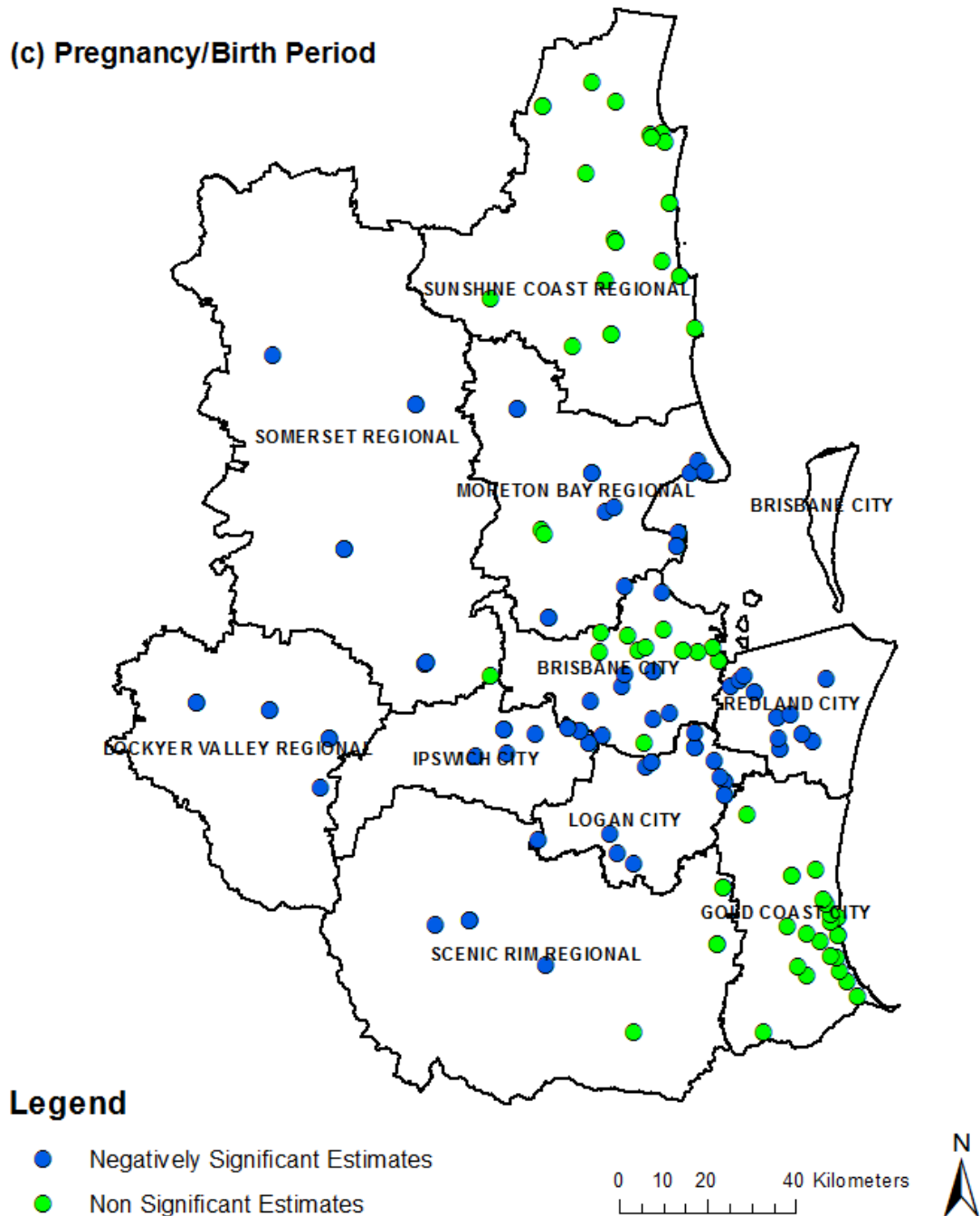


Figure 4.16 (c): Local estimates of the pregnancy period variable in the study area.

The pregnancy period variable showed negative significance in most of the regions except Gold Coast, Sunshine Coast and part of Brisbane where the variable showed no statistical significance in the study area. The results of the GWR model indicate that the virus dispersion is positively related to the density and distribution of the black and grey headed flying foxes in the study area.

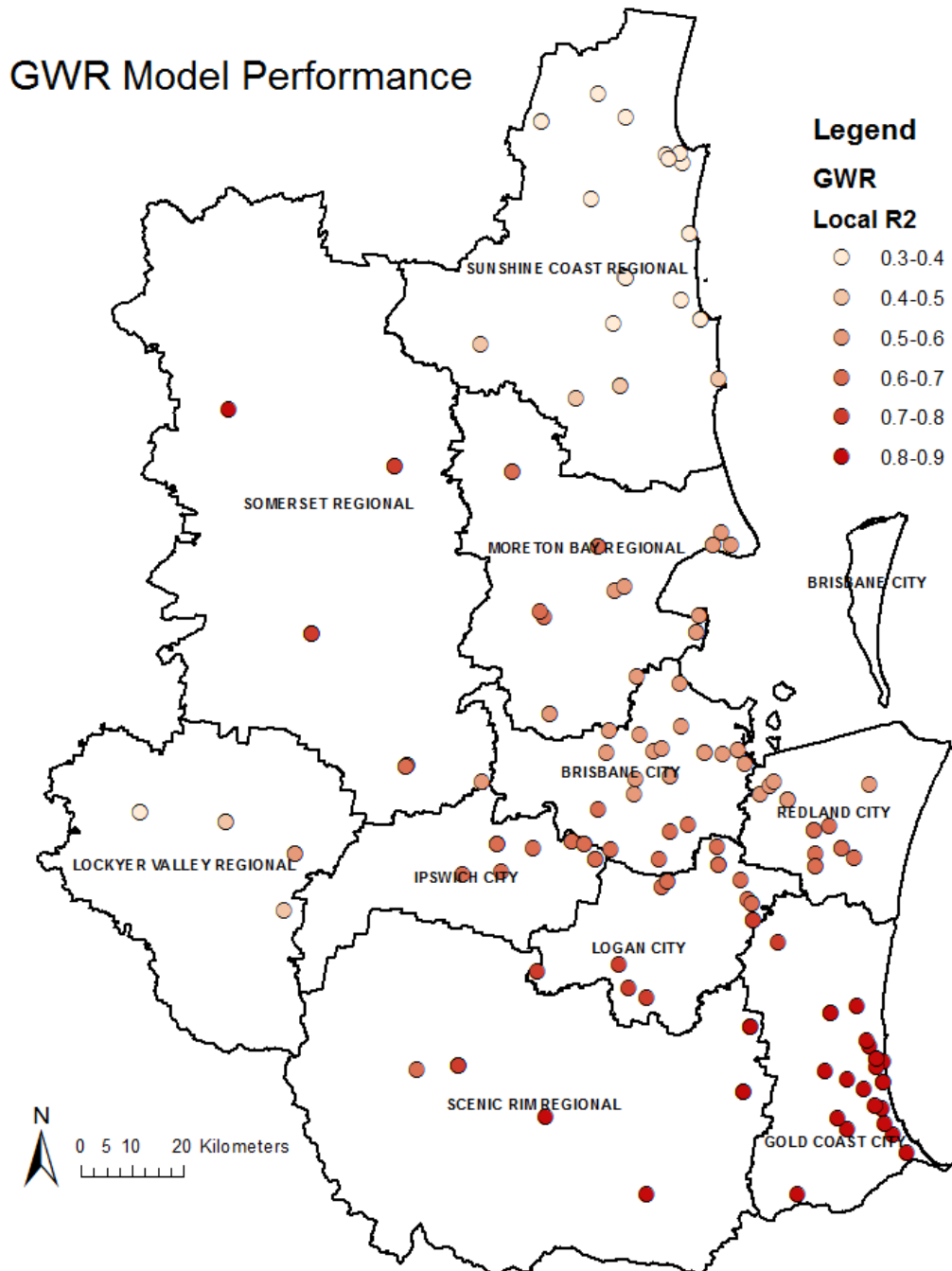


Figure 4.17: Local R-Squared values of the GWR model across the study area.

Figure 4.17 shows the model performance (local R-squared) across the study area. The GWR model performed well in the southern part of the study area where the incident rate is comparatively high and poorly in the northern region of the study area where the incident rate is low. Additional documentation of the local estimates of each variable is provided in *Appendix 3*.

4.4 Food Source Vegetation Analysis (Hypothesis 3)

4.4.1 An Investigation of the Food Sources and Roosting Sites as Potential Factors of HeV Dispersion

4.4.1.1 Black Flying Foxes

Using the Spatial Analyst toolset (see *Section 3.5.2*), the vegetation groups and subgroups on the black flying fox roosting sites were identified. Figure 4.18 shows the black flying fox roosting sites in the study area. For full legend of the MVS and MVG, see *Appendix 1*.

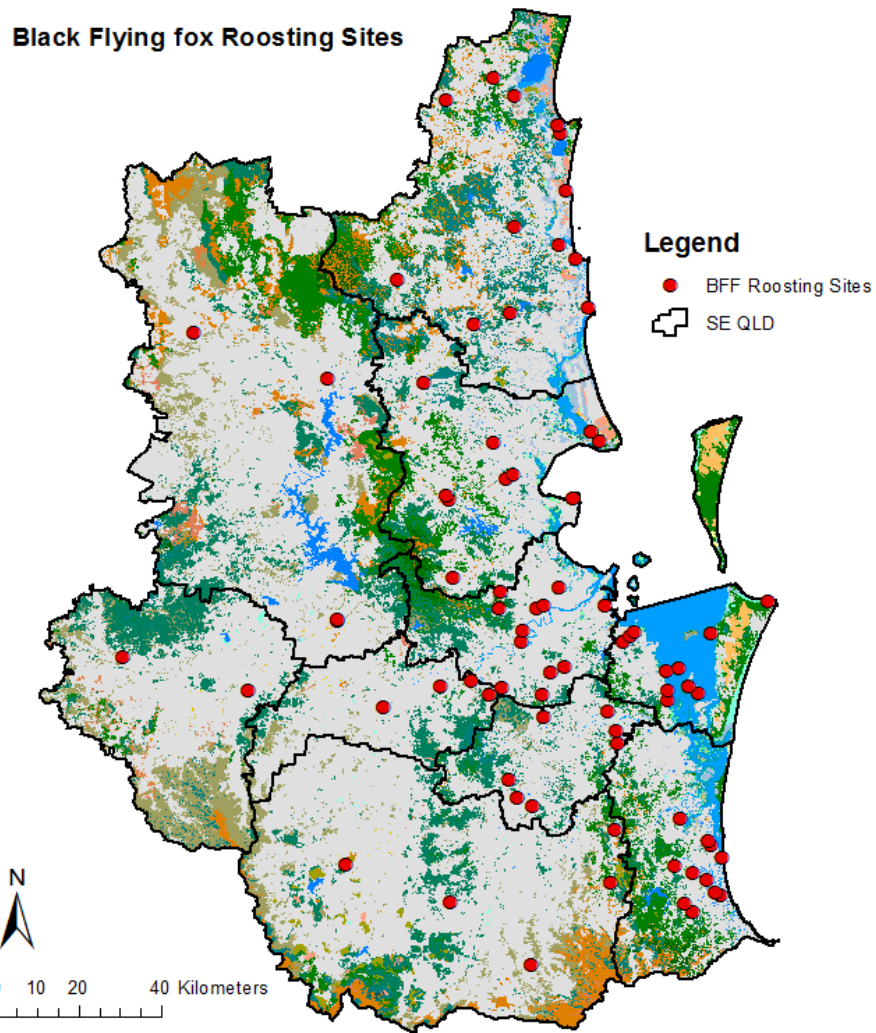


Figure 4.18: Black flying fox roosting sites in the study area.

Table 4.6: Major vegetation groups on the black flying fox roosting sites in the study area.

Value	MVG Name	MVG Common Description
1	Rainforests and Vine Thickets	Rainforests
3	Eucalyptus Open Forests	Eucalyptus Trees (10 to 30 m tall)
5	Eucalyptus Woodlands	Eucalyptus Woodlands (tree crowns not touching)

8	Casuarina Forests and Woodlands	She-oak Forests and Woodlands
9	Melaleuca Forests and Woodlands	Paperbark Forests and Woodlands
23	Mangroves	Mangroves
24	Inland Aquatic – Freshwater, Salt Lakes, Lagoons	Water
25	Cleared, Non-native Vegetation, Buildings	Cleared Vegetation
28	Sea and Estuaries	Sea

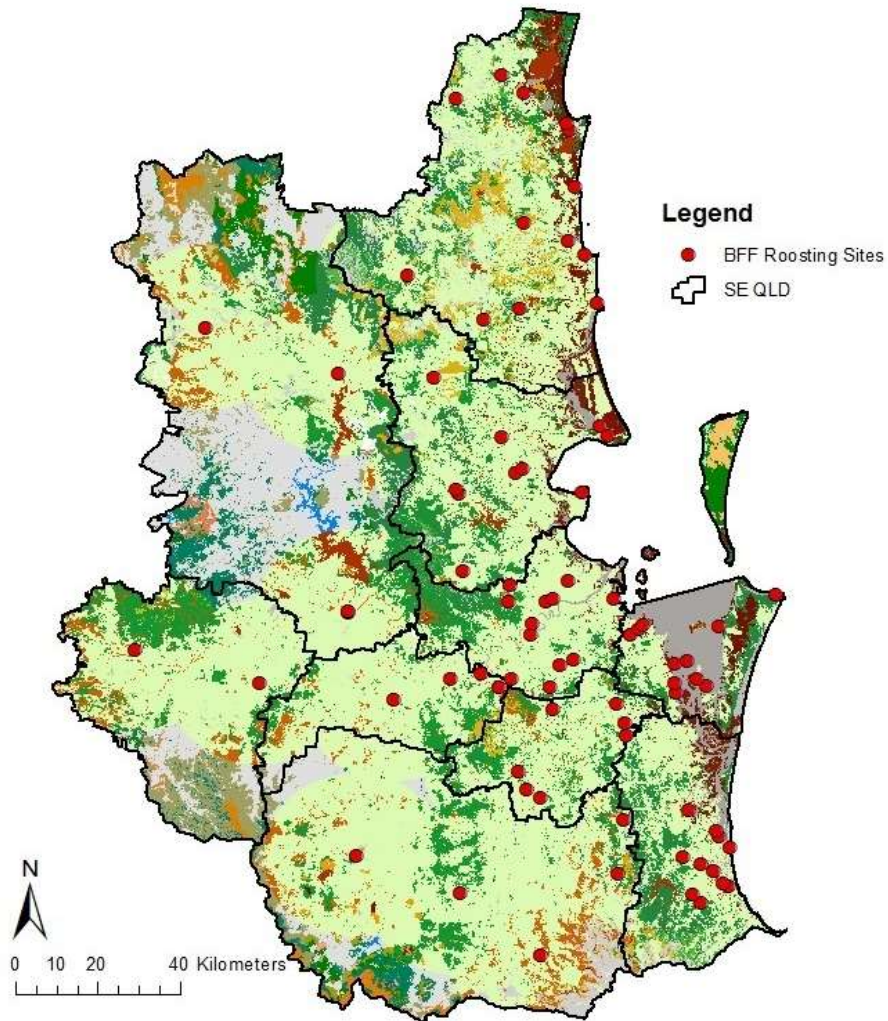
Table 4.6 shows the major vegetation groups and their common description on the black flying fox roosting sites in the study area. Table 4.7 shows the major vegetation subgroups identified on the black flying fox roosting sites in the study area. The field ‘value’ represents the unique ID of the vegetation type. From the list of major vegetation groups and subgroups, it is evident that the black flying fox roosting sites were located near the eucalyptus and rainforests type of vegetation.

Table 4.7: Major vegetation groups on the black Flying fox roosting sites in the study area.

Value	MVS Name
2	Tropical or Sub-tropical Rainforest
5	Eucalyptus Open Forests with a Grassy Understorey
9	Eucalyptus Woodlands with a Tussock Grassy Understorey
15	Melaleuca Forests and Woodlands
26	Casuarina and Allocasuarina Forests and Woodlands
40	Mangroves
44	Freshwater, Dams, Lakes, Lagoons or aquatic Plants
46	Sea and Estuaries (includes seagrass)
98	Cleared, Non-native Vegetation, Buildings

Using the buffer analysis and extract by mask tool, the vegetation subgroups near the black roosting sites was identified. Area covering 20 kms from the roosting sites has been chosen for the study as it the minimum foraging range of both the species. Figure 4.19 shows the identification of the major vegetation subgroups within 20 kms buffer range of the black flying fox roosting sites in the study area. For a full list of vegetation subgroups identified, see *Appendix 4*.

Identification of MVS within 20 kms Buffer Range of the Black Flying fox Roosting Sites



List of Notable Vegetation Subgroups Identified

MVS_NAME

- Casuarina and Allocasuarina forests and woodlands
- Cleared, non-native vegetation, buildings
- Dry rainforest or vine thickets
- Eucalyptus (+/- tall) open forest with a dense broad-leaved and/or tree-fern understorey (wet sclerophyll)
- Eucalyptus open forests with a grassy understorey
- Eucalyptus open forests with a shrubby understorey
- Eucalyptus tall open forests and open forests with ferns, herbs, sedges, rushes or wet tussock grasses
- Eucalyptus woodlands with a shrubby understorey
- Eucalyptus woodlands with a tussock grass understorey
- Freshwater, dams, lakes, lagoons or aquatic plants
- Low closed forest or tall closed shrublands (including Acacia, Melaleuca and Banksia)
- Mangroves
- Melaleuca open forests and woodlands

Figure 4.19: Major vegetation subgroups within 20 kms range of the black flying fox roosting sites.

Identification of Black Flying Fox Food Resources within 20 kms Buffer Range

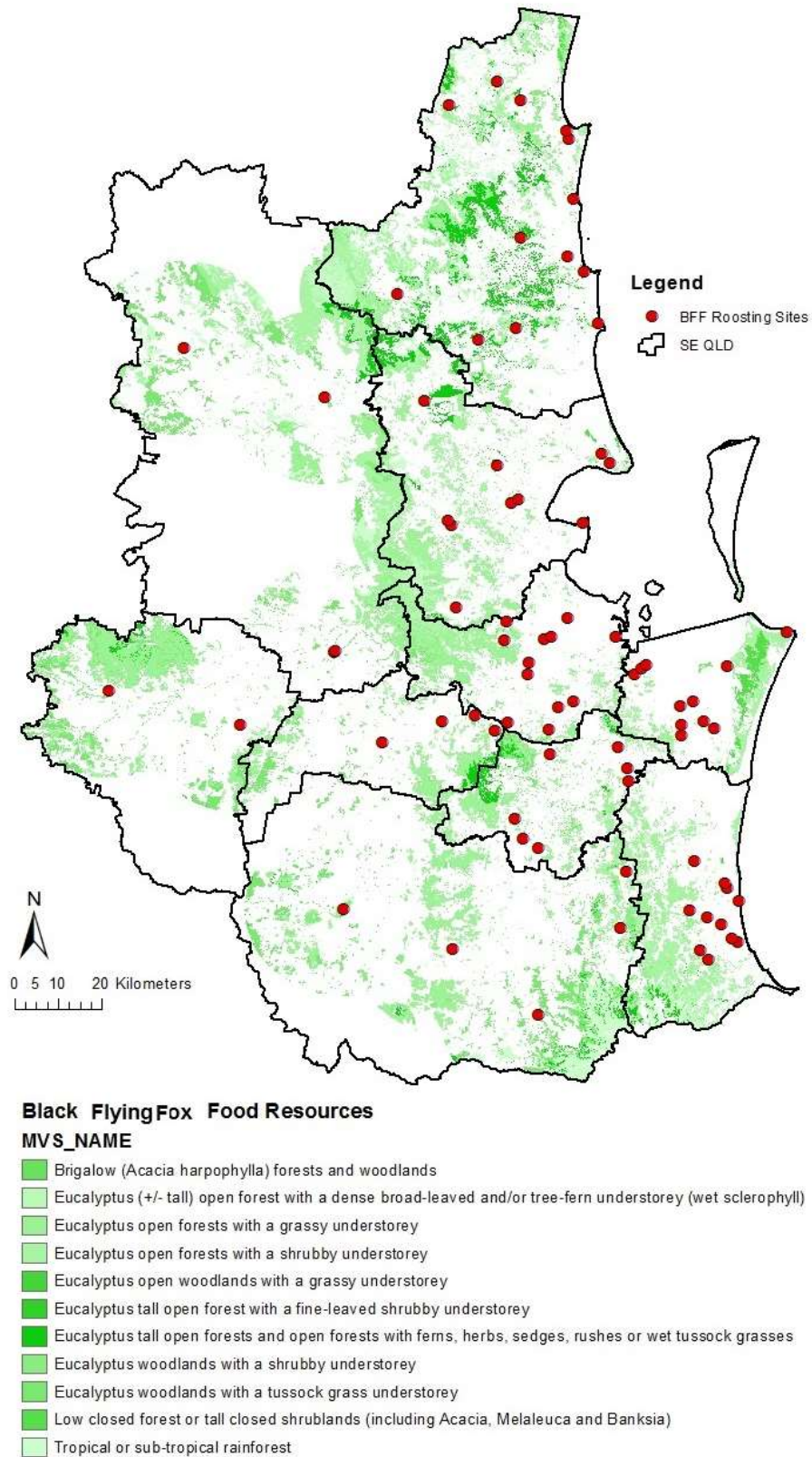


Figure 4.20: Identification of food resources within 20 kms range of the black flying fox roosting sites.

Using extract by attributes tool, the possible food resources for black flying fox species near the roosting sites were identified. Figure 4.20 shows the food resources identified within the minimum foraging range of the black flying foxes in the study area. Table 4.7 shows the food source vegetation of the black flying foxes in a descending order to study the most occurring food source vegetation.

Table 4.8: List of black flying fox food source vegetation and its count in the study area.

Value	Count	MVS Name
5	190355	Eucalyptus open forests with a grassy understorey
4	123885	Eucalyptus open forests with a shrubby understorey
9	77878	Eucalyptus woodlands with a tussock grass understorey
2	68127	Tropical or Sub-tropical Rainforest
60	46374	Eucalyptus tall open forests and open forests with ferns, herbs, sedges, rushes or wet tussock grasses
3	15429	Eucalyptus (-/+) open forests with a dense broad-leaved and/or tree-fern understorey
8	8633	Eucalyptus woodlands with a shrubby understorey
28	6809	Low closed forest or tall closed shrub lands (including Acacia, Melaleuca and Banksia)
13	829	Brigalow forests and woodlands
54	66	Eucalyptus tall open forest with a fine-leaved shrubby understorey
48	48	Eucalyptus open woodlands with a grassy understorey

Table 4.9: Summary of the cluster analysis results of black flying foxes food source vegetation.

Distance Threshold	Getis-Ord General G Statistic Report	High/low Clustering
3 kms	Observed General G – 0.000002 z-Score – 20.21 p-value – 0.00000	High Clustering
5 kms	Observed General G – 0.000003 z-Score – 14.48 p-value – 0.00000	High Clustering
10 kms	Observed General G – 0.000005 z-Score – 6.97 p-value – 0.00000	High Clustering

High/low Clustering (Getis-Ord General G) analysis was performed on the food source vegetation of the black flying foxes at various thresholds (3, 5, and 10 kms) to examine the clustering. Table 4.8 shows the summary of the results of High/low clustering analysis of the black flying fox food source vegetation. The analysis returned high clustering at a confidence level of 99% at all the thresholds tested. For the full report of the analyses, see *Appendix 4*.

4.4.1.2 Grey-headed Flying Foxes

Using the Spatial Analyst toolset (see *Section 3.5.2*), the vegetation groups and subgroups on the grey-headed flying fox roosting sites were identified. Figure 4.21 shows the grey-headed flying fox roosting sites in the study area. For full legend of the MVS and MVG, see *Appendix 1*.

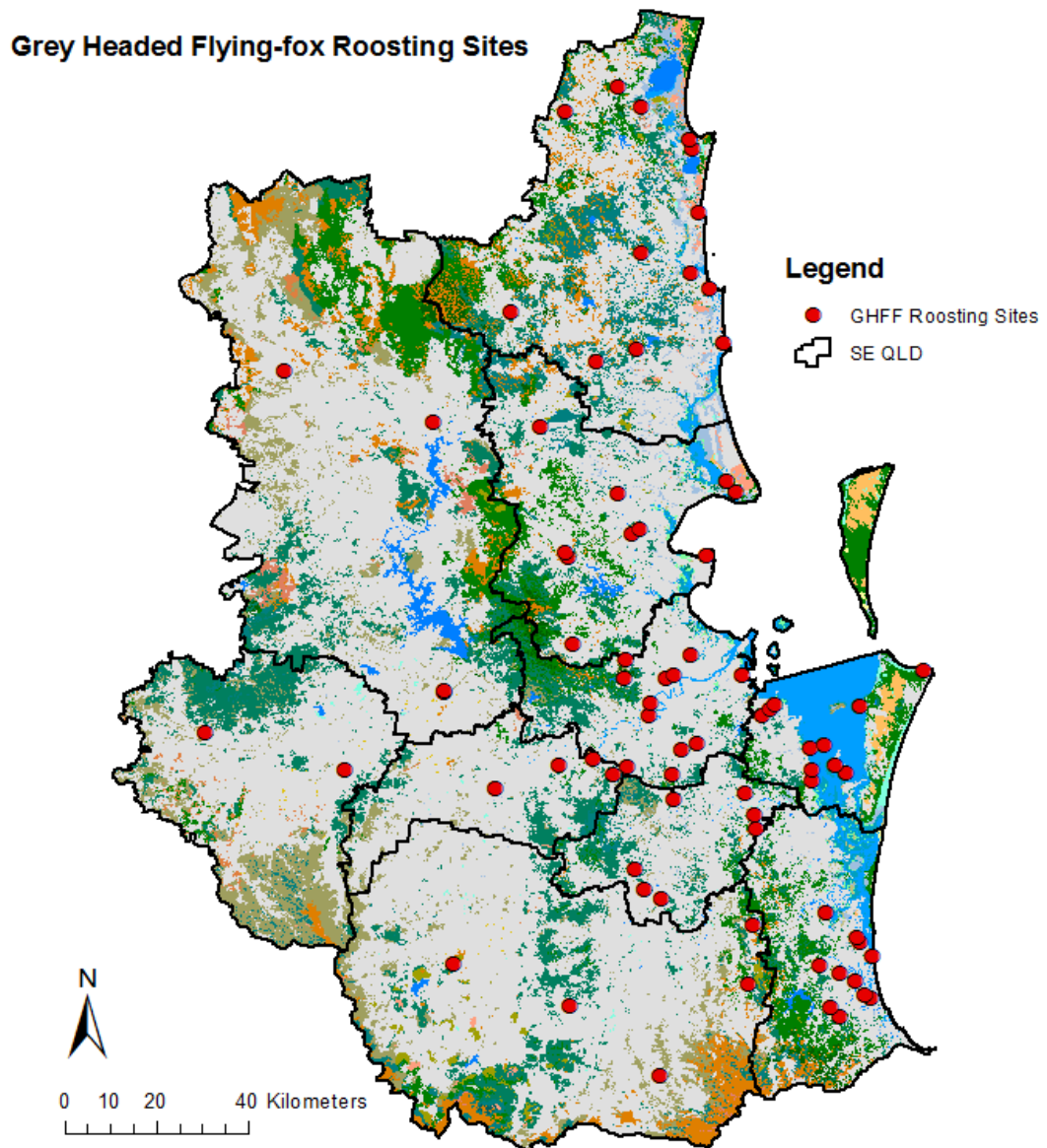


Figure 4.21: Grey-headed flying fox roosting sites in the study area.

Table 4.10 shows the major vegetation groups and their common description on the grey-headed flying fox roosting sites in the study area. Table 4.11 shows the major vegetation subgroups identified on the grey-headed flying fox roosting sites in the study area. From the list of major vegetation groups and subgroups, it is evident that the grey-headed flying foxes prefer eucalyptus and rainforests type of vegetation as their roosting sites. The grey-headed flying foxes roosting site vegetation is almost same as the black flying fox species.

Table 4.10: List of major vegetation groups on the grey-headed flying fox roosting sites in the study area.

Value	MVG Name	MVG Common Description
1	Rainforests and Vine Thickets	Rainforests
3	Eucalyptus Open Forests	Eucalyptus Trees (10 to 30 m tall)
5	Eucalyptus Woodlands	Eucalyptus Woodlands (tree crowns not touching)
8	Casuarina Forests and Woodlands	She-oak Forests and Woodlands
9	Melaleuca Forests and Woodlands	Paperbark Forests and Woodlands
23	Mangroves	Mangroves
24	Inland Aquatic – Freshwater, Salt Lakes, Lagoons	Water
25	Cleared, Non-native Vegetation, Buildings	Cleared Vegetation
28	Sea and Estuaries	Sea

Table 4.11: List of major vegetation subgroups on the grey-headed flying fox roosting sites in the study area.

Value	MVS Name
2	Tropical or Sub-tropical Rainforest
5	Eucalyptus Open Forests with a Grassy Understorey
9	Eucalyptus Woodlands with a Tussock Grassy Understorey
15	Melaleuca Forests and Woodlands
26	Casuarina and Allocasuarina Forests and Woodlands
40	Mangroves
44	Freshwater, Dams, Lakes, Lagoons or aquatic Plants
46	Sea and Estuaries (includes seagrass)
98	Cleared, Non-native Vegetation, Buildings

Using the buffer analysis and extract by mask tool, the vegetation subgroups near the grey-headed flying fox roosting sites was identified. Figure 4.22 shows the identification of the major vegetation subgroups within 20 kms buffer range of the grey-headed flying fox roosting sites in the study area. For a full list of vegetation subgroups identified, see *Appendix 4*.

Identification of MVS within 20 kms Buffer Range of the Grey Headed Flying-fox Roosting Sites

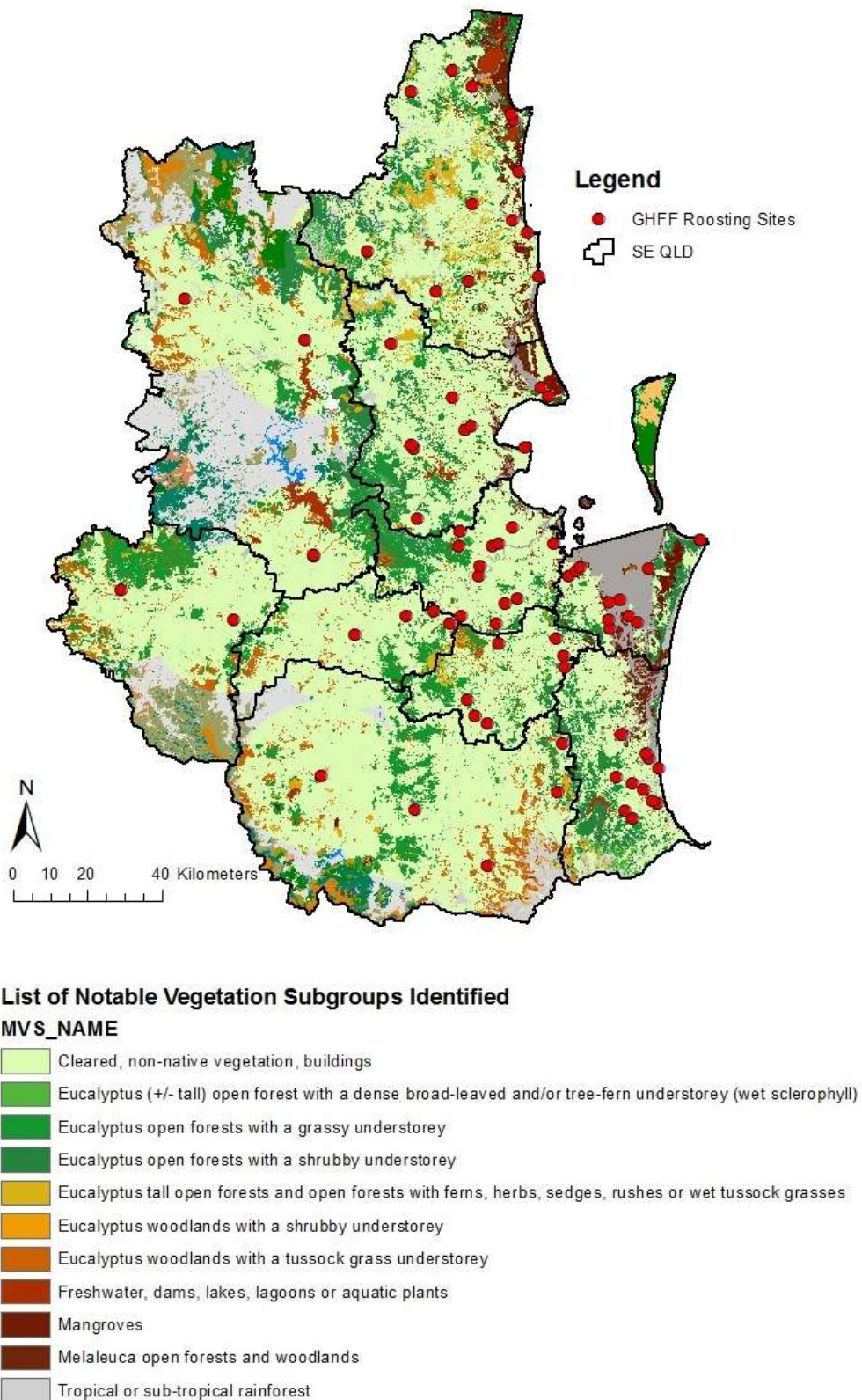


Figure 4.22: Major vegetation subgroups within 20 kms range of the grey-headed flying fox roosting sites.

Identification of Grey Headed Flying-fox's Food Resources within 20 kms Buffer Range

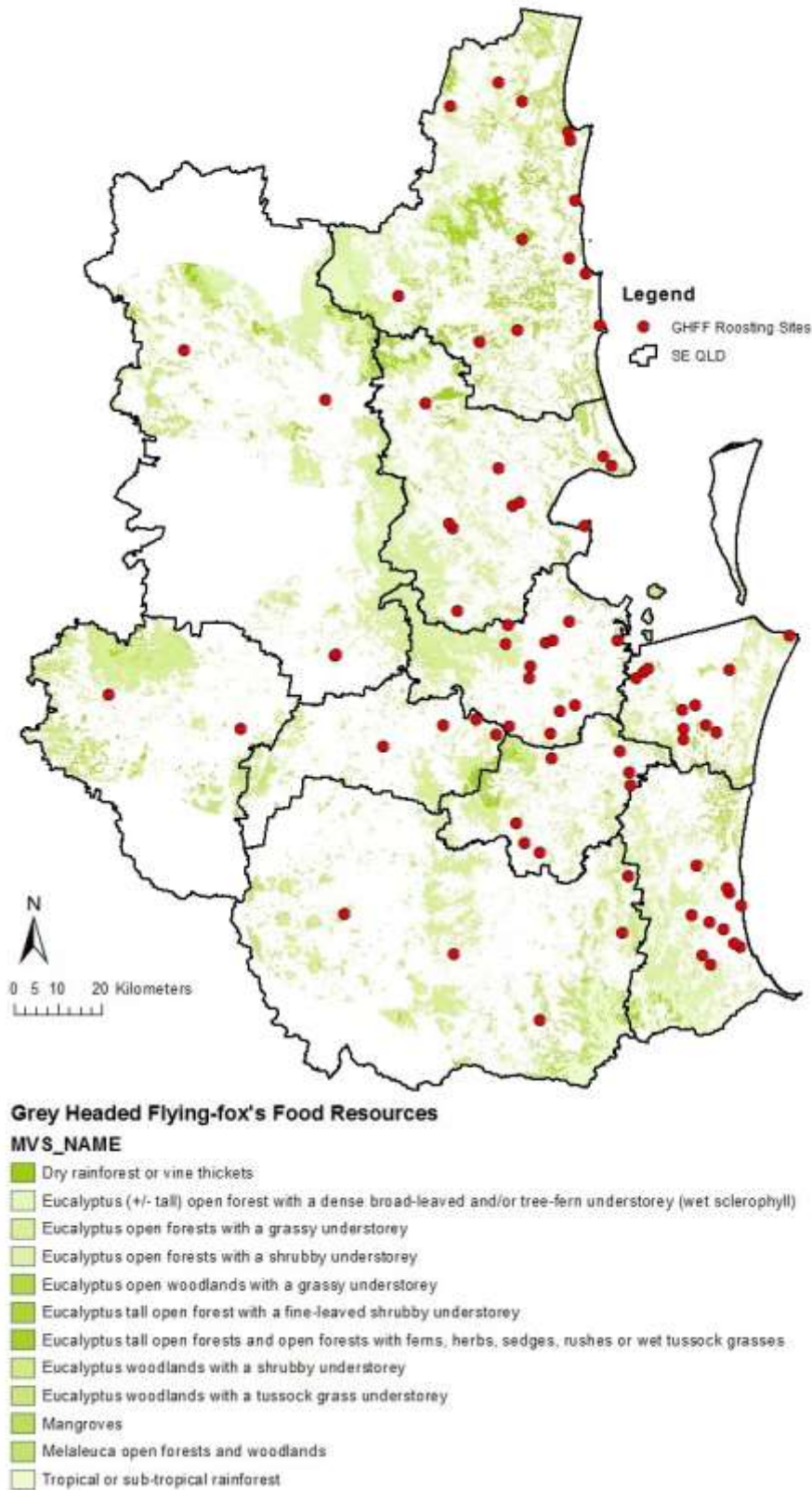


Figure 4.23: Identification of food resources within 20 kms range of the grey-headed flying fox roosting sites.

Using extract by attributes tool, the possible food resources for grey-headed flying fox species near the roosting sites were identified. Figure 4.23 shows the food resources identified within the minimum foraging range of the grey-headed flying foxes in the study area. Table 4.12 shows the food source vegetation of the grey-headed flying foxes in a descending order to study the most occurring food source vegetation.

Table 4.12: List of grey-headed flying fox food source vegetation and its count in the study area.

Value	Count	MVS Name
5	190355	Eucalyptus open forests with a grassy understorey
4	123885	Eucalyptus open forests with a shrubby understorey
9	77878	Eucalyptus woodlands with a tussock grass understorey
2	68127	Tropical or Sub-tropical Rainforest
60	46374	Eucalyptus tall open forests and open forests with ferns, herbs, sedges, rushes or wet tussock grasses
15	26736	Melaleuca open forests and woodlands
3	15429	Eucalyptus (-/+) open forest with a dense broad-leaved and/or tree-fern understorey (wet sclerophyll)
40	15232	Mangroves
8	8633	Eucalyptus woodlands with a shrubby understorey
62	4454	Dry rainforest or vine thickets

High/low Clustering (Getis-Ord General G) analysis was performed on the food source vegetation of the grey-headed flying foxes at various thresholds (3, 5, and 10 kms) to examine the clustering. Table 4.13 shows the summary of the results of High/low clustering analysis of the grey-headed flying fox food source vegetation. The analysis gave high clustering at a confidence level of 99% at all the thresholds tested. For the full report of the analyses, see *Appendix 4*.

Table 4.13: Summary of the cluster analysis results of grey-headed flying foxes food source vegetation.

Distance Threshold	Getis-Ord General G Statistic	High/low Clustering Report
3 kms	Observed General G – 0.000002 z-Score – 17.72 p-value – 0.00000	High Clustering
5 kms	Observed General G – 0.000003 z-Score – 11.89 p-value – 0.00000	High Clustering
10 kms	Observed General G – 0.000004 z-Score – 115.12 p-value – 0.00000	High Clustering

4.4.1.3 HeV Outbreak Incidents

Using the Spatial Analyst toolset (see Section 3.5.2), the vegetation groups and subgroups on the grey-headed flying fox roosting sites were identified. Figure 4.24 shows the HeV outbreak events in the study area. For full legend of the MVS and MVG, see *Appendix 1*.

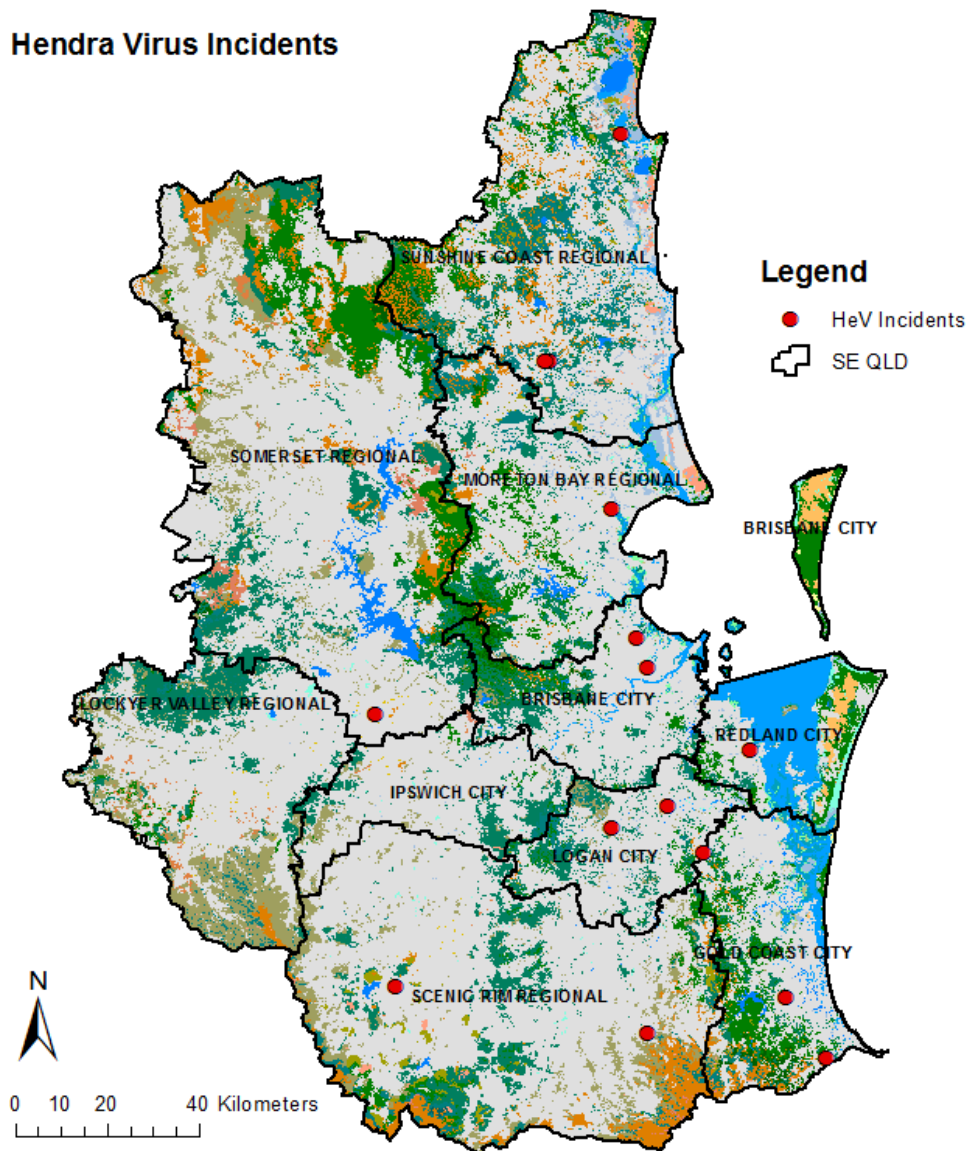


Figure 4.24: HeV outbreak events with MVS in the study area.

Table 4.14 shows the list of the major vegetation groups on the HeV outbreak sites in the study area. Table 4.15 shows the list of the major vegetation subgroups identified on the outbreak sites. The major vegetation subgroups identified on the incident location indicated 10 out of 14 incidents occurred on a ‘cleared, non-native vegetation, buildings’.

Table 4.14: List of major vegetation groups on the HeV outbreak sites in the study area.

Value	MVG Name	MVG Common Description
3	Eucalyptus Open Forests	Eucalyptus Trees (10 to 30 m tall)
25	Cleared, Non-native Vegetation, Buildings	Cleared Vegetation

Table 4.15: List of major vegetation subgroups on the HeV outbreak sites in the study area.

Value	MVS Name
5	Eucalyptus Open Forests with a Grassy Understorey
98	Cleared, Non-native Vegetation, Buildings

Using the buffer analysis and extract by mask tool, the vegetation subgroups near the incidence sites was identified. For the vegetation study near the incidence, a 10 kms range has been chosen for a detailed study. Figure 4.25 shows the identification of the major vegetation subgroups within 10 kms buffer range of the incidence sites in the study area. For a full list of vegetation subgroups identified, see *Appendix 4*.

Identification of MVS within 10 kms Buffer Range of the HeV Incident Locations

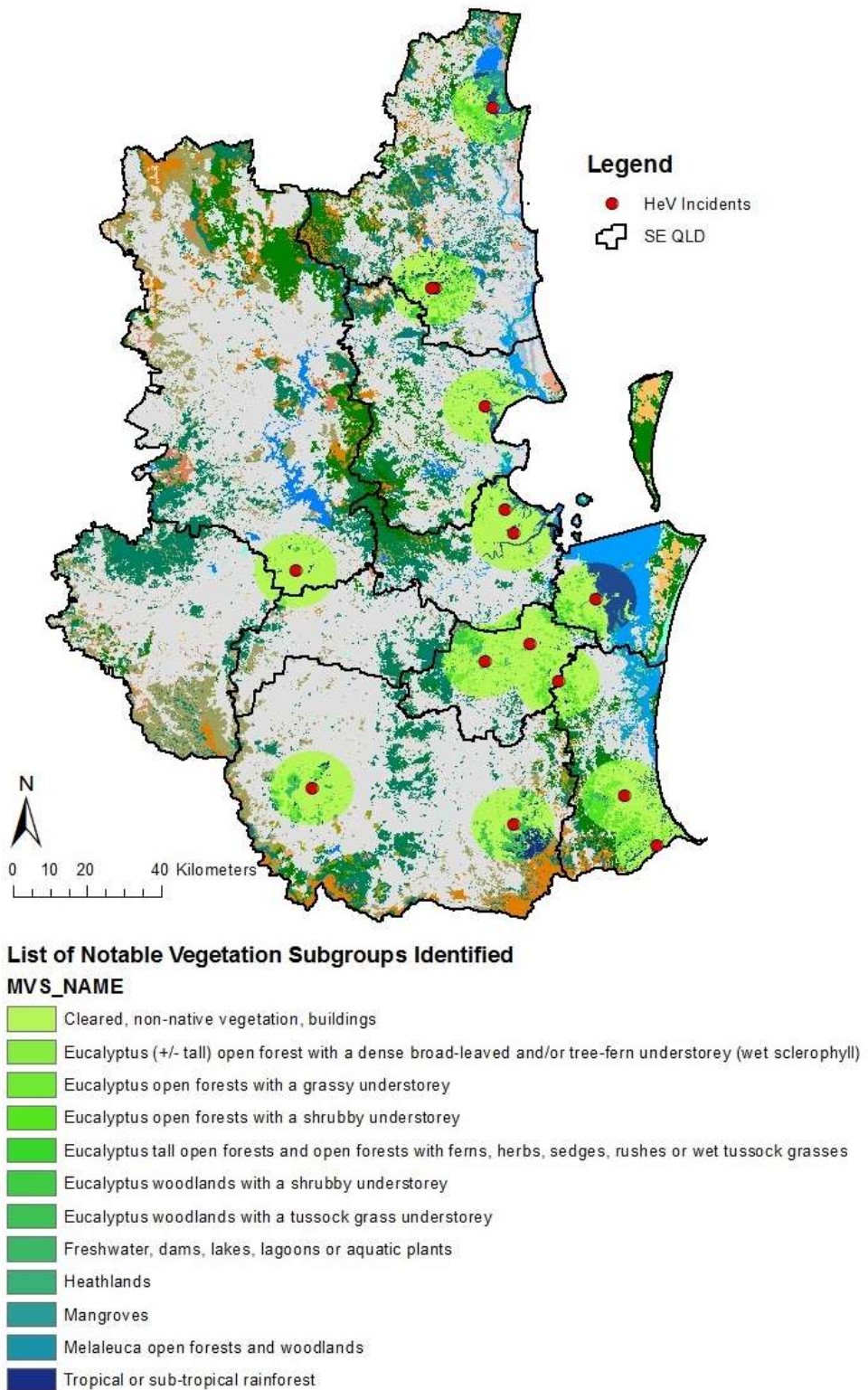
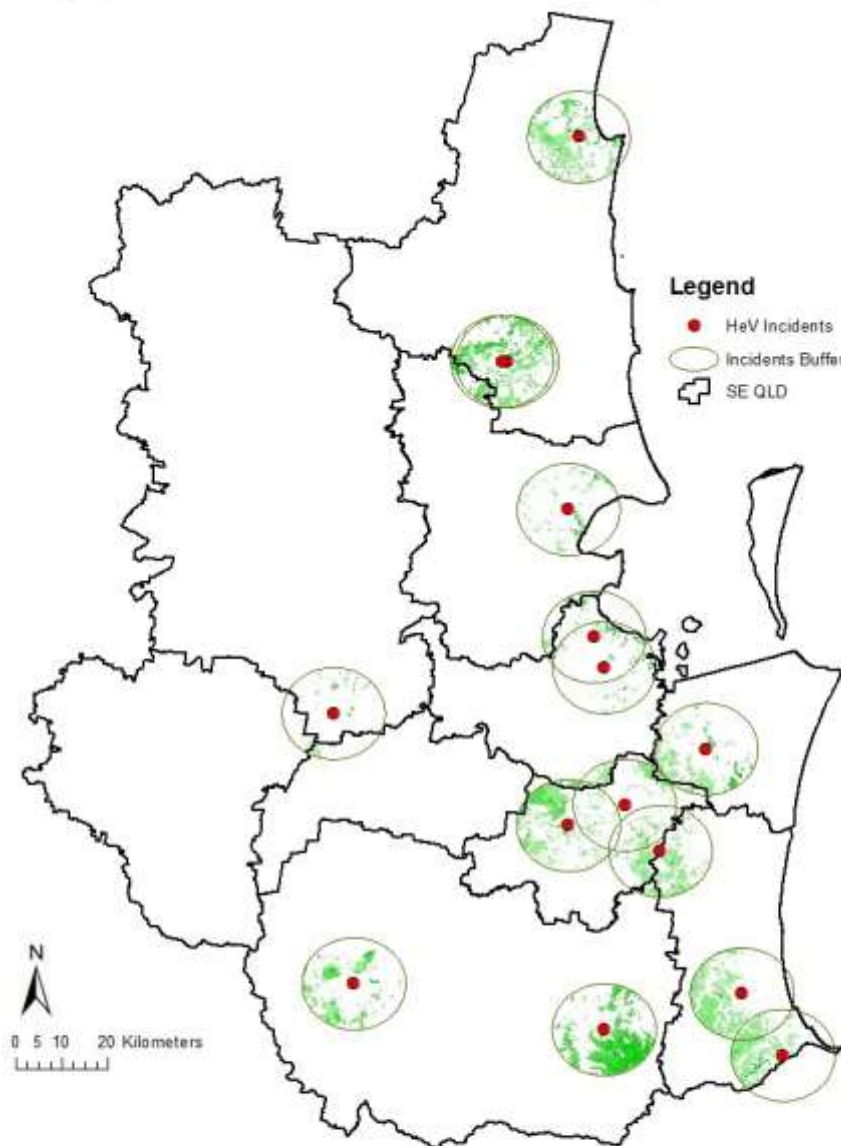


Figure 4.25: Major vegetation subgroups within 10 kms range of the HeV outbreak sites.

Flying-fox's Food Resources within 10 kms Buffer Range of the Incidents



Flying-fox's Food Resources Present within 10 kms Range of the Incidents

MVS_NAME

- Banksia woodlands
- Bngalow (*Acacia harpophylla*) forests and woodlands
- Dry rainforest or vine thickets
- Eucalyptus (+/- tall) open forest with a dense broad-leaved and/or tree-fern understorey (wet sclerophyll)
- Eucalyptus open forests with a grassy understorey
- Eucalyptus open forests with a shrubby understorey
- Eucalyptus open woodlands with a grassy understorey
- Eucalyptus tall open forests and open forests with ferns, herbs, sedges, rushes or wet tussock grasses
- Eucalyptus woodlands with a shrubby understorey
- Eucalyptus woodlands with a tussock grass understorey
- Low closed forest or tall closed shrublands (including *Acacia*, *Melaleuca* and *Banksia*)
- Mangroves
- Tropical or sub-tropical rainforest

Figure 4.26: Identification of flying fox food resources within 10 kms range of the HeV outbreak sites.

Using “extract by attributes” tool, the possible food resources for both black and grey-headed flying fox species within 10 kms range of the outbreak incidents were identified. Figure 4.26 shows the food resources of flying foxes identified within 10 kms range of the outbreak events in the study area. Table 4.16 shows the food source vegetation of the flying foxes in a descending order to study the most occurring food source vegetation near the incident sites.

Table 4.16: List of flying fox food source vegetation and its count near the outbreak events in the study area.

Value	Count	MVS Name
5	26833	Eucalyptus open forests with a grassy understorey
4	16936	Eucalyptus open forests with a shrubby understorey
9	11658	Eucalyptus woodlands with a tussock grass understorey
2	8676	Tropical or Sub-tropical Rainforest
60	7921	Eucalyptus tall open forests and open forests with ferns, herbs, sedges, rushes or wet tussock grasses
40	3680	Mangroves
8	2486	Eucalyptus woodlands with a shrubby understorey
3	1855	Eucalyptus (-/+) open forest with a dense broad-leaved and/or tree-fern understorey (wet sclerophyll)
13	271	Brigalow (Acacia harpophylla) forests and woodlands
50	209	Banksia Woodlands
28	190	Low closed forest or tall closed shrub lands

		(including Acacia, Melaleuca and Banksia)
48	47	Eucalyptus open woodlands with a grassy understorey
62	45	Dry rainforest or vine thickets

High/low Clustering (Getis-Ord General G) analysis was performed on the food source vegetation of the flying foxes at various thresholds (3, 5, and 10 kms) to examine the clustering. Table 4.17 shows the summary of the results of High/low clustering analysis of the fox food source vegetation within 10 kms range of the outbreak events. The analysis gave high clustering at a confidence level of 90% at 3 and 4 kms thresholds. At 5 kms, the clustering was random and at 10 kms range; the analysis gave a low clustering. For the full report of the analyses, see *Appendix 4*. It is evident that the HeV outbreak events had high clustered food source vegetation of both species within 4 kms range, which could be a probable cause for the outbreak.

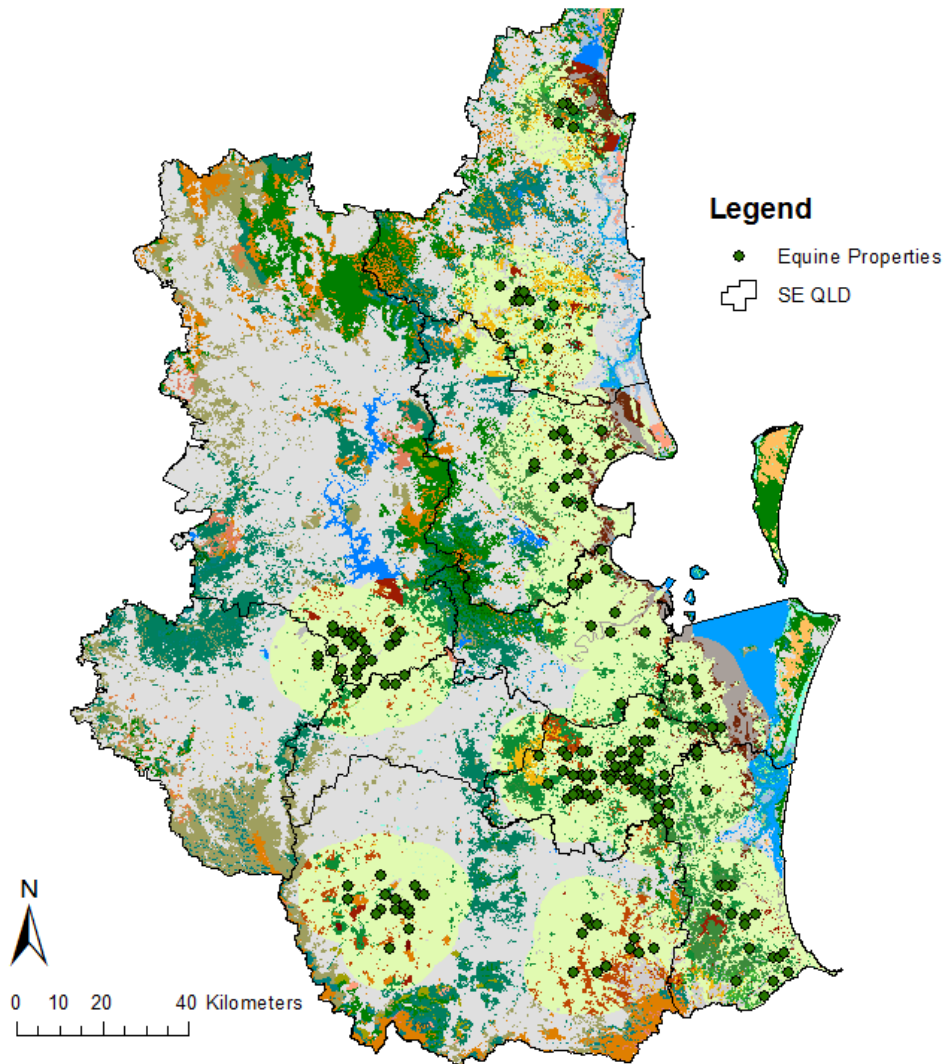
Table 4.17: Summary of the cluster analysis results of food source vegetation near the outbreak events.

Distance Threshold	Getis-Ord General G Statistic Report	High/low Clustering
3 kms	Observed General G – 0.000006 z-Score – 2.99 p-value – 0.002	High Clustering
4 kms	Observed General G – 0.000007 z-Score – 1.87 p-value – 0.006	High clustering
5 kms	Observed General G – 0.000008 z-Score – 0.64 p-value – 0.51	Random Clustering
10 kms	Observed General G – 0.000013 z-Score – -3.65 p-value – 0.00026	Low Clustering

4.4.2 Examining the Spatial Relationship between the Equine Population and Food Source Vegetation of the Flying Foxes

A 10 Km range from the equine properties was chosen to examine the spatial relationship between the equine properties and the food source vegetation of the flying foxes in the study area. Using buffer analysis and extract by mask, the major vegetation subgroups present near the equine population was identified. Figure 4.27 shows the identification of major vegetation subgroups within 10 Km buffer range of the equine population in the study area. A full list of vegetation subgroups in the map is provided in *Appendix 4*.

Identification of MVS within 10 kilometers of the Equine Properties



List of Notable Vegetation Subgroups Identified

MVS_NAME

- Casuarina and Allocasuarina forests and woodlands
- Cleared, non-native vegetation, buildings
- Eucalyptus (+/- tall) open forest with a dense broad-leaved and/or tree-fern understorey (wet sclerophyll)
- Eucalyptus open forests with a grassy understorey
- Eucalyptus open forests with a shrubby understorey
- Eucalyptus tall open forests and open forests with ferns, herbs, sedges, rushes or wet tussock grasses
- Eucalyptus woodlands with a shrubby understorey
- Eucalyptus woodlands with a tussock grass understorey
- Melaleuca open forests and woodlands

Figure 4.27: Major vegetation subgroups within 10 kms range of the equine properties.

Food Source Vegetation Identified within 10 kilometers of the Equine Properties

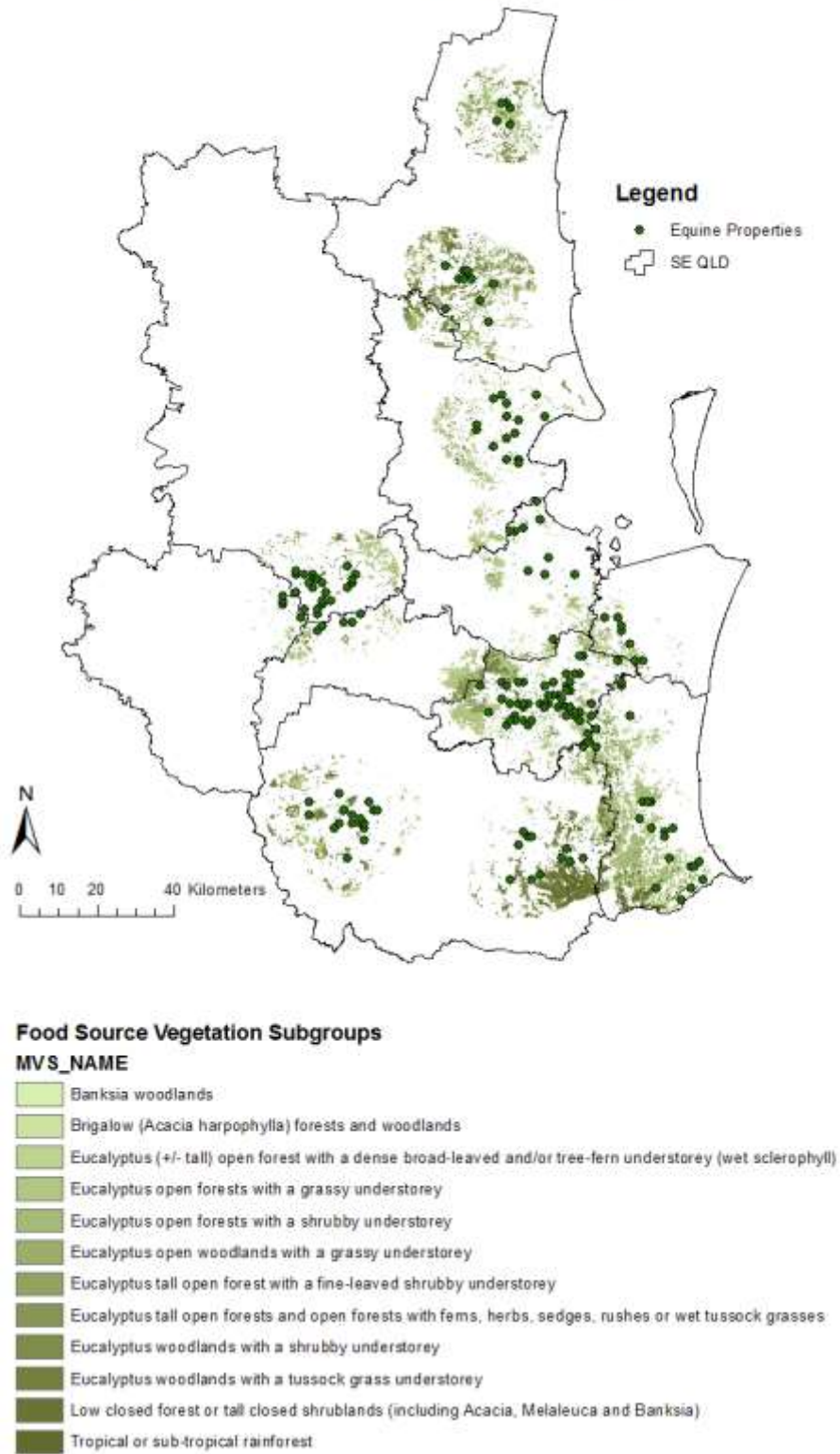


Figure 4.28: Identification of flying fox food resources within 10 kms range of the equine properties.

Using “extract by attributes” tool, the possible food sources for black and grey headed flying foxes near the equine population were identified. Figure 4.28 shows the food source vegetation of the flying foxes identified within 10 Km range of the equine population. Table 4.18 shows the food source vegetation of the flying foxes in a descending order to study the most occurring food source vegetation near the equine population in the study area.

Table 4.18: List of flying fox food source vegetation and its count near the outbreak events in the study area.

Value	Count	MVS Name
5	67865	Eucalyptus open forests with a grassy understorey
4	41845	Eucalyptus open forests with a shrubby understorey
9	26659	Eucalyptus woodlands with a tussock grass understorey
2	21435	Tropical or Sub-tropical Rainforest
60	21346	Eucalyptus tall open forests and open forests with ferns, herbs, sedges, rushes or wet tussock grasses
3	5784	Eucalyptus (-/+) open forest with a dense broad-leaved and/or tree-fern understorey (wet sclerophyll)
8	5510	Eucalyptus woodlands with a shrubby understorey
13	476	Brigalow (Acacia harpophylla) forests and woodlands
28	449	Low closed forest or tall closed shrub lands (including Acacia, Melaleuca and Banksia)
50	413	Banksia Woodlands

The food source vegetation near the equine properties was examined using high/low clustering (Getis-Ord General G Statistic) method. The clustering of the vegetation was studied at 3, 5 and 10 Km from the equine population. The analysis showed a significant high clustering of the food source vegetation at all the distance thresholds. Table 4.19 shows the high/low clustering report of the food source vegetation of flying-foxes at different distance thresholds. For the full report of the analyses, see *Appendix 4*. This study revealed that the equine properties in the study area have high clustered food source vegetation of both species in the range with Eucalyptus varieties being the most occurring vegetation group.

Table 4.17: Summary of the cluster analysis results of food source vegetation near the equine properties.

Distance Threshold	Getis-Ord General G Statistic Report	High/low Clustering
3 kms	Observed General G – 0.000007 z-Score – 69.1 p-value – 0.00000	High Clustering
5 kms	Observed General G – 0.000011 z-Score – 65.15 p-value – 0.00000	High Clustering
10 kms	Observed General G – 0.000016 z-Score – 54.83 p-value – 0.00000	High Clustering

4.5 Models to Identify Population ‘at risk’ (Hypothesis 4)

4.5.1 Model 1

This model identifies the ‘at risk’ equine properties based on the presence of positively significant black flying foxes roosting sites from the GWR model (see *Section 4.3.5*) and their food source vegetation (see *Section 4.4.1*) in significantly

high clusters within 20 kms from the properties. These two factors are extremely significant in this model based on the GWR model results and food source vegetation study. Flowering season of the food source vegetation adds an additional risk factor due its importance in attracting the flying foxes and previous outbreaks in these seasons. However, even without flowering season as a risk factor, the properties remain 'at risk' with the presence of black flying fox species and their food source vegetation in range.

An equine property located within 20 kms range from a positively significant black flying fox roosting site with significantly high clusters of their food source vegetation in the study area were considered as 'at risk' population in model 1. Figure 4.29 shows the equine population 'at risk' based on model 1.

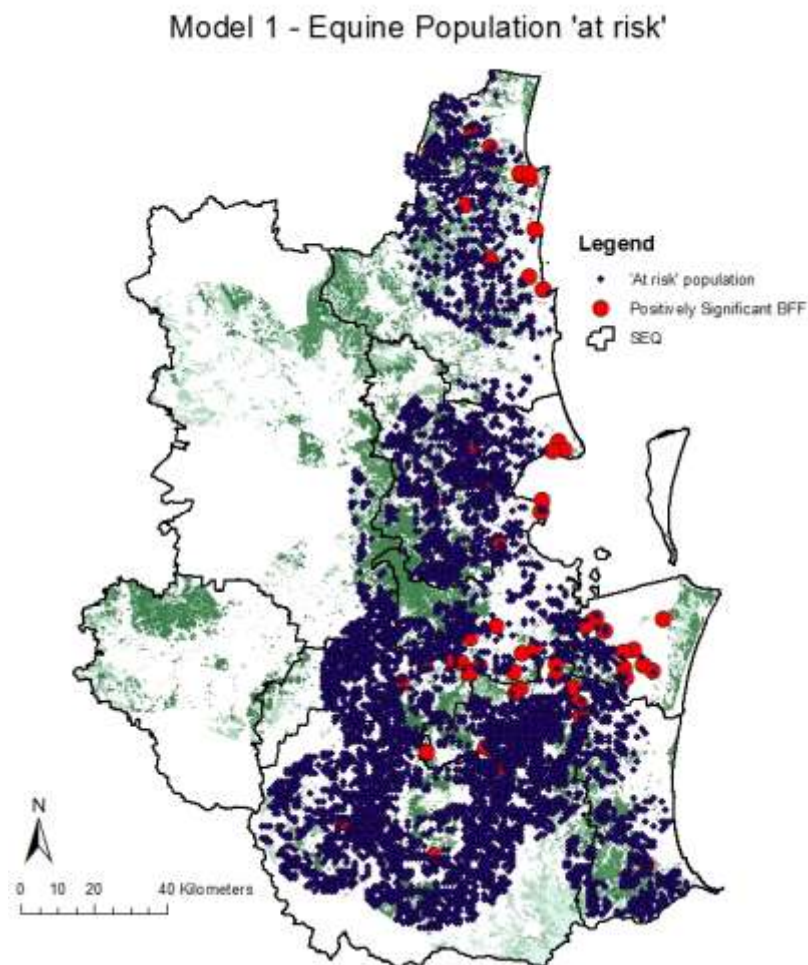


Figure 4.29: Equine population 'at risk' in the study area based on model 1.

Table 4.18: Cluster analysis results of black flying foxes food source vegetation near the equine population ‘at risk’.

Distance Threshold	Getis-Ord Statistic Report	General G	High/low Clustering
3 kms	Observed General G – 0.000001 z-score – 21.67 p-value – 0.00000		High clustering
5 kms	Observed General G – 0.000002 z-score – 16.38 p-value – 0.00000		High clustering
10 kms	Observed General G – 0.000004 z-score – 8.85 p-value – 0.00000		High Clustering
15 kms	Observed General G – 0.000005 z-score – 4.68 p-value – 0.000003		High Clustering
20 kms	Observed General G – 0.000006 z-score – 1.83 p-value – 0.0667		High Clustering

Table 4.18 shows the summary of the high/low clustering results at various distance thresholds of the black flying fox food source vegetation near the equine population ‘at risk’ based on model 1. The vegetation clusters were significantly high at all 3, 5, 10, 15 and 20 kms tested. For full reports of the cluster analysis, see *Appendix 4*. The flowering and fruiting season of the food source vegetation that attracts the black flying foxes is mostly around the winter months (various sources as references and these eucalyptus varieties often depend on birds and mammals to spread the pollen in winter months) which adds an additional risk factor for a possible outbreak in flowering season (Catchpole 2005). The flowering season of the food source vegetation of the black flying foxes overlaps with their pregnancy period. Pregnancy period/birth period showed a significant negative relationship in the GWR model with the outbreak events in the study area. Regardless of the pregnancy/birth factor, flowering season remains as an important element.

Assumption:

Based on an assumption that the distance to the significantly positive black flying fox roosting site contributes to 40% of the risk, clustering of the food source vegetation (significantly high, random or low) to 40% of the risk and flowering season (yes or no) to another 20% of the risk; based on these factors the relative risk of a probable outbreak on a selected equine property 'at risk' can be calculated.

Risk factor of Farm based on model 1 (%)

$$\begin{aligned} &= \text{Distance to the significant roosting site (BFF) in kms}(\%) \\ &+ \text{food source vegetation clustering} (\%) \\ &+ \text{flowering season} (\%) \end{aligned}$$

Equation 4.1

For example, a farm 'A' is located 5 kms (5kms of total 20 kms range i.e. 10%) from a black flying fox roosting site with significant high cluster of food source vegetation (40%), it has a 50% chance of a probable outbreak in non-flowering season (0%) and 85% chance of a probable outbreak in flowering season (20%) based on model 1. This chance of probable outbreak can be calculated for any equine property based on the exact distance, food source vegetation cluster type and season.

4.5.2 Model 2

This model identifies the 'at risk' equine properties based on the presence of positively significant grey-headed flying foxes roosting sites from the GWR model (see *Section 4.3.5*) and their food source vegetation (see *Section 4.4.1*) in significantly high clusters within 20 kms from the properties. Flowering season of the food source vegetation adds an additional risk factor due its importance in attracting the flying foxes and previous outbreaks in these seasons. However, even without flowering season as a risk factor, the properties remain 'at risk' with the presence of grey-headed flying fox species and their food source vegetation in range.

An equine property located within 20 kms range from a positively significant grey-headed flying fox roosting site with significantly high clusters of their food source vegetation in the study area were considered as 'at risk' population in model 2. Figure 4.30 shows the equine population 'at risk' based on model 2.

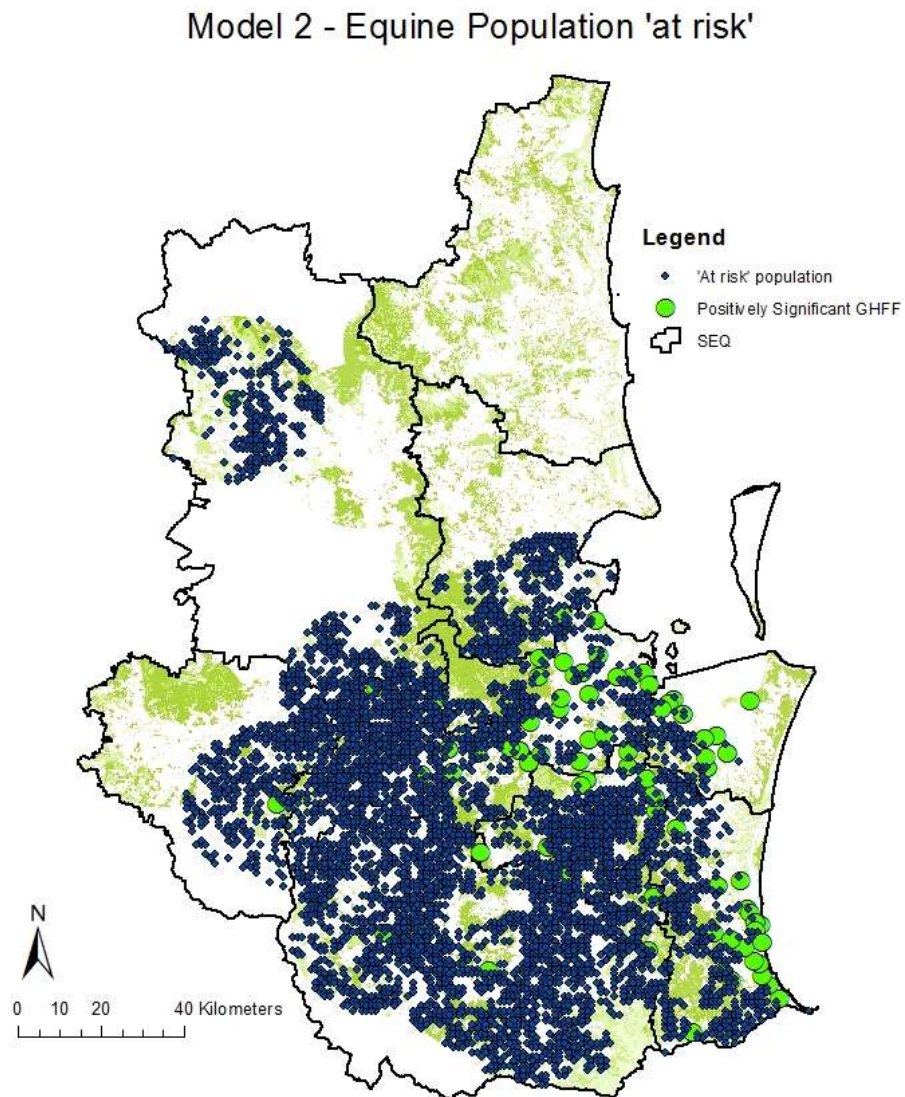


Figure 4.30: Equine population 'at risk' in the study area based on model 2.

Table 4.19: Cluster analysis results of grey-headed flying Foxes food source vegetation near the equine population ‘at risk’.

Distance Threshold	Getis-Ord General G Statistic Report	High/low Clustering
3 kms	Observed General G – 0.000001 z-score – 19.26 p-value – 0.00000	High clustering
5 kms	Observed General G – 0.000002 z-score – 13.79 p-value – 0.00000	High clustering
10 kms	Observed General G – 0.000003 z-score – 5.99 p-value – 0.00000	High Clustering
15 kms	Observed General G – 0.000004 z-score – 1.44 p-value – 0.14	Random Clustering
20 kms	Observed General G – 0.000006 z-score – -1.42 p-value – 0.15	Random Clustering

Table 4.19 shows the summary of the high/low clustering results at various distance thresholds of the grey-headed flying fox food source vegetation near the equine population ‘at risk’ based on model 2. The vegetation clusters were significantly high at all 3, 5 and 10 kms tested. For full reports of the cluster analysis, see *Appendix 4*. The flowering and fruiting season of the food source vegetation that attracts the grey-headed flying foxes is mostly around the winter months, which is the same as the black flying foxes.

Assumption:

Based on an assumption that the distance to the significantly positive grey-headed flying fox roosting site contributes to 40% of the risk, clustering of the food source

vegetation (significantly high, random or low) to 40% of the risk and flowering season (yes or no) to another 20% of the risk; based on these factors the relative risk of a probable outbreak on a selected equine property 'at risk' can be calculated.

$$\begin{aligned} & \textit{Risk factor of Farm based on model 2 (\%)} \\ & = \textit{Distance to the significant roosting site (GHFF) in kms(\%)} \\ & + \textit{food source vegetation clustering (\%)} + \textit{flowering season (\%)} \end{aligned}$$

Equation 4.2

For example, a farm 'B' is located 15 kms (15 kms out of total 20 kms range i.e. 18.75%) from grey-headed flying fox roosting site with low cluster of food source vegetation (0%), it has an 18.75% chance of a probable outbreak in non-flowering season and 38.75% chance of a probable outbreak in flowering season (20%) based on model 2. This chance of probable outbreak can be calculated for any equine property based on the exact distance, food source vegetation cluster type and season.

4.5.3 Model 3

This model identifies the 'at risk' equine properties based on the presence of either black or grey-headed or both species roosting sites and their food source vegetation in significantly high clusters within 20 kms from the properties. Flowering season of the food source vegetation adds an additional risk factor due its importance in attracting both flying fox species and previous outbreaks in these seasons.

An equine property located within 20 kms range from a positively significant roosting site of either species with significantly high clusters of their food source vegetation in the study area were considered as 'at risk' population in model 3. Figure 4.31 shows the equine population 'at risk' based on model 3.

Model 3 - Equine Population 'at risk'

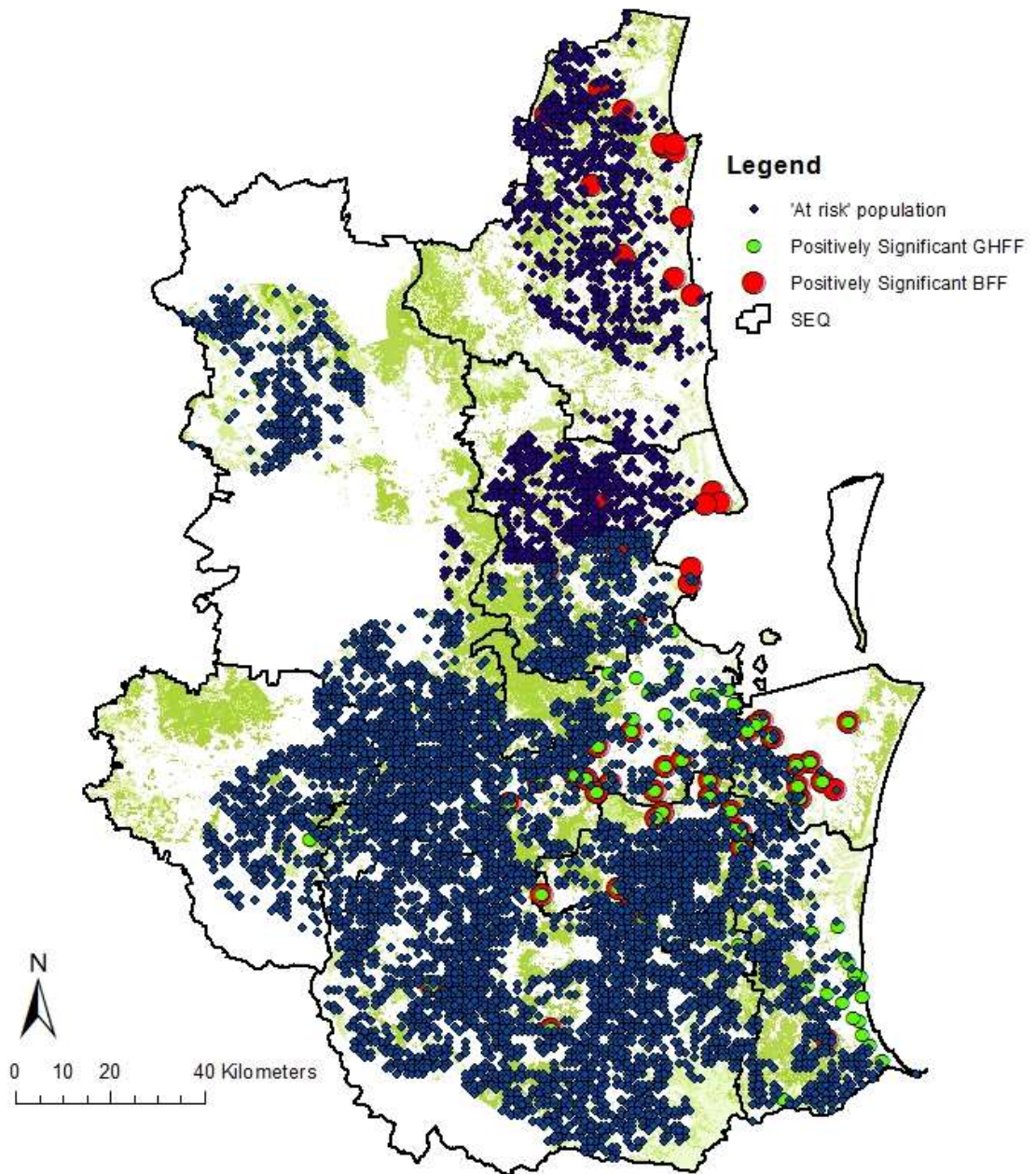


Figure 4.31: Equine population 'at risk' in the study area based on model 3.

The clustering of the food source vegetation for this model needs to be calculated depending on the equine property 'at risk' and the species identification at the roosting site in their range. The assumptions remain the same as models 1 and 2.

4.6 Flowchart of the Results

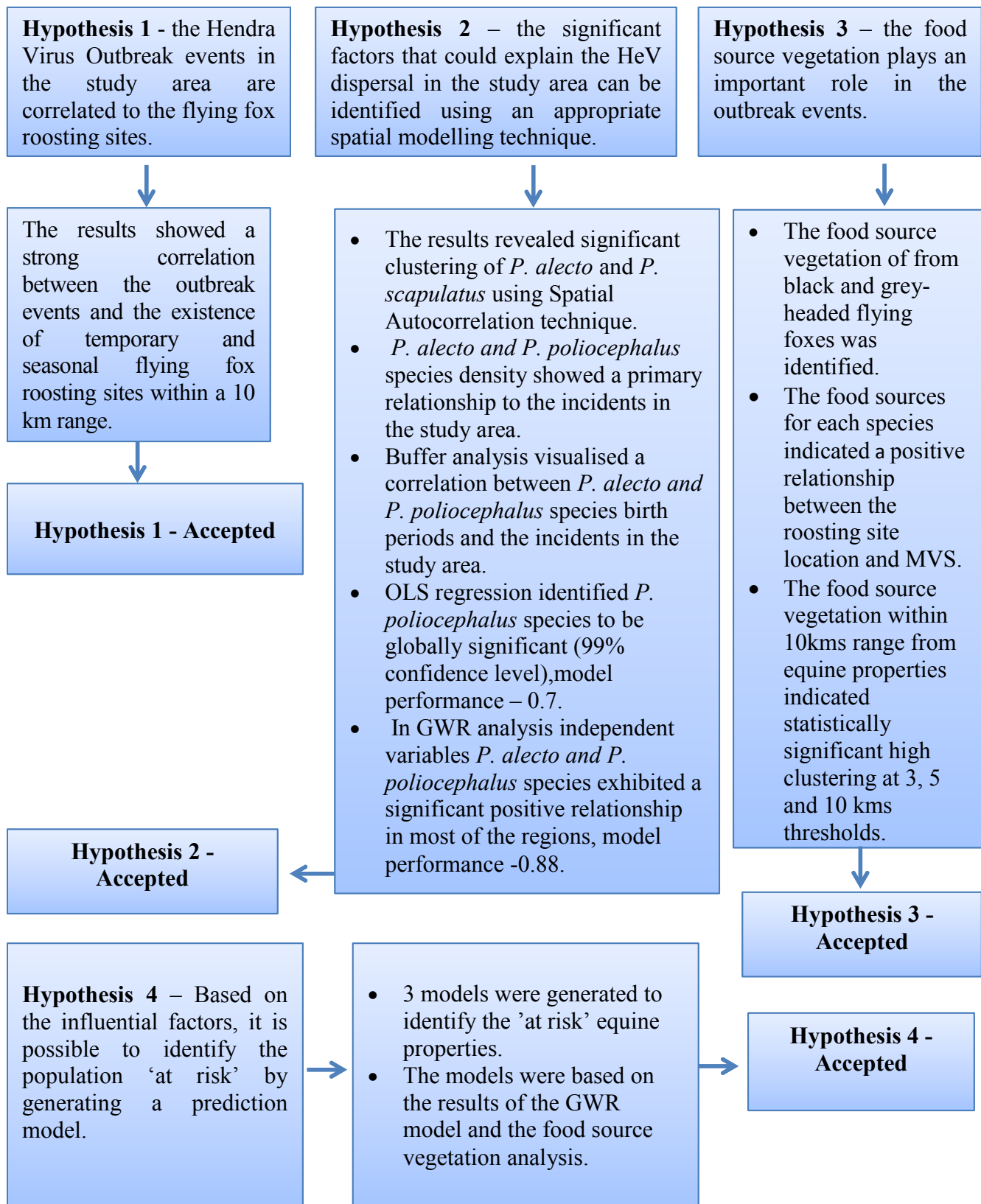


Figure 4.32: Summary of the results.

4.7 Summary

A summary of the conclusion of each hypothesis tested was presented in Figure 4.32 (see *Section 4.6*). The preliminary spatial analysis of the flying fox roosting sites results showed a strong correlation between the outbreak events and the existence of temporary and seasonal flying fox roosting sites within a 10kms range. A very few disease outbreak incidents have a permanent roosting site in their buffer range. The results provided a strong case for investigation into the seasonal behaviour of flying foxes, particularly in breeding season.

4.7.1 Spatial Autocorrelation

The spatial autocorrelation of the black flying foxes showed significant clustering at all the foraging range intervals (20 to 50 kms range) with high occurrence at 50 kms, which is their maximum foraging range. Grey-headed flying foxes showed random clustering at 10, 20 and 30 kms range. The maximum clustering for grey headed flying foxes occurred at 40 kms foraging range. The results of the little red flying foxes showed maximum significant clustering occurring at 10 kms range.

4.7.2 Kernel Density Estimation

The Kernel density estimation (KDE) identified a primary relationship between black flying foxes and grey-headed flying foxes density and the HeV outbreak incidents in the study area. Buffer analysis indicated a correlation between the black flying fox and grey-headed flying fox birth periods and the incidents in the study area. Pregnancy period of the flying foxes is considered to exhibit high correlation with Hendra disease outbreaks in other study areas (Field et al. 2007). A total of ten incidents have fallen within the birth period of the black flying foxes and grey-headed flying foxes with one or more roosting sites in the buffer range of 10 kms. Buffer analysis was able to establish the initial correlation between the birth periods of individual species and incidents in the study area.

4.7.3 Regression Analysis

Ordinary least squares (OLS) regression identified *P. poliocephalus* species to be significant among the other explanatory variables in the model. The OLS model has a statistically significant heteroscedasticity ($p < 0.05$) which suggests the use of Robust P to determine the coefficient significance for consideration. Goodness-of-fit measure indicated a model performance of 0.7. The variance inflation factor (VIF) values indicated no redundancy among the variables. Moran's I test ($Index = -0.02, P = 0.8$) indicated no significant clustering among the residuals. The results indicate that the presence of the camps with high density grey headed flying-fox species have high incident rate across the study area globally. Geographically weighted regression (GWR) analysis was performed to identify the local relationships between the dependent and independent variables. *P. alecto* and *P. poliocephalus* species exhibited a significant positive relationship in most of the regions where as pregnancy period variable exhibited a significant negative relationship to the HeV incidents in the study area. The goodness-of-fit measure indicated an improvement from 0.7 (global model) to 0.8. Moran's I test ($Index = -0.02, P = 0.9$) indicated no significant clustering among the residuals. The spatial variability of the local parameter estimates of each variable has been tested using GWR4 software and significant spatial variability was present in the variables. The t value of each parameter estimate of the independent variables was mapped for a detailed study of the local relationships.

4.7.4 Vegetation Analysis

The food source vegetation analysis identified the major vegetation subgroups present within the minimum foraging range (20 kilometers) from the black and grey-headed flying foxes temporary and seasonal roosting sites. From the identified subgroups, the potential food sources for each species were identified. The abundance of food sources for each species within their minimum foraging range indicates a positive relationship between the roosting site locations and the vegetation subgroups present near them. The vegetation subgroup identification on the incident site location indicated that 10 out of 11 incidents are rather located on

'Cleared, non-native vegetation, buildings' subgroup and the other one incident is located vegetation subgroup 'Eucalyptus open forests with a grassy understorey'.

Further study on the vegetation subgroups within 10 kilometers range from the incident sites identified a range of vegetation including a good amount of possible food sources for both black and grey-headed flying foxes. High/low clustering method was employed to study the clustering of the food sources near the incident sites. The results indicated a significant high clustering at 3 kilometers distance threshold. The p-value of 0.002 indicates 99% significance and the positive z-score indicated clustering among the high values. However, the clustering started dispersing as the distance threshold increased. At 4 kilometer distance threshold, the clustering was still statistically significant but at 90% confidence level. At 5 kilometer distance threshold, the clustering is random and at 8 kilometer distance threshold, the result is dispersed.

The food source vegetation within 10 kilometers range from equine properties was examined using high/low clustering method. Unlike the food source vegetation study near the outbreak events in the study area which was clustered at 3 kilometer threshold and then started dispersing, the results indicated statistically significant high clustering at all 3, 5 and 10 kilometers distance thresholds. The study of the most occurring food source vegetation types near the equine population indicated that it mainly consists of 'Eucalyptus' related subgroups. This established a strong spatial relationship between the registered equine properties and the food source vegetation of the flying foxes.

4.7.5 Prediction Models

Based on the results achieved thus far, 3 models were generated to identify the equine population 'at risk' in the study area. These models concentrate on the presence of positively significant roosting sites of both species from the GWR model and their food source vegetation clustering within 20 kms range from the equine properties. Flowering season was also considered as an additional risk factor in these models due its importance in attracting the flying foxes and previous outbreaks in these seasons. The flowering and fruiting season of the food source vegetation that

attracts these species is mostly around the winter months (various sources as references and these eucalyptus varieties often depend on birds and mammals to spread the pollen in winter months) which adds an additional risk factor for a possible outbreak in flowering season (Catchpole 2005).

A detailed discussion on the methods used, hypothesis tested, results achieved and the limitations of the work has been presented in the following *Chapter 5*.

5. Chapter Five - Discussion

HeV is responsible for the cause of a zoonotic disease with very high mortality rate. The disease is transmitted to humans from bats of the genus *Pteropus*, commonly known as fruit bats via an intermediate equine host. HeV infections have been seen only in Australia, where the virus is endemic in flying foxes. The research on HeV has been given a high public health significance due to the high mortality rate of >79 per cent. HeV is transmitted mainly by ingesting food or water contaminated with infected flying fox body fluids and excretions in horses. The virus can then be passed onto humans who come into close contact with infected horse's nasal discharge, blood, saliva or urine (AAW 2012). The studies show strong evidences that the disease is not bat-to-human transmissible and horses act as medium for disease transmission to humans. Horses to other species and bats to other species transmissions are however possible (Australian Biosecurity 2009).

HeV is considered as a serious public health concern, particularly in Queensland and New South Wales. Its effective prevention and control are being considered by the government as a matter of priority. While there is a new development in the HeV control strategy by mean of, vaccination to the horses against the disease is the only solution so far. As a *Zoonoses* category disease, there is always a possibility to determine the causes that promote the virus transmission. It is important to explore the possible environmental, ecological and other related factors that may influence the prevention and control measures in terms of the public and environmental health safety.

Hypothesis-1

To study the relationship between the flying fox roosting sites and the outbreak events, a preliminary study incorporating buffer analysis was conducted. The results showed a strong relationship between the outbreak events in the study area and the existence of temporary and seasonal flying fox roosting sites within a 10km range. Very few disease outbreak incidents have a permanent roosting site in their buffer range. The results of the preliminary analysis are consistent with the NFFMP's findings. The recent findings of NFFMP revealed that the distribution of flying foxes is highly variable, with the animals

moving in and out of camps seasonally, apparently in response to varying food resources available. The grey headed and spectacled flying foxes - whose entire distributions were covered by the monitoring, have shown a dramatic change in their distribution over the last decades with a shift to smaller camps located in urban and peri urban areas. This is a similar distribution pattern to that of horses (DoE 2013). The results provided a strong case for research into the seasonal behaviour of flying foxes, particular in breeding season.

Hypothesis-2

Global statistics such as Spatial Autocorrelation tool assess the overall pattern and trend of the data. It is a useful technique to identify the trend of the data over space-time (Getis et al 1992). Spatial Autocorrelation tests results of the flying fox species at various distance thresholds indicated that the species - black flying foxes and little red flying foxes are significantly clustered at threshold distance of 10 kms. The spatial autocorrelation of the black flying foxes showed significant clustering at all the foraging range intervals (20 to 50 kms range) with high occurrence at 50 kms, which is their maximum foraging range. Grey-headed flying foxes showed random clustering at 10, 20 and 30 kms range. The maximum clustering for grey headed flying foxes occurred at 40 kms foraging range, which is the nocturnal foraging range of the flying foxes (Markus et al 2004). The results of the little red flying foxes showed maximum significant clustering occurring at 10 kms range.

Similar to a recent study on the HeV patterns (Smith et al. 2014); the kernel density estimation (KDE) technique showed that the black flying foxes density is particularly higher near the incident locations in the study area; however the density of grey headed flying foxes is also high near the incidents in the study area unlike the study. KDE identified a primary relationship between black headed flying foxes and grey-headed flying foxes density and the incidents in the study area. It is an ideal technique to examine large scale trends in point pattern analysis (So et al. 2008). The bandwidth for the KDE analysis for each species was 0.4598 degrees, which was calculated by the default search radius (bandwidth) algorithm of ArcGIS 10.2.1 (ESRI 2016). The study (Smith et al 2014) suggested that there are unidentified risk

factors that exist at the property level apart from the density of horses, climatic and vegetation variables.

Buffer analysis indicated a correlation between the black flying foxes and grey-headed flying fox birth periods and the incidents in the study area. Pregnancy period of the flying foxes is considered to exhibit high correlation with Hendra disease outbreaks in other study areas (Field et al. 2007). A total of ten incidents have fallen within the birth period of the black flying-foxes and grey-headed flying foxes with one or more roosting sites in the buffer range of 10 kms. Buffer analysis was able to establish the initial correlation between the birth periods of individual species and incidents in the study area. The black and grey-headed flying foxes were considered as significant species for the regression model as explanatory variables based on the results of KDE analysis and the birth period correlation study.

The model for the regression analyses was calibrated using the GWR technique in an exploratory method (Fotheringham et al 2012). The explanatory variables for this study were selected considering the previous studies (Breed et al. 2011, Smith et al. 2014, Plowright et al. 2008 and Field et al. 2007) as well as the preliminary analysis conducted in this study to establish the initial correlations to identify the unspecified risk factors and patterns of the disease dispersal using spatial analysis techniques. The model calibration technique introduced by Fotheringham et al (2012) uses a statistical model-building procedure in order to establish if any further reduction in the set were possible. By doing this, a reduced set of highly significant explanatory variables (black flying foxes, grey-headed flying foxes and the average pregnancy/birth period) of HeV outbreak events were achieved.

The implementation of the OLS technique has provided a global understanding of the HeV disease across the study area. The analysis was carried out using the 'incident rate' as a dependent variable and black flying foxes, grey-headed flying foxes and pregnancy period as independent variables. The OLS regression technique identified grey-headed flying foxes as significant explanatory variable in the global context across the study area. The independent variable 'grey-headed flying foxes' was globally significant at 99% confidence level across the study area. The variance inflation factor (VIF) values indicated no redundancy among the variables in the

model. This model has a statistically significant heteroscedasticity ($p < 0.05$) which suggests the use of Robust P to determine the coefficient significance for consideration. Goodness-of-fit measure indicated a model performance of 0.7 (70%). Moran's I test ($Index = -0.02, P = 0.8$) indicated no significant clustering among the residuals. Field et al (2011) suggested that some flying fox species may play a greater role on the HeV transmission of infection to horse, which indicates that the virus dispersal highly depends on the presence of particular flying fox species based on the geographic location. In the current study, it can be interpreted that the grey-headed flying fox species play primary role in the HeV dispersal across the study area globally.

The GWR technique is a local model of the variable or process for understanding the spatial patterns by fitting a regression equation to every feature in the data set. The model produced (explanatory variables - black flying fox density, grey-headed flying fox density and pregnancy period) using statistical model-building procedure was used to study the locally varying spatial trends of the HeV incidents across the study area. The spatial variability among the local parameter estimates produced by GWR analysis of each variable has been tested using GWR4.0 software. The significant spatial variability test indicated that it was present among the variables. The goodness-of-fit measure indicated an improvement from 0.7 (global model) to 0.88 (88%). The good-of-fit measure value indicates that the chosen explanatory variables explain 88% of the virus dispersal locally in the study area. Moran's I test ($Index = -0.02, P = 0.9$) indicated no significant clustering among the residuals.

The GWR results revealed a significant positive relationship between black and grey headed flying foxes density and the incidents in the study area. The result supports the statement of Westcott (2016), who argued that the HeV in horses mostly correlated with the incursions of the spectacled flying foxes and black flying foxes. A study by Smith et al (2014) identified the density of black and spectacled flying foxes as a significant risk factor in eastern Australia. The local trends of these two species observed across the study region would be highly beneficial in further disease modelling. Even though the pregnancy factor (Plowright et al. 2008) was considered as a potential risk for the Hendra outbreak and showed an initial possible correlation to the incidents in the study area, it exhibited a negative relationship at

local level. This indicates that there are other unidentified risk factors such as vegetation, migration strategies and seasonal change that need to be assessed together with the birth and lactating periods for more detailed local analysis.

The black flying foxes showed positive significance in the regions of Logan, Redland, Scenic Rim and parts of Brisbane, Moreton Bay, and Sunshine Coast Regions. The grey-headed flying foxes showed positive significance in the regions of Brisbane, Ipswich, Gold Coast, Scenic Rim, Logan and Redland regions in the study area. The black flying foxes showed a positive correlation where the grey-headed flying foxes displayed a negative correlation in the region of Sunshine Coast. The grey-headed flying foxes showed no significance in the region of Moreton Bay where black flying foxes showed a strong positive correlation in the study area. The pregnancy period variable showed negative significance in most of the regions except Gold Coast, Sunshine Coast and part of Brisbane where the variable showed no statistical significance in the study area. The results of the GWR model reveal that the virus dispersion is positively related to the density and distribution of the black and grey headed flying foxes in the study area. The GWR model performed well (local R-squared value > 0.8) in the southern part of the study area where the incident rate is comparatively high and poorly in the northern region of the study area where the incident rate is low.

Hypothesis-3

An in-depth investigation of the food source vegetation of the flying foxes and their roosting sites as potential factors of HeV dispersal has identified the major vegetation subgroups present within the minimum foraging range (20 kilometers) from the black and grey-headed flying foxes temporary and seasonal roosting sites in the study area. Flying foxes largely depend on nectar and pollen from eucalypts, melaleucas and banksias; however they are attracted to a broad range of flowering and fruiting trees, and vegetation, as food sources (Wildlife QLD 2016). Department of primary industries, NSW investigated the type of vegetation present on some of the virus infected properties which included a range of fig trees, bottlebrushes, cocoas palm, stone fruits such as mangoes and papaws, palms, lilly-pillies and

grevilleas (DPI 2012). Black flying foxes prefer blossom of eucalypts, paperbarks and turpentine's, as well as a variety of other native and introduced blossom and fruits. They have been seen to eat the leaves of trees by chewing the leaves into a bolus, swallowing the liquid and then spitting out the fibre (Wildlife QLD 2016, Australian Museum 2013). Grey-headed flying foxes forage on fruits and blossoms of more than 80 species of plants and mostly refer eucalypt blossom with native figs being the most popular fruit. They chew leaves and appear to eat the salt glands from mangroves. They also forage in gardens, parks and orchards and may fly many kms from roost site to feed (Wildlife QLD 2016).

Based on the above information, the potential food sources for each species were identified. The black flying fox food resources included major Eucalyptus open forests varieties, Eucalyptus woodlands varieties, Tropical or Sub-tropical Rainforest, Low closed forest or tall closed shrub lands (including Acacia, Melaleuca and Banksia) and Brigalow forests and woodlands. The grey-headed flying fox resources included Eucalyptus open forests varieties, Eucalyptus woodlands varieties, Tropical or Sub-tropical Rainforest, Melaleuca open forests and woodlands, Mangroves and Dry rainforest or vine thickets. The abundance of food sources for each species within their minimum foraging range indicates a positive relationship between the roosting site locations and the vegetation subgroups present near them.

High/low Clustering (Getis-Ord General G) analysis was performed on the food source vegetation of the black flying foxes and grey-headed flying foxes at various thresholds (3,5, and 10 kms) to examine the clustering. The results of High/low clustering analysis of the black flying fox food source vegetation returned high clustering at a confidence level of 99% at all the thresholds tested. The results of High/low clustering analysis of the grey-headed flying fox food source vegetation returned high clustering at a confidence level of 99% at all the thresholds tested. The results indicate that the roosting site locations are majorly dependent on the availability of the food source vegetation especially in high clusters.

Further study on the vegetation subgroups within 10 kilometers range from the incident sites identified a range of vegetation including a good amount of possible food sources for both black and grey-headed flying foxes. High/low clustering

method was employed to study the clustering of the food sources near the incident sites. The results indicated a significant high clustering at 3 kilometers distance threshold. The p value of 0.002 indicates 99% significance and the positive Z score indicated clustering among the high values. However, the clustering started dispersing as the distance threshold increased. At 4 kilometers distance threshold, the clustering was still statistically significant but at 90% confidence level. At 5 kilometers distance threshold, the clustering is random and at 8 kilometers distance threshold, the result is dispersed.

The major vegetation subgroups present within 10 Km range of the equine population in the study area were examined. From the major vegetation subgroups, the food source vegetation of black and grey-headed flying foxes were identified. The food source vegetation within 10 Km range from equine properties was examined using high/low clustering method. Unlike the food source vegetation study near the outbreak events in the study area which was clustered at 3 Km threshold and then started to disperse widely, the results indicated statistically significant high clustering at all 3, 5 and 10 Km distance thresholds. The study of the most occurring food source vegetation types near the equine population indicated that it mainly consists of 'Eucalyptus' related subgroups. It can be interpreted that these food resources present near the equine properties attract the flying foxes and thus the chances of an outbreak is more likely at a property with highly clustered food source vegetation.

Hypothesis-4

Based on the results from the GWR model and the food resource vegetation analysis of the flying foxes, three models that could identify the equine population 'at risk' (thus identifying the human population 'at risk' of a potential outbreak) were generated. Model 1 identified the 'at risk' equine properties based on the presence of positively significant black flying foxes roosting sites from the GWR model and their food source vegetation in significantly high clusters within 20 kms from the properties. Model 2 identified the 'at risk' equine properties based on the presence of positively significant grey-headed flying foxes roosting sites from the GWR model and their food source vegetation in significantly high clusters within 20 kms from the

properties. Model 3 identified the 'at risk' equine properties based on the presence of either black or grey-headed or both species roosting sites and their food source vegetation in significantly high clusters within 20 kms from the properties. Flowering season of the food source vegetation was considered as an additional risk factor in all three models due its importance in attracting the flying foxes and previous outbreaks in these seasons. Each factor was given a 'weighted percentage' in assumptions to calculate the 'relative risk of a probable outbreak event' involved for individual equine property in the study area. The risk percentage of a probable outbreak event varies for each equine property depending on their exact location and their contributing factors. By incorporating the prediction models generated, the early warning messages can be issued to the equine properties 'at risk' in the study area, thus by identifying the human population 'at risk'.

Research Limitations

The findings of this research were based on the empirical data driven analysis and are highly dependent on the data accuracy. The data was validated and any duplicates were removed to reduce the degree of possible error. The results of the study are only applicable to the study area. The results may vary when the dynamics of the HeV dispersal and its influential factors are to be studied at a larger scale or geographical area.

The flying fox species data is recorded manually, which may be prone to some degree of error. The species data is continuous by the EHP and is updated every 3 months. The data used in this research has been manipulated to best reflect the occupancy of the roosting sites at the time of the events.

It is important to note that this research is a spatial GIS-based approach to understand the HeV disease outbreak events, its transmission and the factors influencing the disease dispersal in the study area. This study is built on the research that have been published so far on the HeV, its biology, transmission and their reservoir host – flying foxes. The future biological researches may find contrary to results achieved in this research.

Future Research

Hypothesis 2 indicated a significant negative relationship with the average pregnancy/birth period variable of the flying fox species in the study area. A further examination into the flying fox pregnancy, birth and lactation periods of the flying foxes may reveal any underlying spatial patterns of this correlation to the HeV incidents in the study area. This may be effective in improvising the prediction models generated and thus helps in generating accurate warning signals.

It will be advantageous to study further into the most re-occurring food sources (at least 3 vegetation subgroups) near the flying fox roosting sites, equine properties and the incidents to identify the individual correlations. This may help identify if the virus dispersion could be linked to a particular major vegetation subgroup(s) in the study area. Studying the HeV dispersal and its influential factors at a larger or smaller scale (geographical context) would be useful in understating the changes in the pattern(s) and how the influential factors affect the study area(s) at various scales/geographical contexts. This will be beneficial for state and local governments to plan mitigation policies appropriately and achieve the best outcome for human, equine and flying fox populations.

By using the current study as a base, this research provides a platform for potential automated disease forecasting and surveillance system for HeV disease. As HeV is a highly fatal disease, the automated system could have significant impact on both public health and equine industries. The automated surveillance systems require sophisticated data acquisition and analysis; there is still a gap in current research due to limitations in lack of infrastructure for such data acquisition, lack of awareness and also shortage of trained personnel. However, in the near future the automated disease surveillance system would be a cost and time effective approach in monitoring public health.

6. Chapter Six – Conclusion

The overall aim of this research was to analyse the spatial patterns of the HeV cases, study the factors that may explain the HeV dispersal in the study area and identify the population ‘at risk’ using a prediction model by incorporating GIS techniques. Using the spatial analytical tools, this research established a relationship between the outbreak events and their influential factors such as species, foraging range, pregnancy period, birth and lactation period, seasons and food source vegetation. This study successfully filled in the requirement of a good GIS-based epidemiological research to study the HeV outbreaks in the study area spatially and temporally, which addresses the pressing need announced by Queensland Government (DAF 2015). The results of Hypothesis 1 showed strong correlations between the outbreak events and the existence of temporary and seasonal flying fox roosting sites within a 10kms range of the incidents in the study area. A very few outbreak incidents (18%) have a permanent roosting site in their buffer range. The findings provided a strong case for investigation into the seasonal behaviour of flying foxes, particularly in breeding season.

The findings of Hypothesis 2 have provided excellent understanding the factors influencing the dispersal of HeV outbreak events in the study area. Global Moran’s I method (inverse distance conceptualisation) was used to identify the presence of significant spatial clustering of the three flying fox species at various foraging ranges (10, 20, 30, 40 and 50 kms) in the study area. Global Moran’s I revealed significant clustering of *P. alecto* and *P.scapulatus* species. The analysis of *P. alecto* species showed significant clustering at all foraging range intervals with high occurrence at 50 kms, which is their maximum foraging range. The findings of *P.scapulatus* species showed maximum significant clustering occurring at 10 kms range. Kernel density estimation (KDE technique) analysis helped in establishing a strong relationship between *P. alecto* and *P.scapulatus* species density and the outbreak events in the study area and revealed the density hotspots of these species. Buffer analysis established an initial relationship between *P. alecto* and *P. poliocephalus* species birth periods and the outbreak incidents.

Ordinary least squares (OLS) regression identified *P. poliocephalus* species to be significant among the other explanatory variables in the model. Goodness-of-fit measure indicated a model performance of 0.7. The results indicated that the presence of the camps with high density grey headed flying-fox species have high incident rate across the study area globally. Geographically weighted regression (GWR) analysis was performed to identify the local relationships between the dependent and independent variables. *P. alecto* and *P. poliocephalus* species exhibited a significant positive relationship in most of the regions where as pregnancy period variable exhibited a significant negative relationship to the HeV incidents in the study area. The goodness-of-fit measure indicated an improvement from 0.7 (global model) to 0.8. The t values of each parameter estimate of the independent variables were mapped for a detailed study of the local relationships, which facilitated in identifying and understanding the local relationships of the HeV incidents with the explanatory variables.

In Hypothesis 3, the findings identified the major vegetation subgroups present within the minimum foraging range (20 kilometers) from the black and grey-headed flying foxes temporary and seasonal roosting sites. Subsequently, the food source vegetation of each species was identified. The abundance of food sources for each species within their minimum foraging range indicates a positive relationship between the roosting site locations and the vegetation subgroups present near them. Further study on the vegetation subgroups within 10 kilometers range from the incident sites identified a range of vegetation including a good amount of possible food sources for both black and grey-headed flying foxes. The clustering of the food resource vegetation present near the incidence was studied using Getis-Ord General G Statistic method, which indicated statistically high clustering with 99% confidence level at 3 kms distance threshold. A 10 kms range vegetation study on the equine properties in the study area identified the food source vegetation of both significant species. The clustering of the food source vegetation present near the equine properties was studied using high/low clustering/Getis-Ord General G Statistic method, which indicated statistically significant high clustering at 3, 5 and 10 kms distance thresholds. The vegetation analysis revealed strong correlations between the roosting sites, food source vegetation and the equine properties.

Hypothesis 4 resulted in identifying the equine population ‘at risk’ based on the three prediction models generated. The risk percentage of a probable outbreak event varied for each equine property depending on their exact location and their contributing factors. The prediction model(s) was an effective tool to identify the potential population (both equine and human) ‘at risk’, which could help in health service planning, policy implications, decision making and ongoing disease surveillance in the study area. This study revealed the capability of GIS-based surveillance system to issue early warnings and precautionary measures to the identified population ‘at risk’. This research also made evidence based practice of disease mitigation, planning and prevention and control strategies for HeV achievable.

References

AAW. (2012). HeV Fact Sheet. Retrieved April 19, 2017, from http://www.australiananimalwelfare.com.au/app/webroot/files/upload/files/Equivac_HeV_fact_sheet_about_Hendra_virus.pdf

Albert, D., Gesler, W., and Horner, R. D. (2000). Geographic Information Systems and Health Services Research. Spatial Analysis, GIS, and Remote Sensing Applications in the Health Sciences, Michigan: Ann Arbor Press, pp 55-75.

Ali, M., Wagatsuma, Y., Emch, M., and Breiman, R. (2003). Use of a geographic information system for defining spatial risk for dengue transmission in Bangladesh: role for *Aedes albopictus* in an urban outbreak. *The American journal of tropical medicine and hygiene*, 69(6), pp.634-640.

Andrienko, G., and Andrienko, N. (2001). Exploring spatial data with dominant attribute map and parallel coordinates. Retrieved April 20, 2017, from <http://geoanalytics.net/and/papers/ceus01.pdf>

Anselin, L. (1988). *Spatial Econometrics: Methods and Models*. Dordrecht: Kluwer Academic.

Auchincloss, A. H., Gebreab, S. Y., Mair, C., and Roux, A. V. (2012, April). A Review of Spatial Methods in Epidemiology, 2000–2010. Retrieved April 19, 2017, from <https://www.ncbi.nlm.nih.gov/pmc/articles/PMC3638991/>

AURIN. (2016). Getis-Ord Local G. Retrieved April 19, 2017, from <https://docs.aurin.org.au/portal-help/analysing-your-data/spatial-statistics-tools/localg-workflow/>

Australian Biosecurity CRC for Emerging Infectious Disease. (2009). HeV Update. CRC Australia.

Australian Pteropus Species. (2013). Fact Sheet. Retrieved April 19, 2017, from <http://www.aawhg.org/uploads/7/8/7/3/78739940/australian-pteropus-species-fact-sheets-v1.1.pdf>

AVA. (2016). HeV. Retrieved April 18, 2017, from <http://www.ava.com.au/hendra-virus>

Bailey, T. C., and Gatrell, A. C. (1995). Interactive Spatial Data Analysis, England. Longman Group Limited.

Baker, M. (2016). Spikes in HeV spillover: early warning through the bat urinary metabolome. Compendium of findings from the National HeV Research Program, pp. 14-15. doi:ISBN 978-1-74254-847-0

Barr, J., Smith, C., Smith, I., Jong, C. D., Todd, S., Melville, D., . . . Wang, L. (2015). Isolation of multiple novel paramyxoviruses from pteropid bat urine. Journal of General Virology, 96(Pt_1), 24-29. doi:10.1099/vir.0.068106-0

Bat Rescue Inc. (2017). Found a Bat? Retrieved April 20, 2017, from <http://batrescue.org.au/new/special-projects/colony-reveg.html>

Baum, S., Kendall, E., Muenchberger, H., Gudes, O. and Yigitcanlar, T. (2010). Geographical information systems: An effective planning and decision-making platform for community health coalitions in Australia. Health Information Management Journal, 39(3):28-33.

Bazemore, A., Phillips, R., and Miyoshi, T. (2003). Using Geographic Information Systems to Define Healthcare Access in an Urban Community Health Centre Network. ESRI International Health GIS Conference.

Beck, L. R., Rodriguez, M. H., Dister, S. W., Rodriguez, A. D., Rejmankova, E., Ulloa, A., . . . Spanner, M. A. (1994, September). Remote sensing as a landscape epidemiologic tool to identify villages at high risk for malaria transmission. Retrieved April 19, 2017, from <https://www.ncbi.nlm.nih.gov/pubmed/7943544>

Better Health Victoria. (2014). HeV. Retrieved April 19, 2017, from <https://www.betterhealth.vic.gov.au/health/conditionsandtreatments/hendra-virus#lp-h-1>

Bithell, J. (2000). A classification of disease mapping methods. *Statistics in Medicine*, 19(1718):2203-2215.

Boots, B., and Getis, A. (1988). *Point Pattern Analysis*. Sage University Paper Series on Quantitative Applications in the Social Sciences, series no. 07-001. Sage Publications.

Bordoloi, U. D., Kao, D. L., and Shen, H. (2004, June 04). Visualization and exploration of spatial probability density functions: a clustering-based approach. Retrieved April 19, 2017, from <http://proceedings.spiedigitallibrary.org/proceeding.aspx?articleid=837014>

Breed, A. C., Breed, M. F., Meers, J., and Field, H. E. (2011). Evidence of Endemic HeV Infection in Flying-Foxes (*Pteropus conspicillatus*)—Implications for Disease Risk Management. *PLoS ONE*, 6(12). doi:10.1371/journal.pone.0028816.

Brooker, S., and Utzinger, J. (2007). Integrated disease mapping in a polyparasitic world. *Geospatial Health*, pp. 141-146.

Brunsdon, C., Fotheringham, A. S., and Charlton, M. (1996). Geographically weighted regression: a method for exploring spatial Nonstationarity. *Geographical Analysis*, 28 281–298.

Buja, A., Cook, D., and Swayne, D. F. (1996). Interactive high-dimensional data visualization. *Journal of Computational and Graphical Statistics*, 5, 78-99.

Burnham, J., and Chong, A. K. (2016). An Investigation of the Food Sources and Roosting Sites as Potential Factors of HeV Dispersion in South East Queensland, Australia. International conference on GIS and Geomatics Engineering 2016

(ICGGE'16), (In progress to be published in the 'International Journal of Applied Engineering Research (IJAER)' SCOPUS ISSN no 0973-4562).

Burnham, J., and Chong, A. K. (2016). Examining the Spatial Relationship between Equine Population and Food Source Vegetation of Flying-foxes in South East Queensland, Australia. In the proceedings of The 8th National Cartographic Conference, GeoCart'2016, and the 4th ICA Regional Symposium on Cartography for Australasia and Oceania.

Burnham, J., and Chong, A. K. (2016). Factors Explaining the Dispersal of HeV Disease in South-East Queensland. Geocarto International, pp 1-16. DOI: 10.1080/10106049.2016.1161080

Burnham, J., Chong, A. K., Liu, X., and Moore, A. (2015). Preliminary spatial analysis of Hendra disease outbreaks in South East Queensland. The Globe, Vol 76, pp 39-45.

Busgeeth, K., and Rivett, U. (2004). The use of a spatial information system in the management of HIV/AIDS in South Africa. International Journal of Health Geographics, vol.3, no.1, pp.3-13.

Calisher, C. H., Childs, J. E., Field, H. E., Holmes, K. V., and Schountz, T. (2006, July 01). Bats: Important Reservoir Hosts of Emerging Viruses. April 19, 2017, <http://dx.doi.org/10.1128/cmr.00017-06>

Catchpole, H. (2005, May 05). Winter-flowering gums. Retrieved April 20, 2017, from <http://www.abc.net.au/science/articles/2005/05/05/3299439.htm>

CDC GIS Exchange. (2012). Highlights from the Chronic Diseases GIS Exchange, Newsletter, CDC. Retrieved April 19, 2017, from http://www.cdc.gov/dhdsp/docs/GIS_Exchange_Highlights_Aug2012.pdf

CDC. (2014, March 17). HeV Disease. Retrieved April 18, 2017, from <https://www.cdc.gov/vhf/hendra/index.html>

CDNA. (2010). HeV. Retrieved April 19, 2017, from [http://www.health.gov.au/internet/main/publishing.nsf/Content/0E7D7BF4F17C1A96CA257BF0001CBF10/\\$File/Hendra-virus-SoNG.pdf](http://www.health.gov.au/internet/main/publishing.nsf/Content/0E7D7BF4F17C1A96CA257BF0001CBF10/$File/Hendra-virus-SoNG.pdf)

CFSPH. (2015). HeV Infection. Retrieved April 19, 2017, from <http://www.cfsph.iastate.edu/Factsheets/pdfs/hendra.pdf>

Chainey, S. (2010). Understanding hotspots. Retrieved April 21, 2017, from <http://www.popcenter.org/conference/conferencepapers/2010/Chainey-Understandinghotspots.pdf>

Charlton, M., Fotheringham, S., and Brunson, C. (2006). Geographically Weighted Regression. Retrieved April 20, 2017, from <http://eprints.ncrm.ac.uk/90/1/MethodsReviewPaperNCRM-006.pdf>

Christensen, L. A. (1997). Introduction to building a linear regression model. Proceedings of the Twenty-Second Annual SAS Users Group International Conference, March 16–19, San Diego, CA.

Churchill, S. (2008). Australian bats (2nd ed. ed.). Crows Nest, NSW: Allen and Unwin. doi:9781741754612

Clarke, K. C., McLafferty, S. L., and Tempalski, B. J. (1996). On epidemiology and geographic information systems: a review and discussion of future directions. Retrieved April 20, 2017, from <https://www.ncbi.nlm.nih.gov/pubmed/8903207>

Clements, A., Moyeed, R., and Brooker, S. (2006). Bayesian geostatistical prediction of the intensity of infection with *Schistosoma mansoni* in East Africa. *Parasitology*, vol. 133, 711–719.

Colak, E. (2005). Using GIS to Produce Cancer Incidence Maps: A Case Study of Trabzon, Turkey. Retrieved April 19, 2017, from

[http://www.academia.edu/382092/Using_GIS_to_Produce_Cancer_Incidence_Maps
A Case Study of Trabzon Turkey](http://www.academia.edu/382092/Using_GIS_to_Produce_Cancer_Incidence_Maps_A_Case_Study_of_Trabzon_Turkey)

Cressie, N. (2000). Geo-statistical Methods for Mapping Environmental Exposure in Spatial Epidemiology, Methods and Applications. Oxford University Press, doi:10.1093/acprof:oso/9780198515326.003.0010

Cromley, E. K., and McLafferty, S. L. (2002). Analysing Access to Health Services, GIS and Public Health. Guilford Press.

CSIRO. (2016, July 19). HeV Identification. Retrieved April 18, 2017, from <https://csiropedia.csiro.au/hendra-virus-identification/>

CSIRO. (2016, March 08). Developing the world's first Hendra vaccine. Retrieved April 18, 2017, from <http://www.csiro.au/en/Research/BF/Areas/Protecting-Animal-and-Human-Health/Zoonotic-capability/Hendra>

DAF - National HeV Research Program. (2015). Retrieved April 19, 2017, from <https://www.daf.qld.gov.au/animal-industries/animal-health-and-diseases/a-z-list/hendra-virus/intergovernmental-hendra-virus-taskforce/national-hendra-virus-research-program>

Davenhall, B. (2002). Health Geography. Retrieved April 19, 2017, from <http://www.esri.com/news/arcuser/0702/overview.html>

DeHaven, C. (2005). Pteropus poliocephalus. Animal Diversity Web. Retrieved April 18, 2017, from http://animaldiversity.org/accounts/Pteropus_poliocephalus/

Department of the Environment and Energy. (2013, February 12). Australia's bioregions (IBRA) . Retrieved April 20, 2017, from <http://www.environment.gov.au/land/nrs/science/ibra>

Department of the Environment and Energy. (2015). Australia - Present Major Vegetation Subgroups - NVIS Version 4.2 (Albers 100m analysis product).

Retrieved April 20, 2017, from <http://www.environment.gov.au/fed/catalog/search/resource/details.page?uuid=%7BBADF81BD-CAFF-42A1-8A88-FE90A427588A%7D>

Department of the Environment and Energy. (2015). Australia - Pre-1750 Major Vegetation Groups - NVIS Version 4.2 (Albers 100m analysis product). Retrieved April 21, 2017, from <http://www.environment.gov.au/fed/catalog/search/resource/details.page?uuid=%7B3B0B4F84-AA9E-40FB-B5C1-0DB9019CB1A1%7D>

Department of the Environment. (2017). National Flying-fox monitoring viewer. Retrieved April 20, 2017, from <http://www.environment.gov.au/webgis-framework/apps/ffc-wide/ffc-wide.jsf>

DEPI VIC. (2011, February 10). An Assessment of the HeV Situation in Victoria. Retrieved April 18, 2017, from <http://agriculture.vic.gov.au/agriculture/pests-diseases-and-weeds/animal-diseases/vetsource-information-for-vets/an-assessment-of-the-hendra-virus-situation-in-victoria>

DGILP - South East Queensland Regional Plan. (2017). Retrieved April 20, 2017, from <https://www.dilgp.qld.gov.au/planning/regional-planning/south-east-queensland-regional-plan.html>

DoE. (2013). NERP FAQ's. Retrieved April 19, 2017, from <http://www.environment.gov.au/resource/national-flying-fox-monitoring-program-frequently-asked-questions>

Doll, S. R. (1980). The Epidemiology of Cancer. *Cancer*, 45: 2475–2485. doi:10.1002/1097-0142(19800515)45:10<2475::AID-CNCR2820451004>3.0.CO;2-6

DPI NSW. (2012). HeV FAQ's. Retrieved April 19, 2017, from <http://www.dpi.nsw.gov.au/animals-and-livestock/horses/health-and-disease/hendra-virus/faqs>

DPI NSW. (2016, October 17). HeV. Retrieved April 18, 2017, from <http://www.dpi.nsw.gov.au/about-us/services/laboratory-services/veterinary/hendra-virus>

Dykes, J. A. (1997). Exploring spatial data representation with dynamic graphics. *Computers and Geosciences*, 23(4), 345-370.

Edmondston, J., and Field, H. (2011). Research Update – HeV. Australian Biosecurity CRC for Emerging Infectious Diseases.

Edson, D., Field, H., McMichael, L., Vidgen, M., Goldspink, L., Broos, A., Melville, D., Kristoffersen, J., Jordan, D., Kirkland, P., and Smith, C. (2015). Routes of HeV Excretion in Naturally-Infected Flying-Foxes: Implications for Viral Transmission and Spillover Risk. *Plos One*, 10(10). doi:10.1371/journal.pone.0140670

EHP QLD. (2013). Grey-headed flying-fox. Retrieved April 19, 2017, from https://www.ehp.qld.gov.au/wildlife/animals-az/greyheaded_flyingfox.html

EHP QLD. (2016). Little red flying-fox. Retrieved April 19, 2017, from https://www.ehp.qld.gov.au/wildlife/animals-az/little_red_flyingfox.html

Eisen, L., and Eisen, R. J. (2010). Using Geographic Information Systems and Decision Support Systems for the Prediction, Prevention, and Control of Vector-Borne Diseases. Retrieved April 20, 2017, from <http://ral.ucar.edu/csap/events/climatehealth/2011/Vector-Borne%20Disease-Eisen.pdf>

Electron micrograph of HeV [Photograph]. (n.d.). CSIRO, Australia.

Elliot, P., and Wartenberg, D. (2004). Spatial Epidemiology: Current Approaches and future Challenges. *Environmental Health Perspectives*, 112: 998-1006.

Elliott, P. (2000). *Spatial epidemiology: methods and applications*. Oxford: Oxford University Press.

ESRI. (2013). OLS ArcGIS Help. Retrieved April 19, 2017, from <http://resources.arcgis.com/en/help/main/10.1/index.html#//005p00000022000000>

ESRI. (2016). GWR. Retrieved April 20, 2017, from <http://desktop.arcgis.com/en/arcmap/10.3/tools/spatial-statistics-toolbox/geographically-weighted-regression.htm>

ESRI. (2016). An overview of the Extraction tools. Retrieved April 21, 2017, from <http://desktop.arcgis.com/en/arcmap/10.3/tools/spatial-analyst-toolbox/an-overview-of-the-extraction-tools.htm>

ESRI. (2016). An overview of the Spatial Analyst Toolbox. Retrieved April 21, 2017, from <http://desktop.arcgis.com/en/arcmap/10.3/tools/spatial-analyst-toolbox/an-overview-of-the-spatial-analyst-toolbox.htm>

ESRI. (2016). Buffer (Analysis). Retrieved April 21, 2017, from http://resources.esri.com/help/9.3/arcgisengine/java/gp_toolref/analysis_tools/buffer_analysis_.htm

ESRI. (2016). Geographically Weighted Regression (GWR). Retrieved April 21, 2017, from <http://desktop.arcgis.com/en/arcmap/10.3/tools/spatial-statistics-toolbox/geographically-weighted-regression.htm#GUID-E9FD5D8B-103B-40FC-93DD-E84BB2F1C7E9>

ESRI. (2016). High/Low Clustering (Getis-Ord General G). Retrieved April 21, 2017, from <http://desktop.arcgis.com/en/arcmap/10.3/tools/spatial-statistics-toolbox/high-low-clustering.htm>

ESRI. (2016). How GWR works. Retrieved April 21, 2017, from <http://desktop.arcgis.com/en/arcmap/latest/tools/spatial-statistics-toolbox/how-gwr-regression-works.htm>

ESRI. (2016). Interpreting GWR results. Retrieved April 21, 2017, from <http://desktop.arcgis.com/en/arcmap/latest/tools/spatial-statistics-toolbox/interpreting-gwr-results.htm>

ESRI. (2016). Interpreting OLS results. Retrieved April 21, 2017, from <http://desktop.arcgis.com/en/arcmap/latest/tools/spatial-statistics-toolbox/interpreting-ols-results.htm>

ESRI. (2016). Regression analysis basics. Retrieved April 21, 2017, from <http://desktop.arcgis.com/en/arcmap/latest/tools/spatial-statistics-toolbox/regression-analysis-basics.htm>

ESRI. (2016). What they don't tell you about regression analysis. Retrieved April 20, 2017, from <http://pro.arcgis.com/en/pro-app/tool-reference/spatial-statistics/what-they-don-t-tell-you-about-regression-analysis.htm>

ESRI. (2017). Buffer. Retrieved April 20, 2017, from http://desktop.arcgis.com/en/arcmap/10.3/tools/analysis-toolbox/buffer.htm#ESRI_USAGES_CFF587FA5751438FB7100D0063C456F7

ESRI. (2017). How High/Low Clustering (Getis-Ord General G) works. Retrieved April 21, 2017, from <http://pro.arcgis.com/en/pro-app/tool-reference/spatial-statistics/h-how-high-low-clustering-getis-ord-general-g-spat.htm>

ESRI. (2017). How Kernel Density works. Retrieved April 21, 2017, from <http://pro.arcgis.com/en/pro-app/tool-reference/spatial-analyst/how-kernel-density-works.htm>

ESRI. (2017). How OLS regression works. Retrieved April 21, 2017, from <http://desktop.arcgis.com/en/arcmap/10.3/tools/spatial-statistics-toolbox/how-ols-regression-works.htm>

ESRI. (2017). How Spatial Autocorrelation (Global Moran's I) works. Retrieved April 21, 2017, from <http://pro.arcgis.com/en/pro-app/tool-reference/spatial-statistics/h-how-spatial-autocorrelation-moran-s-i-spatial-st.htm>

ESRI. (2017). Kernel Density. Retrieved April 21, 2017, from <http://desktop.arcgis.com/en/arcmap/10.3/tools/spatial-analyst-toolbox/kernel-density.htm>

ESRI. (2017). Ordinary Least Squares (OLS). Retrieved April 21, 2017, from <http://pro.arcgis.com/en/pro-app/tool-reference/spatial-statistics/ordinary-least-squares.htm>

ESRI. (2017). Spatial Autocorrelation (Global Moran's I). Retrieved April 21, 2017, from <http://pro.arcgis.com/en/pro-app/tool-reference/spatial-statistics/spatial-autocorrelation.htm>

Estimation of A K Function [Photograph]. (1996). Gatrell et al 1996.

Field, H., Edson, D., and McMichael, L. (2016). Flying fox dispersal and HeV risk. Compendium of findings from the National HeV Research Program, pp. 26-27. doi:ISBN 978-1-74254-847-0

Field, H., Jong, C. D., Melville, D., Smith, C., Smith, I., Broos, A., Kung, N., McLaughlin, A., and Zeddeman, A. (2011). HeV Infection Dynamics in Australian Fruit Bats. PLoS ONE, 6(12). doi:10.1371/journal.pone.0028678

Field, H., Jordan, D., Edson, D., Melville, D., Kirkland, P., and Smith, C. (2016). HeV infection and transmission dynamics. Compendium of findings from the National HeV Research Program, pp. 12-13. doi:ISBN 978-1-74254-847-0

Field, H., Jordan, D., Edson, D., Morris, S., Melville, D., Kung, N., Kirkland, P., and Smith, C. (2015). Spatiotemporal Aspects of HeV Infection in Pteropid Bats (Flying-Foxes) in Eastern Australia. Plos One, 10(12). doi:10.1371/journal.pone.0144055

Field, H., Young, P., Yob, J. M., Mills, J., Hall, L., and Mackenzie, J. (2001). The natural history of Hendra and Nipah viruses. *Microbes and Infection*, 3(4), 307-314. doi:10.1016/s1286-4579(01)01384-3

Flying-fox Species [Photograph]. (2017). <https://www.batreach.com/>, Kuranda.

Fotheringham, A. S., Brunson, C., and Charlton, M. (1997). Measuring Spatial Variations in Relationships with Geographically Weighted Regression. *Recent Developments in Spatial Analysis, Spatial Statistics, Behavioural Modelling and Computational Intelligence*, Springer-Verlag, pp 4: 60-82.

Fotheringham, A. S., Brunson, C., and Charlton, M. (2002). Geographically weighted regression the analysis of spatially varying relationships. Chichester: Wiley.

Fotheringham, A. S., Kelly, M., and Charlton, M. (2012). The demographic impacts of Irish famine: towards a greater geographical understanding. *Transactions of the Institute of British Geographers*, 38(2):221-237.

Gao, S., Mioc, D., Anton, F., Yi, X., and Coleman, D. J. (2008). Online GIS services for mapping and sharing disease information. Retrieved April 20, 2017, from <https://ij-healthgeographics.biomedcentral.com/articles/10.1186/1476-072X-7-8>

Gatrell, A. C., and Löytönen, M. (1997). GIS and health. London, Taylor and Francis.

Gatrell, A. C., and Senior, M. (2005). Health and health care applications. Retrieved April 20, 2017, from http://www.colorado.edu/geography/leyk/GIS1/Readings/Gatrell_Senior_2005.pdf

Gatrell, A. C., Bailey, T. C., Diggle, P. J., and Rowlingson, B. S. (1996). Spatial point pattern analysis and its application in geographical epidemiology. *Transactions, Institute of British Geographers*, 21: 256–74.

Getis, A. (2008). A History of the Concept of Spatial Autocorrelation: A Geographer's Perspective. *Geographical Analysis*, 40(3), 297-309. doi:10.1111/j.1538-4632.2008.00727.x

Getis, A., and Ord, J. K. (1992). The Analysis of Spatial Association by Use of Distance Statistics. *Geographical Analysis*, 24(3), 127-145. doi:10.1007/978-3-642-01976-0_10

Getis, A., and Ord, J. K. (1996). Local spatial statistics: an overview. *GeoInformation International*, pp 261-277.

Gold Coast Bulliten. (2016). QLD News: Bats driving Southport residents crazy. Retrieved April 21, 2017, from <http://www.couriermail.com.au/news/queensland/bats-driving-southport-residents-crazy/news-story/bbd1f5c801c4e95344734caad33bc5b5>

Goodchild, M. F. (1986). *Spatial autocorrelation*. Norwich: Geo Books.

Goodchild, M. F., and Haining, R. P. (2004). GIS and spatial data analysis: Converging perspectives. *Papers in Regional Science*, 83: 363–385.

Goodchild, M. F., and Longley, P. A. (2005). The future of GIS and spatial analysis. Retrieved April 20, 2017, from http://www.csiss.org/gispopsci/workshops/2005/PSU/docs/goodchild_future.pdf

Grabowski, M. K., Lessler, J., Redd, A. D., Kagaayi, J., Laeyendecker, O., Ndyanabo, A., . . . Program, T. R. (2014). The Role of Viral Introductions in Sustaining Community-Based HIV Epidemics in Rural Uganda: Evidence from Spatial Clustering, Phylogenetics, and Egocentric Transmission Models. Retrieved April 19, 2017, from <http://journals.plos.org/plosmedicine/article?id=10.1371%2Fjournal.pmed.1001610>

Gupta, R., Jay, D., and Jain, R. (2003). Geographic Information Systems for the study and control of infectious diseases. Retrieved April 19, 2017, from

<https://www.geospatialworld.net/article/geographic-information-systems-for-the-study-and-control-of-infectious-diseases/>

Haining, R. P. (1987). Small area aggregate income models: theory and methods with an application to urban and rural income data for Pennsylvania. *Regional Studies*, 21: 519-30.

Haining, R. P. (1994). Designing spatial data analysis modules for GIS. In A.S.Fotheringham and P. Rogerson, editors, *Spatial Analysis and GIS*, pp. 45-63. London: Taylor and Francis.

Haining, R. P. (1998). *Spatial Statistics and the Analysis of Health Data*. GIS and Health: GIS Data, Taylor and Francis Ltd.

Haining, R. P. (2003). *Spatial data analysis: theory and practise*. Cambridge University Press.

Halpin, K., Young, P., Field, H., and Mackenzie, J. (2000). Isolation of HeV from pteropid bats: a natural reservoir of HeV. *Journal of General Virology*, 81:1927-32. doi:10.1099/0022-1317-81-8-1927

Han, D., and Rogerson, P. A. (2003). Application of a GIS-Based Statistical Method to Access Spatio-Temporal Changes in Breast Cancer Clustering in the Northeastern United States. *Geographic Information Systems and Health Applications*, 114-138. doi:10.4018/978-1-59140-042-4.ch007

Hendra Belt [Photograph]. (n.d.). Agriculture Victoria, Victoria.

HeV Incidents [Photograph]. (2013). Bio Security QLD, CSIRO, Random Analytics and multiple other outlets, Australia.

HeV Temporal Pattern [Photograph]. (2013). Bio Security QLD, CSIRO, Random Analytics and multiple other outlets, Australia.

Hendrickx, G. (2001). Spatial trypanosomosis management: from data-layers to decision making. *Parasitology Today*, 17(1), 35-41. doi:10.1016/s0169-4758(00)01852-4

Hess, I. M., Massey, P. D., Walker, B., Middleton, D. J., and Wright, T. M. (2011). HeV: what do we know? *New South Wales Public Health Bulletin*, 22(6), 118. doi:10.1071/nb10077

Hubert, L. J., Golledge, R. G., and Costanza, C. M. (1981). Generalized Procedures for Evaluating Spatial Autocorrelation. *Geographical Analysis*, 13, 224–32.

Hutcheson, G. D. (2011). Ordinary Least-Squares Regression. In L. Moutinho and G. D. Hutcheson, *The SAGE Dictionary of Quantitative Management Research*. Pages 224-228.

Jarup, L. (2004, June). Health and Environment Information Systems for Exposure and Disease Mapping, and Risk Assessment. Retrieved April 19, 2017, from <https://www.ncbi.nlm.nih.gov/pmc/articles/PMC1247192/>

Jerrett, M., Burnett, R. T., Goldberg, M. S., Sears, M., Krewski, D., Catalan, R., . . . Finkelstein, N. (2003). Spatial analysis for environmental health research: concepts, methods, and examples. Retrieved April 19, 2017, from <https://www.ncbi.nlm.nih.gov/pubmed/12959844>

Jones, K. E., Patel, N. G., Levy, M. A., Storeygard, A., Balk, D., Gittleman, J. L., and Daszak, P. (2007). Global trends in emerging infectious diseases. Retrieved April 20, 2017, from <http://www.nature.com/nature/journal/v451/n7181/full/nature06536.html>

Kaushal, A., and Johnson, C.P. (2003). Disease Surveillance Using GIS and Remote Sensing. Indo-French Workshop on Tele-Epidemiology of Dengue, Pune, Egypt.

Kernel Estimation of a Point Pattern [Photograph]. (1996). Gatrell et al 1996.

Keys, A. (1980). *Seven countries: a multivariate analysis of death and coronary heart disease*. Cambridge, MA: Harvard University Press.

Knigge, L., and Cope, M. (2005). *Grounded visualization: integrating the analysis of qualitative and quantitative data through grounded theory and visualization*. Retrieved April 20, 2017, from http://www.uvm.edu/~mcope/Knigge%26Cope_2006.pdf

Koch, T. (2004). *The Map as Intent: Variations on the Theme of John Snow* . Retrieved April 20, 2017, from [http://www.ph.ucla.edu/epi/snow/cartographica39\(4\)1_14_2004.pdf](http://www.ph.ucla.edu/epi/snow/cartographica39(4)1_14_2004.pdf)

Koch, T. (2005). *Cartographies of Disease: Maps, Mapping, and Medicine*. Redlands, CA: ESRI Press.

Kulldorf, M. (1999). Geographical Information Systems and Community Health: Some statistical Issues. *Journal of Public Health Management*, 5(2): 100-106.

Langford, I., and Bentham, G. (1996). Regional variations in mortality rates in England and Wales – an analysis using multilevel modelling. *Social Science and Medicine*, 42: 987–98.

Lawson, A. B., and Williams, F. L. (2001). *An introductory guide to disease mapping*. New York, NY: John Wiley and Sons, Inc.

Lawson, A., and Williams, F. (2001). *An introductory guide to disease mapping*. Chichester: John Wiley.

Lessler, J., Salje, H., Grabowski, M. K., and Cummings, D. A. (2016). Measuring Spatial Dependence for Infectious Disease Epidemiology. Retrieved April 19, 2017, from <http://journals.plos.org/plosone/article?id=10.1371%2Fjournal.pone.0155249#pone.0155249.ref022>

Levine, N. (2002). CrimeStat: A Spatial Statistical Program for the Analysis of Crime Incidents. *Encyclopedia of GIS*, 187-193. doi:10.1007/978-0-387-35973-1_229

Lopes, S. B., Brondino, N. C., and Rodrigues da Silva, A. N. (2007). EXPLORATORY AND CONFIRMATORY SPATIAL DATA ANALYSIS TOOLS IN TRANSPORT DEMAND MODELING . Retrieved April 20, 2017, from <http://www.redpgv.coppe.ufrj.br/index.php/es/produccion/articulos-cientificos/2007-1/300-062/file>

Luo, W., and Wang, F. (2003). Spatial accessibility to primary care and physician shortage area designation: a case study in Illinois with GIS approaches. *Geographic Information Systems and Health Applications*, Idea Group Publishing, Hershey, PA, pp.260—278.

Maceachren, A. M. (1992). Visualizing Uncertain Information. *Cartographic Perspectives*, (13), 10-19. doi:10.14714/cp13.1000

MacEachren, A. M., and Ganter, J. H. (1990). A pattern identification approach to cartographic visualization. *Cartographica*, 27(2): 64-81.

Maceachren, A. M., and Kraak, M. (1997). Exploratory cartographic visualization: Advancing the agenda. *Computers and Geosciences*, 23(4), 335-343. doi:10.1016/s0098-3004(97)00018-6

Malczewski, J., and Poetz, A. (2004). Residential Burglaries and Neighborhood Socioeconomic Context in London, Ontario: Global and Local Regression Analysis*. *The Professional Geographer*, 57(4), 516-529. doi:10.1111/j.1467-9272.2005.00496.x

Markus, N., and Hall, L. (2004). Foraging behaviour of the black flying-fox (*Pteropus alecto*) in the urban landscape of Brisbane, Queensland. *Wildlife Research*, 31: 345–355.

McCall, J., Pasini, A. K., and Wait, R.B. (2003). Using a GIS and the American Community Survey to Address Community Health Problems. *Medicine, Healthcare, and Life Sciences Book Chapter* | IGI Global.

McCallum, H. (2016). Models to predict HeV prevalence in flying fox populations. *Compendium of findings from the National HeV Research Program*, pp. 10-11. doi:ISBN 978-1-74254-847-0

Mcfarlane, R., Becker, N., and Field, H. (2011). Investigation of the Climatic and Environmental Context of HeV Spillover Events 1994–2010. *PLoS ONE*, 6(12). doi:10.1371/journal.pone.0028374

Middleton D, Pallister J, Klein R, Feng Y, Haining J, Arkinstall R, Frazer L, Huang J, Edwards N, Wareing M, ... Wang, L. (2014). HeV Vaccine, a One Health Approach to Protecting Horse, Human, and Environmental Health. *EID Journal*. Vol 20 No. 3. doi: 10.3201/eid2003.131159

Minitab. (2016). Types of regression analyses. Retrieved April 20, 2017, from <http://support.minitab.com/en-us/minitab/17/topic-library/modeling-statistics/regression-and-correlation/basics/types-of-regression-analyses/>

Miranda, M. L., Casper, M., Tootoo, J., and Schieb, L. (2013, June 20). Putting chronic disease on the map: building GIS capacity in state and local health departments. Retrieved April 20, 2017, from <https://www.ncbi.nlm.nih.gov/pubmed/23786907>

Monmonier, M. (1989). Geographic brushing: enhancing exploratory analysis of the scatterplot matrix. *Cartographical Analysis*, 21, 81-84.

Moore, A., Seng, S. B., and Chong, A. K. (2005). Geostatistical modelling, analysis and mapping of epidemiology of Dengue Fever in Johor State, Malaysia. Retrieved April 19, 2017, from <https://ourarchive.otago.ac.nz/handle/10523/763>

Moran, P. A. (1950). Notes On Continuous Stochastic Phenomena. *Biometrika*, 37(1-2), 17-23. doi:10.1093/biomet/37.1-2.17

Muttitanon, W., Kongthong, P., Kongkanon, C., Yoksan, S., Gonzalez, J.P., and Babazan, P. (2002). Spatial and temporal dynamics of Dengue Hemorrhagic Fever Epidemics (NakhonPathom province, Thailand, 1997-2001). Retrieved April 19, 2017, from <http://www.gisdevelopment.net/application/health/planning/healthp0010pf.htm>

Myers, M., Rogers, D., Cox, J., Flahault, A., and Hay, S. (2000). Forecasting Disease Risk for Increased Epidemic Preparedness in Public Health. Retrieved April 19, 2017, from <https://www.ncbi.nlm.nih.gov/pmc/articles/PMC3196833/>

Nakaya, T. (2016). GWR Windows Application for Geographically Weighted Regression Modelling (Version 4.0) [Program documentation].

National HeV Research Program. (2016). Retrieved April 18, 2017, from <https://www.daf.qld.gov.au/animal-industries/animal-health-and-diseases/a-z-list/hendra-virus/intergovernmental-hendra-virus-taskforce/national-hendra-virus-research-program>

Nobre, F. F., and Carvalho, M. (1995). Spatial and Temporal Analysis of Epidemiological Data. Retrieved April 19, 2017, from <http://www.nzdl.org/gsdmod?e=d-00000-00---off-0envl--00-0----0-10-0---0---0direct-10---4-----0-11--11-en-50---20-about---00-0-1-00-0-0-11-1-0utfZz-8-00-0-0-11-10-0utfZz-8-00andcl=CL2.1.2andd=HASHab27b8a9e2dc0f8c951c5b.4.3>=1>

NPDO. (2016). HeV. Retrieved April 18, 2017, from <http://www.outbreak.gov.au/for-vets-and-scientists/hendra-virus>

Nuckols, J. R., Ward, M. H., and Jarup, L. (2004, June). Using geographic information systems for exposure assessment in environmental epidemiology studies. Retrieved April 19, 2017, from <https://www.ncbi.nlm.nih.gov/pubmed/15198921>

Ogbonna, J. U. (2012). EPIDEMIOLOGICAL GIS: Understanding Emerging Critical Issues. *American Journal of Geographic Information System*, 1(2), 29-32. Retrieved April 20, 2017, from <http://article.sapub.org/10.5923.j.ajgis.20120102.02.html>

Ord, J. K., and Getis, A. (1995). Local Spatial Autocorrelation Statistics: Distributional Issues and an Application. *Geographical Analysis*, 27(4), 286-306. doi:10.1111/j.1538-4632.1995.tb00912.x

Outbreak Distribution Map [Photograph]. (n.d.). Centers for disease control and prevention, USA.

Pang, A. (2001). Visualizing Uncertainty in Geo-spatial Data. Retrieved April 20, 2017, from <ftp://ftp.cse.ucsc.edu/pub/reinas/papers/geo.pdf>

Perry, B. D. (1994). Modelling vector-borne and other parasitic diseases: proceedings of a workshop organized jointly by the International Laboratory for Research on Animal Diseases and the Food and Agriculture Organization of the United Nations, held at ILRAD Nairobi, Kenya, 23 - 27 November 1992. Nairobi: ILRAD.

Pfeiffer, D. U. (1996). Issues related to handling of spatial data. Retrieved April 20, 2017, from ftp://131.252.97.79/Transfer/ES_Pubs/ESVal/spatial_statistics/issues_related_to_spatial_data.pdf

Philbrick, A. K. (1953). Toward a unity of cartographical forms and geographical content. *Professional Geographer*, 5(5): 11-15.

Plowright, R. K., Eby, P., Hudson, P. J., Smith, I. L., Westcott, D., Bryden, W. L., . . . Mccallum, H. (2014). Ecological dynamics of emerging bat virus spillover. *Proceedings of the Royal Society B: Biological Sciences*, 282(1798), 20142124-20142124. doi:10.1098/rspb.2014.2124

Plowright, R. K., Foley, P., Field, H. E., Dobson, A. P., Foley, J. E., Eby, P., and Daszak, P. (2011). Urban habituation, ecological connectivity and epidemic dampening: the emergence of HeV from flying foxes (*Pteropus* spp.). *Proceedings of the Royal Society B: Biological Sciences*, 278(1725), 3703-3712. doi:10.1098/rspb.2011.0522

Plowright, R., Field, H., Smith, C., Divljan, A., Palmer, C., Tabor, G., Daszak, P., and Foley, J. (2008). Reproduction and nutritional stress are risk factors for HeV infection in little red flying foxes (*Pteropus scapulatus*). *Proceedings of the Royal Society*, 275. 861-869. doi: 0.1098/rspb.2007.1260

QLD Horse Council. (2010). Hendra-Property Design. Retrieved April 19, 2017, from <http://www.qldhorsecouncil.com/OldHorseCouncil/media/QHC-Portal/Hendra%20Virus/Hendra-Property-Design.pdf>

QLD Horse Council. (2012). Bats and Trees. Retrieved April 19, 2017, from <http://www.qldhorsecouncil.com/OldHorseCouncil/media/QHC-Portal/Hendra%20Virus/Bats-and-Trees.pdf>

Queensland Government - South east Queensland regional plan 2009-2031. (2009). Retrieved April 21, 2017, from <http://www.statedevelopment.qld.gov.au/resources/plan/seq/regional-plan-2009/seq-regional-plan-2009.pdf>

Queensland Government Data. (2014). Local government area boundaries - Queensland - Data | Queensland Government. Retrieved April 20, 2017, from <https://data.qld.gov.au/dataset/local-government-area-boundaries-queensland>

Queensland Health. (2005). Report on GIS and public health spatial applications. Retrieved April 20, 2017, from <http://citeseerx.ist.psu.edu/viewdoc/download?rep=rep1&andtype=pdf&doi=10.1.1.20.5733>

Queensland Treasury. (2011). Population growth highlights and trends Queensland 2011. Retrieved April 21, 2017, from <http://www.qgso.qld.gov.au/products/reports/pop-growth-highlights-trends-qld/pop-growth-highlights-trends-qld-2011.pdf>

Random Analytics Posts. (2013, July). Retrieved April 18, 2017, from <https://gmgranger.wordpress.com/2013/07/>

Red List. (2008). Pteropus alecto. Retrieved April 19, 2017, from <http://www.iucnredlist.org/details/18715/0>

Red List. (2008). Pteropus conspicillatus. Retrieved April 19, 2017, from <http://www.iucnredlist.org/details/18721/0>

Red List. (2008). Pteropus poliocephalus. Retrieved April 19, 2017, from <http://www.iucnredlist.org/details/18751/0>

Red List. (2008). Pteropus scapulatus. Retrieved April 19, 2017, from <http://www.iucnredlist.org/details/18758/0>

Ripley, B. D. (1981). Spatial statistics. John Wiley, Chichester.

Roberts, B. J., Catterall, C. P., Eby, P. and Kanowski, J. (2012). Latitudinal range shifts in Australian flying-foxes: A re-evaluation. *Austral Ecology*, 37: 12–22. doi:10.1111/j.1442-9993.2011.02243.x

Rogerson, P. A. (2001). Statistical methods for geography. London: Sage.

Scanlan, J. C., Kung, N. Y., Selleck, P. W., and Field, H. E. (2015). Erratum to: Survival of HeV in the Environment: Modelling the Effect of Temperature. *EcoHealth*, 12(2), 390-390. doi:10.1007/s10393-015-1049-9

Seng, S. B. (2005). Geostatistical modelling, analysis and mapping of epidemiology of dengue fever in Johor State, Malaysia (Unpublished Masters dissertation). University of Otago.

Shittu, O. B., Akpan, I., Popoola, T. O., Oyedepo, J. A., and Ogunshola, E. O. (2010). Epidemiological features of a GIS-supported investigation of cholera outbreak in Abeokuta, Nigeria. Retrieved April 20, 2017, from http://www.academicjournals.org/article/article1379409987_Shittu%20et%20al.pdf

Shittu, O., Akpan, T., Popoola, S., Oyedepo, J., and Ogunshola, E. (2010). Epidemiological features of a GIS-supported investigation of cholera outbreak in Abeokuta, Nigeria. *Journal of Public Health and Epidemiology*, vol.2, no.7, pp.152-162.

Sirken, M., Herrmann, D., and White, A. A. (1993). COGNITIVE ASPECTS OF DESIGNING STATISTICAL MAPS . Retrieved April 20, 2017, from http://ww2.amstat.org/sections/srms/Proceedings/papers/1993_097.pdf

Skerratt, L., and Martin, G. (2016). Models that predict risk for HeV transmission from flying foxes to horses. *Compendium of findings from the National Hendra Virus Research Program*, pp. 16-17. doi:ISBN 978-1-74254-847-0

Smith, C., Skelly, C., Kung, N., Roberts, B., and Field, H. (2014). Flying-Fox Species Density - A Spatial Risk Factor for HeV Infection in Horses in Eastern Australia. *PLoS ONE*, 9(6). doi:10.1371/journal.pone.0099965

Snow, J. (n.d.). John Snow Cholera Map [Photograph]. *Epidemiology Inside and multiple Other Sources*.

Snow, J., and Ellis, R. H. (1994). *The case books of dr. John Snow*. London: Wellcome institute for the history of medicine.

Snow, R. W., Gouws, E., Omumbo, J., Rapuoda, B, F. C., . . . Ouma, J. (1998). Models to predict the intensity of Plasmodium falciparum transmission: applications

to the burden of disease in Kenya. Retrieved April 19, 2017, from <https://www.ncbi.nlm.nih.gov/pubmed/10326100>

Sykes, A. O. (1993). An Introduction to Regression Analysis. Coase-Sandor Institute for Law and Economics Working Paper No. 20.

Tanser, F., and Sueur D. (2002). The application of geographical information systems to important public health problems in Africa. *International Journal of Health Geographics*, Vol 1. Issue 4.

Thompson, J. (2016). Foreword. *Compendium of findings from the National HeV Research Program*, pp. 3-4. doi:ISBN 978-1-74254-847-0

Tobler, W. R. (1970). A Computer Movie Simulating Urban Growth in the Detroit Region. *Economic Geography*, 46, 234. doi:10.2307/143141

Ulugtekin, N., Alkoy, S., and Seker, D. Z. (2007). Use of Geographic Information Systems in an Epidemiological Study of Measles in Istanbul. *The Journal of International Medical Research*, vol.35:1, pp 150-154.

Ungerer, M. J., and Goodchild, M. F. (2002). Integrating spatial data analysis and GIS: a new implementation using the Component Object Model (COM). *International Journal of Geographical Information Science*, 16(1): 41-54.

Unwin, D. J. (1996). GIS, spatial analysis and spatial statistics. *Progress in Human Geography*, 20(4), 540-551.

Wakefield, J., Kelsall, J. E., and Morris, S. E. (2001). Clustering, Cluster detection, and Spatial variation in Risk. *Oxford Scholarship Online*.

Waller, L. A. (1996). *Epidemiologic Uses of Geographic Information Systems (GIS)*. Retrieved April 20, 2017, from http://www.csm.ornl.gov/asasie/newsletter/la_walle.html

Walter, S. D. (1993, July 30). Visual and statistical assessment of spatial clustering in mapped data. Retrieved April 19, 2017, from <https://www.ncbi.nlm.nih.gov/pubmed/8210826>

Walter, S. D. (2000). Disease mapping: a historical perspective. In: Spatial Epidemiology: Methods and Applications (Elliott P, Wakefield J, Best N, Briggs DJ, eds). Oxford:Oxford University Press, 223–252.

Westcott, D. (2016). Implementing a national flying fox monitoring program. Compendium of findings from the National HeV Research Program, pp. 8-9. doi:ISBN 978-1-74254-847-0

Wiafe, S., and Davenhall, B. (2007). Extending Disease Surveillance with GIS. Retrieved April 19, 2017, from http://www.esri.com/news/arcuser/0405/disease_surveil1of2.html

Wildlife QLD. (2016). Pteropus poliocephalus. Retrieved April 19, 2017, from <http://wildlife.org.au/grey-headed-flying-fox/>

Wildlife QLD. (2016). Pteropus scapulatus. Retrieved April 19, 2017, from <http://wildlife.org.au/little-red-flying-fox/>

Wildlife QLD. (2016). Pteropus alecto. Retrieved April 19, 2017, from <http://wildlife.org.au/black-flying-fox/>

Wise, S., Haining, R., and Signoretta, P. (1998). The role of visualization in the exploratory spatial data analysis of area-based data. Retrieved April 20, 2017, from http://www.geocomputation.org/1998/81/gc_81.htm

Appendix - 1

Data and Statistics

A1.1 List of HeV Incidents

Table A1.1: List of HeV incidents (Source: Queensland Centre for Emerging Infectious Diseases 2014).

Incident	Date	Latitude	Longitude
1	1/08/1994	-21.12	149.03
2	9/09/1994	-27.42	153.08
3	18/01/1999	-16.79	145.69
4	25/10/2004	-17.09	145.79
5	1/12/2004	-19.38	146.91
6	14/06/2006	-26.82	152.89
7	31/10/2006	-28.33	153.39
8	6/06/2007	-26.82	152.88
9	18/07/2007	-16.78	145.67
10	26/06/2008	-27.58	153.28
11	11/07/2008	-20.57	148.61
12	28/07/2009	-23.27	150.67
13	3/08/2009	-19.99	148.19
14	17/05/2010	-26.38	153.03
15	21/06/2011	-28.04	152.59
16	26/06/2011	-28.13	153.08
17	28/06/2011	-27.69	153.12
18	30/06/2011	-28.79	153.37
19	3/07/2011	-30.73	152.83
20	4/07/2011	-27.73	153.01
21	11/07/2011	-16.89	145.57
22	13/07/2011	-25.33	152.82
23	14/07/2011	-28.72	153.35
24	15/07/2011	-27.36	153.06
25	22/07/2011	-26.75	150.62

26	24/07/2011	-28.54	153.5
27	8/08/2011	-28.88	153.49
28	12/08/2011	-28.54	153.43
29	15/08/2011	-28.71	153.54
30	23/08/2011	-28.18	153.43
31	27/08/2011	-28.79	153.51
32	9/10/2011	-27.11	153.01
33	3/01/2012	-19.59	146.91
34	26/05/2012	-23.39	150.59
35	28/05/2012	-18.63	146.12
36	26/06/2012	-20.99	148.98
37	15/07/2012	-23.39	150.61
38	27/07/2012	-16.93	145.69
39	3/09/2012	-16.53	145.45
40	1/11/2012	-18.66	146.27
41	21/01/2013	-21.82	149.37
42	19/02/2013	-16.88	145.57
43	5/06/2013	-30.69	152.72
44	25/06/2013	-27.51	152.55
45	1/07/2013	-30.71	152.64
46	5/07/2013	-28.06	153.35
47	8/07/2013	-30.85	152.65
48	10/07/2013	-31.09	152.84
49	17/03/2014	-24.93	152.24
50	2/06/2014	-27.78	153.19
51	21/06/2014	-28.33	153.39
52	16/07/2014	-23.98	151.19

A1.2 List of Permanent continuous Use Roosting Sites in the Study Area

Table A1.2: List of permanent continuous use roosting sites in the study area
(Source: EHP 2014).

Longitude	Latitude	Name
151.9837	-28.028	Allora (Dalrymple Creek)
152.6799	-27.9919	Boonah, Bicentennial Park
153.4277	-28.0222	Broadbeach, Cascade Gardens
152.3387	-24.8615	Bundaberg, Harriet Island/Don Tallon Bridge
153.4292	-28.0946	Burleigh, Marymount College
146.2764	-26.3598	Charleville (Warrego)
153.258	-27.5275	Cleveland, Black Swamp
153.3812	-27.8883	Coombabah, Coombabah Creek
153.4672	-28.1453	Currumbin Creek
153.0519	-27.4841	East Brisbane, Norman Creek (Heath Park/Giffin Par
152.4233	-27.2349	Esk
153.1136	-27.444	Hemmant, Lytton Road
152.8128	-25.2456	Hervey Bay, Gatakers bay
152.7044	-26.4048	Kandanga, Hyne Estate Rd
153.1437	-27.445	Lindum, Kianawah Rd.
153.1837	-27.4641	Lota, Wynnum Hospital
152.9255	-27.5444	Mount Ommaney - Westlake Drive
152.7222	-27.4939	Pine Mountain (Camerons Scrub/Sapling Pocket)
153.0988	-27.2315	Redcliffe Botanic Gardens
148.8029	-26.5602	Roma, Bungil Creek
153.0687	-27.3231	Sandgate, Curlew Park
153.1279	-27.0804	Sandstone Point, Bestman Rd
153.1373	-27.6402	Slacks Creek, Meakin Park
153.4134	-27.9951	Southport Golf Club
153.4136	-27.9797	Southport, Akes Avenue,
152.9992	-27.412	Stafford, Sparkes Hill, Clover Street
153.2767	-28.2174	Springbrook N.P, Natural Bridge
153.1363	-27.61	Springwood, Parfrey Road
151.8786	-26.9345	The Palms NP, Cooyar
151.6566	-24.0818	Turkey Beach (now Central Region)
152.926	-27.0809	Wararba Creek, Caboolture
152.7485	-27.6031	Woodend
152.7556	-27.6514	Yamanto
152.2726	-27.5648	Gatton, Amaroo Retirement Village, Tenthill Creek

A1.3 List of Permanent Seasonal Use Roosting Sites in the Study Area

Table A1.3: List of permanent seasonal use roosting sites in the study area (Source: EHP 2014).

Longitude	Latitude	Name
153.2263	-27.5026	Birkdale, Tarradarrapin
152.6085	-28.0009	Boonah - Mount French
152.9714	-27.1527	Burpengary
152.5274	-25.2095	Burrum River (upper), Junction Cherwell River
152.9206	-27.6315	Camira, Pilney Reserve (Barbara Street)
153.1824	-28.0398	Canungra, Beachmont Rd
152.98	-27.8558	Cedar Grove -Brushwood Cres.
151.8965	-25.6147	Coalstoun Lakes Recreation Reserve
153.3312	-27.5724	Coochiemudlo Island
152.0166	-27.45	Crows Nest
151.2601	-27.1897	Dalby, Myall Creek
152.8254	-27.1971	Dayboro, Railway Street
152.8316	-27.2069	Dayboro, Strong Road
152.7272	-25.2682	Dundowran, O'Reagans Creek CP
152.9479	-27.6142	Ellen Grove, Waterford Rd
153.0226	-27.4424	Enoggera Creek Herston
152.785	-27.7928	Flinders Peak, Peak Crossing
153.0471	-25.4019	Fraser Island, Cornwell's Break
151.6109	-25.6239	Gayndah Township
152.6384	-26.1822	Gympie Township, Widgee Crossing
152.0558	-27.3467	Hampton, Wockner Rd
153.3343	-27.9012	Helensvale, Mildura Drive
152.8929	-25.2888	Hervey Bay, Botanic Gardens
152.8472	-25.2818	Hervey Bay, Tooan Tooan
153.0115	-28.2192	Hillview
152.3208	-25.2258	Horton, 59 Station Road
152.9886	-27.5157	Indooroopilly Island
151.8125	-26.5275	Kingaroy, Mt. Wooloorin Reserve
152.1724	-24.7218	Kolan River, Avondale
153.3753	-27.6274	Lamb Island
152.9654	-26.7997	Landsborough, Vidler Crt
152.5903	-27.4657	Lowood (Camp 2) Water Tower
152.5886	-27.4688	Lowood Bend (Camp 1) Brisbane River
153.085	-27.5707	MacGregor, Freesia Street
153.3535	-27.6114	Macleay Island

152.7137	-25.556	Maryborough, Little Tinana Ck
153.107	-26.6824	Mooloolaba, Goonawarra Drive
153.1983	-27.737	Mount Warren Park - Yvonne Cr.
153.3459	-28.0856	Mudgeeraba, Burke Crescent
153.363	-28.1048	Mudgeeraba, Hardys Road/Appaloosa Crt
153.402	-27.499	North Stradbroke Island, Dunwich (Mitchell Cres.)
153.5276	-27.427	North Stradbroke Island, Point Lookout
153.4789	-28.126	Palm Beach, M1
153.0337	-27.6303	Parkinson, Avondale Crescent
151.813	-28.554	Passchendaele SF
152.8873	-26.8232	Peachester
151.6388	-27.7085	Pittsworth, Int. Campbell St and Perham St
152.8802	-27.5996	Redbank (Pan Pacific Peace Garden)
153.3085	-27.6421	Redland Bay, Junee Street Wetlands
153.3068	-27.6209	Redland Bay, Weinam Creek Wetlands (Moores Rd)
152.9759	-26.3279	Ringtail Creek, Tronson Road
152.8405	-27.3761	Samford, Days Road
153.1028	-27.2029	Scarborough, Sunnyside Rd
153.4033	-27.9581	Southport, Loders Creek
153.0524	-27.5826	Sunnybank (Les Atkinson Park)
152.9753	-26.6109	Parklands, Tallangatta Street
153.1935	-27.9237	Tamborine NP (Joalah Sec)
152.9926	-25.9175	Tin Can Bay, Snapper Point
152.9276	-27.0823	Wararba Creek - Colburn way
151.9949	-24.6942	Watalgan SF, Arthur's Ck Rd
153.2355	-27.4952	Wellington Point, Crossley Drive
153.0745	-26.4081	Weyba Creek
152.6895	-27.6572	Willowbank
152.0461	-25.5115	Woocoo NP, Aramara
152.7763	-26.9503	Woodford
153.1725	-27.4378	Wynnum Creek

A1.4 List of Temporary Occupied Roosting Sites in the Study Area

Table A1.4: List of temporary occupied roosting sites in the study area (Source: EHP 2014).

Longitude	Latitude	Name
153.2097	-27.5165	Alexandra Hills, Lawn Terrace
152.616	-26.3607	Amamoor State Forest
152.4689	-24.8316	Bargara, Larder Street
152.5734	-25.1733	Burrum River (lower), Big Shaggy Island
152.3737	-25.2258	Childers (Mango Hill)
152.8264	-26.3375	Cooran - Yellow Belly Reserve
151.2595	-27.1899	Dalby, Wood Street
152.6259	-25.9274	Glenwood Varley Road
150.2869	-28.5383	Goondiwindi (Macintyre River) Sandlewood St.
151.0736	-28.416	Inglewood, Frey Street
152.9275	-26.2886	Kinmond Creek, Cootharaba Road
152.834	-28.0834	Kooralbyn (Routley Drive)
152.3948	-27.6206	Laidley, Laidley Plainlands Road
153.0712	-26.6508	Maroochydore, Stella Maris CS
152.7224	-25.4734	Maryborough, Saltwater Creek
151.0231	-24.7532	Monto
153.3242	-28.003	Nerang, Gilston Road
153.0699	-26.392	Noosaville, Goat Island CP
153.037	-27.68	Regents Park, Emerald Drive
153.412	-28.0629	Robina, Kiralee Dr
152.9419	-27.4443	The Gap, Riaweena St
153.1367	-26.7881	Tooway Creek
151.943	-27.601	Toowoomba, Spring Street
153.3044	-27.5801	Victoria Point, Marianne St/Egret Drive.
153.1592	-27.079	Bongaree, Shirley Creek
153.1773	-27.667	Loganholme, Timor Avenue
153.3624	-28.0179	Carrara, Edelsten Court
152.9631	-27.8147	Undullah, Homestead Drive (Flagstone)
153.4272	-27.9842	Surfers Paradise, Macintosh Island
153.073	-27.3987	Northgate reserve
152.9553	-27.1605	Burpengary Equestrian
153.3916	-28.0332	Carrara, Gooding Drive
151.7204	-27.4356	Oakey - Campbell St
151.857	-28.2677	Warwick, Rockland Rd
152.7199	-26.7276	Conondale, Herron Rd
153.3973	-27.9481	Labrador, Government Rd

152.8127	-27.6124	Bundamba, Paice St
152.9456	-27.4055	Ferny Hills, Kylie Ave
153.0855	-26.5328	Coolum, Cassia Wildlife Corridor
153.0376	-27.4376	Windsor, Enoggera Creek
152.5687	-26.9415	Kilcoy, Kilcoy Creek (Anzac Park)
153.0125	-27.8746	Cedar Vale, Banksia Court
153.4238	-28.0681	Miami, Pizzey Drive
153.1963	-27.709	Beenleigh, Lincoln St
152.2784	-26.8413	Linville, John Street
152.9929	-27.491	Toowong Perrin Park, Josling St
151.6349	-27.7125	Pittsworth, 1 Thomas Street
152.1227	-27.5483	Helidon, Gunn Street
153.1424	-27.0578	Bellara, Warrigal Street

A1.5 List of Temporary Unoccupied Roosting Sites in the Study Area

Table A1.5: List of temporary unoccupied roosting sites in the study area (Source: EHP 2014).

Longitude	Latitude	Name
151.9847	-28.0314	Allora (Dalrymple Park Reserve)
153.3809	-27.9479	Arundal, Biggera Creek
152.0364	-24.5105	Baffle Estuary, Baffle Creek
153.0365	-27.6212	Calamvale, Earnshaw St.
153.3596	-28.0066	Carrara, Nerang Broadbeach Road
152.0978	-28.3992	Cherry Gully, Warwick
150.5813	-26.8012	Chinchilla
153.4223	-28.1865	Coolamon, Currumbin Valley (Nicolls Scrub)
153.0866	-26.5485	Coolum, Hyatt
153.2167	-27.7	Eagleby, Dreyer Road (Carbrook Golf Course)
152.9145	-26.4721	Eerwah Vale
151.6622	-25.5859	Gayndah, Brambah Ck
152.9028	-27.6049	Goodna, Woogaroo Creek
152.778	-26.0485	Goomboorian, Anderleigh Rd Ginger Creek
150.2876	-28.5373	Goondiwindi (Macintyre River) Cairns St.
152.4102	-27.6381	Laidley (Whites Road)
153.1876	-27.7015	Loganholme, Alexander Clark Park
152.7185	-25.5097	Maryborough, Albion Rd Wetlands (Island Plantation
152.7131	-25.5436	Maryborough, Kent Street
152.8185	-27.827	Mount Elliot
152.9737	-26.6113	Nambour, Tallangatta St.
153.3226	-27.9885	Nerang, Bushmead Street
153.3157	-28.0039	Nerang, Riverpark Dr.
153.3138	-28.0025	Nerang, Winchester Dr.
153.2429	-27.7758	Ormeau, Carob Court
152.9726	-26.6073	Parklands, Nambour Bypass (SC)
153.0687	-25.9763	Rainbow Beach, Seary's Creek
153.3038	-27.6166	Redland Bay, Pitt St
153.0481	-27.67	Regents Park - Bennets Drive
153.3888	-27.7037	Russell Island
151.9311	-28.6519	Stanthorpe (Gleason Park - Quart Pot Ck)
152.7692	-25.3749	Sunshine Acres, Black Swamp Creek
153.4448	-28.1144	Tallebudgera Creek
152.6789	-25.5404	Tinana, Franklins Close
151.9315	-27.6009	Toowoomba (Japanese Gardens/University)
151.9972	-27.5633	Toowoomba (Redwood Park)
152.0296	-28.2081	Warwick - Dragon Street

151.9714	-27.5257	Withcott
153.3432	-28.0619	Worongary, Worongary Road
153.157	-27.4338	Wynnum North, Meilandt Street
150.6229	-26.7506	Chinchilla, Dorney Street
152.87	-25.61	Boonaroo Point, Maroom
153.4193	-28.0093	Surfers Paradise, Girung Island
152.954	-26.691	Palmwoods, Dunning Street
152.7912	-27.568	Chuwar, Brodzig Road
152.8742	-25.6133	maaroom, Esplanade
152.7501	-25.2749	Dundowran, Jimilee Street
152.7122	-25.5609	Maryborough, Tinana Island,

A1.6 List of Abandoned Roosting Sites in the Study Area

Table A1.6: List of abandoned roosting sites in the study area (Source: EHP 2014).

Longitude	Latitude	Name
153.2253	-27.5112	Birkdale, Birkdale Tip
151.889	-28.7226	Glen Aplin Caravan Park
150.3058	-28.5431	Goondiwindi, Herbert Street
152.3753	-27.7209	Mulgowie
151.3011	-25.5845	Mundubbera Township, Jones' Weir
152.7566	-25.9983	Neerdie, Power St.
153.07	-25.8172	Rainbow Beach, Inskip Peninsula
152.8665	-28.2149	Rathdowney, John Street
153.3101	-27.6247	Redland Bay, Orchard Beach Wetlands (The Boulevard
152.325	-27.7192	Mount Berryman, Scanlans Scrub
152.9802	-25.768	Tin Can Bay, Dinnies Ck
152.0593	-27.4616	Upper Rocky Creek, Murphys Creek
153.0475	-26.6492	Maroochydore, Eudlo Creek CP
151.3085	-27.6951	Brookstead, 1589 Pampas Horrane Rd
152.3857	-27.6402	Laidley (Deborah Rd)

A1.7 List of Destroyed Roosting Sites in the Study Area

Table A1.7: List of destroyed roosting sites in the study area (Source: EHP 2014).

Longitude	Latitude	Name
153.402	-28	Bundall, Gold Coast Turf Club

A1.8 Full Legend of Major Vegetation Groups (MVG)

Legend





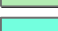
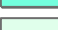






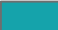
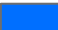

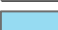




	Rainforest and vine thickets
	Eucalyptus tall open forest
	Eucalyptus open forest
	Eucalyptus low open forest
	Eucalyptus woodlands
	Acacia forests and woodlands
	Callitris forests and woodlands
	Casuarina forests and woodlands
	Melaleuca forests and woodlands
	Other forests and woodlands
	Eucalyptus open woodlands
	Tropical Eucalyptus woodlands/grasslands
	Acacia open woodlands
	Mallee woodlands and shrublands
	Low closed forest and tall closed shrubland
	Acacia shrublands
	Other shrublands
	Heath
	Tussock grasslands
	Hummock grasslands
	Other grasslands, herblands, sedgelands and rushlands
	Chenopod shrublands, samphire shrubs and forblands
	Mangroves
	Inland aquatic - fresh water, salt lakes, lagoons
	Cleared, non-native vegetation, buildings
	Unclassified native vegetation
	Naturally bare -sand, rocks, claypan, mudflat
	Sea and estuaries
	Regrowth, modified native vegetation
	Unclassified Forests
	Other Open Woodlands
	Mallee Open Woodlands and Sparse Shrublands
	Unknown/no data

Figure A1.1: Full legend of MVG (Source: Department of the Environment and Energy 2015).

A1.9 Full Legend of Major Vegetation Subgroups (MVS)

Figure A1.2: Full legend of MVS (Source: Department of the Environment and Energy 2015).

Legend

Major Vegetation Subgroups

■ <-all other values>

Value

- Cool temperate rainforest
- Tropical or sub-tropical rainforest
- Eucalyptus (+/- tall) open forest with a dense broad-leaved and/or tree-fern understorey (wet sclerophyll)
- Eucalyptus open forests with a shrubby understorey
- Eucalyptus open forests with a grassy understorey
- Warm temperate rainforest
- Tropical Eucalyptus forest and woodlands with a tall annual grassy understorey
- Eucalyptus woodlands with a shrubby understorey
- Eucalyptus woodlands with a tussock grass understorey
- Eucalyptus woodlands with a hummock grass understorey
- Tropical mixed spp forests and woodlands
- Callitris forests and woodlands
- Bigalow (Acacia harpophylla) forests and woodlands
- Other Acacia forests and woodlands
- Melaleuca open forests and woodlands
- Other forests and woodlands
- Boulders/rock with algae, lichen or scattered plants, or alpine fieldmarks
- Eucalyptus low open woodlands with hummock grass
- Eucalyptus low open woodlands with tussock grass
- Mulga (Acacia aneura) woodlands +/- tussock grass +/- forbs
- Other Acacia tall open shrublands and [tall] shrublands
- Acacia (+/- low) open woodlands and shrublands with chenopods
- Acacia (+/- low) open woodlands and shrublands with hummock grass
- Acacia (+/- low) open woodlands and shrublands +/- tussock grass
- Acacia (+/- low) open woodlands and sparse shrublands with a shrubby understorey
- Casuarina and Allocasuarina forests and woodlands
- Mallee with hummock grass
- Low closed forest or tall closed shrublands (including Acacia, Melaleuca and Banksia)
- Mallee with a dense shrubby understorey
- Heath
- Saltbush and Bluebush shrublands
- Other shrublands
- Hummock grasslands
- Mitchell grass (Astrebla) tussock grasslands
- Blue grass (Dicanthium) and tall bunch grass (Nivveria syn: Chrysopogon) tussock grasslands
- Temperate tussock grasslands
- Other tussock grasslands
- Wet tussock grassland with herbs, sedges or rushes, herblands or ferns
- Mixed chenopod, samphire +/- forbs
- Mangroves
- Saline or brackish sedgeland or grasslands
- Naturally bare, sand, rock, claypan, mudflat
- Salt lakes and lagoons
- Freshwater, dams, lakes, lagoons or aquatic plants
- Mulga (Acacia aneura) open woodlands and sparse shrublands +/- tussock grass
- Sea, estuaries (includes seagrass)
- Eucalyptus open woodlands with shrubby understorey
- Eucalyptus open woodlands with a grassy understorey
- Melaleuca shrublands and open shrublands
- Banksia woodlands
- Mulga (Acacia aneura) woodlands and shrublands with hummock grass
- Mulga (Acacia aneura) open woodlands and sparse shrublands with hummock grass
- Eucalyptus low open woodlands with a shrubby understorey
- Eucalyptus tall open forest with a fine-leaved shrubby understorey
- Mallee with an open shrubby understorey
- Eucalyptus (+/- low) open woodlands with a chenopod or samphire understorey
- Lignum shrublands and wetlands
- Leptospermum forests
- Eucalyptus woodlands with ferns, herbs, sedges, rushes or wet tussock grassland
- Eucalyptus tall open forests and open forests with ferns, herbs, sedges, rushes or wet tussock grasses
- Mallee with a tussock grass understorey
- Dry rainforest or vine thickets
- Sedgeland, rushes or reeds
- Other grasslands
- Eucalyptus woodlands with chenopod or samphire understorey
- Open mallee woodlands and sparse mallee shrublands with an open hummock grass understorey
- Open mallee woodlands and sparse mallee shrublands with an open tussock grass understorey
- Open mallee woodlands and sparse mallee shrublands with an open open shrubby understorey
- Open mallee woodlands and sparse mallee shrublands with an open dense shrubby understorey
- Callitris open woodlands
- Casuarina and Allocasuarina open woodlands with a tussock grass understorey
- Casuarina and Allocasuarina open woodlands with a hummock grass understorey
- Casuarina and Allocasuarina open woodlands with a chenopod shrub understorey
- Casuarina and Allocasuarina open woodlands with a shrubby understorey
- Melaleuca open woodlands
- Other open woodlands
- Other sparse shrublands and sparse heathlands
- Regrowth or modified forests and woodlands
- Regrowth or modified shrublands
- Regrowth or modified graminoids
- Unclassified forest
- Unclassified native vegetation
- Cleared, non-native vegetation, buildings
- Unknown/No data

A1.10 List of MVG in the Study Area

Table A1.8: List of MVG in the study area.

VALUE	COUNT	MVG_NAME	MVG_COMMON
1	105669	Rainforests and Vine Thickets	rainforests
2	39389	Eucalypt Tall Open Forests	tall eucalypt forests (trees taller than 30 m)
3	419230	Eucalypt Open Forests	eucalypt forests (trees 10 to 30 m tall)
5	153680	Eucalypt Woodlands	eucalypt woodlands (tree crowns not touching)
6	928	Acacia Forests and Woodlands	acacia forests and woodlands
8	3802	Casuarina Forests and Woodlands	she-oak forests and woodlands
9	26880	Melaleuca Forests and Woodlands	paperbark forests and woodlands
10	443	Other Forests and Woodlands	other forests and woodlands
11	48	Eucalypt Open Woodlands	sparse eucalypt woodlands
15	12148	Low Closed Forests and Tall Closed Shrublands	tall dense thickets
17	39	Other Shrublands	other shrublands
18	9349	Heathlands	heathlands (low, dense, fine-leaved shrublands)
21	12066	Other Grasslands, Herblands, Sedgeland and Rushlands	swampy grasses, sedges, etc.
23	14503	Mangroves	mangroves
24	25727	Inland aquatic - freshwater, salt lakes, lagoons	water
25	1395168	Cleared, non-native vegetation, buildings	cleared vegetation
27	1152	Naturally bare - sand, rock, claypan, mudflat	naturally bare
28	10564	Sea and estuaries	sea
31	35	Other Open Woodlands	other sparse woodlands
99	77	Unknown/no data	unknown

A1.11 List of MVS in the Study Area

Table A1.9: List of MVS in the study area.

VALUE	COUNT	MVS_NAME
1	739	Cool temperate rainforest
2	91553	Tropical or sub-tropical rainforest
3	15836	Eucalyptus (+/- tall) open forest with a dense broad-leaved and/or tree-fern understorey (wet sclerophyll)
4	157648	Eucalyptus open forests with a shrubby understorey
5	227628	Eucalyptus open forests with a grassy understorey
6	7452	Warm Temperate Rainforest
8	11450	Eucalyptus woodlands with a shrubby understorey
9	142246	Eucalyptus woodlands with a tussock grass understorey
13	928	Brigalow (<i>Acacia harpophylla</i>) forests and woodlands
15	26903	Melaleuca open forests and woodlands
26	3911	Casuarina and Allocasuarina forests and woodlands
28	12149	Low closed forest or tall closed shrublands (including <i>Acacia</i> , <i>Melaleuca</i> and <i>Banksia</i>)
30	9350	Heathlands
32	45	Other shrublands
40	15232	Mangroves
41	4892	Saline or brackish sedgeland or grasslands
42	1272	Naturally bare, sand, rock, claypan, mudflat
44	25775	Freshwater, dams, lakes, lagoons or aquatic plants
46	61360	Sea, estuaries (includes seagrass)
48	48	Eucalyptus open woodlands with a grassy understorey
50	443	<i>Banksia</i> woodlands
54	346	Eucalyptus tall open forest with a fine-leaved shrubby understorey
60	57246	Eucalyptus tall open forests and open forests with ferns, herbs, sedges, rushes or wet tussock grasses
62	6135	Dry rainforest or vine thickets
63	7321	Sedgeland, rushes or reeds
79	35	Other open woodlands
98	1395023	Cleared, non-native vegetation, buildings
99	90	Unknown/No data

A1.12 Data statistics calculated in the Study

Table A1.10: Statistics calculated in the study of HeV dispersal (Main Source: Queensland Centre for Emerging Infectious Diseases 2014).

Longitude	Latitude	HeV Events	ff_per	b_per	g_per	l_per	Inci_rate	Avg_dist	Avg_preg
153.0115	-28.2192	1	0.00149	0.000403	0.00329	0	0.013549	50	2.1
153.363	-28.1048	1	0.005589	0.006804	0.00754	0	0.05081	50	2.45
153.3459	-28.0856	1	0.046576	0.100796	0.022849	0	0.423417	50	2.8
152.834	-28.0834	1	1.024669	0	0	4.601967	9.315173	30	2
153.4238	-28.0681	1	0.000466	0.00126	0	0	0.004234	50	3
153.412	-28.0629	1	0.013041	0.030239	0	0.008367	0.118557	47.14286	2.857143
153.1824	-28.0398	3	8.212219	7.624751	13.22101	0.016734	223.9696	49.99093	2.343221
153.3916	-28.0332	1	0.382295	0.792255	0.219355	0	3.475406	50	2.766082
153.3624	-28.0179	1	0.557979	0.851221	0.596827	0	5.072535	50	2.56394
153.3242	-28.003	1	0.115322	0.249974	0.052782	0.006275	1.04838	49.75767	2.801292
152.6085	-28.0009	1	1.191504	1.244073	1.794595	0	10.83185	50	2.385975
153.4272	-27.9842	1	0.005869	0.015069	0.000731	0	0.053351	50	2.949206
153.4033	-27.9581	1	0.324373	0.853237	0.021981	0	2.948845	50	2.972374
153.3973	-27.9481	1	0.004024	0.005241	0.005118	0	0.036583	50	2.481481
153.1935	-27.9237	1	0.235767	0.081897	0.499489	0.008367	2.143337	49.84196	2.128408
153.3343	-27.9012	1	7.010972	9.888575	7.882601	0.637582	63.73611	49.59503	2.521391
153.0125	-27.8746	3	0.517924	0.600743	0.716559	0.016734	14.12519	49.85612	2.428777
152.98	-27.8558	3	1.667416	2.06319	1.624001	1.08983	45.47498	47.08939	2.457408
152.9631	-27.8147	2	0.050116	0.012096	0.111962	0	0.911193	50	2.089219
153.1983	-27.737	3	1.610221	3.075029	1.159152	0.004184	43.91511	49.98843	2.705947
153.1963	-27.709	3	0.291938	0.760253	0.026734	0	7.961932	50	2.962668
153.037	-27.68	2	2.822497	2.133596	0.921518	7.44682	51.31813	38.25083	2.279439
153.1773	-27.667	3	0.302743	0.447534	0.180054	0.286995	8.25663	45.77846	2.546462
152.6895	-27.6572	1	0.002608	0.007056	0	0	0.023711	50	3
153.3085	-27.6421	1	1.331511	1.12085	0.367876	3.445619	12.10464	38.47628	2.31118

152.9206	-27.6315	2	3.459841	3.311748	4.642916	1.539567	62.90621	48.01842	2.353842
153.0337	-27.6303	2	3.739203	1.946116	7.09658	0.568971	67.98552	49.32239	2.192397
153.3753	-27.6274	1	0.27014	0.636022	0.085914	0	2.455818	50	2.870345
153.3068	-27.6209	1	0.752387	1.28807	0.677577	0	6.839877	50	2.632859
152.3948	-27.6206	1	0.415457	0.74095	0.250521	0.17705	3.776879	48.10224	2.659283
152.9479	-27.6142	2	0.415457	0.74095	0.250521	0.17705	7.553758	48.10224	2.659283
152.8127	-27.6124	1	0.049762	0.115109	0.017685	0	0.452379	50	2.85511
153.3535	-27.6114	1	0.000373	0.001008	0	0	0.003387	50	3
152.8802	-27.5996	1	0.123352	0.287268	0.037519	0.008367	1.121377	49.69793	2.860897
153.0524	-27.5826	2	0.087246	0.151496	0.076637	0	1.586289	50	2.641896
153.3044	-27.5801	1	0.884662	1.625938	0.67511	0.037652	8.042381	49.81047	2.679415
153.3312	-27.5724	1	0.14582	0.110019	0.257925	0	1.325634	50	2.278906
153.085	-27.5707	1	1.019266	2.125784	0.572607	0	9.266056	50	2.770974
152.1227	-27.5483	1	2.808692	0.013053	0	12.59266	25.53357	30.03436	2.001718
153.2097	-27.5165	1	0.804831	1.422229	0.684569	0	7.316645	50	2.653241
152.9886	-27.5157	1	2.817001	4.955526	2.260313	0.285824	25.6091	49.54816	2.650296
153.2263	-27.5026	1	0.879539	2.358119	0.019194	0	7.995806	50	2.991104
153.402	-27.499	1	0.717082	1.069645	0.688225	0.184581	6.518927	48.85373	2.551416
153.2355	-27.4952	1	0.149266	0.39774	0.005484	0	1.356967	50	2.985022
152.9929	-27.491	1	0.090543	0.160769	0.076317	0	0.823123	50	2.656379
152.5886	-27.4688	1	3.541815	4.5786	3.892906	1.177685	32.19832	48.51928	2.477876
152.5903	-27.4657	1	0.558445	0.698969	0.371121	0.668122	5.076769	44.67223	2.462686
152.9419	-27.4443	1	0.253634	0.117074	0.515986	0	2.305759	50	2.170633
153.0226	-27.4424	1	0.116999	0.262876	0.048624	0	1.063623	50	2.830573
153.1725	-27.4378	1	0.011961	0.032355	0	0	0.108733	50	3
153.0376	-27.4376	1	0.4652	1.258436	0	0	4.229088	50	3
152.9456	-27.4055	1	0.869106	0.587136	1.599461	0	7.90096	50	2.249732
153.073	-27.3987	1	0.267811	0.699271	0.022849	0	2.434647	50	2.965217
152.8405	-27.3761	1	2.687781	2.045349	4.738289	0	24.43438	50	2.281308
152.8316	-27.2069	1	1.660895	0.950505	3.139057	0.133875	15.09905	49.64105	2.211554

153.1028	-27.2029	2	0.082327	0.222708	0	0	1.496864	50	3
152.8254	-27.1971	1	2.522549	2.190041	4.201784	0	22.93226	50	2.320938
152.9553	-27.1605	1	0.286013	0.482056	0.173062	0.167344	2.600119	47.39448	2.623046
152.9714	-27.1527	1	0.11303	0.209504	0.087285	0	1.027548	50	2.685182
152.9276	-27.0823	1	3.175859	2.378126	3.417363	4.058099	28.87145	44.30975	2.27681
153.1592	-27.079	1	0.167673	0.050398	0	0.669377	1.524301	32.22222	2.111111
153.1424	-27.0578	1	0.011625	0.029886	0.001417	0	0.105685	50	2.950321
152.7763	-26.9503	1	5.083811	3.074878	6.761105	5.348072	46.21647	45.31534	2.223587
152.5687	-26.9415	1	0.139728	0.307427	0.063978	0	1.270251	50	2.813333
152.2784	-26.8413	1	0.027387	0.05443	0.017823	0	0.248969	50	2.734694
152.8873	-26.8232	1	0.612938	0.34321	1.192284	0	5.572167	50	2.206991
152.9654	-26.7997	1	0.964847	0.551756	1.86456	0.003347	8.771336	49.98455	2.211396
153.1367	-26.7881	1	0.537672	0.802234	0.362941	0.418361	4.887925	46.535	2.551559
152.7199	-26.7276	1	0.279455	0.665253	0.082258	0	2.540502	50	2.88
153.107	-26.6824	1	0.101591	0.113043	0.032629	0.208846	0.923557	40.84541	2.411333
153.0712	-26.6508	1	4.551393	5.315468	6.337522	0.012551	41.3763	49.98772	2.431723
152.9753	-26.6109	1	1.656424	2.179962	2.086383	0	15.0584	50	2.486503
153.0855	-26.5328	1	0.255236	0.514059	0.159946	0	2.320325	50	2.744526
153.0745	-26.4081	1	1.05839	0.445014	0.243118	3.569453	9.621727	34.98152	2.15543
153.0699	-26.392	1	0.037261	0.080637	0.01828	0	0.338734	50	2.8
152.8264	-26.3375	1	0.290577	0.380958	0.367328	0	2.641614	50	2.484644
152.9759	-26.3279	1	0.037261	0.06718	0.030481	0	0.338734	50	2.6665
152.9275	-26.2886	1	0.566735	0.161173	1.244015	0	5.152137	50	2.105128
153.0491	-26.4007	1	8.708047	0.11783	0	38.91373	79.16406	30.10004	2.005002
153.1373	-27.6402	1	0.931517	1.511938	0.913978	0	8.468339	50	2.6
152.9268	-27.0816	3	0.931517	0.100796	0.091398	3.848918	25.40502	31.6	2.04
152.7763	-26.9503	1	0.931517	0.403183	0.091398	3.346885	8.468339	34	2.16
152.4233	-27.2349	1	0.931517	0.503979	1.028225	1.464262	8.468339	43	2.2
153.4277	-28.0222	1	0.001118	0	0.002742	0	0.010162	50	2
153.4448	-28.1144	1	0.100604	0.201592	0.063978	0	0.914581	50	2.740741

153.4136	-27.9797	1	0.01863	0	0.045699	0	0.169367	50	2
152.6799	-27.9919	1	0.027946	0.030239	0.041129	0	0.25405	50	2.4
152.3753	-27.7209	1	0.149043	0	0.365591	0	1.354934	50	2
152.8185	-27.827	1	0.083837	0	0.205645	0	0.76215	50	2
152.8405	-27.3761	1	0.010098	0.019101	0.007449	0	0.091797	50	2.699262
153.1279	-27.0804	1	0.419183	0.340186	0.719758	0	3.810752	50	2.3
152.9943	-27.3111	1	0.074521	0.075597	0.114247	0	0.677467	50	2.375
152.6799	-27.9919	1	0.149043	0.302388	0.091398	0	1.354934	50	2.75
153.4277	-28.0222	1	0.232879	0.566977	0.057124	0	2.117085	50	2.9
153.4292	-28.0946	1	0.279455	0.680372	0.068548	0	2.540502	50	2.9
153.258	-27.5275	1	0.014904	0.040318	0	0	0.135493	50	3
153.3812	-27.8883	1	0.046576	0.100796	0.022849	0	0.423417	50	2.8
153.4672	-28.1453	1	0.009315	0.015119	0.00914	0	0.084683	50	2.6
153.0519	-27.4841	1	0.02761	0.053775	0.018965	0	0.251002	50	2.719973
152.4233	-27.2349	1	0.065206	0.123475	0.047984	0	0.592784	50	2.7
153.1136	-27.444	1	0.093152	0.125995	0.114247	0	0.846834	50	2.5
153.1437	-27.445	2	0.027014	0.054833	0.016543	0	0.491164	50	2.750345
153.1837	-27.4641	1	0.026138	0.069297	0.00128	0	0.237622	50	2.980043
152.9255	-27.5444	1	0.093152	0.125995	0.114247	0	0.846834	50	2.5
152.7222	-27.4939	1	0.01863	0.050398	0	0	0.169367	50	3
153.0988	-27.2315	2	0.279455	0.100796	0.594086	0	5.081003	50	2.133333
153.0687	-27.3231	1	0.013041	0.020159	0	0.025102	0.118557	41.42857	2.571429
153.1279	-27.0804	1	0.093152	0.125995	0.114247	0	0.846834	50	2.5
153.1373	-27.6402	3	0.139728	0.226791	0.034274	0.188262	3.810752	44	2.6
153.4134	-27.9951	1	0.139728	0.226791	0.034274	0.188262	1.270251	44	2.6
153.4136	-27.9797	1	0.015929	0	0.039073	0	0.144809	50	2
152.9992	-27.412	1	0.037261	0.085676	0.01371	0	0.338734	50	2.85
153.2767	-28.2174	1	0.048159	0.097722	0.029521	0	0.437813	50	2.750097
153.1363	-27.61	2	0.020493	0.055438	0	0	0.372607	50	3
152.926	-27.0809	1	0.037261	0.100796	0	0	0.338734	50	3

152.7485	-27.6031	1	0.014159	0.038302	0	0	0.128719	50	3
152.7556	-27.6514	1	0.014904	0.036287	0.003656	0	0.135493	50	2.9
152.2726	-27.5648	1	0.057903	0.155074	0.001417	0	0.526392	50	2.990026
152.9206	-27.6315	1	0.093152	0.226791	0.022849	0	0.846834	50	2.9
152.7485	-27.6031	1	0.009315	0.025199	0	0	0.084683	50	3
152.9028	-27.6049	2	0.124078	0.26852	0.060871	0	2.255965	50	2.8
152.8802	-27.5996	1	0.000932	0.00252	0	0	0.008468	50	3
152.9028	-27.6049	2	0.007452	0.01008	0.00914	0	0.135493	50	2.5
152.3948	-27.6206	1	0.023661	0.061485	0.002285	0	0.215096	50	2.96063
152.2726	-27.5648	1	0.060176	0.089708	0.066263	0	0.547055	50	2.551084
152.1227	-27.5483	1	0.242194	0	0	1.087738	2.201768	30	2
153.1876	-27.7015	3	0.093152	0.25199	0	0	2.540502	50	3
153.0481	-27.67	2	0.074521	0.120955	0.01828	0.100407	1.354934	44	2.6
153.1983	-27.737	3	0.027946	0.075597	0	0	0.76215	50	3
153.0988	-27.2315	2	0.186303	0.050398	0.41129	0	3.387336	50	2.1
153.046	-26.3944	1	0.037261	0.080637	0.01828	0	0.338734	50	2.8
153.0491	-26.4007	1	0.055891	0.105836	0.034274	0.012551	0.5081	49	2.7
153.3535	-27.6114	1	0.014904	0.008064	0.029247	0	0.135493	50	2.2
153.258	-27.5275	1	0.046576	0.125995	0	0	0.423417	50	3
153.3044	-27.5801	1	0.025151	0.040822	0.024677	0	0.228645	50	2.6
153.1824	-28.0398	3	0.040987	0.033263	0.070376	0	1.117821	50	2.3
152.6799	-27.9919	1	0.006539	0.017639	4.57E-05	0	0.059448	50	2.997151
152.5903	-27.4657	1	0.034	0.03679	0.05004	0	0.309094	50	2.4
152.5886	-27.4688	1	0.037261	0.080637	0.01828	0	0.338734	50	2.8
152.5687	-26.9415	1	0.093152	0.201592	0.045699	0	0.846834	50	2.8
152.9145	-26.4721	1	0.01863	0.000504	0.045242	0	0.169367	50	2.01
152.9726	-26.6073	1	0.046576	0.062997	0.057124	0	0.423417	50	2.5
152.9654	-26.7997	1	0.030367	0.004082	0.070788	0	0.276068	50	2.049693
152.9753	-26.6109	1	0.065206	0.151194	0.022849	0	0.592784	50	2.857143
152.8264	-26.3375	1	0.003726	0.00504	0.00457	0	0.033873	50	2.5

153.107	-26.6824	1	0.372607	0.503979	0.456989	0	3.387336	50	2.5
153.0855	-26.5328	1	0.027946	0.075597	0	0	0.25405	50	3
152.954	-26.691	1	0.037261	0.070557	0.027419	0	0.338734	50	2.7
153.1136	-27.444	1	0.024219	0.065517	0	0	0.220177	50	3
152.7485	-27.6031	1	0.372607	0.907163	0.091398	0	3.387336	50	2.9
152.9028	-27.6049	1	0.037261	0.090716	0.00914	0	0.338734	50	2.9
153.1963	-27.709	3	0.040987	0	0.100538	0	1.117821	50	2
153.0519	-27.4841	1	0.232879	0.566977	0.057124	0	2.117085	50	2.9
153.2429	-27.7758	1	0.046576	0.113395	0.011425	0	0.423417	50	2.9
153.3343	-27.9012	2	0.093152	0.176393	0.068548	0	1.693668	50	2.7
153.1373	-27.6402	1	0.55891	0.302388	1.096773	0	5.081003	50	2.2
153.0481	-27.67	1	0.260825	0.423343	0.255914	0	2.371135	50	2.6
153.3085	-27.6421	1	0.014904	0.032255	0.007312	0	0.135493	50	2.8
153.1935	-27.9237	1	0.020493	0	0.050269	0	0.186303	50	2
152.4233	-27.2349	1	0.694446	0.375716	0.68137	1.247552	6.313147	42	2.2

Appendix - 2

Regression Model Calibration Results

A2.1 GWR Result of Significant Model 1 (ArcGIS)

GWR2_supp			
	OID	VARIABLE	DEFINITION
▶	0	Bandwidth	0.307129
	1	ResidualSquares	13152.724905
	2	EffectiveNumber	17.060652
	3	Sigma	9.592504
	4	AICc	1189.29804
	5	R2	0.829074
	6	R2Adjusted	0.809869
	7	Dependent Field	0 Inci_rate
	8	Explanatory Field	1 g_per

Figure A2.1: GWR result of the significant model 1 using ArcGIS.

A2.2 GWR Result of Significant Model 1 (GWR4.0 for Spatial Variability)

```

*****
GWR (Geographically weighted regression) result
*****
Bandwidth and geographic ranges
Bandwidth size: 160.000000
Coordinate      Min      Max      Range
-----
X-coord        152.122694  153.467210  1.344516
Y-coord        -28.219245  -26.288550  1.930695

Diagnostic information
Residual sum of squares: 76855.607619
Effective number of parameters (model: trace(S)): 1.753194
Effective number of parameters (variance: trace(S^2)): 1.281134
Degree of freedom (model: n - trace(S)): 158.246806
Degree of freedom (residual: n - 2*trace(S) + trace(S^2)): 157.774746
ML based sigma estimate: 21.916833
unbiased sigma estimate: 22.070849
-2 log-likelihood: 1441.983914
Classic AIC: 1447.488303
AICC: 1447.620572
BIC/MDL: 1455.954855
CV: 490.070498
R square: 0.001225
Adjusted R square: -0.012952

*****
<< Geographically varying (Local) coefficients >>
*****
Estimates of varying coefficients have been saved in the following file.
Listwise output file: c:\users\Mike_Hell\Desktop\vegetationdata\gwr\gwr_L1listwise.csv

Summary statistics for varying (Local) coefficients
Variable      Mean      STD
-----
Intercept     7.795263  0.329167

Variable      Min      Max      Range
-----
Intercept     7.298309  8.315202  1.016893

Variable      Lwr quartile  Median  Upr quartile
-----
Intercept     7.440591     7.929675  8.111941

Variable      Interquartile R  Robust STD
-----
Intercept     0.671349        0.497665
(Note: Robust STD is given by (interquartile range / 1.349) )

*****
GWR ANOVA Table
*****
Source      SS      DF      MS      F
-----
Global Residuals  76949.869  159.000
GWR Improvement  94.262    1.225    76.932
GWR Residuals    76855.608  157.775    487.122  0.157932

*****
Geographical variability tests of local coefficients
*****
Variable      F      DOF for F test  DIFF of Criterion
-----
Intercept     0.257684  0.753  138.247  1.366108

Note: positive value of diff-Criterion (AICC, AIC, BIC/MDL or CV) suggests no spatial variability in terms of model selection criteria.
F test: in case of no spatial variability, the F statistics follows the F distribution of DOF for F test.

*****
Program terminated at 4/04/2017 11:33:46 AM

```

Figure A2.2: GWR result of the significant model 1 using GWR4.0 (Spatial Variability Test).

A2.3 Spatial Autocorrelation Report of the Significant Model 1 Residuals

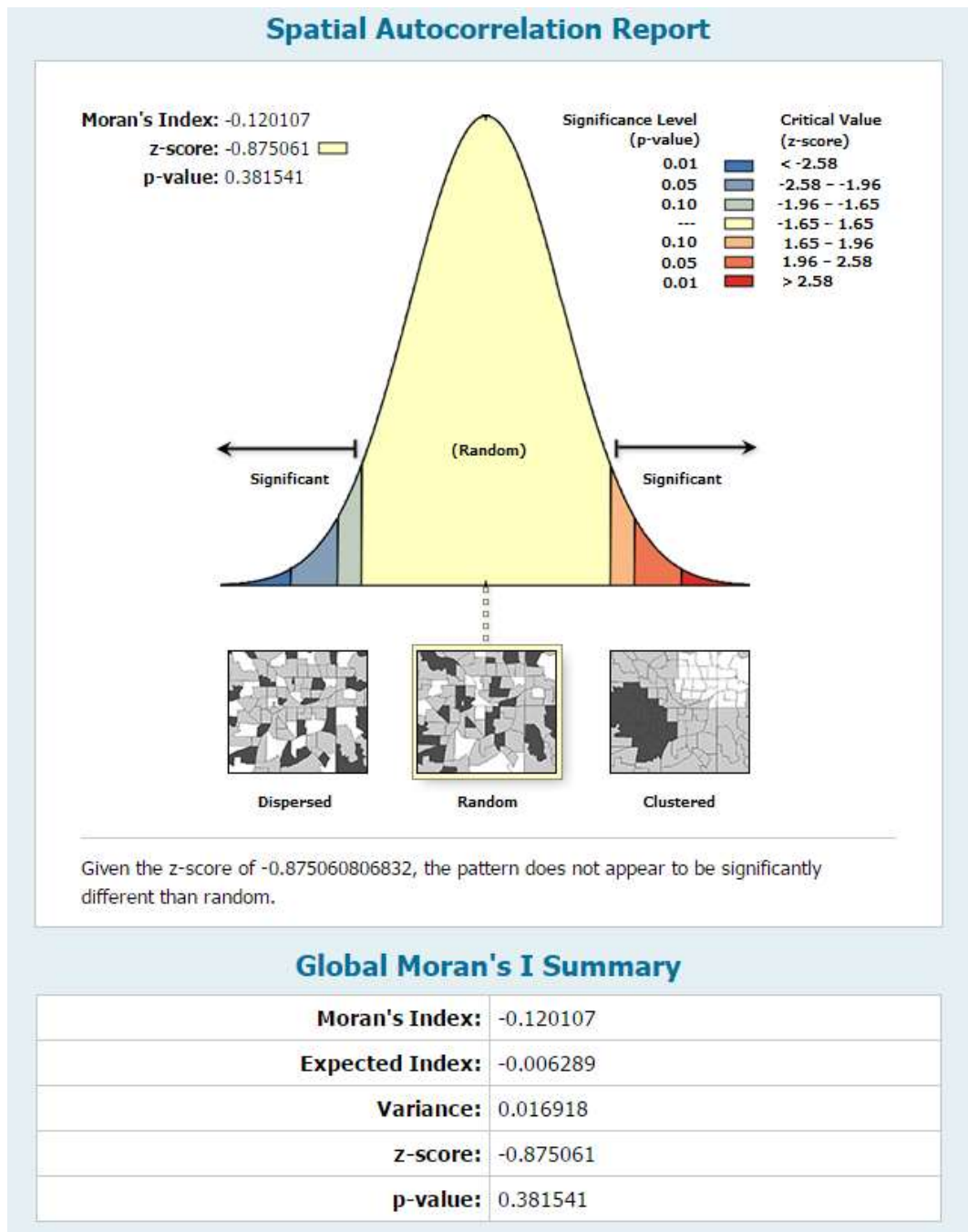


Figure A2.3: Spatial Autocorrelation test of significant model 1 residuals.

A2.4 GWR Result of Significant Model 2 (ArcGIS)

GWR5_supp				
	OID	VARNAME	VARIABLE	DEFINITION
▶	0	Bandwidth	0.307129	
	1	ResidualSquares	10646.168549	
	2	EffectiveNumber	22.024348	
	3	Sigma	8.784063	
	4	AICc	1165.557703	
	5	R2	0.861648	
	6	R2Adjusted	0.840566	
	7	Dependent Field	0	lnci_rate
	8	Explanatory Field	1	b_per
	9	Explanatory Field	2	g_per

Figure A2.4: GWR result of the significant model 2 using ArcGIS.

A2.5 GWR Result of Significant Model 2 (GWR4.0 for Spatial Variability)

```

*****
GWR (Geographically weighted regression) result
*****
Bandwidth and geographic ranges
Bandwidth size: 160.000000
Coordinate      Min      Max      Range
-----
x-coord      152.122694  153.467210  1.344516
y-coord      -28.219245  -26.288550  1.930695

Diagnostic information
Residual sum of squares: 76855.607619
Effective number of parameters (model: trace(S)): 1.753194
Effective number of parameters (variance: trace(S'S)): 1.281134
Degree of freedom (model: n - trace(S)): 158.246806
Degree of freedom (residual: n - 2*trace(S) + trace(S'S)): 157.774746
ML based sigma estimate: 21.916833
Unbiased sigma estimate: 22.070849
-2 log-likelihood: 1441.981914
Classic AIC: 1447.488303
AICC: 1447.620572
BIC/MDL: 1453.954855
CV: 490.070498
R square: 0.001225
Adjusted R square: -0.012952

*****
<< Geographically varying (Local) coefficients >>
*****
Estimates of varying coefficients have been saved in the following file.
Listwise output file: C:\Users\Mike Hell\Desktop\vegetationdata\gwr\gwr_2_listwise.csv

Summary statistics for varying (Local) coefficients
variable      Mean      STD
-----
Intercept      7.795263  0.329167

variable      Min      Max      Range
-----
Intercept      7.298309  8.315202  1.016893

variable      Lwr Quartile  Median  Upr Quartile
-----
Intercept      7.440591  7.929675  8.111941

variable      Interquartile R  Robust STD
-----
Intercept      0.671349  0.497665
(Note: Robust STD is given by (interquartile range / 1.349) )

*****
GWR ANOVA Table
*****
Source      SS      DF      MS      F
-----
Global Residuals  76949.869  159.000
GWR Improvement  94.262  1.225  76.932
GWR Residuals  76855.608  157.775  487.122  0.157932

*****
Geographical variability tests of local coefficients
*****
variable      F      DOF for F test  DIFF of Criterion
-----
Intercept      0.257684  0.753  158.247  1.366108

NOTE: positive value of diff-criterion (AICC, AIC, BIC/MDL or CV) suggests no spatial variability in terms of model selection criteria.
F test: in case of no spatial variability, the F statistics follows the F distribution of DOF for F test.

*****
Program terminated at 4/04/2017 11:30:41 AM
*****

```

Figure A2.5: GWR result of the significant model 2 using GWR4.0 (Spatial Variability Test).

A2.6 Spatial Autocorrelation Report of the Significant Model 2 Residuals

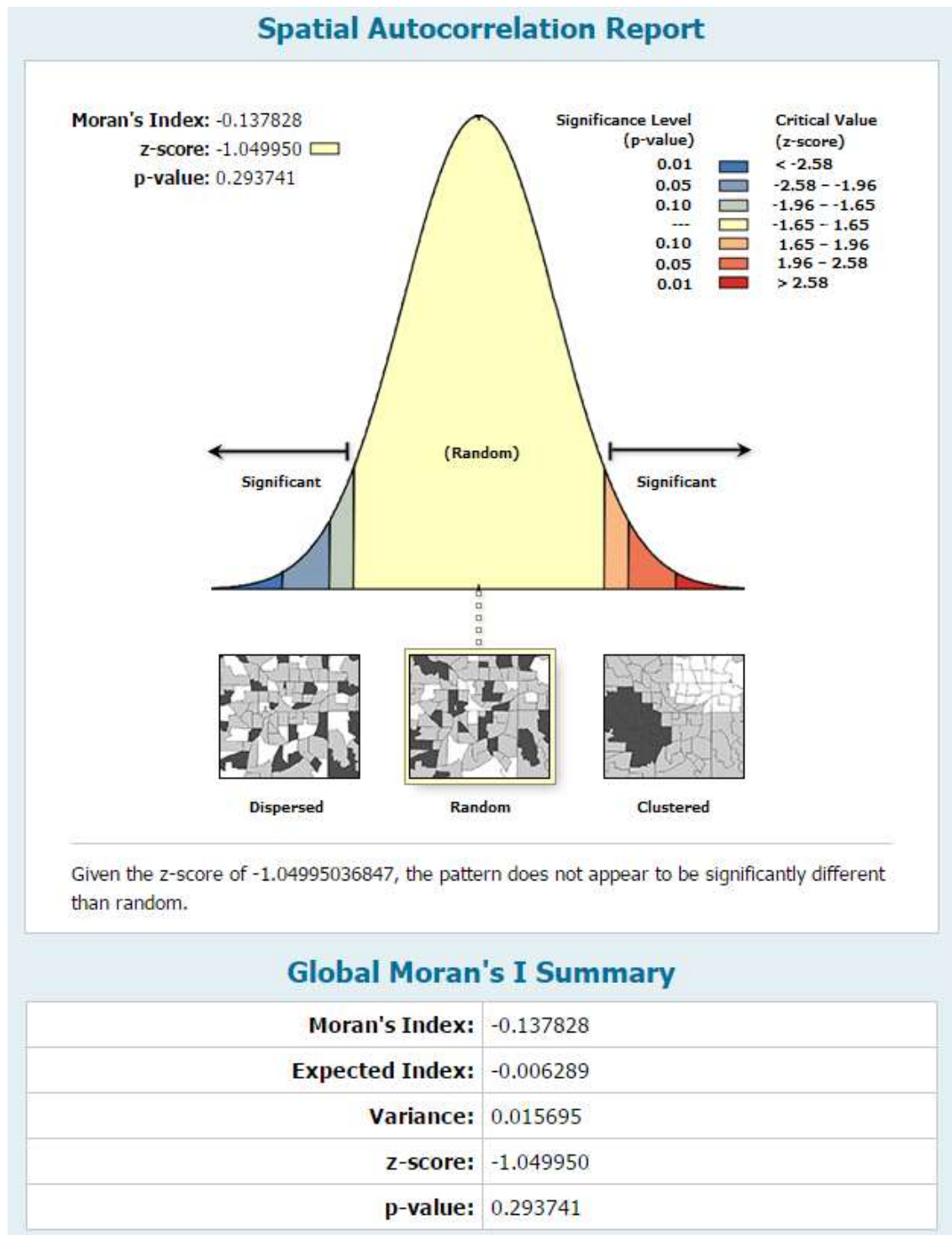


Figure A2.6: Spatial Autocorrelation test of significant model 2 residuals.

A2.7 GWR Result of Significant Model 3 (ArcGIS)

GWR9_supp				
	OID	VARNAME	VARIABLE	DEFINITION
▶	0	Bandwidth	0.322621	
	1	ResidualSquares	8523.058328	
	2	EffectiveNumber	28.821755	
	3	Sigma	8.06059	
	4	AICc	1143.849672	
	5	R2	0.889239	
	6	R2Adjusted	0.865747	
	7	Dependent Field	0	Inci_rate
	8	Explanatory Field	1	b_per
	9	Explanatory Field	2	g_per
	10	Explanatory Field	3	Avg_preg

Figure A2.7: GWR result of the final model using ArcGIS.

A2.8 GWR Result of Significant Model 3 (GWR4.0 for Spatial Variability)

```

*****
GWR (Geographically weighted regression) result
*****
Bandwidth and geographic ranges
Bandwidth size: 54.241546
Coordinate      Min      Max      Range
-----
X-coord        132.122094  153.467210  1.344516
Y-coord        -28.219243  -26.288550  1.930693

Diagnostic information
Residual sum of squares: 7560.016997
Effective number of parameters (model: trace(s)): 25.230016
Effective number of parameters (variance: trace(s's)): 18.292323
Degree of freedom (model: n - trace(s)): 134.769084
Degree of freedom (residual: n - 2*trace(s) + trace(s's)): 127.830401
ML based sigma estimate: 6.873871
Unbiased sigma estimate: 7.690316
-2 log-likelihood: 1070.933115
Classic AIC: 1123.394948
AICC: 1134.134861
BIC/MDL: 1204.059175
CV: 330.416663
R square: 0.901754
Adjusted R square: 0.876833

*****
GWR ANOVA Table
*****
source      SS      DF      MS      F
-----
Global Residuals  22116.428  196.000
GWR Improvement  14556.411  28.170  516.744
GWR Residuals    7560.017  127.830  59.141  8.737491

*****
Geographical variability tests of local coefficients
*****
Variable      F      DOF for F test  DSW of Criterion
-----
Intercept     4.583933  6.893  134.769  -14.786551
perB          18.343303  3.689  134.769  -54.737133
perG          35.094427  3.065  134.769  -85.240322
perK          7.145171  5.597  134.769  -26.075265

Note: positive value of diff-criterion (AICC, AIC, BIC/MDL or CV) suggests no spatial variability in terms of model selection criteria.
F test: in case of no spatial variability, the F statistics follows the F distribution of DOF for F test.
*****
Program terminated at 20/05/2015 8:53:40 AM

```

Figure A2.8: GWR result of the final model using GWR4.0 (Spatial Variability Test).

A2.9 Spatial Autocorrelation Report of the Significant Model 3 Residuals

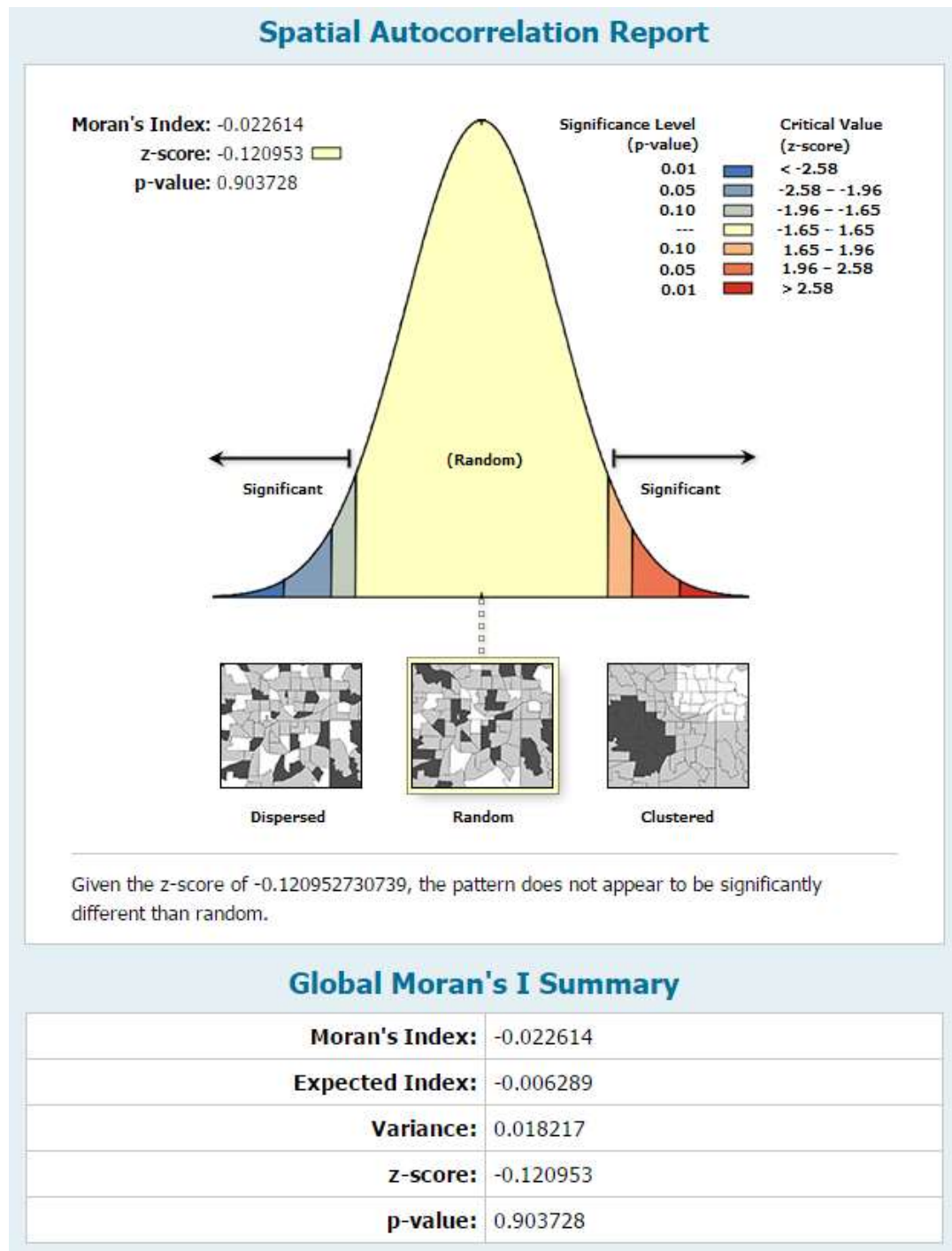
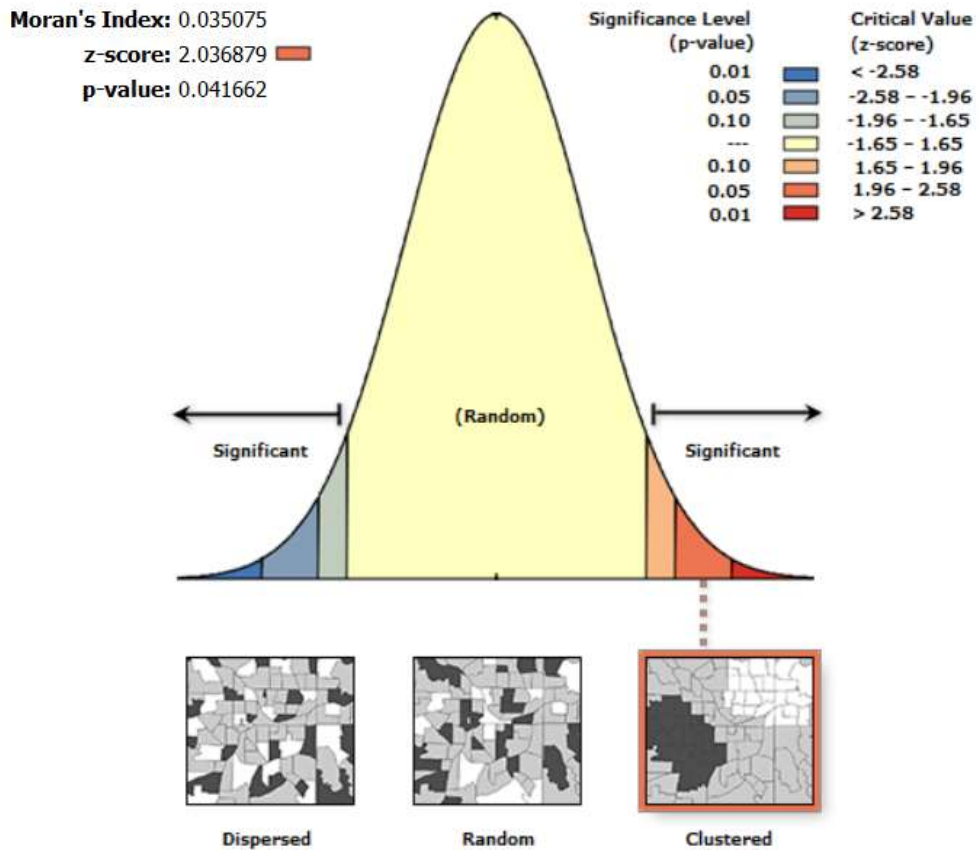


Figure A2.9: Spatial Autocorrelation test of the final model residuals.

Appendix - 3

Spatial Autocorrelation and Regression Analysis

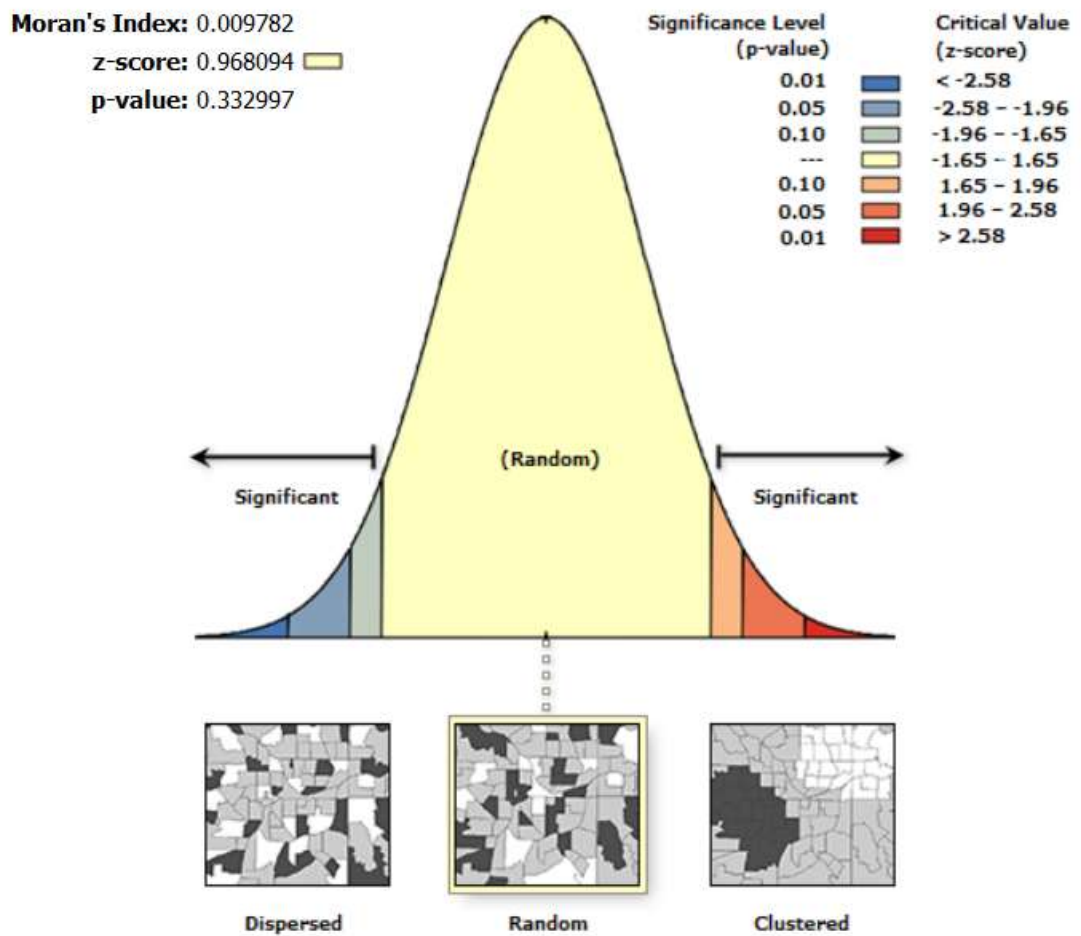
A3.1 Spatial Autocorrelation Report of the Black Flying Foxes at 20 kms



Given the z-score of 2.04, there is a less than 5% likelihood that this clustered pattern could be the result of random chance.

Figure A3.1: Spatial Autocorrelation report of the black flying foxes at their minimum foraging range.

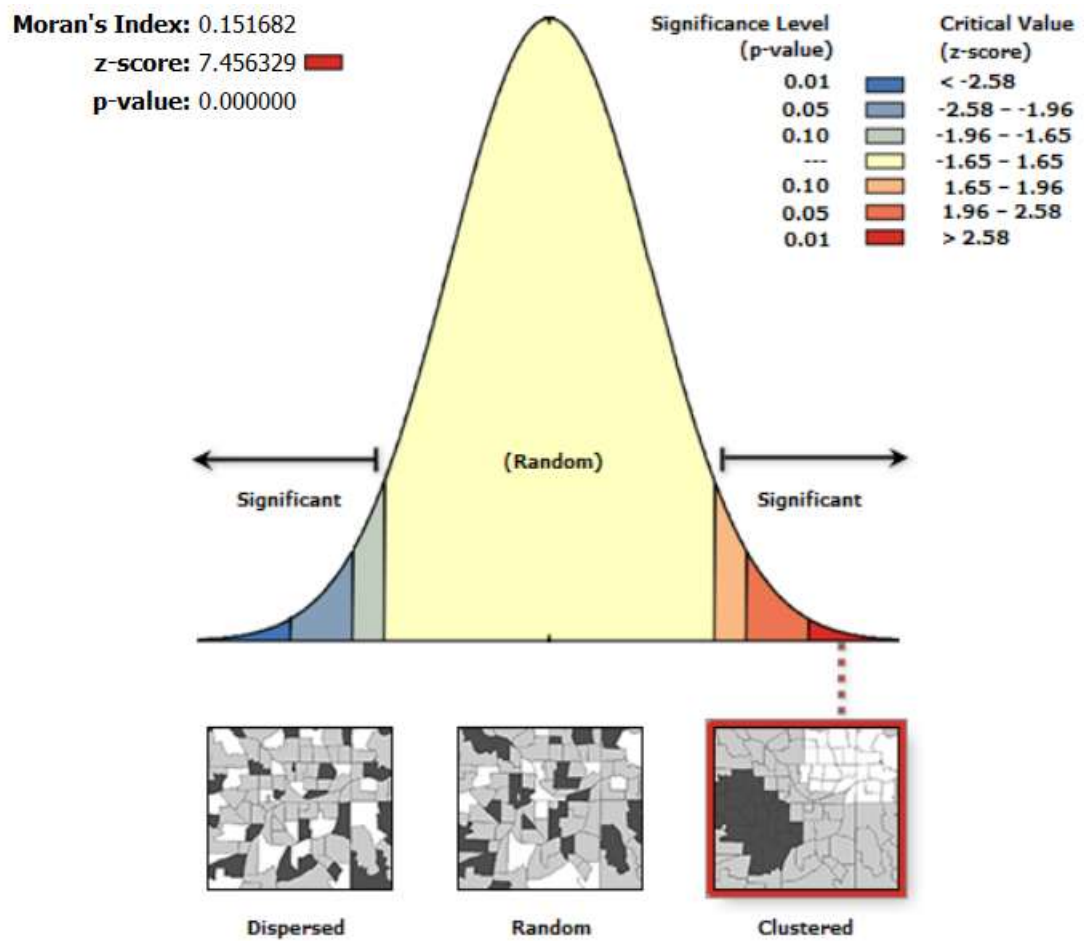
A3.2 Spatial Autocorrelation Report of the Grey-headed Flying Foxes at 20 kms



Given the z-score of 0.97, the pattern does not appear to be significantly different than random.

Figure A3.2: Spatial Autocorrelation report of the grey-headed flying foxes at their minimum foraging range.

A3.3 Spatial Autocorrelation Report of the Little Red Flying Foxes at 20 kms



Given the z-score of 7.46, there is a less than 1% likelihood that this clustered pattern could be the result of random chance.

Figure A3.3: Spatial Autocorrelation report of the little red flying foxes at their minimum foraging range.

A3.4 Summary of the OLS Results

Summary of OLS Results - Model Variables

Variable	Coefficient [a]	StdError	t-Statistic	Probability [b]	Robust_SE	Robust_t	Robust_Pr [b]	VIF [c]
Intercept	7.679160	8.203830	0.936046	0.350687	12.986101	0.591337	0.555153	-----
B_PER	1.739899	1.378975	1.261733	0.208931	2.823398	0.616243	0.538634	3.584622
G_PER	9.807887	1.101032	8.907900	0.000000*	3.697125	2.652842	0.008803*	3.807780
AVG_PREG	-2.705768	3.143792	-0.860670	0.390731	4.683835	-0.577682	0.564315	1.141511

Figure A3.4: Summary of the OLS results.

A3.5 Variable Distributions and Relationships of the OLS Model

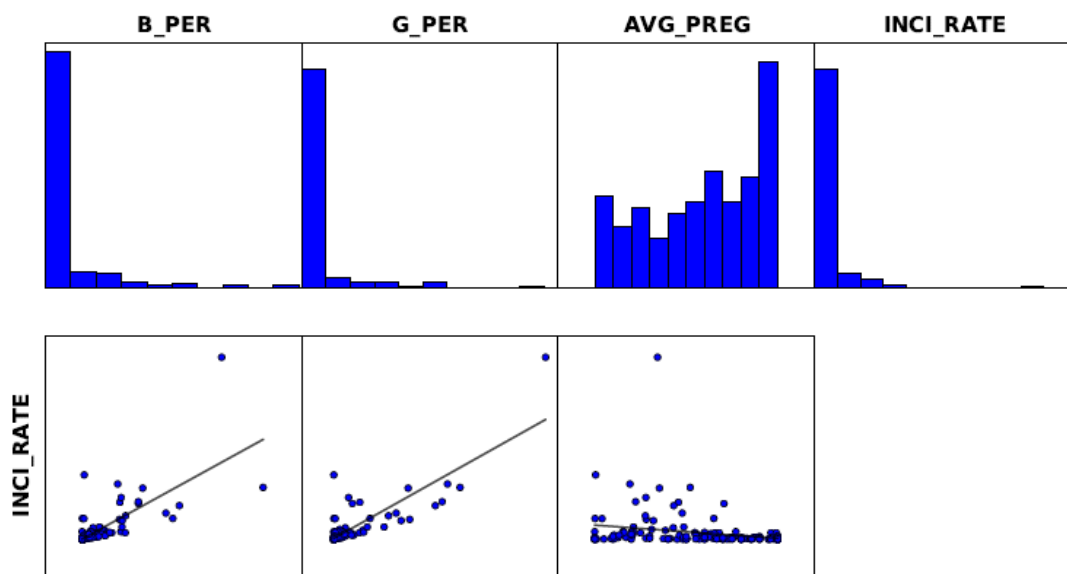


Figure A3.5: The variable distributions and relationships of the OLS model.

A3.6 Histogram of the OLS Model's Standard Residuals

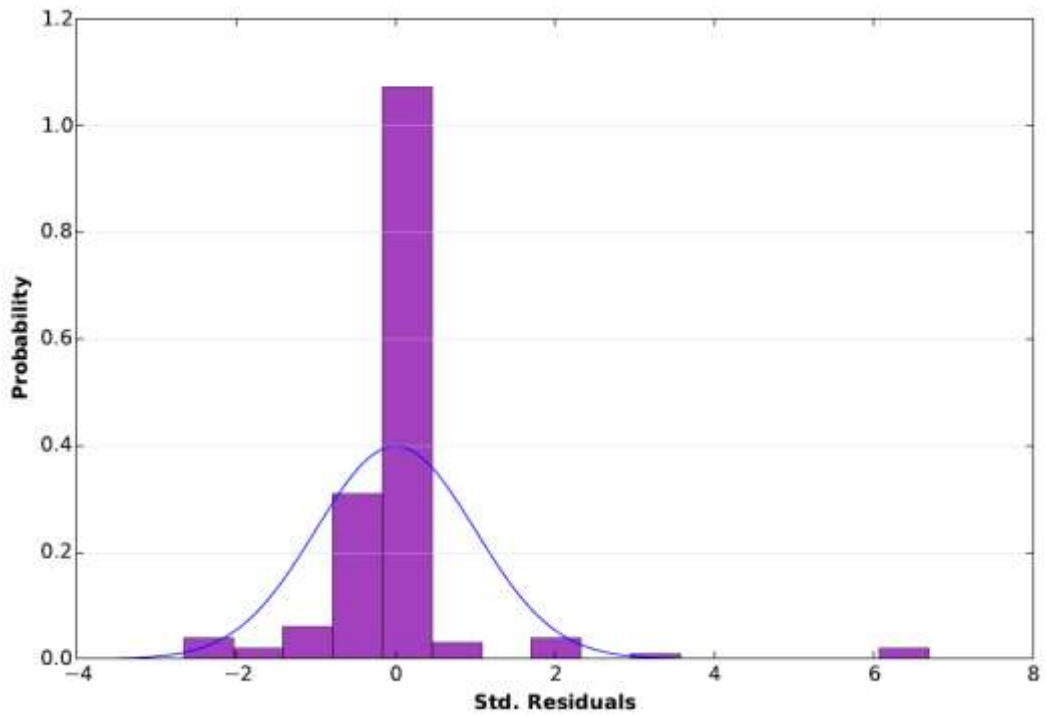


Figure A3.6: The histogram of the OLS model's standard residuals.

A3.7 Spatial Autocorrelation Report of the OLS Standard Residuals

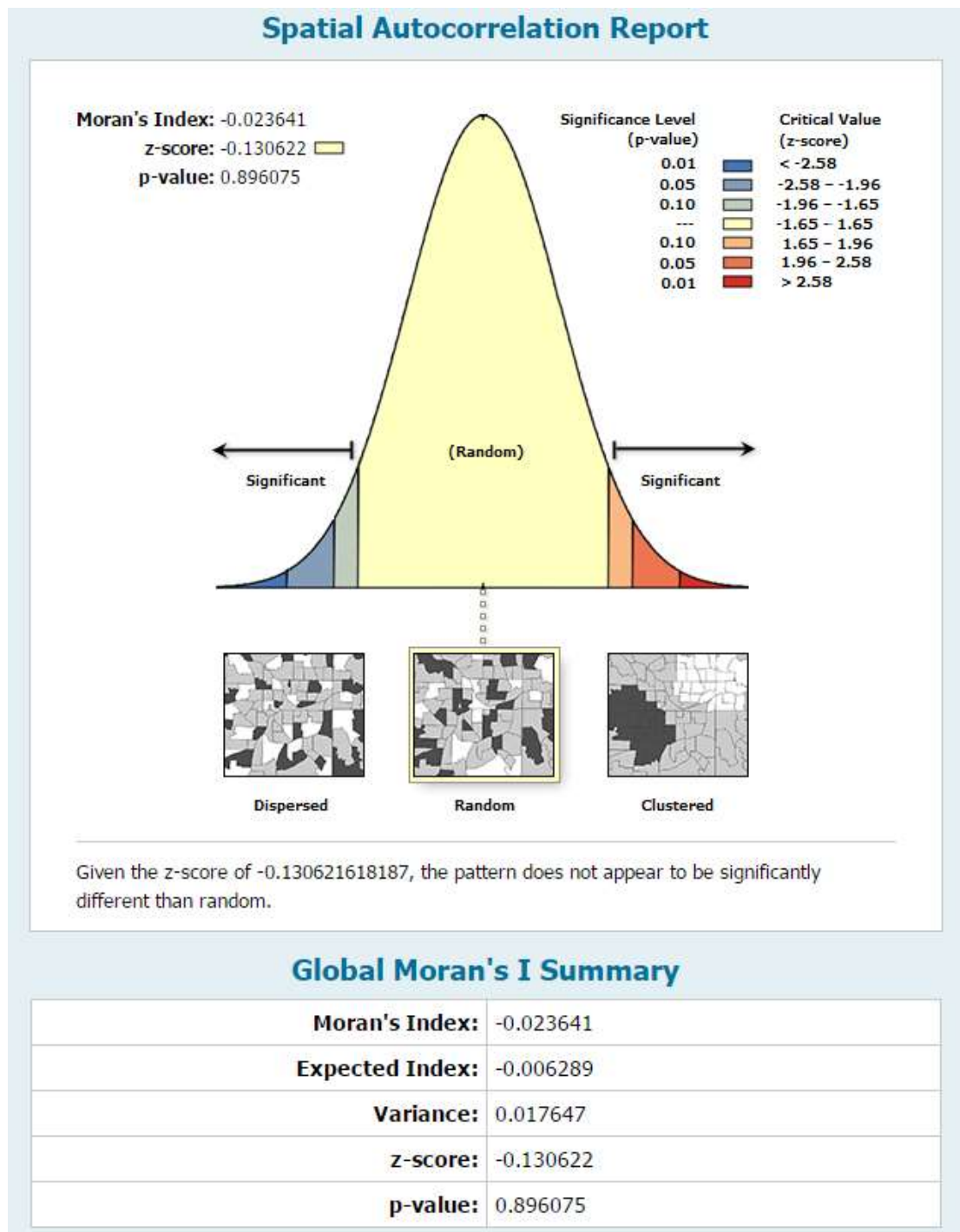


Figure A3.7: Spatial Autocorrelation report of the OLS standard residuals.

A3.8 GWR – Significantly Positive Estimates of Black Flying Foxes

Table A3.1: Significantly positive estimates of black flying foxes in the study.

Longitude	Latitude	t_perB
153.2355	-27.4952	1.977073
153.1424	-27.0578	1.991723
153.107	-26.6824	1.992049
153.107	-26.6824	1.992049
153.0712	-26.6508	2.058989
153.1592	-27.079	2.068613
152.9943	-27.3111	2.075467
152.9886	-27.5157	2.081071
152.9753	-26.6109	2.08645
152.9753	-26.6109	2.08645
152.9726	-26.6073	2.091106
153.1279	-27.0804	2.092699
153.1279	-27.0804	2.092699
152.926	-27.0809	2.110843
152.9276	-27.0823	2.114754
152.9268	-27.0816	2.115554
152.8254	-27.1971	2.14875
153.2263	-27.5026	2.204321
152.8405	-27.3761	2.205218
152.8405	-27.3761	2.205218
152.8316	-27.2069	2.222608
153.402	-27.499	2.228568
152.9553	-27.1605	2.296992
152.9145	-26.4721	2.307189
152.9714	-27.1527	2.316948
152.9255	-27.5444	2.33432
153.0855	-26.5328	2.335555
153.0855	-26.5328	2.335555
153.2097	-27.5165	2.354085
153.0988	-27.2315	2.359386
153.0988	-27.2315	2.359386
152.8264	-26.3375	2.422655
152.8264	-26.3375	2.422655
153.1028	-27.2029	2.42798
152.7556	-27.6514	2.472741
153.0491	-26.4007	2.488751
153.0491	-26.4007	2.488751
153.046	-26.3944	2.495121
153.0745	-26.4081	2.498721
153.0699	-26.392	2.512301
152.9759	-26.3279	2.515952
152.9275	-26.2886	2.521906
153.258	-27.5275	2.723098
153.258	-27.5275	2.723098
152.8127	-27.6124	2.765369
153.3312	-27.5724	2.777747
152.9479	-27.6142	2.783501
152.8802	-27.5996	2.795979
152.8802	-27.5996	2.795979
152.6085	-28.0009	2.799839
152.9028	-27.6049	2.82481
152.9028	-27.6049	2.82481
152.9028	-27.6049	2.82481
153.3535	-27.6114	2.847462
153.3535	-27.6114	2.847462
153.0524	-27.5826	2.891925
153.085	-27.5707	2.913427
153.3753	-27.6274	2.950768
153.3044	-27.5801	2.975222
153.3044	-27.5801	2.975222

153.3068	-27.6209	3.036823
153.3085	-27.6421	3.111871
153.3085	-27.6421	3.111871
152.9206	-27.6315	3.153736
152.9206	-27.6315	3.153736
153.0337	-27.6303	3.691208
153.363	-28.1048	3.74396
152.834	-28.0834	3.74396
153.1983	-27.737	3.862661
153.1983	-27.737	3.862661
152.6799	-27.9919	3.910496
152.6799	-27.9919	3.910496
152.6799	-27.9919	3.910496
153.1363	-27.61	4.010195
153.1963	-27.709	4.078136
153.1963	-27.709	4.078136
153.1876	-27.7015	4.452935
153.1373	-27.6402	4.648864
153.1373	-27.6402	4.648864
153.1373	-27.6402	4.648864
153.1773	-27.667	4.801027
153.0481	-27.67	4.81446
153.0481	-27.67	4.81446
153.037	-27.68	4.95088
153.0125	-27.8746	5.114505
152.8185	-27.827	5.408792
152.98	-27.8558	6.782161
152.9631	-27.8147	6.832482

A3.9 GWR – Significantly Positive Estimates of Grey-headed Flying Foxes

Table A3.2: Significantly positive estimates of grey-headed flying foxes in the study.

Longitude	Latitude	t_perG
152.2784	-26.8413	1.988214
152.3753	-27.7209	2.023214
152.9943	-27.3111	2.22698
153.3535	-27.6114	2.247036
153.3535	-27.6114	2.247036
152.5903	-27.4657	2.499218
152.5903	-27.4657	2.499218
152.5886	-27.4688	2.507069
152.5886	-27.4688	2.507069
152.8405	-27.3761	2.507216
152.8405	-27.3761	2.507216
153.0687	-27.3231	2.647021
153.402	-27.499	3.145594
153.3085	-27.6421	3.274762
153.3085	-27.6421	3.274762
153.1983	-27.737	3.664597
153.1983	-27.737	3.664597
153.3068	-27.6209	3.940209
152.9456	-27.4055	4.006327
152.7222	-27.4939	4.044717
153.3312	-27.5724	4.125248
153.1963	-27.709	4.424874
153.1963	-27.709	4.424874
152.8185	-27.827	4.431801
152.6799	-27.9919	4.620385
152.6799	-27.9919	4.620385
152.6799	-27.9919	4.620385
153.1876	-27.7015	4.641239
153.3044	-27.5801	4.693948
153.3044	-27.5801	4.693948
152.9419	-27.4443	5.054344
153.0481	-27.67	5.086084
153.0481	-27.67	5.086084
153.037	-27.68	5.103839
153.1773	-27.667	5.219118
152.9992	-27.412	5.341215
153.1373	-27.6402	5.365255
153.1373	-27.6402	5.365255
153.1373	-27.6402	5.365255
153.2355	-27.4952	5.403071
153.0337	-27.6303	5.536634
153.1363	-27.61	5.575357
153.258	-27.5275	5.593176
153.258	-27.5275	5.593176
153.2263	-27.5026	5.664311
153.1725	-27.4378	5.675319
153.1437	-27.445	5.692899
153.073	-27.3987	5.703284
153.2097	-27.5165	5.812297
152.7485	-27.6031	5.813112
152.7485	-27.6031	5.813112
152.7485	-27.6031	5.813112
153.1837	-27.4641	5.818728
152.6895	-27.6572	5.823178

153.1136	-27.444	5.842799
153.1136	-27.444	5.842799
152.9479	-27.6142	5.856523
152.6085	-28.0009	5.884588
153.0524	-27.5826	5.900043
153.085	-27.5707	5.997791
152.9206	-27.6315	6.025978
152.9206	-27.6315	6.025978
152.9255	-27.5444	6.087288
152.7556	-27.6514	6.116684
152.8127	-27.6124	6.13014
152.9028	-27.6049	6.134064
152.9028	-27.6049	6.134064
152.9028	-27.6049	6.134064
152.8802	-27.5996	6.154785
152.8802	-27.5996	6.154785
152.9886	-27.5157	6.297904
153.0226	-27.4424	6.303629
152.9929	-27.491	6.33866
153.0376	-27.4376	6.353046
153.0519	-27.4841	6.545723
153.0519	-27.4841	6.545723
152.9631	-27.8147	6.583615
152.834	-28.0834	6.698205
152.98	-27.8558	7.717512
153.2429	-27.7758	8.02133
153.0125	-27.8746	10.20315
153.0115	-28.2192	16.80109
153.3812	-27.8883	17.15241
153.1935	-27.9237	17.19
153.1935	-27.9237	17.19
153.3343	-27.9012	17.36283
153.3343	-27.9012	17.36283
153.1824	-28.0398	17.4745
153.1824	-28.0398	17.4745
153.3973	-27.9481	17.50434
153.4033	-27.9581	17.52036
153.4272	-27.9842	17.53264
153.4136	-27.9797	17.54608
153.4136	-27.9797	17.54608
153.2767	-28.2174	17.5636
153.4134	-27.9951	17.56649
153.4672	-28.1453	17.56983
153.4277	-28.0222	17.57322
153.4277	-28.0222	17.57322
153.4448	-28.1144	17.58548
153.4292	-28.0946	17.59191
153.4238	-28.0681	17.59318
153.412	-28.0629	17.59866
153.3242	-28.003	17.59982
153.3916	-28.0332	17.60324
153.3624	-28.0179	17.6041
153.363	-28.1048	17.64172
153.3459	-28.0856	17.65492

A3.10 GWR – Significantly Negative Estimates of Grey-headed Flying Foxes

Table A3.3: Significantly negative estimates of grey-headed flying foxes in the study.

Longitude	Latitude	t_perG
153.0699	-26.392	-0.47518
152.9759	-26.3279	-0.46257
152.9275	-26.2886	-0.45976
153.0745	-26.4081	-0.45455
153.046	-26.3944	-0.44445
153.0491	-26.4007	-0.43021
153.0491	-26.4007	-0.43021
152.8264	-26.3375	-0.26563
152.8264	-26.3375	-0.26563
153.0855	-26.5328	-0.19587
153.0855	-26.5328	-0.19587
152.9145	-26.4721	-0.08518

A3.11 GWR – Significantly Negative Estimates of Pregnancy/Birth Period

Table A3.4: Significantly negative estimates of pregnancy/birth period in the study.

Longitude	Latitude	t_pregR
152.1227	-27.5483	-1.90201
152.1227	-27.5483	-1.90201
152.9553	-27.1605	-1.86312
153.037	-27.68	-1.85979
153.0481	-27.67	-1.8447
153.0481	-27.67	-1.8447
152.926	-27.0809	-1.83001
152.9276	-27.0823	-1.82963
152.9268	-27.0816	-1.82923
152.9714	-27.1527	-1.8109
152.2726	-27.5648	-1.73539
152.2726	-27.5648	-1.73539
152.9479	-27.6142	-1.72758
152.7763	-26.9503	-1.64797
152.7763	-26.9503	-1.64797
152.4233	-27.2349	-1.59545
152.4233	-27.2349	-1.59545
152.4233	-27.2349	-1.59545
153.0524	-27.5826	-1.56208
152.9206	-27.6315	-1.53991
152.9206	-27.6315	-1.53991
152.5687	-26.9415	-1.46177
152.5687	-26.9415	-1.46177
153.1279	-27.0804	-1.387
153.1279	-27.0804	-1.387
152.3948	-27.6206	-1.35478
152.3948	-27.6206	-1.35478
152.3753	-27.7209	-1.34618
152.2784	-26.8413	-1.34402
153.1424	-27.0578	-1.33949
153.1592	-27.079	-1.30087
153.1028	-27.2029	-1.27243
153.085	-27.5707	-1.26456
152.9028	-27.6049	-1.2023
152.9028	-27.6049	-1.2023
152.9028	-27.6049	-1.2023
153.0988	-27.2315	-1.13981
153.0988	-27.2315	-1.13981
152.8185	-27.827	-1.00232
152.8802	-27.5996	-0.99716
152.8802	-27.5996	-0.99716
153.1373	-27.6402	-0.96871
153.1373	-27.6402	-0.96871
153.1373	-27.6402	-0.96871
153.1363	-27.61	-0.96758
152.9631	-27.8147	-0.9505
153.1963	-27.709	-0.81794
153.1963	-27.709	-0.81794
152.9943	-27.3111	-0.79495
153.1876	-27.7015	-0.79306
152.8127	-27.6124	-0.77176
152.98	-27.8558	-0.7572
153.1983	-27.737	-0.7357
153.1983	-27.737	-0.7357

152.9255	-27.5444	-0.67276
152.834	-28.0834	-0.6562
153.1773	-27.667	-0.64613
152.7556	-27.6514	-0.62096
152.6799	-27.9919	-0.56116
152.6799	-27.9919	-0.56116
152.6799	-27.9919	-0.56116
152.9886	-27.5157	-0.51943
153.3085	-27.6421	-0.5096
153.3085	-27.6421	-0.5096
153.3068	-27.6209	-0.50359
153.3753	-27.6274	-0.46767
153.3535	-27.6114	-0.41753
153.3535	-27.6114	-0.41753
152.6085	-28.0009	-0.40495
153.3044	-27.5801	-0.38729
153.3044	-27.5801	-0.38729
153.3312	-27.5724	-0.34841
152.7485	-27.6031	-0.34279
152.7485	-27.6031	-0.34279
152.7485	-27.6031	-0.34279
153.0687	-27.3231	-0.32994
152.6895	-27.6572	-0.28692
153.0125	-27.8746	-0.24696
153.258	-27.5275	-0.22125
153.258	-27.5275	-0.22125
153.2097	-27.5165	-0.2212
153.402	-27.499	-0.18917
152.9929	-27.491	-0.18831
153.2263	-27.5026	-0.14257
153.0519	-27.4841	-0.12116
153.0519	-27.4841	-0.12116
152.8405	-27.3761	-0.10901
152.8405	-27.3761	-0.10901
152.5886	-27.4688	-0.09805
152.5886	-27.4688	-0.09805
152.5903	-27.4657	-0.09365
152.5903	-27.4657	-0.09365
153.2355	-27.4952	-0.06739

Appendix – 4

Food Source Vegetation Analysis

A4.1 List of MVS Identified within 20 Kms Range of Black Flying Foxes

Legend

MVS within 20 Kms Buffer Range of the Black Flying-fox Roosting Sites

MVS_NAME


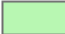
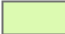

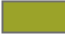













	Banksia woodlands
	Brigalow (Acacia harpophylla) forests and woodlands
	Casuarina and Allocasuarina forests and woodlands
	Cleared, non-native vegetation, buildings
	Cool temperate rainforest
	Dry rainforest or vine thickets
	Eucalyptus (+/- tall) open forest with a dense broad-leaved and/or tree-fern understorey (wet sclerophyll)
	Eucalyptus open forests with a grassy understorey
	Eucalyptus open forests with a shrubby understorey
	Eucalyptus open woodlands with a grassy understorey
	Eucalyptus tall open forest with a fine-leaved shrubby understorey
	Eucalyptus tall open forests and open forests with ferns, herbs, sedges, rushes or wet tussock grasses
	Eucalyptus woodlands with a shrubby understorey
	Eucalyptus woodlands with a tussock grass understorey
	Freshwater, dams, lakes, lagoons or aquatic plants
	Heathlands
	Low closed forest or tall closed shrublands (including Acacia, Melaleuca and Banksia)
	Mangroves
	Melaleuca open forests and woodlands
	Naturally bare, sand, rock, claypan, mudflat
	Other open woodlands
	Other shrublands
	Saline or brackish sedgeland or grasslands
	Sea, estuaries (includes seagrass)
	Sedgeland, rushes or reeds
	Tropical or sub-tropical rainforest
	Unknown/No data
	Warm Temperate Rainforest

Figure A4.1: Legend of the MVS identified within 20 kms range of the black flying fox roosting sites in the study area.

A4.2 High/Low Clustering Reports of the Black flying Foxes Food Source Vegetation at 3, 5 and 10 Kms

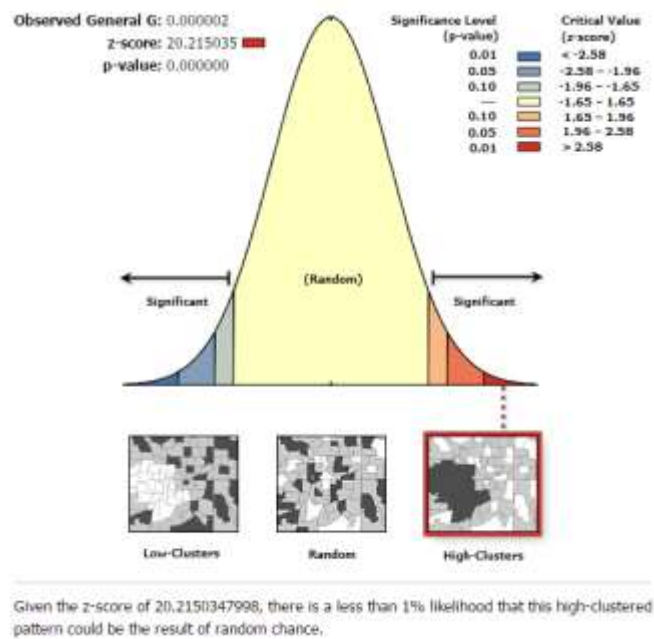


Figure A4.2 (a): High/Low Clustering report of the food source vegetation of black flying foxes at 3 kms.

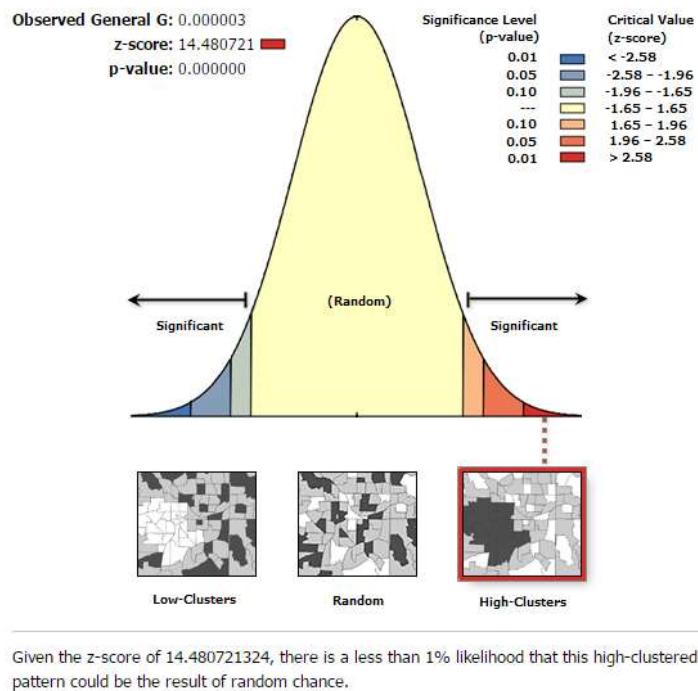
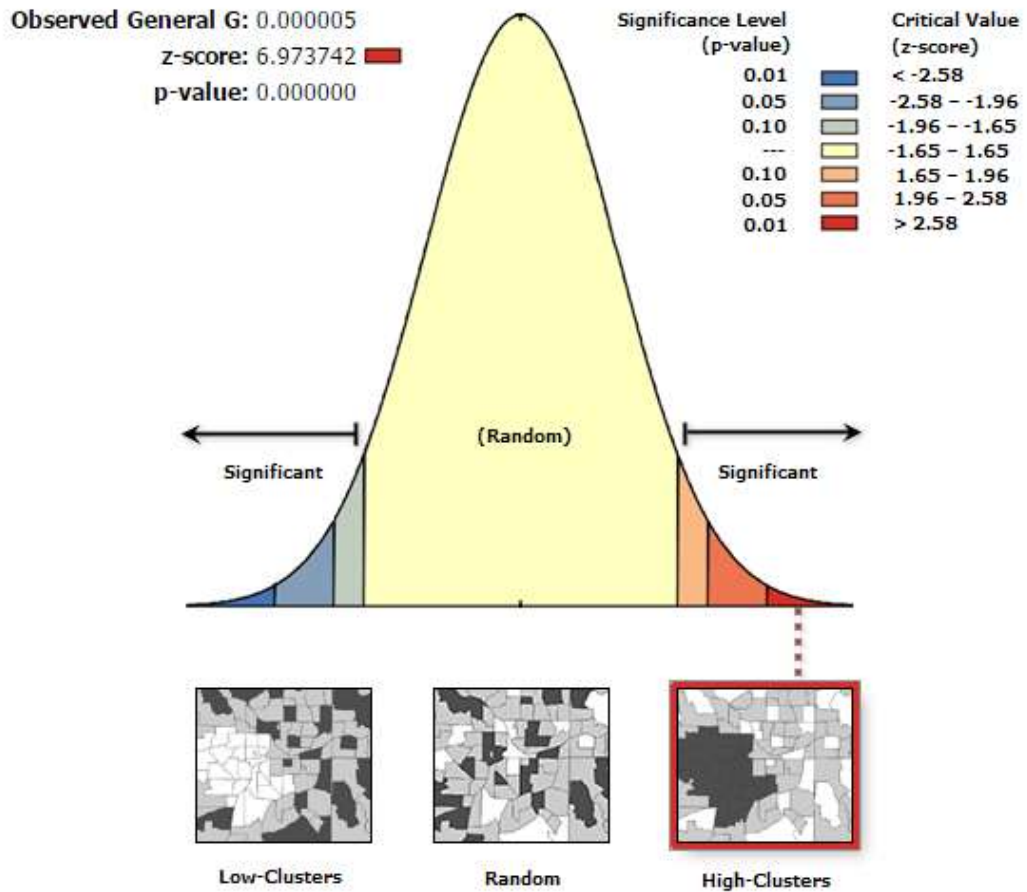


Figure A4.2 (b): High/Low Clustering report of the food source vegetation of black flying foxes at 5 kms.



Given the z-score of 6.97374231917, there is a less than 1% likelihood that this high-clustered pattern could be the result of random chance.

Figure A4.2 (c): High/Low Clustering report of the food source vegetation of black flying foxes at 10 kms.

A4.3 List of MVS Identified within 20 Kms Range of Grey-headed Flying Foxes

Legend

MVS within 20 Kms Buffer Range of the Grey Headed Flying-fox Roosting Sites

MVS_NAME


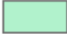
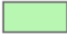
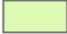
























	Banksia woodlands
	Brigalow (Acacia harpophylla) forests and woodlands
	Casuarina and Allocasuarina forests and woodlands
	Cleared, non-native vegetation, buildings
	Cool temperate rainforest
	Dry rainforest or vine thickets
	Eucalyptus (+/- tall) open forest with a dense broad-leaved and/or tree-fern understorey (wet sclerophyll)
	Eucalyptus open forests with a grassy understorey
	Eucalyptus open forests with a shrubby understorey
	Eucalyptus open woodlands with a grassy understorey
	Eucalyptus tall open forest with a fine-leaved shrubby understorey
	Eucalyptus tall open forests and open forests with ferns, herbs, sedges, rushes or wet tussock grasses
	Eucalyptus woodlands with a shrubby understorey
	Eucalyptus woodlands with a tussock grass understorey
	Freshwater, dams, lakes, lagoons or aquatic plants
	Heathlands
	Low closed forest or tall closed shrublands (including Acacia, Melaleuca and Banksia)
	Mangroves
	Melaleuca open forests and woodlands
	Naturally bare, sand, rock, claypan, mudflat
	Other open woodlands
	Other shrublands
	Saline or brackish sedgelands or grasslands
	Sea, estuaries (includes seagrass)
	Sedgelands, rushes or reeds
	Tropical or sub-tropical rainforest
	Unknown/No data
	Warm Temperate Rainforest

Figure A4.3: Legend of the MVS identified within 20 kms range of the grey-headed flying fox roosting sites in the study area.

A4.4 High/Low Clustering Reports of the Grey-headed flying Foxes Food Source Vegetation at 3, 5 and 10 Kms

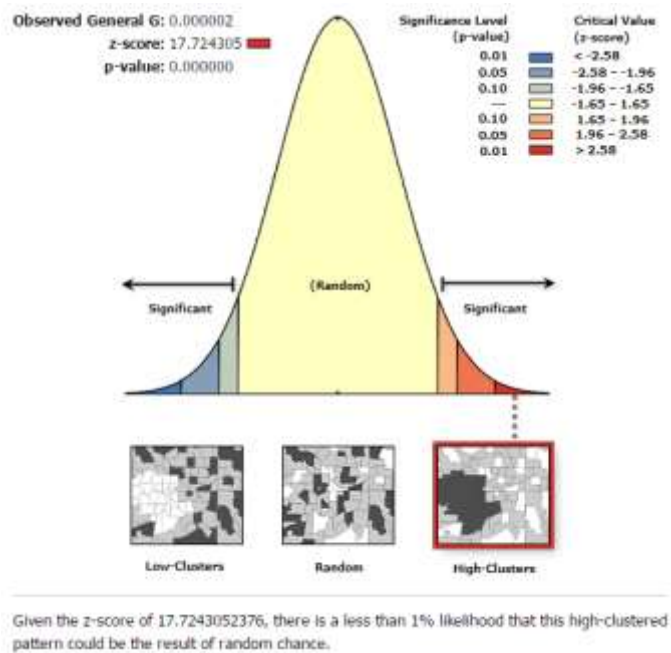


Figure A4.4 (a): High/Low Clustering report of the food source vegetation of grey-headed flying foxes at 3 kms.

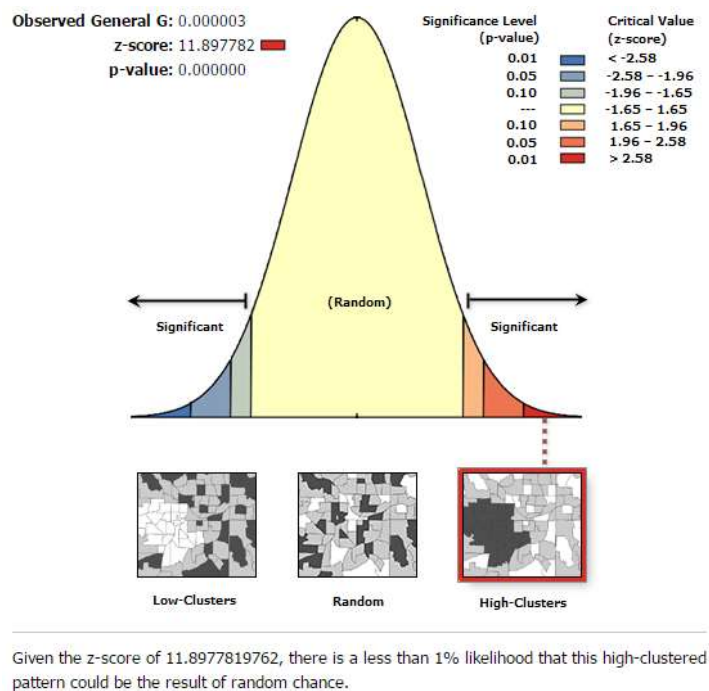
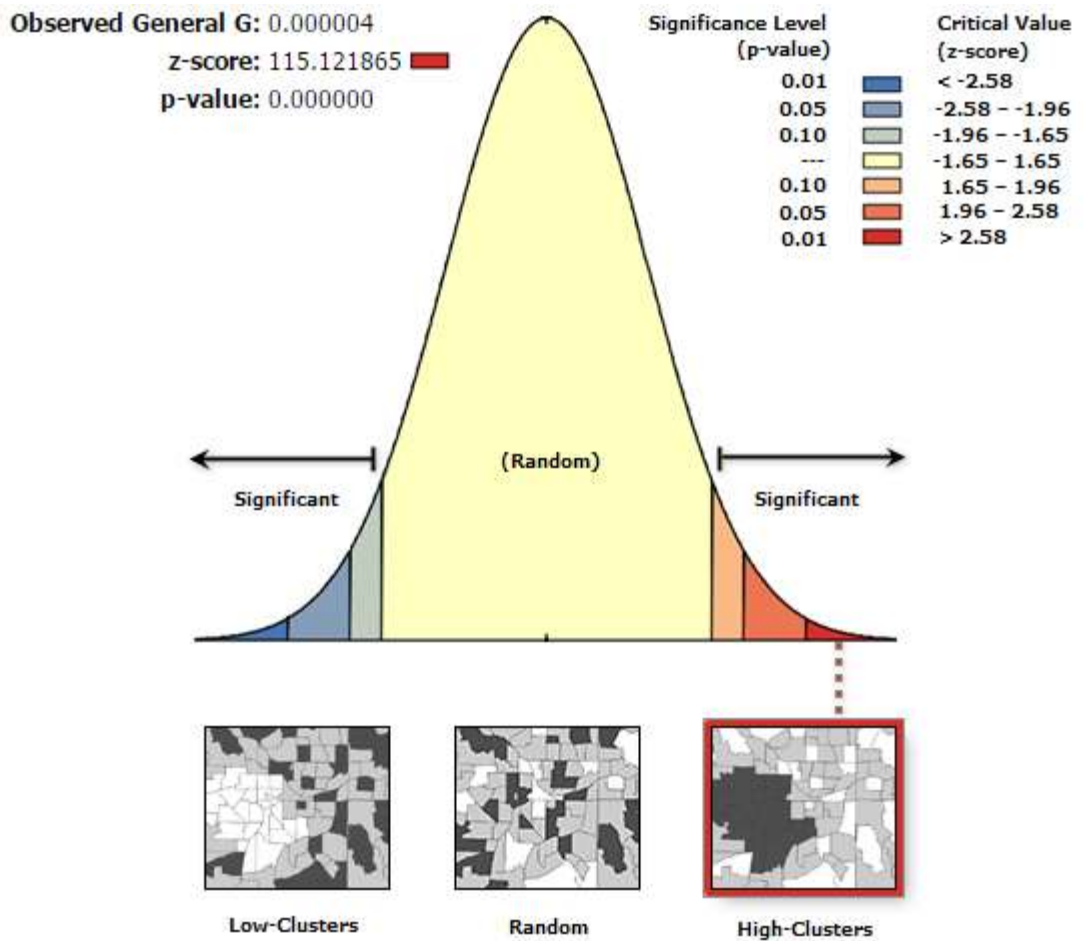


Figure A4.4 (b): High/Low Clustering report of the food source vegetation of grey-headed flying foxes at 5 kms.



Given the z-score of 115.121864934, there is a less than 1% likelihood that this high-clustered pattern could be the result of random chance.

Figure A4.4 (c): High/Low Clustering report of the food source vegetation of grey-headed flying foxes at 10 kms.

A4.5 List of MVS Identified within 10 Kms Range of HeV Incidents

Legend

MVS within 10 Kms Buffer Range of the Incidents

MVS_NAME

	Banksia woodlands
	Brigalow (Acacia harpophylla) forests and woodlands
	Casuarina and Allocasuarina forests and woodlands
	Cleared, non-native vegetation, buildings
	Dry rainforest or vine thickets
	Eucalyptus (+/- tall) open forest with a dense broad-leaved and/or tree-fern understorey (wet sclerophyll)
	Eucalyptus open forests with a grassy understorey
	Eucalyptus open forests with a shrubby understorey
	Eucalyptus open woodlands with a grassy understorey
	Eucalyptus tall open forests and open forests with ferns, herbs, sedges, rushes or wet tussock grasses
	Eucalyptus woodlands with a shrubby understorey
	Eucalyptus woodlands with a tussock grass understorey
	Freshwater, dams, lakes, lagoons or aquatic plants
	Heathlands
	Low closed forest or tall closed shrublands (including Acacia, Melaleuca and Banksia)
	Mangroves
	Melaleuca open forests and woodlands
	Other open woodlands
	Other shrublands
	Saline or brackish sedgelands or grasslands
	Sea, estuaries (includes seagrass)
	Sedgelands, rushes or reeds
	Tropical or sub-tropical rain forest
	Unknown/No data
	Warm Temperate Rainforest

Figure A4.5: Legend of the MVS identified within 10 kms range of the HeV incidents in the study area.

A4.6 High/Low Clustering Reports of the Food Source Vegetation of Flying Foxes within 10 kms Range of the Incidents at 3, 4, 5 and 10 Kms

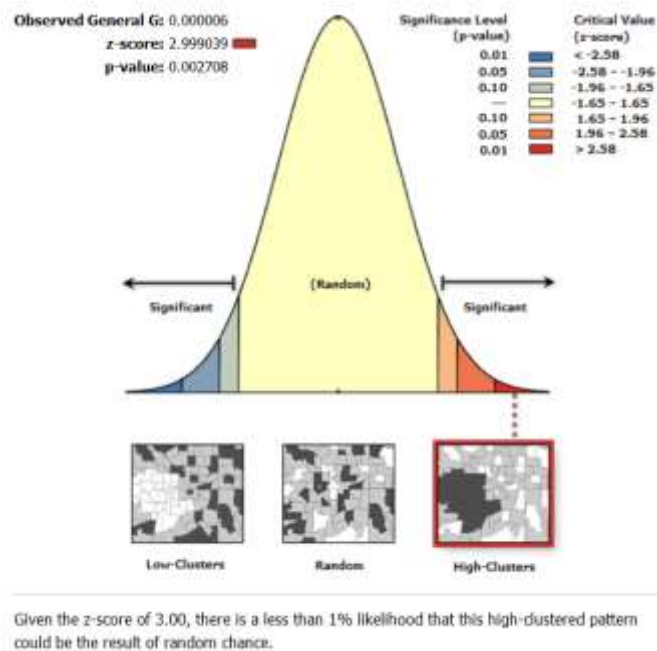


Figure A4.6 (a): High/Low Clustering report of the flying foxes food source vegetation within 10 kms incident range at 3 kms.

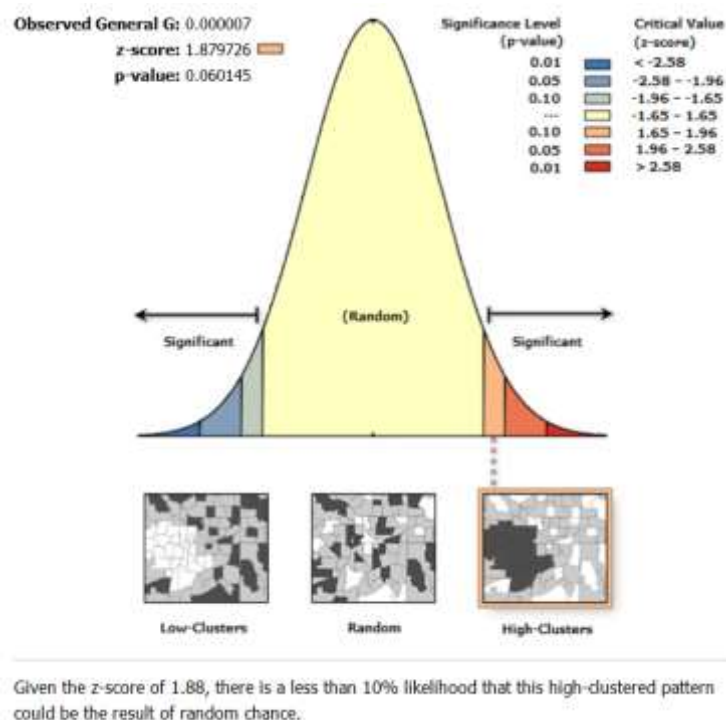
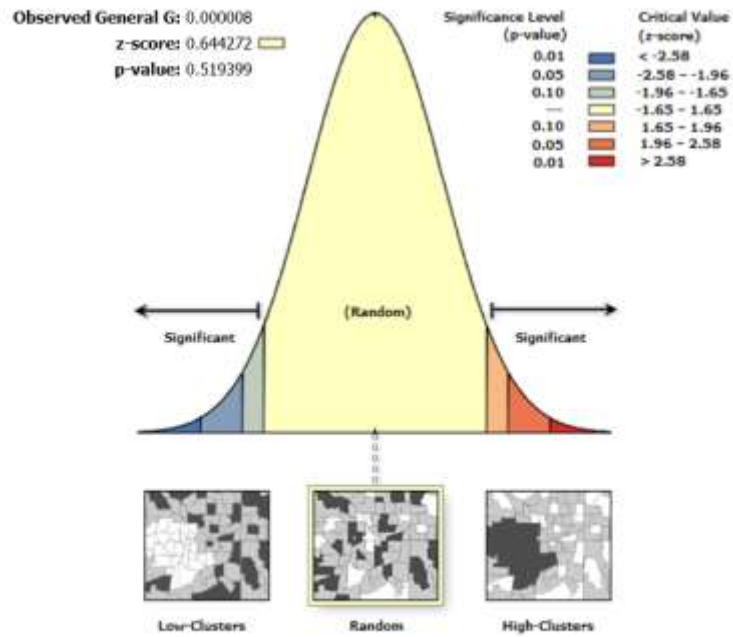
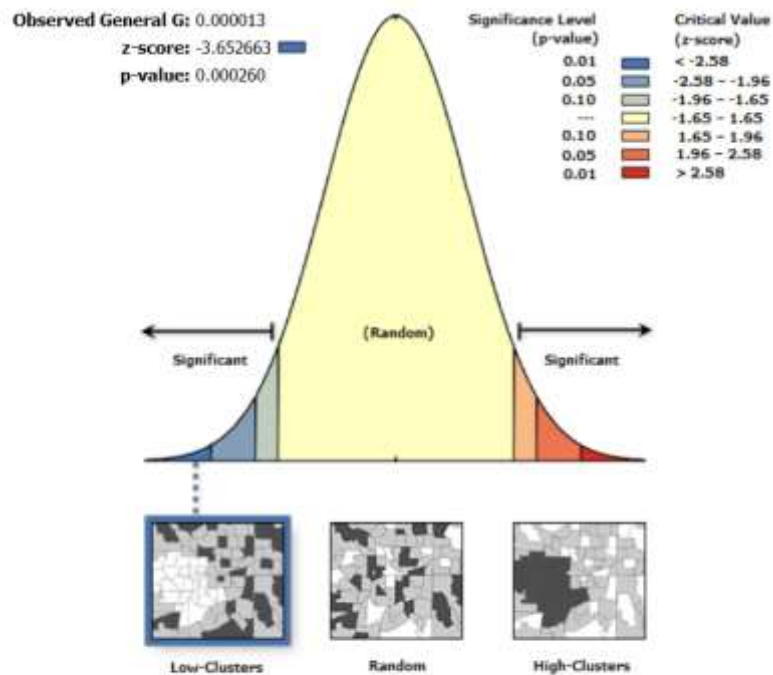


Figure A4.6 (b): High/Low Clustering report of the flying foxes food source vegetation within 10 kms incident range at 4 kms.



Given the z-score of 0.64, the pattern does not appear to be significantly different than random.

Figure A4.6 (c): High/Low Clustering report of the flying foxes food source vegetation within 10 kms incident range at 5 kms.



Given the z-score of -3.65, there is a less than 1% likelihood that this low-clustered pattern could be the result of random chance.

Figure A4.6 (d): High/Low Clustering report of the flying foxes food source vegetation within 10 kms incident range at 10 kms.

A4.7 List of MVS Identified within 10 Kms Range of Registered Equine Properties

Legend

List of MVS Identified within 10 Kilometers of the Equine Properties

MVS_NAME

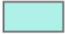
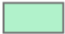
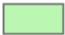
























	Banksia woodlands
	Brigalow (<i>Acacia harpophylla</i>) forests and woodlands
	Casuarina and Allocasuarina forests and woodlands
	Cleared, non-native vegetation, buildings
	Cool temperate rainforest
	Dry rainforest or vine thickets
	Eucalyptus (+/- tall) open forest with a dense broad-leaved and/or tree-fern understorey (wet sclerophyll)
	Eucalyptus open forests with a grassy understorey
	Eucalyptus open forests with a shrubby understorey
	Eucalyptus open woodlands with a grassy understorey
	Eucalyptus tall open forest with a fine-leaved shrubby understorey
	Eucalyptus tall open forests and open forests with ferns, herbs, sedges, rushes or wet tussock grasses
	Eucalyptus woodlands with a shrubby understorey
	Eucalyptus woodlands with a tussock grass understorey
	Freshwater, dams, lakes, lagoons or aquatic plants
	Heathlands
	Low closed forest or tall closed shrublands (including <i>Acacia</i> , <i>Melaleuca</i> and <i>Banksia</i>)
	Mangroves
	<i>Melaleuca</i> open forests and woodlands
	Other open woodlands
	Other shrublands
	Saline or brackish sedgeland or grasslands
	Sea, estuaries (includes seagrass)
	Sedgeland, rushes or reeds
	Tropical or sub-tropical rainforest
	Unknown/No data
	Warm Temperate Rainforest

Figure A4.7: Legend of the MVS identified within 10 kms range of the registered equine properties in the study area.

A4.8 High/Low Clustering Reports of the Food Source Vegetation of Flying Foxes within 10 kms Range of the Equine Properties at 3, 5 and 10 Kms

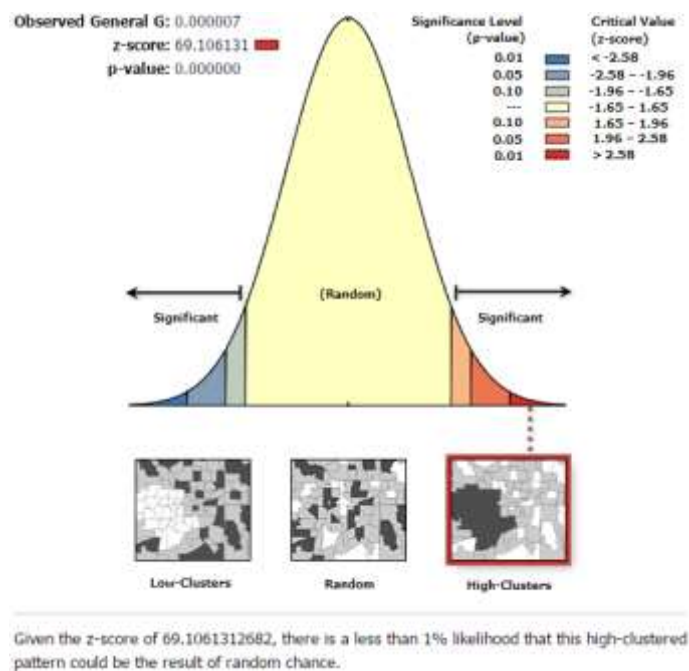


Figure A4.8 (a): High/Low Clustering report of the flying foxes food source vegetation within 10 kms range of equine properties at 3 kms.

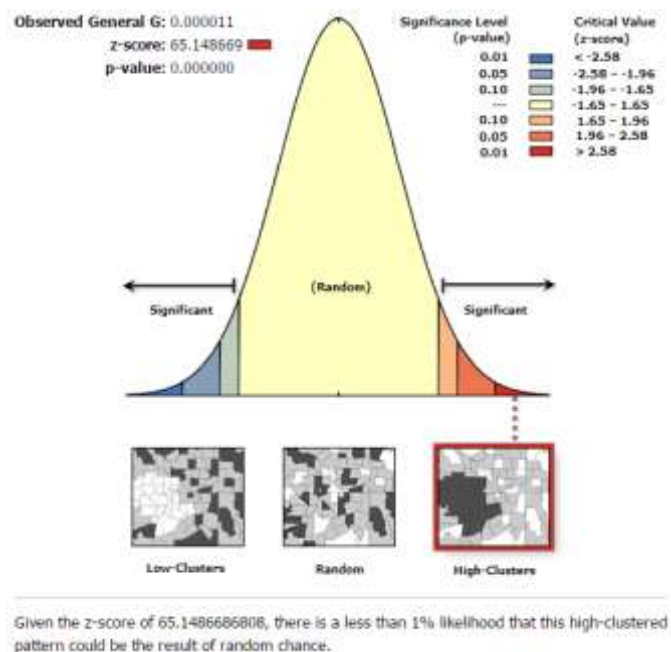
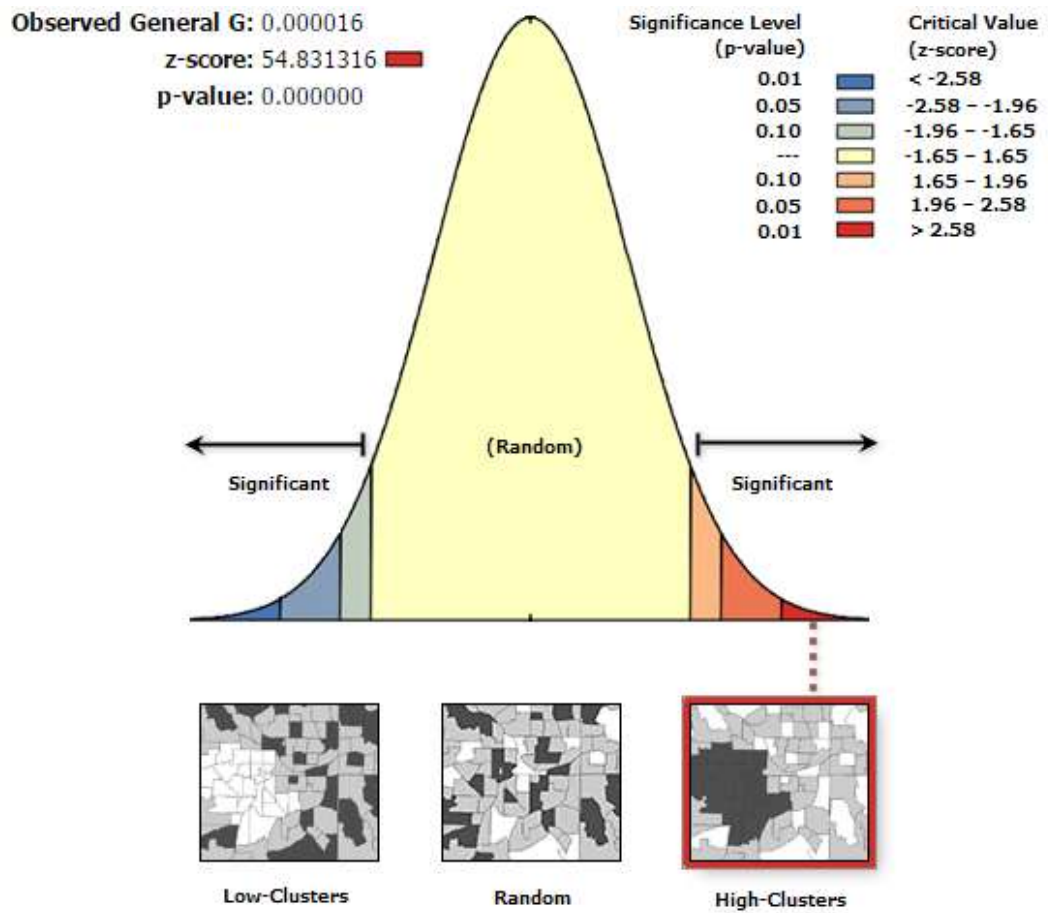


Figure A4.8 (b): High/Low Clustering report of the flying foxes food source vegetation within 10 kms range of equine properties at 5 kms.



Given the z-score of 54.831316114, there is a less than 1% likelihood that this high-clustered pattern could be the result of random chance.

Figure A4.8 (c): High/Low Clustering report of the flying foxes food source vegetation within 10 kms range of equine properties at 10 kms.

A4.9 High/Low Clustering Reports of the Food Source Vegetation of the Black Flying Foxes near the Equine Properties ‘at risk’ at 3, 5, 10, 15 and 20 Kms

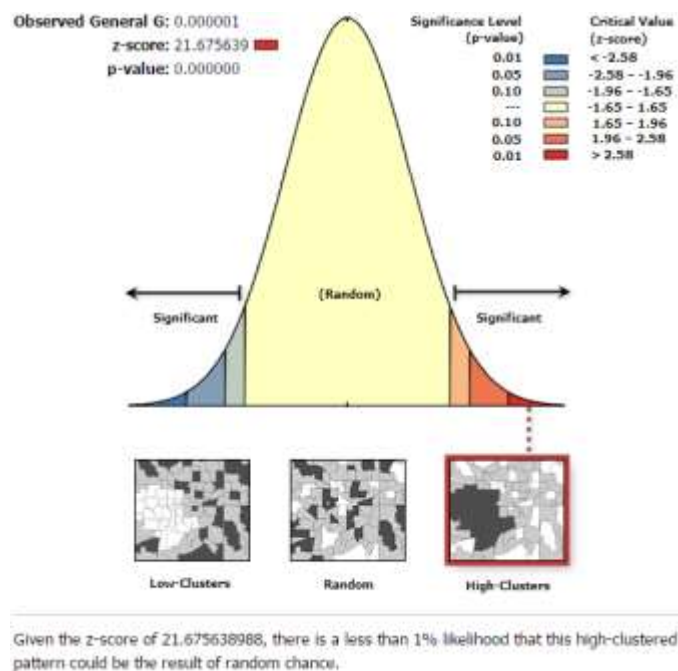


Figure A4.9 (a): High/Low Clustering report of the black flying foxes food source vegetation near the equine Properties ‘at risk’ at 3 kms.

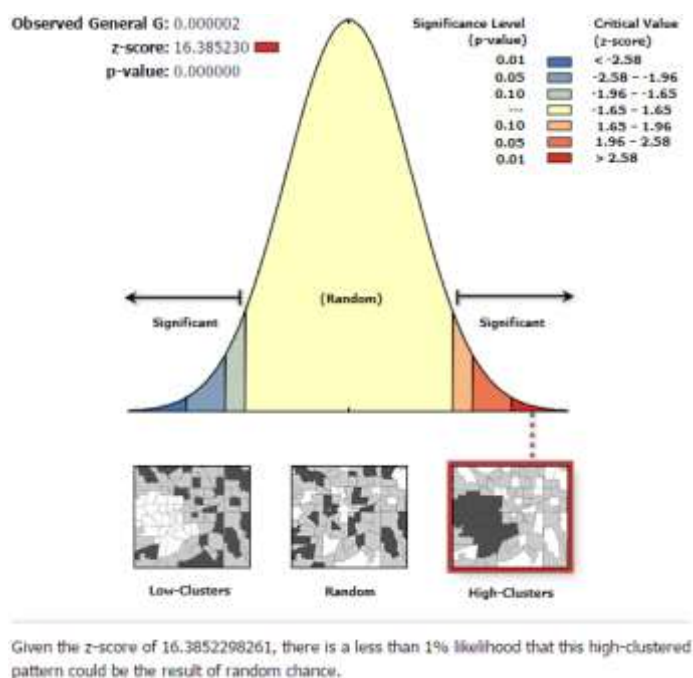
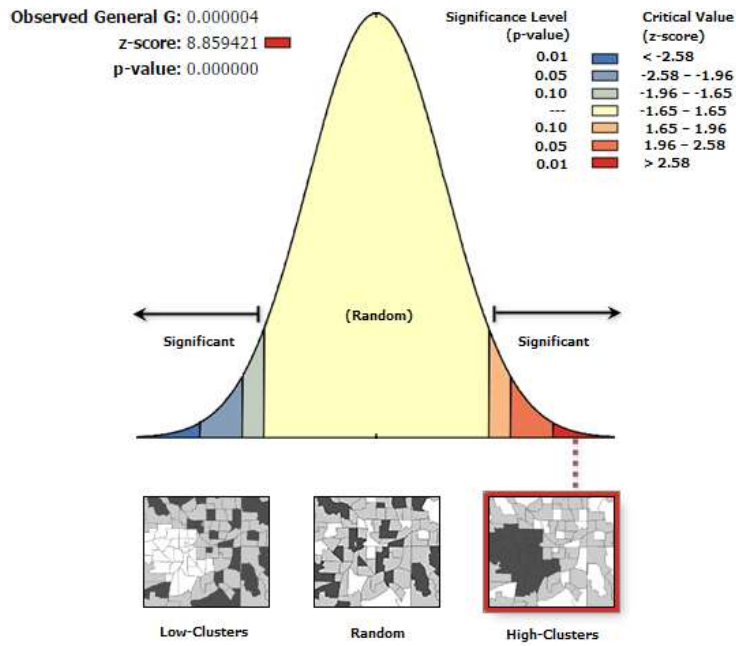
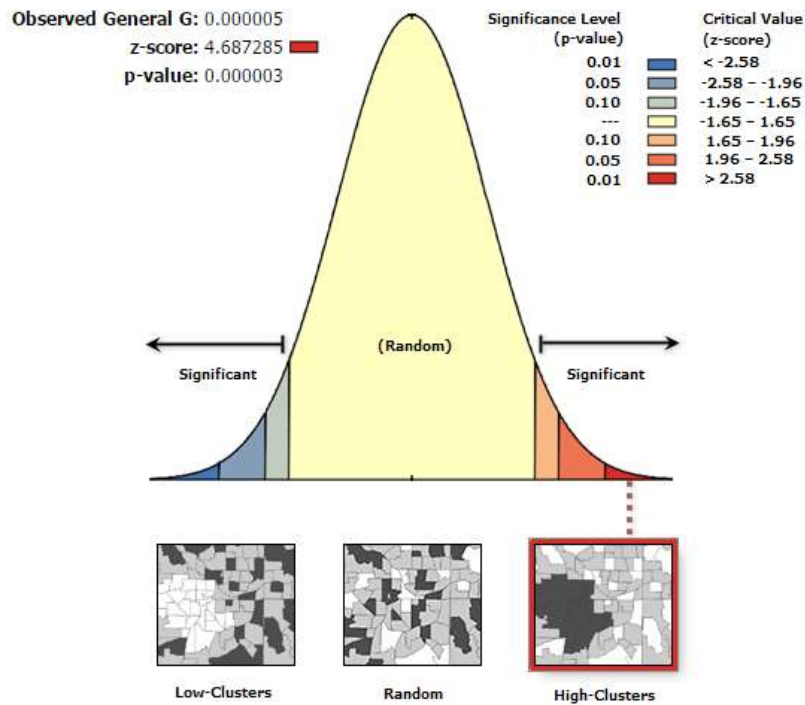


Figure A4.9 (b): High/Low Clustering report of the black flying foxes food source vegetation near the equine properties ‘at risk’ at 5 kms.



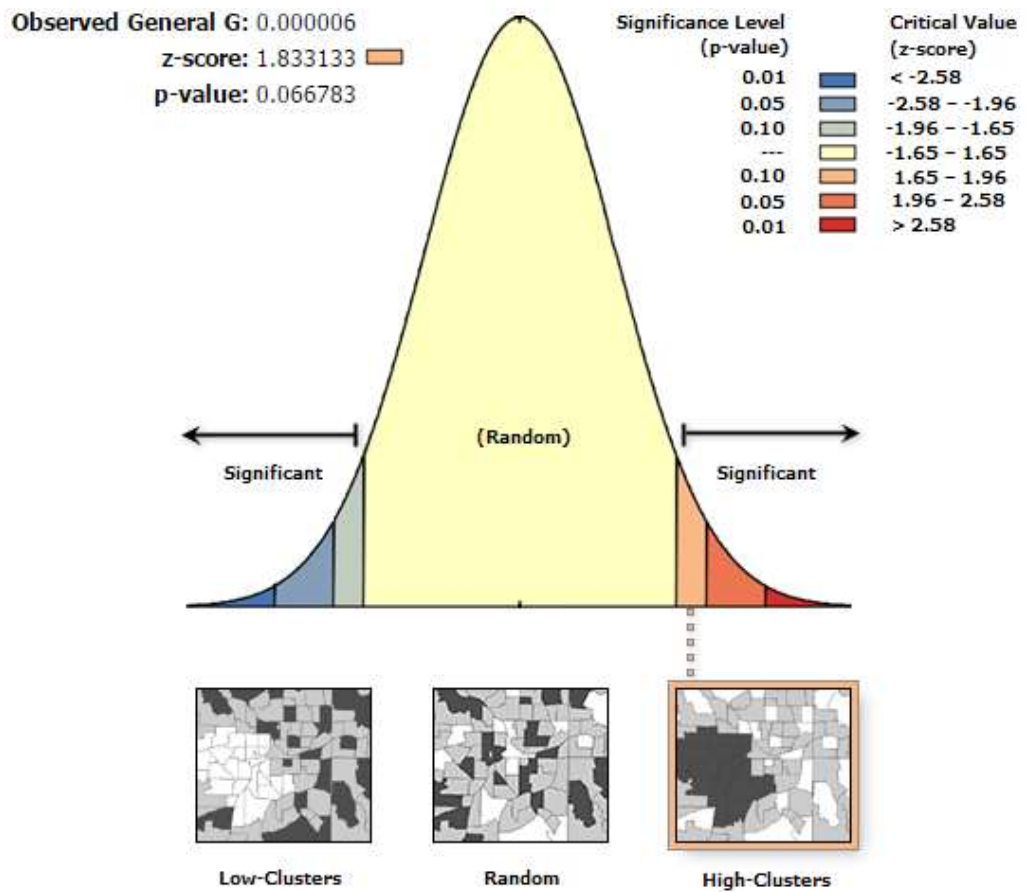
Given the z-score of 8.85942051884, there is a less than 1% likelihood that this high-clustered pattern could be the result of random chance.

Figure A4.9 (c): High/Low Clustering report of the black flying foxes food source Vegetation near the equine properties ‘at risk’ at 10 kms.



Given the z-score of 4.68728450336, there is a less than 1% likelihood that this high-clustered pattern could be the result of random chance.

Figure A4.9 (d): High/Low Clustering report of the black flying foxes food source Vegetation near the equine properties ‘at risk’ at 15 kms.



Given the z-score of 1.83313336949, there is a less than 10% likelihood that this high-clustered pattern could be the result of random chance.

Figure A4.9 (e): High/Low Clustering report of the black flying foxes food source Vegetation near the equine properties 'at risk' at 20 kms.

A4.10 High/Low Clustering Reports of the Food Source Vegetation of the Grey-headed Flying Foxes near the Equine Properties ‘at risk’ at 3, 5, 10, 15 and 20 Kms

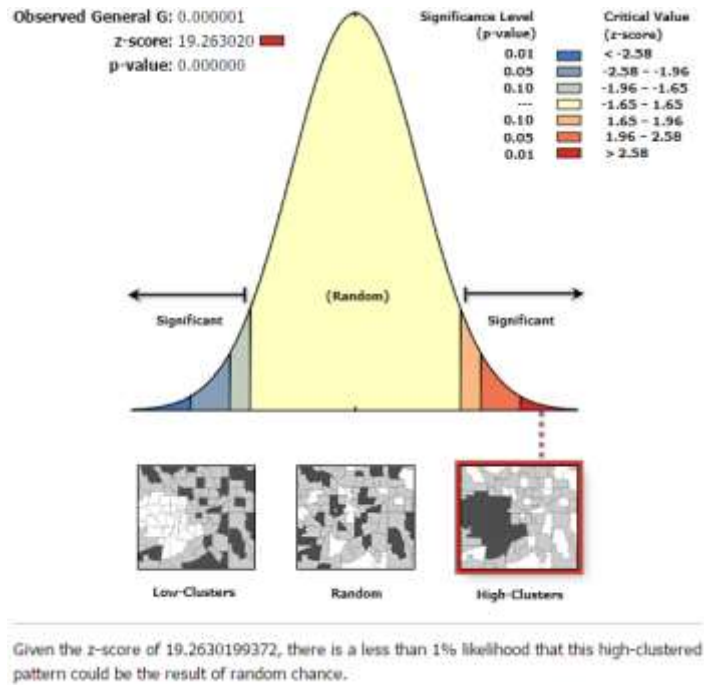


Figure A4.10 (a): High/Low Clustering report of the grey-headed flying foxes food source vegetation near the equine properties ‘at risk’ at 3 kms.

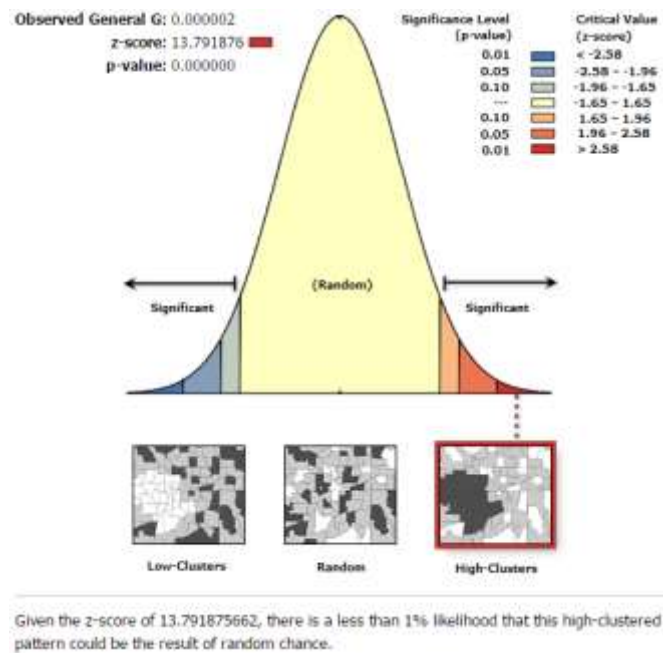
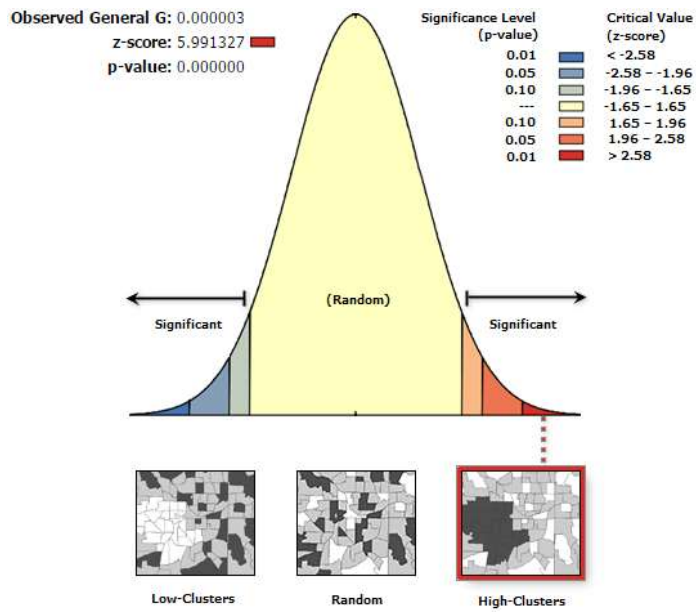
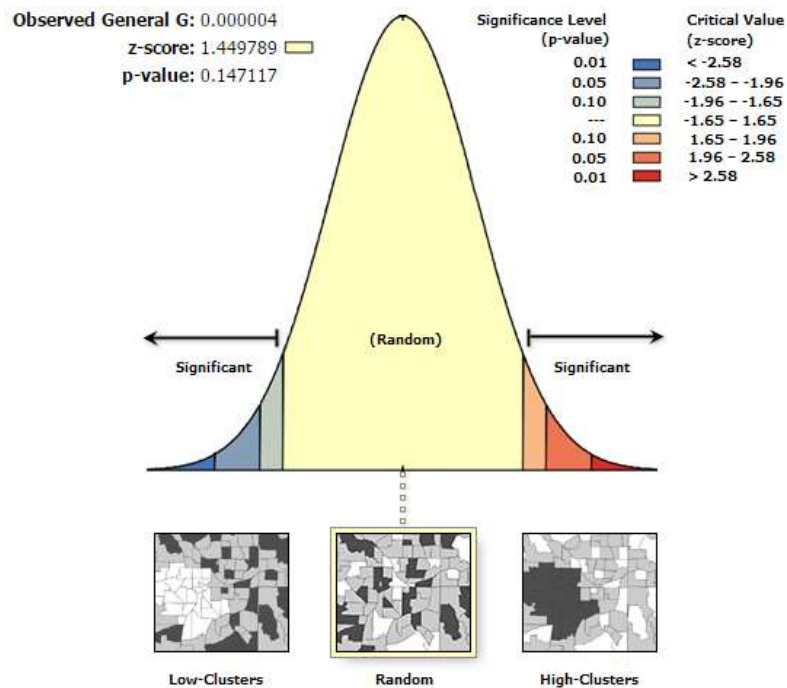


Figure A4.10 (b): High/Low Clustering report of the grey-headed flying foxes food source vegetation near the equine properties ‘at risk’ at 5 kms.



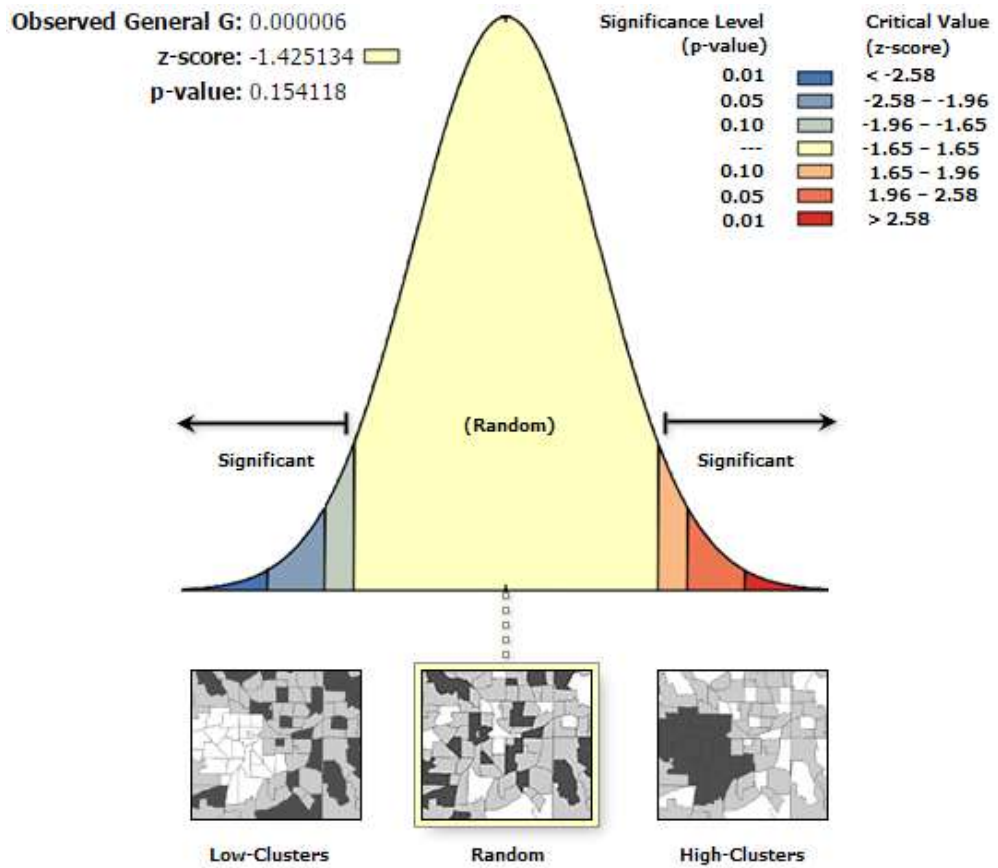
Given the z-score of 5.99132656821, there is a less than 1% likelihood that this high-clustered pattern could be the result of random chance.

Figure A4.10 (c): High/Low Clustering report of the grey-headed flying foxes food source vegetation near the equine properties 'at risk' at 10 kms.



Given the z-score of 1.44978944457, the pattern does not appear to be significantly different than random.

Figure A4.10 (d): High/Low Clustering report of the grey-headed flying foxes food source vegetation near the equine properties 'at risk' at 15 kms.



Given the z-score of -1.42513429067, the pattern does not appear to be significantly different than random.

Figure A4.10 (e): High/Low Clustering report of the grey-headed flying foxes food source vegetation near the equine properties 'at risk' at 20 kms.

Appendix - 5

Abstracts of the Associated Publications

A5.1 Preliminary Spatial Analysis of Hendra Disease Outbreaks in South East Queensland

Abstract: HeV was first reported in the suburb of Hendra, Brisbane in 1994. It has proven to be fatal to both humans and horses, with the first outbreak resulting in the death of 13 horses and a trainer. Since then, there have been several other outbreaks reported across Queensland, from Cairns to the New South Wales border at Murwillumbah. Due to the frequent incidents of the virus outbreak, the Queensland Government's Department of Agriculture, Fisheries and Forestry (DAFF) stated that there is a pressing need for current research on the spatial and temporal occurrences of the virus infections (DAFF 2012). This paper presents an overview of the research, and the preliminary results of the relationship between the Hendra disease outbreaks and the roosting sites of flying-foxes in the south-east Queensland. The results show a strong relationship (92% of the incidents) between temporary and seasonal roosting sites (rather than the permanent continuous roosting sites) and the outbreak locations. This finding suggests the need for detailed cluster analysis and regression models to identify the risk factors for the spread of the disease.

Keywords: Hendra disease, Horses, Flying-foxes, Outbreaks, Spatial analysis

A5.2 Factors Explaining the Dispersal of HeV Disease in South East Queensland

Abstract: HeV (HeV) was first described in 1994 following the outbreak of a new disease fatally affecting horses and humans in south-east Queensland. The disease kills 70% of the infected horses and under some circumstances the virus is spread to humans who have had close contact with the infected horses. Fruit bats (*Pteropus* spp.) commonly known as flying-foxes have been identified as the natural host of the virus. A preliminary analysis of the incidents and the flying-fox roosting sites revealed a strong relationship between the temporary and seasonal roosting sites in the south-east Queensland (Burnham et al. 2014). The aim of this paper is to determine the potential factors that can explain the dispersal of HeV incidents in the study area. Based on the preliminary results, a further analysis was done on the roosting sites by considering factors such as the species of flying-foxes, foraging range and pregnancy period. Spatial autocorrelation (Global Moran's I) revealed significant clustering of *P. alecto* and *P. scapulatus* species. Kernel density estimation analysis helped in identifying a strong relationship between *P. alecto* and *P. scapulatus* species density and the outbreak events in the study area. Buffer analysis established an initial relationship between *P. alecto* and *P. poliocephalus* species birth periods and the incidents. Ordinary least squares (OLS) regression identified *P. poliocephalus* species as statistically significant at a global context across the study area. Geographically weighted regression (GWR) analysis was performed to study the local spatial variations of the explanatory variables. *P. alecto* and *P. poliocephalus* species exhibited a significant positive relationship in most of the regions where as pregnancy period variable exhibited a significant negative relationship to the HeV incidents in the study area.

Keywords: Hendra disease, Incidents, Dispersal, Flying-foxes, Spatial Analysis

A5.3 An Investigation of the Food Sources and Roosting Sites as Potential Factors of HeV Dispersion in South East Queensland, Australia

Abstract: HeV (HeV) was first identified in 1994 following the outbreak of a new disease which is fatally affecting horses and humans in south-east Queensland. Since this outbreak, there have been subsequent incidents reported in south-east Queensland. Fruits Bats (*Pteropus* spp.) commonly known as flying-foxes have been identified as the natural host of the virus. In this paper, an in-depth analysis is carried out to determine the correlation between food source vegetation and the flying-foxes roosting sites. This investigation may determine whether clustered or dispersed vegetation has more impact on the incidence. Using spatial analyst tools, the major vegetation subgroups (MVS) present within 20 kilometers buffer range of grey headed flying-foxes and black flying-foxes roosting sites are identified. The identification of abundance of food sources for individual species within their minimum foraging range indicated a strong correlation between their site locations and vegetation subgroups present. A 10 kms range vegetation study on the incident locations identified the presence of 'food sources' of both species. The clustering of the food resource vegetation present near the incidence was studied using Getis-Ord General G Statistic method, which indicated statistically high clustering with 99% confidence level at 3 kms distance threshold. The findings suggest that the presence of potential 'food resource' of the flying-foxes within certain proximity increases the risk of HeV disease transmission to horses.

Keywords: Flying-foxes, Vegetation, Clustering

A5.4 Examining the Spatial Relationship between Equine Population and Food Source Vegetation of Flying-foxes in South East Queensland, Australia

Abstract: HeV (HeV) was first identified and described in 1994 following the outbreak of a new disease fatally affecting horses and humans in south-east Queensland. Since the outbreak, there are subsequent incidents reported in eastern Australia mainly in south-east Queensland. Fruits Bats (*Pteropus* spp.) commonly known as flying-foxes have been identified as the natural host of the virus. This paper examines the spatial relationship(s) between the equine population and food source vegetation of flying-foxes in the study area. A 10 Km range vegetation study on the equine properties in the study area identified the food source vegetation of both black and grey headed flying-foxes. The clustering of the food source vegetation present near the equine properties was studied using Getis-Ord General G Statistic method, which indicated statistically significant high clustering at 3, 5 and 10 Km distance thresholds.

Keywords: HeV, Flying-foxes, Food source vegetation, Equine population